UNIVERSITÀ DEGLI STUDI DI MILANO

Scuola di Dottorato Terra, Ambiente e Biodiversità
Dipartimento di Scienze della Terra "A. Desio"
Corso di Dottorato in Scienze Naturalistiche ed Ambientali

BIOMINERALIZATION AND GLOBAL CHANGES: BRACHIOPOD SHELLS AS ARCHIVES OF THE END PERMIAN EVENTS

CLAUDIO GARBELLI
Matricola R09749

TUTOR
Prof. Andrea Tintori
Prof. Lucia Angiolini

COORDINATORE DEL DOTTORATO
Prof. Nicola Saino

A.A. 2014

...to those who trust me...

Contents

Abstract

The Permian has been the theatre of major global changes in the Earth's geodynamics, climate, seawater and atmosphere geochemistry, and thus it represents an interesting case study to understand the response of organisms to environmental changes, a topic which is of increasing interest to the scientific community, who has to face the current global change. In fact, in the Permian the biotic response was dramatic, culminating at the end of the period with the greatest mass extinction of the Phanerozoic. Noteworthy, the end Permian mass extinction coincided with one of the largest known continental eruptions, the Siberian trap basalts, that are considered to have generated more than 100,000 Gt of CO_2 as well as CH_4, leading to ocean acidification and global warming. Brachiopods, which are low buffered organisms with a heavily calcified shell, can be the perfect candidates to record the trends related to changes in seawater chemistry during this critical interval.

The aim of this research is thus to study the biomineralization of brachiopod shells to unravel the patterns of biotic changes caused by the extreme Late Permian events.

To reach this goal, I organized my research in three different phases, starting to investigate the main differences in the shell fabric of the brachiopod groups ruling the benthic communities in the Late Permian, that are the classes Rhynchonellata and Strophomenata (phase 1); then comparing the stratigraphic distribution of brachiopod genera during the Late Permian in a paleogeographic perspective (phase 2); finally, analyzing in great details, both qualitatively and quantitatively, the shell fabric of several taxa from Tethyan Permian-Triassic Boundary (PTB) successions, to unravel the biomineralization activity at generic level(phase 3).

To develop this research I investigated brachiopods belonging to different

paleogeographic localities in the Tethyan realm. The specimens were in part collected by myself during field activity, in part already available from the collections of Dipartimento di Scienze della Terra "A. Desio" and also provided by external partners. The studied brachiopods come from:

1. Nesen Formation, Alborz Mountains, northern Iran;
2. Julfa Formation, Ali Bashi Formation and Boundary Clay, Ali Bashi Mountains,
Northwestern Iran;
3. Selong Group, southern Tibet;
4. Gyanyima Formation, southwestern Tibet;
5. Bulla Member, Dolomites, Northern Italy;
6. Gomaniibrik Formation, Hazro, Turkey;
7. Changhsing Limestone and Dalong Formation, South China

These data were integrated with the analysis of the available published literature on Upper Permian brachiopods, in particular to develop step 1 and 2.

The methods used to develop this research may be grouped in four main categories:

1. Microscopical analysis of the shell structure using SEM (phases 1 and 3)
2. Geochemical analysis of the calcitic shell contents for trace elements (Mg, Sr, Fe, Mn) and stable isotopes (C and O)(phase 1)
3. Image analysis to acquire quantitative parameters of the shell ultrastructure (phase 3)
4. Statistical analysis of the stratigraphic distribution of brachiopod taxa using the logistic regression in order to test association between environmental variable and taxonomic composition (phase 2).

Performing phase 1, I discovered important differences in the structural and chemical composition of the shell in the two main Upper Permian brachiopod classes: the Strophomenata and the Rhynchonellata. These taxa bear a different calcitic shell fabric: the former possesses a double or triple layer shell consisting of a primary layer, a secondary layer with cross-bladed laminae and

a prismatic tertiary layer; the latter have a shell succession similar to extant ones, which is composed of a primary layer of crystallites, a secondary layer of discrete fibers and, eventually, a tertiary layer of prisms. Their different fabric corresponds to differences in the chemical composition. In particular the Strophomenata, which have a laminar fabric enriched in organic compounds, have higher Sr and Mg contents and a lower $\delta^{13}C$ in their shells than co-occurring Rhynchonellata.

In phase 2, the logistic regression analysis has shown that important changes in terms of taxonomic composition took place from the Wuchiapingian to the Changhsingian, with the Strophomenata being the dominant group in terms of abundance, but the Rhynchonellata being more prone to high rank diversification.

In phase 3, the detailed study of the shell structure at the SEM, has revealed that Upper Permian genera can produce different type of shells, especially regarding the ratio between the organic and inorganic content. In particular, the taxa occurring during the first part of the Late Permian (Wuchiapingian and early Changhsingian) biomineralized thick shells with a relatively high inorganic content. Instead, in the late Changhsingian, brachiopod taxa produced shells with a higher organic content.

In addition, the quantitative analysis of the fabric, based on the measured size of its structural units, revealed different trends in the two classes. Rhynchonellata reduced the size of the structural units (fibers) of their shell as approaching the PTB. On the other hand, the Strophomenata show a more complex response, either continuing in their normal biomineralization activity or increasing the size of their structural units (laminae).

Through this research, two important conclusions were reached: the first concerns the paleobiological implications of the different biomineralization processes performed by brachiopods, and the second is related to the brachiopod response to the end Permian global environmental changes. It is now clear that the brachiopod classes of Strophomenata and Rhynchonellata have

profound differences in terms of the structural and elemental composition of their shell. These differences are likely related to the biomineralization process responsible for the formation of their shell, a collective process where arrays of mantle cells secrete the biocomposite in the Strophomenata, versus a discrete, single cell driven process in the Rhynchonellata .

The observed changes in brachiopod shell biomineralization in the latest Permian are compatible with a change in the carbonate saturation state of seawater and thus with ocean acidification, related to Siberian Traps flood basalt volcanism. In fact, a general trend toward production of calcitic shells with higher organic content is recorded up to the PTB in most brachiopod groups. This may have been likely the result of changes in the physical and chemical composition of seawater that produced an increase in the energetic cost for carbonate precipitation in low buffered organisms such as brachiopods.

Chapter 1
Introduction: biomineralization of brachiopods and an overview on low magnesium calcite shells

Biomineralization concerns those processes through which organisms form minerals (e.g. Simkiss and Wilbur 1989, Mann 2001, Dove *et al.* 2003, Knoll 2003). Even if biominerals meet the criteria for being true minerals, they also possess other characteristics that distinguish them from their inorganic counterparts. In fact the control exerted by organisms on mineral formation characterizes this process, making possible to differentiate these minerals from abiotic ones. The most evident trait is that biogenic minerals have unusual external morphologies, but there are other important properties which mark them (Dove *et al.* 2003). These properties are tightly bounded with the organism producing the biomineral itself. Despite the fact that the hallmark of biomineralization is the control that organisms exert over the mineralization process, during the last 60 years it has been noted that biominerals often contain, embedded within their structure, signatures that reflect the external environment in which the animal lived (Lowenstam 1961, Morrison and Brand 1983, Carpenter and Lohmann 1995, Buening and Spero 1996, Curry and Fallick 2003, Brand *et al.* 2003, Parkinson *et al.* 2005, Parkinson and Cusack 2007). Thus, most of the geochemists have focused on extracting the signal for past seawater temperatures, salinities, productivities, extent of sea water saturation, and more (e.g. Angiolini *et al.* 2009, Brand *et al.* 2012). This is particularly true when the biomineral is formed in equilibrium with the seawater in which the organism lives, with no vital effect during the biomineralization process (e.g. Epstein *et al.* 1953, Grossman and Ku 1986, Lécuyer *et al.* 2004, Schöne *et al.* 2005, Brand *et al.* 2011). At the base of the Cambrian, about 540 myr ago, organisms of many

different phyla had already evolved the ability to form many of the 64 different minerals known today (e.g. Knoll 2003). The diversity of minerals employed in early skeletalized animals suggests a limit to the role of ocean geochemistry in the emergence of skeletons, although the primary acquisition of particular skeletal carbonate mineralogies was likely driven by the ocean geochemistry (Bengtson 1994, 2004, Ushatinskaya and Zhuravlev 1994, Hardie and Stanley 1997, Stanley and Hardie 1998, Porter, 2007, Zhuravlev and Wood 2008, 2009). From their first appearance, calcium carbonate biominerals became the most abundant biogenic minerals, both in terms of quantity produced and of distribution among many different taxa (Kouchinsky *et al.* 2012). Brachiopods with a calcitic shells appeared very soon in the Early Paleozoic and have been the dominant sessile fauna until the Permian-Triassic mass extinction. For this reason their calcitic shells are the most widespread tools to reconstruct Paleozoic seawater environmental conditions.

1.1 The structure of the brachiopod calcitic shell: a multilayered biocomposite

The brachiopod shell calcite is a biomineral built under the effect of different constrains, which fundamentally encompass the body plan of the taxon, the type of secretory regime, and the nature of the organic substrate on which calcium carbonate nucleates.

The shell wall is a multilayered biocomposite, composed of several layers which differ on the basis of their fabric, namely on the ratio between organic and inorganic component and on microstructural features of the inorganic component. Despite this large scale heterogeneity, observations on modern Rhynchonelliformea brachiopods have shown that the carbonate component is structurally very similar in all the layers at the microscale. It is composed by nanometric calcite granules, which assemble together after granular exocytosis (Cusack and Williams 2001). However, recent investigations underline that at this scale there may subtle differences in the nanometric structure of Rhyn-

chonelliformea brachiopods (Pérez-Huerta *et al.* 2013). This underscores that the knowledge on shell secretory mechanisms is far to be exhaustively known and that the brachiopods shell structure cannot be fully understand without taking in account their evolutionary history. Cambrian-Ordovician brachiopods have evolved different types of organocarbonate fabric. Among these, two classes, belonging to the Rhynchonelliformea, dominated the benthic communities of Paleozoic seas: the extinct Strophomenata and the extant Rhynchonellata. These two classes show general differences in their body-plan organization and in their secretory mechanism of the shell (Williams 1997, Cusack and Williams 2001, Garbelli *et al.* 2014a). Strophomenata brachiopods produced two or three layered shells , with a primary layer of randomized granular calcite, a secondary layer of cross-bladed laminar calcite – in case accessorized with pseudopunctae - and, at times, a tertiary layer of large prismatic calcite. The secondary layer was highly variable in the organization of their structural units. Contemporaneous, but still extant, Rhynchonellata also have shells with two or three layers, but their secondary layer consists of calcite fibers, and it may be perforated by punctae. Their secondary layer fibers are more uniform and less variable in terms of structural unit organization. Furthermore, there is less inter-crystalline space in the secondary fibrous layer of the Rhynchonellata than in the laminar one of the Strophomenata, which has been retained to be more organic rich (Garbelli *et al.* 2014a and references therein).

The shell wall may be or not crossed and/or perforated by different structures: pseudopunctae in the Strophomenata and punctae (sensu lato) in the Rhynchonellata. A pseudopuncta essentially consists in an inclined trail of cone-in-cone lamellae affecting the laminae of the secondary layer and sometimes it emerges along the internal surface of the valve as a tubercle or endospine. On the other hand a puncta is an originally hollow funnel shaped or tubular feature generated by outwardly deflected fibers of the secondary layer and in vivo occupied by mantle caeca. Pseudopunctae and punctae are totally different from a structural and a functional point of view. These features are

important systematic tools and probably underlie biological/physiological differences between groups.

Despite these differences, a common feature is present in the two classes: both groups could, in several species, develop a prismatic layer. This layer is secreted under a special secretory regime, in which the cell of the mantle cease to migrate and stop to produce the organic matrix that control and frame the secondary layer. This character crosses the taxonomical subdivisions of the rhynchonelliformean brachiopods because tertiary prismatic layer secretion is reported for all the principal classes and orders and do not seem to have substantial differences. The change in secretory regime is reversible and it is possible to find alternation between tertiary and secondary layer in the shell of the brachiopods. What is puzzling is that, despite the deep differences in the secretory mechanism of the secondary layers between the two classes, the pattern of alternation between secondary and tertiary layer is very similar in species phylogenetically very distant.

1.2 Biomineralization, environmental influences and fitness

It is widely accepted that organic substances regulate or influence the structure of biominerals and recently Okumura *et al.* (2013) have shown that the crystallographic microstructures in biotic calcites arise from incorporated intracrystalline organic molecules. Through the evolution, these biominerals became essential for the survivorship of the species fulfilling a broad set of functions. In this way biominerals production undergoes different selective natural processes. On one way there is the requirement to perform the function for which they have been selected. On another the phylogenetic history and the environment give constrains for the production of the biominerals.

For example, in brachiopods the shell meets the function of support and protection. As most biological processes, shell biomineralization is strongly influenced by environmental conditions. Because skeletal biomineralization requires energy related to the extraction of the carbonate and calcium ions from

the environment, it is possible that changes in chemical composition and physical properties of seawater cause a change in the metabolic cost for shell secretion, making more easy or more difficult the formation of the shell to fulfill its support and protection functions.

Even if this concept is relatively simple and clear, the metabolic response to seawater physicochemical variation and its effect on biomineral production was poorly known, at least for brachiopods, until the last years, when several researches have been performed studying the effects of environment variables on biomineralization processes (e.g. Parkinson at al. 2005). Olson *et al.* (2012a, 2012b) studied the nacre of eight mollusk species, showing that the ultrastructure of nacre is sensitive to the seawater hydrostatic pressure and temperature in which the mollusks live and to which they have adapted. Watson *et al.* (2012) have proved that total inorganic content, a proxy for skeletal $CaCO_3$ content, decreases with latitude, decreasing seawater temperature, and decreasing seawater carbonate saturation state (for $CaCO_3$ as calcite (Ωcal)) in several taxa of brachiopods, bivalves, echinoids and gastropods. Hahn *at al.* (2014), studying the bivalve *Mytilus edulis*, showed that low sea water pH affect biomineralization patterns in term of microstructure and crystallographic arrangement. The scientific community is thus increasingly aware that environmental changes influence biomineralization at different scales.

1.3 The end Permian global changes and mass extinction

The Permian has been the theatre of major global changes in the Earth's geodynamics, climate, and seawater/atmosphere geochemistry. In that changing world, the biotic response was dramatic, culminating in the latest Permian mass extinction (e.g. Erwin 2006, Shen *et al.* 2011, Brand *et al.* 2012), possibly triggered by flood basalt volcanism, high PCO_2 and associated rapid warming (Retallack 2013, Burgess *et al.* 2014). Approximately 90% of marine species, 70% of terrestrial vertebrate species (Maxwell 1992, Jin *et al.* 2000, Ward *et al.* 2005), 30% of insect orders (Labandeira and Sepkoski, 1993) and an indeter-

minate percentage of terrestrial and marine plants disappeared during this catastrophe (Raup 1979, Retallack 1995, Kozur and Weems, 2011). Great uncertainty still surrounds the exact nature and process of the extinction (e.g. Erwin 1994, Jin *et al.* 2000, White 2002, Racki and Wignall 2005, Knoll *et al.* 2007), as well as the duration and extent of the event (e.g. White 2002, Brayard *et al.* 2011, Retallack *et al.* 2011, Shen *et al.* 2011, Angiolini *et al.* 2011). A plethora of trigger and kill mechanisms have been take in account to explain the crisis, but before addressing them, a distinction between the two categories is necessary. A kill mechanisms is a disruptive process causing the death of the organisms. The trigger mechanism is the event bringing the kill mechanisms into play. It is clear that the trigger mechanisms could work in a synergistic way and that a kill mechanism may be fueled by more triggers. The triggers purposed over the years for the end Permian mass extinction are the following: bolide impact, volcanism, ocean anoxia, seafloor methane and thermogenic methane emissions (e.g. Erwin 1994, Racki and Wignall 2005, Retallack and Jahren 2008, Shen *et al.* 2011, Burgess *et al.* 2014). Extraterrestrial triggers are likely to be excluded because there are not evidence and a terrestrial cause of the extinction is more reliable (Erwin 1990).

Kill mechanisms refers to: 1) niche (habitat) loss, 2) hypercapnia, 3) global cooling, 4) hyposalinity, 5) global warming - CO2, 6) global warming - CH4, 7) low atmospheric oxygen, 8) global depletion of stratospheric ozone, 9) ocean acidification, 10) nutrient limitation (shutdown of terrestrial and marine productivity), 11) acid rain, 12) poisoning from toxic gases, and other related mechanisms such as 13) biosphere upheaval through forced migration and increased competition, 14) extraordinary spread and transmission of disease, and 15) life cycle disruption(s) due to increased environmental stresses (e.g. Erwin 1994, Kidder and Worsley 2004, Racki and Wignall 2005, Knoll *et al.* 2007, Wignall 2007, Grasby *et al.* 2011, Brand *et al.* 2012). The general though of the scientific community ruminate the idea of complex interactions and related causes and effects (e.g. Erwin 1994, Knoll *et al.* 2007, Wignall 2007).

Noteworthy the Permian–Triassic mass extinction coincided with one of the largest known continental eruptions, the Siberian Trap basalts that, by the metamorphism of organic matter and petroleum could have generated more than 100,000 Gt of CO_2 as well as CH_4 (Svensen *et al.* 2009, Shen *et al.* 2011, Burgess *et al.* 2014). These large amount of gasses injected in the atmosphere have likely changed the carbonate saturation levels of seawater.

Recently $\delta^{44/40}Ca$ trends in carbonate rocks and conodonts at the PTB have been related to a change in the $\delta^{44/40}Ca$ of seawater, which could be interpret to reflect an imbalance between calcium weathering and burial fluxes, triggered by ocean acidification (Hinojosa *et al.* 2012). In fact there are evidences that the extinction was selective for heavily calcified marine animals (e.g. Knoll *et al.* 1996, Clapham and Payne 2011) . Despite this, the response of organisms to ocean acidification is difficult to evaluate, because the level of carbonate saturation may be alternatively coupled or not with pH variation, depending on the rate of CO_2 injection. Low rates of CO_2 release lead to a small and subtle seawater $CaCO_3$ saturation response, which may induce a differential biotic response (Hönisch *et al.* 2012). The main pulse of volcanism is localized close to the PTB, but some minor events related to the Siberian Traps are dated already 1 my before the extinction event (Reichow *et al.* 2009). So it is possible to hypothesize that a progressive change in $CaCO_3$ saturation of seawater has affected organisms in the time interval before the PTB. Brachiopods, which are low buffered organisms with a heavily calcified shell, can be the perfect candidates to record the trends related to subtle changes in seawater chemistry during this critical interval.

Chapter 2
Main aim and framework of the research

The general aim of this research is to unravel the biomineralization of brachiopod shells during one of the most critical time intervals of the biotic evolution on Earth, which is the end of the Upper Permian. This period was a time of global warming and environmental changes affecting the marine ecosystem through different processes among which the so called ocean acidification (Knoll *et al.* 2007, Svensen *et al.* 2009, Joachimski *et al.* 2012, Hinojosa *et al.* 2012). The effect of ocean acidification on modern organisms is hardly investigated by biologists (e.g. Hahn *et al.* 2014, Cross *et al.* 2015, Fitzer *et al.* 2014) but its role in the history of the biosphere is far to be understood, especially during the end Permian events which culminated with the most dramatic biotic crisis of all geological times (Erwin 1993, 2006).

To study this subject, I structured my research at three different levels spanning from a general and global viewpoint to specific and particular topics. Through a process similar to that of the increasing magnification in the microscope using different lenses, I have progressively addressed various questions corresponding to specific levels.

The first level (phase 1) concerns the general study of biomineralization in Upper Permian brachiopods. I started to investigate the main differences in the shell fabric of principal calcifying brachiopod groups of the Late Permian: the classes Strophomenata and Rhynchonellata. They represent the majority of the brachiopods during this time interval.

At a second more detailed level (phase 2) , I inspected the stratigraphic distribution of brachiopod genera during the Late Permian. I did this both in a general view, with low time resolution, and in a paleogeographical perspective coupled

with a more detailed stratigraphic resolution, investigating the composition of brachiopod associations bed by bed. The brachiopod genera have been grouped by their shell fabric to test if there are some patterns of selectivity relative to their biomineralization ability during the Late Permian.

In the third level of my research (phase 3), I analyzed the shell fabric of several genera in detail. This was done in selected stratigraphic successions of different paleogeographic regions: South China, Tibet, Iran, Turkey, and Dolomites. The basic idea is that the type of shell sequence is informative of the biomineralization capacity of a single genus. As consequences, the recurrence of certain taxa with specific shell structure could be a signal of a change in the carbonate availability dissolved in the seawater. Since it is becoming increasingly clear that calcifying organisms can modify their biomineral skeletons according to the environment (Watson *et al.* 2012), I tried to use a new and unconventional approach for studying the shell. I quantified some features of the shell ultrastructure in some selected brachiopod genera in order (1) to unravel the presence of fine changes of the fabric, (2) to compare it along the stratigraphic record and (3) to find a correlation with environmental changes. Using this approach, I tried to decipher if there is any change in the biomineralization process through time. In fact, assuming that the shell ultrastructure is strongly influenced by ontogenetic constrains, it is theoretically possible to test if there are effects of the End Permian environmental changes on biomineralization process considering specimens belong to different populations of the same species. These changes could have reduced survivorship ability of brachiopods, culminated with the End Permian mass extinction. Finding fine changes in brachiopods shell ultrastructure has further implications on understanding the evolution of shell fabrics and Paleozoic brachiopods phylogenesis.

To develop the research I investigated brachiopods already present in the collection of the Earth Science Department "A. Desio". In addition I had collected brachiopods from selected stratigraphic sections to implement the material already available. The specimens are described and determined in order to obtain

a consistent taxonomy from generic to specific level depending on the quality of the material.

The methods used to develop this research may be grouped in four main categories:

1. Microscopical analysis of the shell structure (during phase 1 and 2)
2. Geochemical analysis of the calcitic shell (phase 1)
3. Image analysis to acquire parameters of the shell ultrastructure (phase 3)
4. Statistical analysis of the stratigraphic distribution and of the ultrastrucural parameters (phase 2 and 3).

2.1 Methods

2.1.1 Microscopical analysis of the shell structure

The study of brachiopod fossil shells with SEM was introduced in the fifty's by Sir Alwyn Williams to investigate shell fabric features. Despite this, only a relatively small number of fossil brachiopods were studied from this point of view with respect to the variety of brachiopod fossil record (i.e. Williams 1968, Armstrong 1968, MacKinnon 1974, Grunt 1982, Gaspard 1982, Komarov 1991, Angiolini *et al.* 1993, Cusack and Williams 2001, Dewing 2004). In this work I had investigated the shell structure of several species belonging to 39 different genera of Upper Permian brachiopods. A total of 364 brachiopods shell have been analyzed.

The brachiopod specimens under investigation (Appendix C) were cut along their longitudinal and transverse axis, embedded in resin, polished and then etched with 5% HCl for 15 seconds. In addition, acetate peels of some specimens were prepared with a cellulose acetate film and acetone $(CH_3)_2CO$. The exposed surfaces were metal coated with Au by the sputtering process and then inspected with the scanning electron microscopy (SEM) Cambridge S-360 featuring a LaB6 source and an acceleration voltage of 20kV.

Thin sections of specimens were also analyzed by cathodoluminescence with a cold cathode luminoscope (Nuclide ELM2) operating at 10 kV with

a beam current of 5–7 mA. Exposure to the electronic beam (before taking the photo) was on the order of 15–30 seconds, not to force shell material to luminesce, and it was consistent for all specimens. Also, photographic exposure time was uniform and set to seconds for consistency with a Nikon Coolpix 4500 operating at 400 ISO.

Cathodoluminescence (CL) microscopy is a powerful technique to study biominerals and it is particularly important in paleontology to asses preservation of carbonatic shells (Barbin 2013). The calcite luminescence is controlled by the molar ratio of Fe/Mn. High Mn content in the calcite lattice is an activator of luminescence, whereas Fe is a quencher of luminescence (Machel *et al.* 1991, Machel 2000). Mn is generally low (< 200 ppm) in unaltered in both recent and fossil brachiopod shells (e.g. Brand *et al.* 2003, 2011), where it may be preferentially incorporated during diagenesis (Brand and Veizer 1980). Fe contents are generally lower than 140 ppm in recent brachiopod shells, although much higher values have also been reported (Brand *et al.* 2003). As consequences, when Mn and Fe are low the shell is non-luminescent; when Mn increases compared to Fe, the shell is luminescent.

2.1.2 Geochemical analysis of the calcitic shells

Brachiopod shells and the relative enclosing rocks were analyzed for trace element composition to provide the diagenetic evaluation of their micromorphology. Brachiopod shells were separated from their enclosing whole rock and cement and cleaned from all the adhering material, and where possibly separated into their sublayers.

Powders of 10–20 mg were weighed to four decimal places and digested in 8 mL doubly distilled HNO3. Modifiers were added to each solution to counter chemical interferences during the analyses. Reference standards (Delta Scientific) were used to calibrate the atomic absorption spectrophotometer (AAS), and all samples were analyzed on a Varian 400P AAS for Ca, Mg, Sr, Mn and Fe. Precision and accuracy of analytical work was 4.8 and 0.99 for Ca; 5.58 and 0.65 for Mg; 8.31 and 1.26 for Sr; 5.33 and 1.91 for Mn; 11.11 and 3.13 for Fe

relative percent (±), respectively, based on the mean of 61 analyses of NBS 633 (NIST) standard reference material (SRM).

A subset of samples, brachiopods and whole rock, was analyzed for their carbon and oxygen isotope compositions. About 200 μg of powder, for each sample, was digested with 100% pure orthophosphatic acid at 75 °C in a Thermo-Finnegan Gasbench II. Liberated carbon di oxide was introduced into a T-F Delta V mass spectrometer. Precision and accuracy of NBS-19 standard values for carbon and oxygen isotopes were within 0.05‰ (VPDB). Isotope values ($\delta^{13}C$, $\delta^{18}O$) are reported as per mil (‰) deviations of the isotopic ratios ($^{18}O/^{16}O$ and $^{13}C/^{12}C$) calculated to the V-PDB scale using a within-run laboratory standard (KMC) calibrated against the international NBS standards (NBS19)

2.1.3 Image analysis

SEM microphotographs were analyzed using ImageJ, a public domain Java image processing program. For further details on the software see the website (http://imagej.nih.gov/ij/). Several measures of the structural units of the brachiopods shell fabric were acquired using this software. In particular, two types of measurements were taken:

1. the thickness of laminae in taxa belonging to theStrophomenata
2. the width and the area of fibers, in cross section, for the taxa belonging to the Rhynchonellata

For laminar fabric the thickness of the laminae has been acquired. To reduce measurement errors, thickness of packed laminae was measured and divided by the counted number of laminae. When the laminae were sectioned with blades in cross section, it has been possible to observe the presence of space between single units. These inter-units spaces, here after called porosity, can be easily measured and they represent a measurement of structural features related to the shell fabric. For fibrous fabric it has been possible to take measurements on transversal section of every single fiber. The measures acquired for the single fibers were the width and the area. From these metric parameters it has been

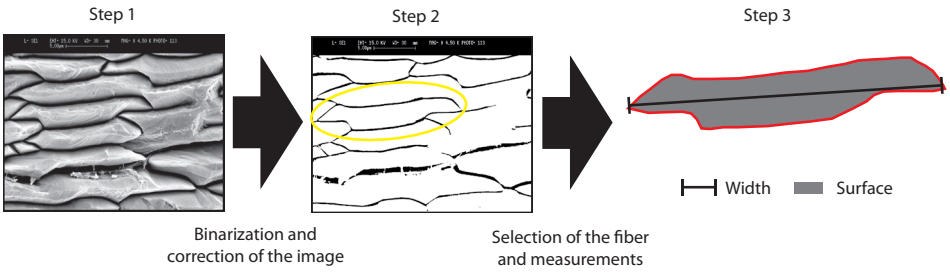

Figure 2.1. Images showing trasverse sections of the fibers were selected (step 1) and subsequentely binarized and corrected to delimit manually the outline where the image contrast was not sufficient to allow the automatical binarization by the software (step 2). The fiber to be measured was then selected with the ImageJ selection tool and a number of measurements and morphological descriptors were acquired by the software (step 3).

also possible to calculate morphological descriptors. The procedures used to acquire measurements in fibrous fabric is summarized in Figure 2.1. For the investigation purposed it will be basically used the width of the fibers.

2.1.4 Statistical analysis of the stratigraphic distribution

To study the change in brachiopod fabrics distribution through the Late Permian, I analyzed three different types of datasets: (1) the genera occurrences downloaded from the Paleobiology database (OccPD -Appendix B), (2) the occurrences of individual species bed by bed on different Lopingian sequences (OccB - Appendix B) recorded from recent literature (see Table 2.1).

The OccPD dataset contains 14961 occurrences of rhynchonelliformean brachiopods and information related to the time interval of occurrence (i.e. stage). For every genus occurrence, a type of fabric was assigned based on its taxonomic position inside the Rhynchonellata and Strophomenata. Four categories were assigned for the type of secondary layer and its feature: (1) laminar fabric with pseudopunctae without taleolae, (2) laminar fabric with pseudopunctae bearing the taleola, (3) impunctate fibrous fabric , (4) punctate fibrous fabric. These data were examined to obtain general information on abundance and distribution of brachiopods based on the characteristic secretory pathway

of the secondary layer, which is the most differentiated among the calcitic layers of rhynchonelliformea shells. Frequencies histograms have been built to compare abundance during Wuchiapingian, Changhsingian, Induan and Olenekian stages and to analyze the relative change in distribution.

The OccB contains a total of 1184 occurrences of species from 312 stratigraphic levels belonging to 22 Late Permian sections of different paleogeographical regions. For every stratigraphic bed, the following topics were recorded: the distance from the Permian-Triassic boundary (when it is present in the section), the stage (Wuchiapingian vs Changhsingian), the depth of the environment, the paelogeographical region and the outcrop name. For every stratigraphic horizon, the number of species classified on the basis of shell fabric was counted (in this case only laminar vs fibrous fabrics have been considered, see Appendix B). A multiple logistic regression was applied to evaluate the effect of environmental, paleogeographical and stratigraphical variables on the frequencies of fabric types. The statistical model considers simultaneously the paleogeography, the environment, the time frame in terms of stage and the stratigraphic position in terms of distance fromto the PTB. Due to differences in sedimentation retes, the latter has been nested to each specific stratigraphic section.

The logistic regression is a statistical model to describe the relationship between a discrete or a categorical response variable and one or more explanatory variables. The major difference between the logistic regression model and the linear regression model is that the dependent variable in logistic regression is binary or dichotomous (Hosmer *et al.* 2013).

If we consider that the response variable y_i is binary and it is coded by 1 or 0, respectively for the presence or for the absence of a positive response, then:

$$yi \begin{cases} 1 \; if \; the \; i-th \; is \; positive \\ 0 \; if \; the \; i-th \; is \; negative \end{cases}$$

We can consider $\boldsymbol{y}_i$ as the realization of a random variable $\boldsymbol{Y}_i$ that can be 1 with the probability π_i and 0 with the probability ***1-*** π_i. The random variable assumes the Bernoulli distribution:

$$\Pr\{Y_i = y_i\} = \pi_i^{y_i}(1-\pi_i)^{1-y_i}$$

and the expected value and variance of $\boldsymbol{Y}_i$ are:

$$\mathrm{E}(Y_i) = \mu_i = \pi_i, \text{ and}$$

$$\mathrm{var}(Y_i) = \sigma_i^2 = \pi_i(1-\pi_i).$$

One important consequence is that a model assuming that predictors affect the mean but not variance will be not appropriate for binary data. To find the relationship between the probabilities π_i, dependent on a vector of observed covariates $\boldsymbol{x}_i$, a linear function has to be built:

$$\pi_i = \mathbf{x}_i'\boldsymbol{\beta},$$

where β is the vector of the regression coefficients and $\boldsymbol{x}_i\beta$ can assume any real value. As consequences, because the probability π has only value between 0 and 1, the predicted values are not in the correct range until the range restrictions are not suppressed. It is possible to remove the range restrictions with a simple transformation including two steps: (1) we move from the probability π to the ***odds***$_i$:

$$\mathrm{odds}_i = \frac{\pi_i}{1-\pi_i},$$

which is the ratio of the probability that the event happens on the probability it does not happen; (2) we take the logarithm of the ***odds***$_i$, calculating the logit or log-odds:

$$\eta_i = \text{logit}(\pi_i) = \log \frac{\pi_i}{1 - \pi_i},$$

as consequences, when the probability is equal to zero the odds goes down to zero and the logit approaches to -∞. At the other extreme, as the probability approaches to one, the odds approaches to +∞ and so does the logit. It is now possible to build the generalized linear model with a binomial response and the linked logit. Supposing to have k independent observations $\boldsymbol{y_1}$….. $\boldsymbol{y_k}$, and that the ***i-th*** observation is the realization of a random variable $\boldsymbol{Y_i}$, $\boldsymbol{Y_i}$ is assumed to have a binomial distribution:

$$Y_i \sim B(n_i, \pi_i)$$

with a binomial denominator $\boldsymbol{n_i}$ and a probability π_i. The individual datum ni has value 1 for all ***i***. This is the stochastic structure of the model. Let's suppose then that the logit of the underlying probability π_i is a linear function of the predictors:

$$\text{logit}(\pi_i) = \mathbf{x}_i'\boldsymbol{\beta},$$

where $\boldsymbol{x_i}$ is the vector of the covariates and β is the vector of the regression coefficients. This is the systematic structure of the model.

The logistic regression model has the following features:

1. the mean value of the outcome variable must be bounded between zero and one and the logistic regression satisfies this constraint;
2. the binomial distribution describes the distribution of the errors and the analysis is based on this statistical distribution
3. the principles that guide an analysis used for the linear regression also guide the logistic one.

To better know the details concerning the statistical model see Hosmer *et al.* (2013).

Locality	Paleogeographic position (Fig. 2.2)	Formation	Section
Southern Alps (Dolomites)	1	Bellerophon and Werfen	Tesero
			Bulla
			Sass de Putia
Northern Iran	2	Julfa, Ali Bashi and Elikah	Main valley
			Ali Bashi 1-3
			Zal
		Nesen	Mangol Quarry +Restaurant
			Bear Gully
			Elikah River
			Abredan
South Pamir	3	Takhtabulak	Kuristyk
South China	4	Changhsing	Beifengjing
			Daijaigou
			Zhongliang hill
		Dalong	Shangsi
		Shaiwa Group	Shaiwa
		Talung	Dongpan
		Lungtan and Changhsing	Meishan C
			Meishan D
			Well H2
Turkey	5	Gomaniibrik	Hazro
		Pamucak	Çürük Dağ
Southwestern Tibet	6	Gyanyima	Gyanyima
	7	Selong Group	Selong Xishan
		Qubuerga	Qubu
			Tulong
Pakistan	8	Wargal Chhidru	Salt Range
Kashmir	9	Zewan	Kashmir

Table 2.1

Sampling and Paleontological analysis	**SEM analysis**	**Geo-chemis-try**	**Data from literature**	**References**
literature	NO	NO	YES	Posenato 2009
YES	YES	NO	YES	
literature	NO	NO	YES	
YES	YES	YES	YES	Ghaderi *et al.* 2014, Garbelli *et al.* 2014b
YES	YES	YES	YES	
YES	YES	YES	NO	NA
YES	YES	YES	YES	Angiolini and Carabelli 2010
YES	YES	YES	YES	
YES	YES	YES	YES	
YES	YES	YES	YES	
aa	NO	NO	YES	Angiolini *et al.* in press
YES	YES	NO	NO	NA
YES	YES	NO	NO	NA
YES	YES	NO	NO	NA
YES	YES	NO	NO	NA
literature	NO	NO	YES	Chen *et al.* 2009
literature	NO	NO	YES	He *et al.* 2005, 2007
literature	NO	NO	YES	Wang *et al.* 2006; Li and Shen 2008, Chen and Liao 2009
literature	NO	NO	YES	
literature	NO	NO	YES	
YES	YES	NO	NO	NA
aa	NO	NO	YES	Angiolini *et al.*, 2007
NO	YES	YES	YES	Shen *et al.*, 2010
YES	YES	NO	YES	Shen *et al.*, 2006
NO	NO	NO	YES	
NO	NO	NO	YES	
NO	NO	NO	YES	
NO	NO	NO	YES	

Table 2.1

2.2 Materials

To investigate the biomineralization of brachiopod during the Late Permian I study several materials from different localities (Fig. 2.2) and with the differents approach explained in the Methods paragraph. I synthetic overview of the material and the type investigation performed on it is presented in the Table 2.2.1. To know better the deatils on the materials see the Appenidx A containing the statigraphic sections sampled for this research. For the data of occurences (OccPD and OccB) and the materials studied with SEM see Appendix B and C respectively.

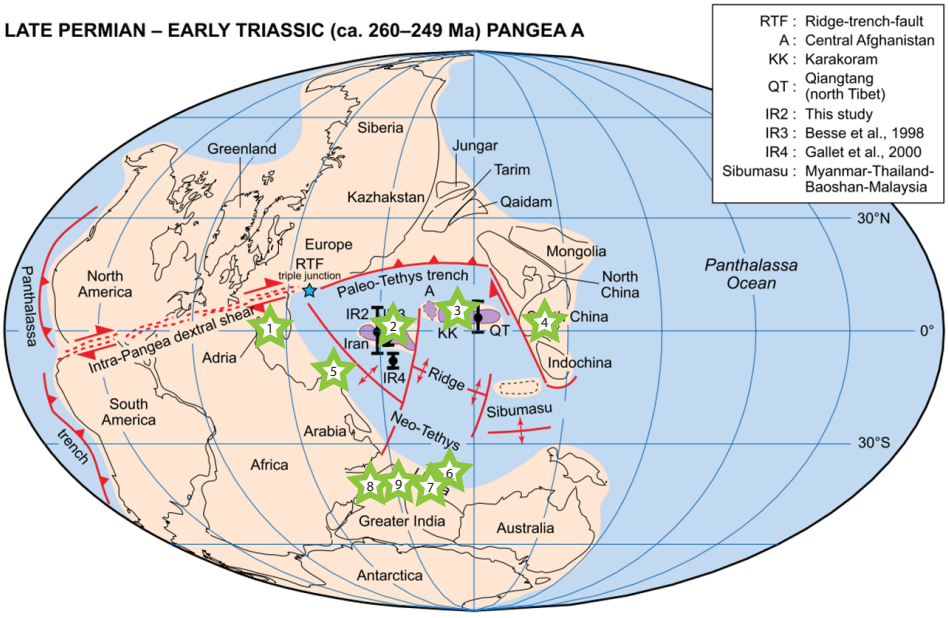

Figure 2.1. Late Permian paleogeographic reconstruction showing the position of the formation under investigations. The green star referes to the paleogeographic position of the different localities studied: 1-Southern Alps (Dolomites), 2 - Northern Iran, 3 - South Pamir (Tajikistan), 4 - South China, 5 - Turkey, 6 - Southwestern Tibet (Gyanyima Fm.), 7 - Southwestern Tibet (peri-Gondwanan region), 8 - Salt Range (Pakistan), 9 - Kashmir (Pakistan), (modified after Muttoni *et al.* 2009).

Chapter 3
Biomineralization differences in fossils brachiopods

Rhynchonelliformean brachiopods branched in the Cambrian, giving rise to five different classes: Chileata, Obolellata, Kutorginata, Strophomenata and Rhynchonellata (Williams *et al.* 1996).

The Strophomenata and Rhynchonellata were the dominant groups of brachiopods through most of the Paleozoic; the Strophomenata became extinct at the Permian-Triassic boundary (PTB), whereas the Rhynchonellata are currently represented by about 300 species. Since these two classes were an important component of the benthic fauna in the Paleozoic, deciphering paleobiological differences may be useful to understand environmental changes in ancient oceans, especially during critical intervals such as the Permian-Triassic transition.

Here, I try to summarize the fundamental differences between the two ruling classes of the Permian (i.e. Strophomenata and Rhynchonellata), focusing on those characters related to the biomineralization process and shell fabric. In fact, because these classes have a low magnesium calcitic shell (bLMCs), which is highly resistant to processes of alteration, it is possible to decode paleobiological characteristics of the two groups by studying original features of their shells.

3.1 Main differences between Rhynchonellata and Strophomenata

Strophomenata and Rhynchonellata dominated the late Paleozoic seas (e.g. Curry and Brunton 2007). They branched very early in the Cambrian and their

synapomorphies include (1) an organocarbonate shell with a fibrous secondary layer, (2) the presence of a pedicle without a coelomic core and (3) the development of a recognizable diductor muscle system controlling the opening of the valves (Williams *et al.* 1997). During the Paleozoic they evolved important differences in their body-plane organization and in the secretory mechanism of the shell.

The Strophomenata were the most widespread group of all brachiopods with more than 1500 genera ranging throughout the Paleozoic Era and they were the major constituents of many ecosystem during this time interval. They adopted a broad range of life-styles, including bivalve-like infaunal style, and a coral-like growth habit in some groups. This brachiopod class shows an incredible morphological diversification, including the most bizarre species of the phylum. The shell might have a biconvex to concavo convex form, extremely modified into a conical form with a lid (coral like form); the life habit may be infaunal to attached, and even encrusting. Many groups develop prominent spines and, during the Late Permian, the order Productida became the dominant group in term of taxonomic diversity and numeric abundance.

The Rhynchonellata is the only class of Rhynchonelliformea brachiopods with extant genera, currently represented by three different orders: Rhynchonellida, Terebratulida and Theicideida. During the Phanerozoic, seven additional order were present: Protorthida, Orthida, Pentamerida, Atrypida, Athyridida, Spiriferida and Spiriferinida. Note that Theicideida appear during the Mesozoic; Athyridida and Spiriferinida range to the Jurassic; Orthida and Spiriferida became extinct at the PTB; Protorthida, Pentamerida and Atrypida disappeared in the late Devonian. The Rhynchonellata are represented by about 3,000 genera ranging through all the Phaneorozoic with the synapomorphy represented by the presence of a pedicle. They differentiate linages by several ways (i.e. reduction of pedicle rudiment, modification of the loops), with shells usually from slightly to strongly biconvex.

Without doubts the most distinctive feature of the two classes is the second-

ary shell fabric, even if there are difficulties to formulate a theory explaining their evolution and phylogenetic relationships (Williams and Cusack 2007). Since Strophomenata have no extant record, becoming extinct at the end of the Permian, the knowledge about their shell fabric is exclusively inferred from fossils. They possess a double or triple layer shell consisting of a primary layer, a secondary layer with cross-bladed calcitic laminae and a prismatic tertiary layer (Figs 3.1A, B, C; Williams 1968, 1997, Williams and Cusack 2007). Fossil Rhynchonellata have a shell succession similar to extant ones, which, below an organic periostracum, is composed of a primary layer of calcite crystallites, a secondary layer of discrete fibers ensheathed in a glyco-proteinaceous membrane and, sometimes, a tertiary layer of prisms (Figs 3.1D, E, F, e.g. Williams 1968, MacKinnon 1974, Azmy *et al.* 2006, Williams and Cusack 2007, Cusack *et al.* 2008, Pérez-Huerta and Cusack 2008, Goetz *et al.* 2009, Cusack *et al.* 2010). The thickness of the secondary and tertiary layers, and their relative proportion in the shells, may vary at the generic and supra-generic levels in both the Rhynchonellata and Strophomenata (e.g. Williams 1997, Garbelli *et al.* 2012).

The difference in the secondary shell fabric of the two classes of brachiopods is probably related to the mechanism of shell secretion. In Rhynchonellata each fiber is secreted by a single cell of the mantle and wrapped by a glycoproteinaceous membrane (e.g., Williams 1968, MacKinnon 1974, Cusack and Williams 2001, Williams and Cusack 2007, Cusack *et al.* 2008). In almost all Strophomenata the secondary layer is secreted as a layer of calcite which is segregated into aligned calcitic units (blades) by impersistent protein strands exuded by the cells surface; this mechanism produces a recurring succession on a membranous substrate consisting of coated, ordered laths or blades of calcite forming the composite laminar layer (Williams and Cusack 2007). In Strophomenata, unlike Rhynchonellata, partitions of calcitic units do not coincide with cell boundaries and it is likely that several independent centers of calcite secretion simultaneously exist on the plasma membrane of

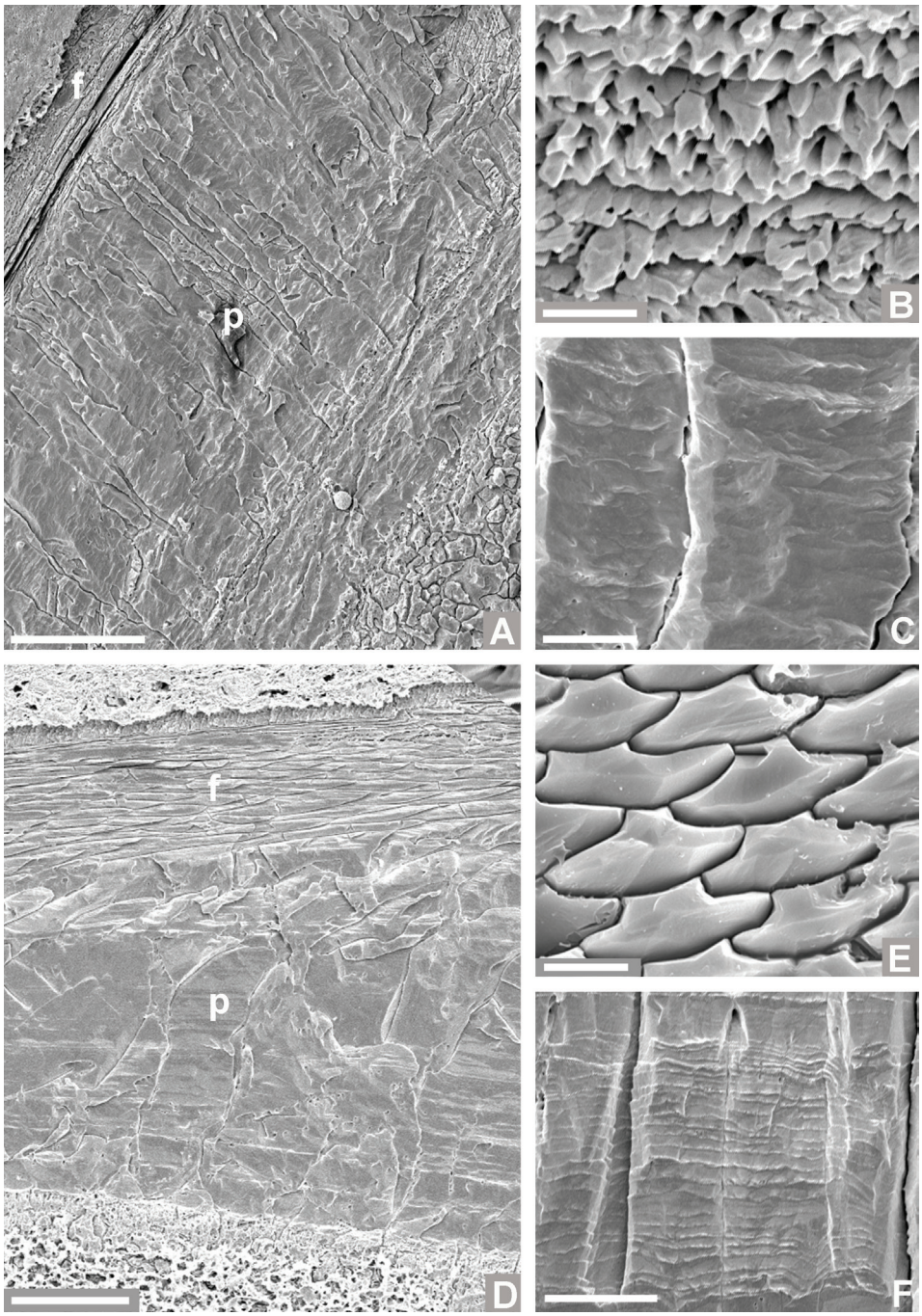

Figure 3.1

each cell (Williams 1968). The composition of the organic substrate in the Strophomenata shells may have been different from that of the Rhynchonellata. A chitino-proteinaceous composition has been tentatively proposed for the Strophomenata organic substrate by Williams and Cusack (2007). The origin of the Rhynchonellata fibrous fabric seems to be related to a shift from collectively secreted calcite laminae to the discrete cellular formation of fibers ensheathed in glycoproteinaceous strips (Williams 1968, Williams and Cusack 2007). In contrast, the origin of the composite laminar layer of the Strophomenata is more complex and seems to have convergently evolved from the coarse laminae of the Billingselloids and from the flat fibers of the Plectambonitoids (Williams 1970, Brunton, 1972, Williams and Cusack 2007). Angiolini *et al.* (2008, 2009) speculated that Strophomenata have a higher in vivo organic matter content, based on their "more open" fabric of the secondary laminar layer. These profound differences in biomineralzation of the shells, in their structure and, possibly, in organic matter-calcium carbonate ratio have to be discussed and accounted to use brachiopod shells as geochemical proxy of past ocean composition. Furthermore, Garbelli *et al.* (2012) have shown that diagenetic alteration may depend on shell fabric and the fibrous secondary layer of the Rhynchonellata is often better preserved than its laminar counterpart of the Strophomenata; a process independent from host rock lithology and possibly related to the amount of in vivo organic matter. These features may play a major role in the ultimate geochemical composition of the Strophomenata and Rhynchonellata.

Figure 3.1. (A) Shell succession of a Productida (*Spinomarginifera spinosocostata*, JU1-3, Lopingian, North Iran) showing an outer laminar layer (l) and an inner prismatic one (p), scale bar 50 μm; (B) details of a laminar secondary layer of a Productida (*Spinomarginifera helica*, IR875-12) in which it is evident the cross section of structural units (blades or laths) that form laminae, scale bar 2.5 μm; (C) detail of a prismatic tertiary layer of a Productida (*Tyloplecta persica*, 314-bis5) showing two distinct prisms with no defined accretionary bands, scale bar 25 μm; (D) shell succession of an Athyridida (*Transcaucasathyris* sp., JU10-4) composed by an outer fibrous layer (f) and an inner prismatic one (p), scale bar 100 μm; (E) fibers in cross section of a Spiriferida, scale bar 10 μm; (F) details of the prismatic layer of an Athyridida (*Comelicania* sp., VB9B-2) showing a neat growth banding, scale bar 20 μm.

3.2 Results of the geochemical investigation on the brachiopods shells

The shells of brachiopods from the Lopingian Nesen Formation and Gyanyima Formation (see paragraph 1.1 and 1.2; appendix B of Garbelli *et al.* 2012; appendix 1 in Garbelli *et al.* 2014a) were analyzed both for trace elements and stable isotopes. In addition, I made a survey on the literature, selecting the material for which taxonomy coupled with geochemical analyses were available. Here below, I summarize the results obtained from shells considered pristine based on microstructural analysis (SEM), cathodoluminecence and geochemical analysis. These results show that brachiopods have a characteristical geochemical composition which could be primarily related to their taxonomy.

3.2.1 Trace elements

The first analyzed dataset comprisethe brachiopods from the Nesen Fm., North Iran. It has returned the first evidence of differentiation between the shell geochemical composition in the two main classes of Permian brachiopods. The shells of the Rhynchonellata have lower Mg and Sr than those of the Strophomenata (Fig. 3.2A). Apparently, the Mg and Sr concentrations seem to covary with shell fabric, with Rhynchonellata having lower Sr contents (from 256 to 423 ppm) and Mg contents (from 834 to 1347 ppm), whereas Strophomenata showing higher Sr (from 547 to 811 ppm) and Mg (from 2382 to 4619 ppm, with 8099 considered a questionable outlier; see appendix 1 in Garbelli *et al.* 2012). In these specimens, Fe contents follow the observed trends in Mn variation between the two classes, an indication of their prowess as diagenetic indicators (cf. Brand and Veizer, 1980). A similar result is obtained from the geochemical analysis of brachiopod shells coming from the Gyanyima Fm. (Tibet, Appendix 3 in Garbelli *et al.*, submitted). The shells deemed to be pristine show differences in Sr content between the two classes; however the difference in Mg composition is less marked in this dataset. In fact, the cross-plot (Fig. 3.2B) shows a region of superimposition for the Mg and Sr concentration. It is noteworthy that a species of *Richthofenia* (Strophomenata), which has a lami-

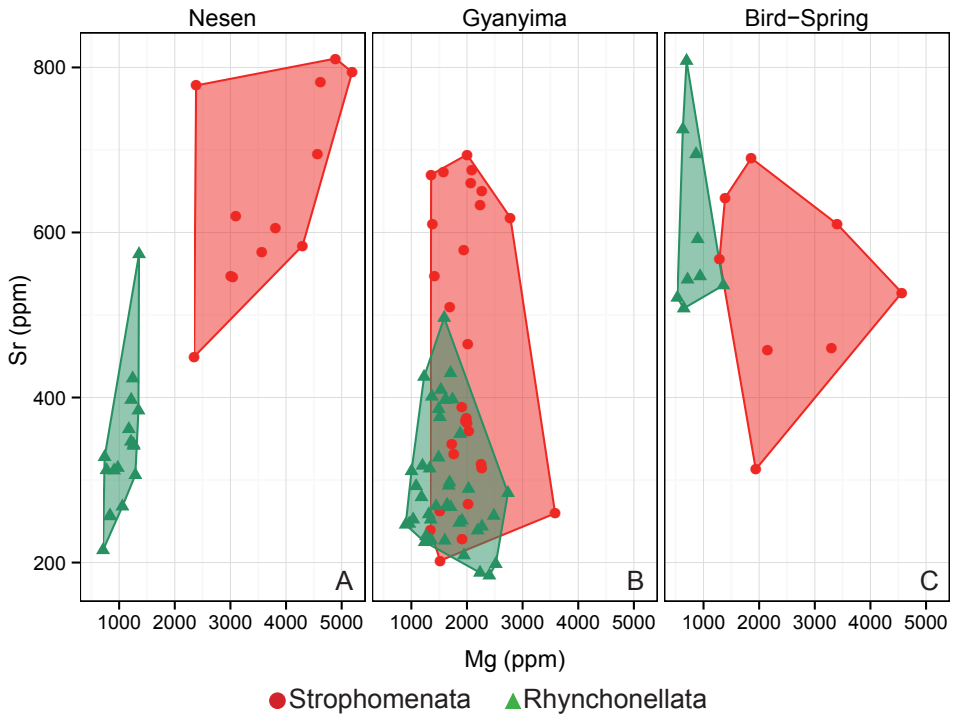

Figure 3.2. (A) Cross-plot of magnesium and strontium content in different groups of Paleozoic brachiopod. A, Permian of Iran (Lopingian, Garbelli *et al.* 2012, 2014a); (B) Permian of Tibet (Changhsingian, Garbelli *et al.* submitted); (C) Carboniferous of Nevada (Serpukhovian-Bashkirian, Brand *et al.* 2003).

nar fabric, seems to have lower Sr if compared with coeval co-occuring species of *Permorphricodothyris* (Rhynchonellata), making more complex the interpretation of the chemiostructural differences between the two classes. However, Mn and Fe in *Richthofenia* show a slight enrichment if compared with preserved samples from the same stratigraphic horizon. This could be due to the high porosity of the shell wall in *Richthofenia*, which is characterized by a huge density of pseodopuncta crossing the shell wall.

The analysis of the available literature shows the same results. Popp *et al.* (1986) presented some Strophomenata and Rhynchonellata from the Visean of Great Britain. They documented lower Sr and Mg contents in the typical

	Strophomenata			Rhynchonellata			
	N	Mean	SD	N	Mean	SD	Δ
Mg							
Nesen	12	3736	281	17	1071	55	2665
Gyanyima	28	1952	88	43	1619	68	333
Bird-Spring	8	2487	407	9	807	82	1680
Other Paleozoic	22	4383	1695	19	941	280	3442
Sr							
Nesen	12	649	35	17	338	20	311
Gyanyima	28	451	32	43	295	12	155
Bird-Spring	8	534	43	9	608	36	75

Table 3.1. Mean Trace Elements composition (Mg and Sr) of Paleozoic brachiopod classes from different localities. Nesen Fm., Permian of Iran (Lopingian, Garbelli *et al.* 2014a); Gyanyima Fm., Permian of Tibet (Changhsingian, unpublished data); Bird Spring Fm., Carboniferous of Nevada (Serpukhovian-Bashkirian, Brand *et al.* 2003) Other Paleozoic , Carboniferous of Great Britain (Visean, Popp *et al.* 1986)

fibrous fabric of pristine Spiriferida, with respect to Productida with a cross-bladed laminar fabric. The Mg contents are distinctly different between the two classes of brachiopods from Great Britain, similarly to what observed in the two groups from the Permian of North Iran and Tibet (Table 3.1). Brand *et al.* (2007) studied the brachiopod composition of mid Carboniferous brachiopods from Bird Spring Fm (Arrow Canyon, Nevada). Even in this case there is an evident difference in the Mg-Sr composition between the two classes (Fig. 3.2C), but with a different pattern. The enrichment seems to involve only magnesium with only a slight differentiation in strontium content (Table 3.1).

3.2.2 Stable isotopes

Rhynchonellata shells from the Nesen Fm. of North Iran have $\delta^{18}O$ and $\delta^{13}C$ values in the range from −3.16‰ to −4.80‰ and from +3.61‰ to +4.52‰ (VPDB), respectively. Pristine Strophomenata secondary and tertiary layers have similar isotopic values. Their $\delta^{18}O$ values range from −3.31 to −5.48‰ (VPDB). A moreinteresting observation is that the $\delta^{18}O$ values of the two classes of brachiopods show a considerable overlap. In contrast to the similarity of their $\delta^{18}O$ values, $\delta^{13}C$ values of the two classes of brachiopods are significantly different at the 95% of the confidence interval (Table 3.2, Fig. 3.3A).

This difference between the Strophomenata and Rhynchonellata amounts

to 1.95‰ for the brachiopods of the Lopingian Nesen Formation of North Iran. A similar result was obtained from the brachiopods of the Gyanyima Fm. (Garbelli *et al*. submitted). Pristine secondary and tertiary layers of Strophomenata have $\delta^{18}O$ values ranging from –5.68 to –2.55‰ (VPDB) and $\delta^{13}C$ from +1.85 to +4.96 ‰. Shells of Rhynchonellata have $\delta^{18}O$ and $\delta^{13}C$ values in the range of –6.30‰ to –2.19 and from +2.56‰ to +6.30‰ (VPDB). Once again, $\delta^{13}C$ values are rather different, with the Strophomenata being lighter in $\delta^{13}C$ on average of 3.88‰ , in spite of the similar range of $\delta^{18}O$ values (Fig. 3.3B, Table 3.2).

The trend in $\Delta^{13}C$ continues with a difference of 1.46‰ when we examine

	Strophomenata			Rhynchonellata			
	N	Mean	SD	N	Mean	SD	Δ
$\delta^{13}C$							
Carboniferous, Visean (Great Britain)	14	2	0,17	6	3,68	0,08	-1,68
Carboniferous, Serpukhovian-Bashkirian (Nevada)	6	2,08	0,2	8	2,99	0,07	-0,91
Carboniferous, Serpukhovian, (Russia)	31	2,3	0,23	68	5,07	0,17	-2,77
Permian, Lopingian (Iran)	9	2,07	0,25	13	4,13	0,07	-2,06
Permian, Asselian (Russia)	3	3,82	0,02	19	5,28	0,13	-1,46
Permian, LopingianTibet	32	0,63	0,11	45	4,52	0,1	-3,88
ALL	95	1,71	0,12	159	4,71	0,092	-2,99
$\delta^{18}O$							
Carboniferous, Visean (Great Britain)	14	-3,24	0,11	6	-1,96	0,04	-1,29
Carboniferous, Serpukhovian-Bashkirian (Nevada)	6	3,23	0,48	8	0,67	0,19	2,56
Carboniferous, Serpukhovian, (Russia)	31	-2,92	0,13	68	-3,05	0,09	0,12
Permian, Lopingian (Iran)	9	-4,35	0,23	13	-3,95	0,16	-0,4
Permian, Asselian (Russia)	3	-1,38	0,02	19	-1,93	0,05	0,55
Permian, LopingianTibet	32	-4,21	0,2	45	-3,61	0,21	-0,6
ALL	95	-3,1	0,2	159	-2,92	0,11	-0,18

Table 3.2. Differences in mean isotopic composition of stable isotopes between the Strophomenata and the Rhynchonellata from different geological times and localities. Permian of Iran (Lopingian, Garbelli *et al.* 2014a), Permian of Tibet (Changhsingian, unpublished data), Permian of Russia (Asselian, Popp *et al.* 1986), Carbonifeous of Russia (Serpukhovian, Mii *et al.* 2001; undifferentiated Carboniferous, Bruckschen *et al.* 1999), Carboniferous of Nevada (Serpukhovian-Bashkirian, Brand *et al.* 2007), Carboniferous of Great Britain (Visean, Popp *et al.* 1986)

the two classes from the Permian of Russia (Grossman *et al.* 2008, Table 3.2, Fig. 3.3C). A similar pattern is evident even in Carboniferous brachiopods. The Strophomenata from the Visean (Popp *et al.* 1986) have lower $\delta^{13}C$ values than those of associated Rhynchonellata (Fig. 3.3E); as a matter of fact the differences are statistically significant (Table 3.1). The $\Delta^{13}C$ of 1.75‰ in the Visean pair is similar to 1.95‰ recorded in the Strophomenata/Rhynchonellata pair from the Permian of Iran (Table 3.1; Fig. 3.3).

Considering the data from the Carboniferous of Russia (Mii *et al.* 2001, Bruckschen *et al.* 1999), the mean difference in $\Delta^{13}C$ is 2.77‰, even if there is

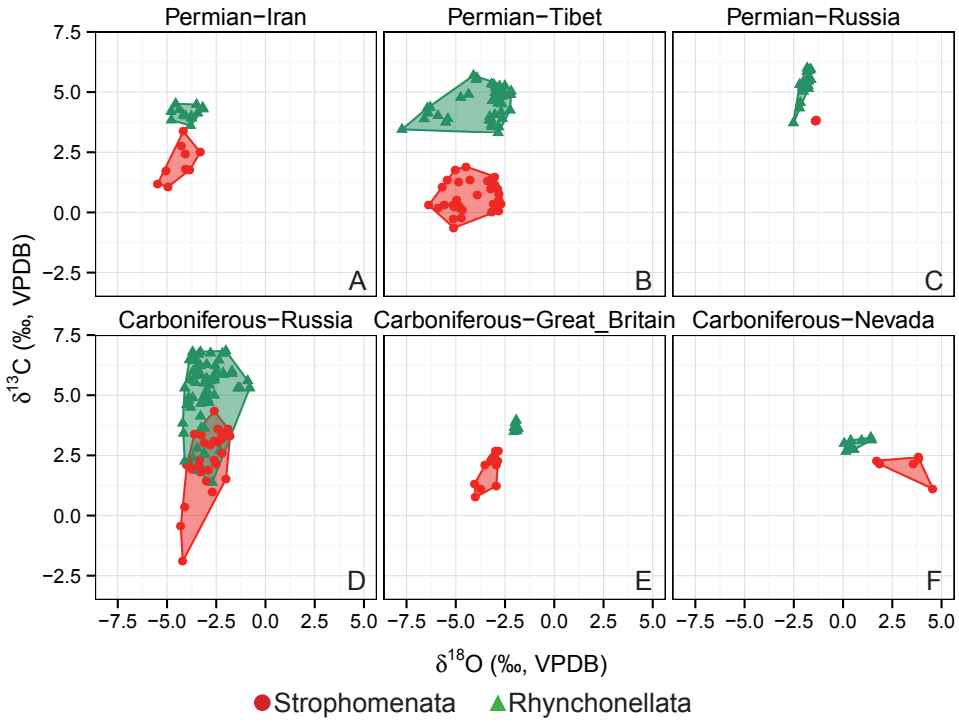

Figure 3.3. Cross plot of oxygen and carbon stable isotopes for different geological time intervals and localities. (A) Permian of Iran (Lopingian, Garbelli *et al.* 2014a); (B) Permian of Tibet (Changhsingian, unpublished data); (C) Permian of Russia (Asselian, Grossman *et al.* 2008); (D) Carboniferous of Russia (Serpukhovian, Mii *et al.* 2001; Tournaisian–Moscovian, Bruckschen *et al.* 1999); (E) Carboniferous of United Kingdom (Visean, Popp *et al.* 1986); (F) Carboniferous of Nevada (Serpukhovian-Bashkirian, Brand *et al.* 2003)

an overlap between the values. This is partially due to the different time interval considered (from Tournaisian to Moscovian). The $\Delta^{18}O$ mean difference between the two classes is only 0.12‰. In the Serpukhovian-Bashkirian transition of Nevada the values for stable isotopes are completely separated for both classe (Brand *et al.* 2007). The Strophomentata are lighter in $\delta^{13}C$ with a mean difference of 0.91‰, but they are enriched of $\delta^{18}O$ in mean of 2.56 ‰ (Fig. 3.3F, Table 3.2). Overall, the difference in $\Delta^{13}C$ values between Strophomenata and Rhynchonellata amounts to 2.99‰ (Table 3.2), which may be significant when evaluating the $\delta^{13}C$ of fossil brachiopods. The impact on $\delta^{18}O$ is less consistent, with an overall difference of 0.18‰.

3.3 Discussion

3.3.1 The relationships between fabric differences and the geochemical composition

Calcitic shells of Strophomenata and Rhynchonellata show a certain amount of differences in the geochemical composition. Since the inclusion of elements in the calcite lattice is primarily driven by the biomineralization process, it is possible to speculate that the differences in the geochemical composition is produced by underlying different mechanisms of shell secretion. Actually the two classes show a very different type of organization of secondary layers, which is a clear indication of different biomineralization mechanisms: a collective one in the Strophomenata and single-cell secretion in Rhynchonellata. This fact has several consequences on the biological ability in building the shell wall. Let me produce some illustrative cases based on personal observations and literature.

The first example concerns that, when brachiopods reach a large size, they have to thicken the shell for structural and functional reasons. Even if this is apparently trivial, they could get the shell thicker in different manners. In the investigated Rhynchonellata, the thickening is mainly reached through a shell sequence which includes the production of the tertiary prismatic layer; intercalation of fibrous and prismatic layers may also occur, (Fig. 3.4A, B, C). However, more rarely, Rhynchonellata may reach shell thickening through a very thick

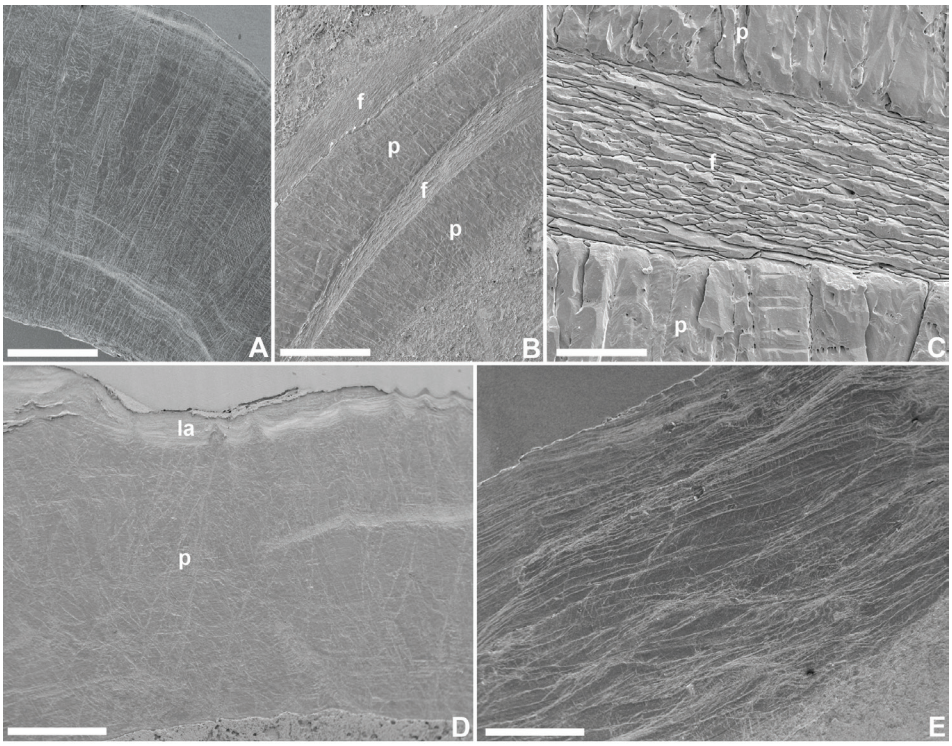

Figure 3.4. (A) Shell of an Athyridida (*Comelicania* sp., PK56-1) that is mostly composed of a prismatic layer, scale bar 500 µm; (B) shell of a Spiriferida (*Permophricodothyris iranica*, IR367-2) composed of alternated fibrous (f) and prismatic (p) layers, scale bar 500 µm; (C) details of (B) illustrating the alternation between secondary (f) and tertiary (p) layers, 60 µm; (D) shell of a Productida (*T. yangtzeensis*, IR310-1) with an outer laminar layer (l) and an inner thick prismatic one (p), scale bar 1 mm; (E) shell of a Productida (*Costiferina indica*, GY79) composed entirely of a laminar fabric, scale bar 1 mm.

secondary layer made of convolute fibers (see for instance the shell of *Pachycyrtella omanensis* in in Angiolini *et al.* 2008)

In the Strophomenata the thickening may be reached by at least two alternative strategies. In fact there are genera with shell wall thickened by a tertiary prismatic layer (fig 3.4D), but several taxa have shells more than 2 mm-thick entirely composed by a secondary laminar fabric (fig. 3.4E). A second example is the deep difference in the secretion pattern of spines as well as illustrated

by Pérez-Huerta (2011) and Alvarez and Brunton (2001). The last two authors show that taxa of Productida grew spines through a radically different process from representatives of the Rhynchonellata. As they stated (p. 108-109):

> *"The former grew from a separate bud of generative epithelium at valve margin which grew rapidly away from the valve surface, producing a complete tube of shell; the latter grew from a portion of marginal generative epithelium which grew forward more rapidly so as to become separate from the rest of the margin as an extended lamellose outgrowth which became rolled and fused on it commissural side to form a sutured hollow spine."*

A third important difference is inherent to the type of structures crossing the shell wall. Rhynchonellata may be impunctated or punctated. In the Rhynchonellata groups with shell perforation, the punctae have different structure but show basically the same order of magnitude, type of organization and, probably, the same function. The pattern of punctae distribution in the shell wall is homogeneous in the same species and probably does not show great variability between taxa (Fig. 3.5A, B). A likely hypothesis for the formation and growth of punctae has been proposed by Pérez-Huerta *et al.* (2009, p. 65-66):

> *"For brachiopods, a bilayered sheath of generative cells, resulting from an evagination of the outer ephithelium, would create the space for the caecum. The same cells would simultaneously contribute to the formation of caecum and the mineralisation of calcite in the primary layer and fibres of the secondary layer laterally, from the margins of the punctae. This mechanism would satisfy the observation of the caecum forming as an evagination of the outer ephithelium (Williams, 1968) and the location of peripherial cells inside the punctae (Figs. 5 and 6). These peripherial cells would be the residuals of the original sheath of generative cells. They purposed that a bilayered sheath of generative cells, resulting from an evagination of the outer mantle ephithelium, would create the space for the caecum. The same cells would simultane-*

ously contribute to the formation of caecum and the mineralisation of calcite in the primary layer and fibres of the secondary layer laterally, from the margins of the punctae".

They point out that there are significant differences in shell formation mechanisms in punctate brachiopods compared to taxa which lack punctae.

In the Strophomenata the situation is completely different. The structures crossing the shell are called pseudopunctae, which are not perforations, but they are slightly arcuate, anteriorly inclined trail of cone in cone inwardly deflection of the laminae. The pseudpunctae may be a simple inwardly inflection of laminae or may posses an inner core of calcite called taleola (Figs 3.6A, B and C). They vary greatly in diameter and length in the same shell (fig. 3.6D) and they can be differently spaced depending on the shell position and taxon. The function of pseudopunctae is still unclear, but the main idea is that they provided holdfast for mantle filaments (Williams 1956). Excluding early stocks, all the Strophomenata bear pseudopunctae, which shows a very different level of complexity. For example, the accelerated apical growth of pseudopunctae can produce tubercles or spines in the interior valve (Fig. 3.6E), which is well developed especially in Productida (Williams 1997). In certain Richthofenioids the endospines of the ventral valve branched and amalgamated to form

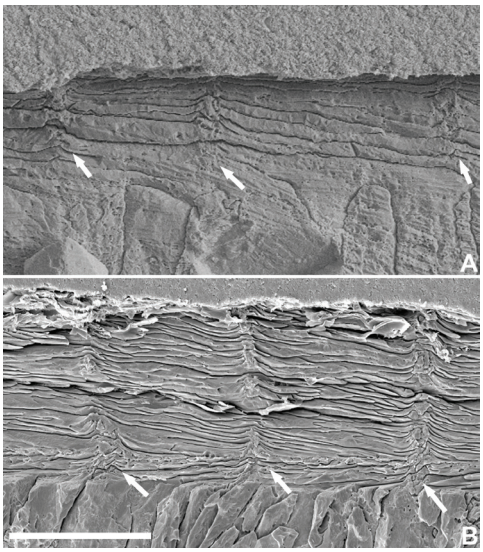

Figure 3.5. Comparison of thesize and distribution of punctae (arrows) in two different taxa of Rhynchonellata. (A) *Notothyris* sp. (GY47) and (B) *Enteletes lateroplicatus* (IR332-1) respectively, scale bar 100 μm. Despite the two specimens belong to different orders, the Terebratulida and the Orthida respectively, the secondary layers in longitudinal section show that the punctae have a very similar size andalso a very similar spacing.

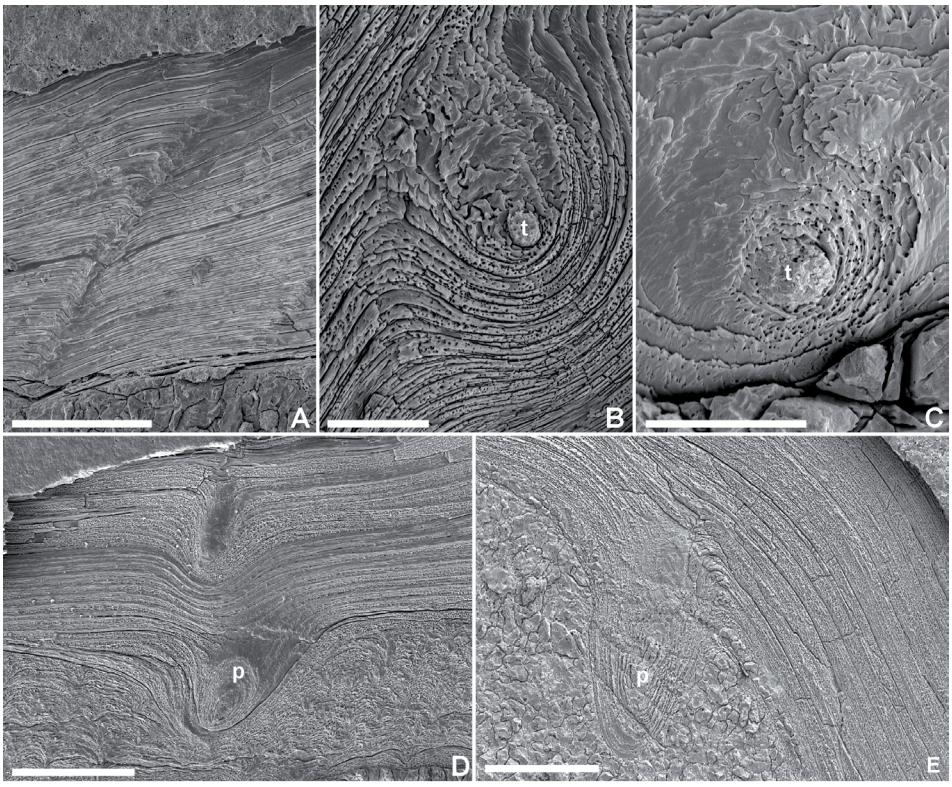

Figure 3.6. (A) Pseudopuncta formed by inwarly deflected laminae in an Orthothetida (*Alathorthotetina* sp., EBHZ 70-8); (B, C) pseudopunctae in the Produtida *Spinomarginifera* sp., formed by cone in cone inwardly deflection of the laminae with an inner core of calcite, the taleola (t), in cross section (specimen JU115-1) and in planar view (specimen JU117-1) respectively; (D) shell wall of a Productida (*Spinomarginifera ciliata*, IR354-11) crossed by a large pseudopuncta (p) in the outer layer and by many small pseudopunctae (arrows) in the inner part of the shell; (E) pseudopuncta producing an endospine in the valve interior (*Tyloplecta yangtzeensis*, IR871-7)

a net, the so called coscinidium, which was covered by the mantle ephitelium, being more exposed to the environment. We can affirm that the biological function of pseudpunctation and punctation of Rhycnhonellata is so different that would not make sense to make a comparison.

Although these three examples are oversimplified, they clarify how deeply different is the shell secretion mechanism in these two classes, without taking in account the basic differences in the ultrastructural units. The rising idea is

that the geochemical differences between the two classes are related to the different secretory mechanism (collective vs. discrete). The real question is which is the mechanism that could link shell secretion and chemical compositions of the brachiopods Low Magnesium Calcite (bLMC).

Modern calcifying organisms usually produce calcite by secreting amorphous calcium carbonate (ACC), which is a precursor of the crystallized phase, because the ACC is anisotropic and can be more easily manipulated by organisms to form a specific shape (Addadi *et al.* 2003). The transient phase of ACC is manipulated by organisms through the addition of mismatched cations and organic material, because they promote the initial stabilization of this highly disorganized phase. It is known that modern brachiopods are able to secrete ACC in order to repair their shell (Griesshaber *et al.* 2009). The basic idea is that the different amount in Mg^{2+} and Sr^{2+} replacing Ca^{2+} in the calcite lattice is linked to the different plasticity of the two fabric types, with the laminar one naturally enriched in mismatched cations. What makes the idea stronger is that $\delta^{13}C$ tells the same story (see paragraph 3.2.2). Even if it is plausible that Strophomenata probably had an higher in vivo organic matter content, it is not clear if this higher organic cntent could have caused the carbon shift. One idea is that there is more intracrystalline organic matter trapped in the shell which is enriched in ^{12}C being a methabolic product

The tertiary layer in the two classes appears superficially quite similar. In greater detail however the prismatic layer of the Rhynchonellata is more neatly organized into distinct prisms which are invariably crossed by micrometrics growth steps. Strophomenata on the other hand tend to have a rougher level of organization into macroscopic growth bands separated by growth lines (fig. 1 in Garbelli *et al.* 2014a, fig. 4 in Angiolini *et al.* 2010)

This hypothesis is very attractive as I found differences into the carbon composition not only in the secondary layers, but also in the tertiary layers of some Strophomenata and Rhynchonellata (Table 3.3), which have a morphological identical prismatic fabric. Nevertheless, prismatic layers of Productida (such

	$\delta^{13}C$		
	Mean	SD	N
Strophomenata	1.74	0.37	7
Rhychonellata	3.88	0.04	6

Table 3.3. Mean values of the $\delta^{13}C$ composition of the tertiary prismatic layer in coeval Strophomenata and Rhycnhonellata from Nesen Fm. (North Iran).

as *Tyloplecta, Araxilevis, Spinomarginifera*) is different from the prismatic layers of Spiriferida or other Rhynchonellata for theri organization at SEM (Fig. 3.1). Prisms of the Rhynchonellata show basically well organazed bands of growing, intead Strophomenta are less organized (Fig. 3.1C, F). In addition prism interruption of growth in the Rhynchonellata are clearly marked by a return in the secretion of a likely secondary fibrous layer (Fig. 3.4 B). In the Strohomenata, there is not always a production of secondary devloperd layer (see fig. 4 in Angiolini *et al.*, 2010). England *et al.* (2007) reported a similar variation in Mg contents in extant representatives of two different subphyla, Craniiformea e a Rhynchonelliformea . They showed that *Novocrania anomala* (Craniiformea), which has a secondary fabric rich in organic matter, is more enriched in Mg than the co-occurring *Terebratulina retusa* (Rhynchonelliformea). The two taxa are characterized by very distinct shell fabrics, so different that *N. anomala* and *T. restusa* do not bear a common structure even at nanometric levels: this could be interpreted as the result of different biomineralization mechanisms (Pérez-Huerta *et al.* 2013). The latest evidence based on a large database of modern brachiopods (Brand *et al.* 2013) shows the same variability in trace element contents between groups with different fabric. Previous researches of England *et al.* (2007) showed that the two groups have a different sulfur content, which is higher in the more organic-rich fabric of Craniiformea. All these evidences show that the chemical composition of calcite is strongly related to the fabric of the shell (i.e. the ratio of organic matter/biomineral and their relative organization). However, other processes may have had a role .

For example, a different amount of mismatched cations or a different $\delta^{13}C$ value in the calcite lattice could be the result of different shell growth rate

(Brand *et al.* 2013, Yamamoto *et al.* 2013); the signature of $\delta^{13}C$ could even be associated to different sources or to metabolic prioritization (Cusak *et al.* 2012). What is clear is that, in the same subphylum, different structures of the shell bring different chemical signals.

Notwithstanding there is not a clear mechanism linking shell structure and geochemical signal and how this evolved, the evidence of differences among higher taxonomic ranks has important implications and consequences in the application of bLMC as a paleoproxy.

3.3.2 Implications and consequences of the taxonomic control on the chemical composition of brachiopod shells

Since brachiopods are low buffering organism which grow their shell in chemical equilibrium with the environment in which they thrive, they are one of the most important archives to reconstruct the chemio-physical structure of Paleozoic seawater. To use them as a paleoproxy, it is necessary that they are deemed pristine based on screening tests (see paragraph 2.1). Some investigators used static and modern brachiopod-based limits of trace elements values to discriminate between preserved and altered material (e.g. Korte *et al.* 2005). This could be considered relevant for those elements not usually present in the seawater such as Mn, which is more abundant in diagenetic fluids of meteoric origin. On the contrary, static limits have the deficiency not to take into account the natural variation in the environment and in geological time of elements such as Mg and Sr which are abundant in seawater. For this reason, some authors preferred to use dynamic limits (e.g. Bates and Brand 1991, Brand 2004). The finding of different trace elements inclusion in fabric reinforces this position: different limits have to be taken in account for different taxonomic groups in the same environmental condition, due to the taxonomic control on shell geochemistry. For example, at Gyanyima, a certain content of a trace element (for instance Sr) could be compatible either with a preserved shell in one group or with an altered shell in another one (see Fig. 3.7). This happens because different taxa have different original background values of elemental composition

In this case, other screening tests are necessary to discriminate altered material and the pattern of geochemical data is simply explained by original differences in the chemical composition of shells. Then, since different fabrics incorporate different amount of mismatched cations, the use of strict cut-offs is not recommended.

Another important implication is that the reconstruction of Paleozoic seawater curves based on brachiopods calcite must consider the influence of differences in the $\delta^{13}C$ values between classes of brachiopods (see fig. 3.7). Indeed a $\delta^{13}C$ shift of about 2-3‰ could be simply due to the fact that the analyzed

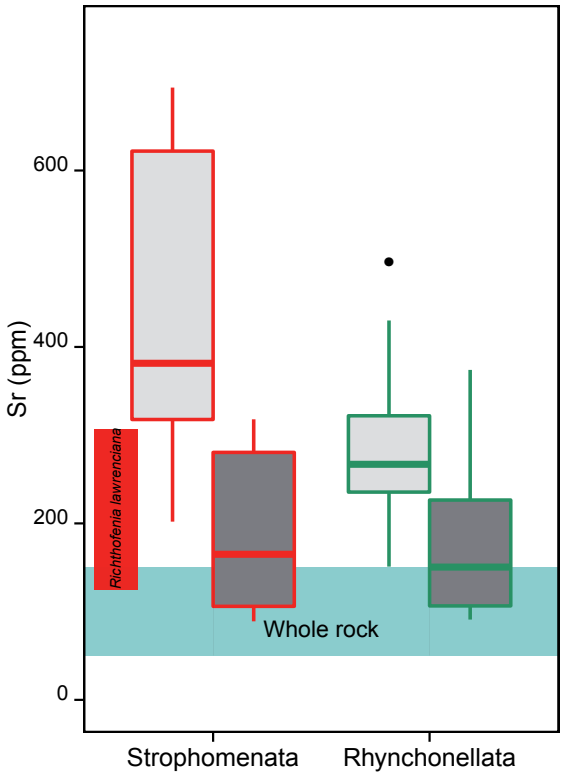

Fig. 3.7. Box plots of Sr content vs. shell fabric showing that distinct brachiopod classes have different Sr content. This enables us to use dynamic limits to evaluate preservation and alteration; in fact preserved material of Rhynchonellata have values overlapping with those of altered Strophomenata. *Richthofenia lawrenciana* has anomalously low values for Sr, different from typical laminar fabric ones. Light gray represents preserved shell fabric, dark gray altered ones.

material belongs to different brachiopod classes. This is particularly true when the systematic position of the analyzed brachiopod shells is not stated (e.g. Schobben *et al.* 2014). An example of a possible misinterpretation is provided in the paper by Grossman *et al.* (2008), where they assume that a negative shift of $\delta^{13}C$ found in brachiopods from the Urals during the Serpukhovian may be related to diagenetic exposure. Nevertheless, most of the brachiopod analyzed for this interval possess a laminar fabric and are naturally impoverished in $\delta^{13}C$.

Last but not least, the differences between taxa and their fabric composition pose the question about the effect of evolution of biomineralization mechanisms and its consequences on the geochemical composition. Coeval brachiopods could be divided by a long evolutive time that, despite the same molecular mechanism of biomineralization, could have evolved different secretory regimes that responded differently to environmental changes, modifying the geochemical composition. In the past, other authors posed the question about the taxonomic variability in isotopic composition (e.g. Carpenter and Lohmann 1995) effect on brachiopod geochemical composition but nobody has considered shell fabric as a possible cause. Indeed, the study of the shell fabric could be a key to understand differences observed in cooccuring brachiopods. This topic will require more investigation in the future.

Chapter 4
The stratigraphy of Upper Permian brachiopods from a biomineralization perspective

During the Permian, brachiopods probably reached the greatest diversity ever, with a peak during the Roadian (Middle Permian). The Productida represented about the 50% of the generic abundance (Curry and Brunton 2007). During the Late Permian, the brachiopod generic abundance slightly declined and, at the end of this period, the most important event of the brachiopod history occurred with the end Permian mass extinction event (Afanasjeva 2010). Over 90% of the genera present in the Changhsingian disappeared at the end of this stage. This was also the largest crisis in absolute numerical terms regarding the genera that went extinct: 199 genera according to Curry and Brunton (2007). In this chapter,I try to analyze the demise pattern of Rhynchonelliformea brachiopods throughout the Late Permian, taking into account the type of shell fabric and the biomineralization processes. Since some authors question if the high generic diversity numbers are biologically realistic or are the result of intense research work by numerous specialists studying this key interval (i.e. Curry and Brunton 2007), I used different type of data to describe the demise patter (see Materials and Methods paragraphs 2.1.4 and 2.2) and I analyzed data using both high rank taxa such as family, order and class, and low rank such as genus and species.

4.1 Results of the stratigraphic investigation on Upper Permian brachiopods

4.1.1 The occurence pattern of brachiopods during the Late Permian and the Early Triassic

Statistical results. A general linear model for a binomial response to a categorical variable was applied to the data OccPD (Appendix B, see paragraph 2.1.4 and 2.1for the details on method and description of the dataset) to test if there is a significant difference in the number of occurrences of the two main brachiopod classes between the Wuchiapingian and the Changhsingian stages. The results highlight that there is a significant difference in the proportion of the occurrences of brachiopods of the two classes between the two stages (Table 4.1).

	Df	Deviance Resid.	Df	Resid. Dev.	Pr(>Chi)
NULL			1	101.33	
stage	1	101.33	0	0	<0.0001***

Table 4.1. Summary results of the anova test for the logistic regression between number of occurrences per class (Strophomenata vs. Rhynchonellata, binomial dependent variable) and the chronostratigraphic unit (Wuchiapingian/Changhsingian stage, categorical predictor). The chi square test reveals a significative difference in the number of occurrences of the two classes between stages.

Descriptive results. The data downloaded from the Paleobiology database on date 17/10/2014 (OccPD data in Appendix B) return interesting numerical information in term of generic occurrences and high rank taxon composition of brachiopods during the Late Permian. In this time interval, Strophomenata and Rhynchonellata are represented by 8 different orders, some of which survive to the end Permian mass extinction. The two orders of the Strophomenata, the Productida and the Orthotetida, became extinct at the end of the Lopingian, with a total loss of 26 family and 212 genera of which 148 disappeared in the Changhsingian. During the Wuchiapingian-Changhsingian transition, the

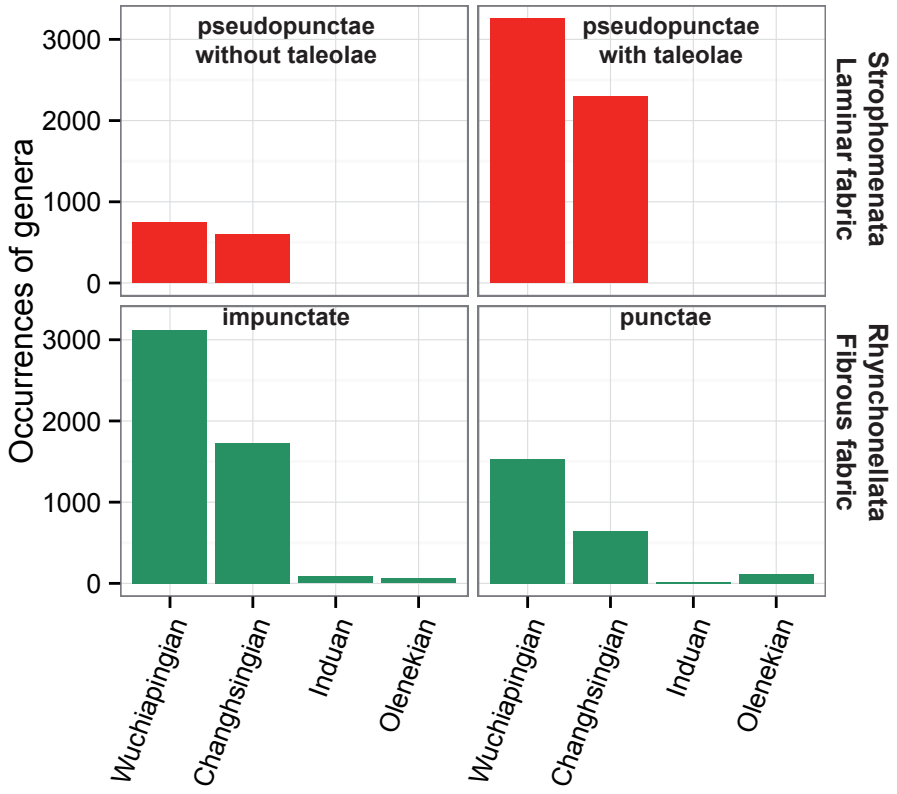

Figure 4.1B. Bar chart summarizing the number of generic occurrences based on the type of secondary fabric and structures crossing the shell in the Late Permian and the Early Triassic obtained from the OccPD (see Appendix B for details).

number of family remains constant, with only the Pulsiidae never found in the Changhsingian and the Cyclacanthariidae not found in the Wuchiapingian.

The Rhynchonellata comprise six different orders: Athyridida, Orthida, Spiriferida, Spiriferinida, Terebratulida and Rhynchonellida, for a total number of 48 families and 181 genera in the Lopingian; 9 families and 45 genera present in the Wuchiapingian have never been found in the Changhsingian; however 5 new families have been found in this last stage. A dramatic decrease in the number of families happened at end of Permian, with the disappearance of 28 families (72% of the total); the decrease is even more striking looking at the amount of genera, as the 90% of the genera had their last occurrence (total

number 126). A total of only 22 families and 36 genera were found in the Upper Triassic. Of these, 9 families and 17 genera are totally new.

The end of the Permian is undoubtedly the most important bottleneck in the history of the phylum Brachiopoda, reducing their taxonomic diversity and pauperizing our potential knowledge of the biology of these organisms. However, taking into account that brachiopod shells could preserve a high degree

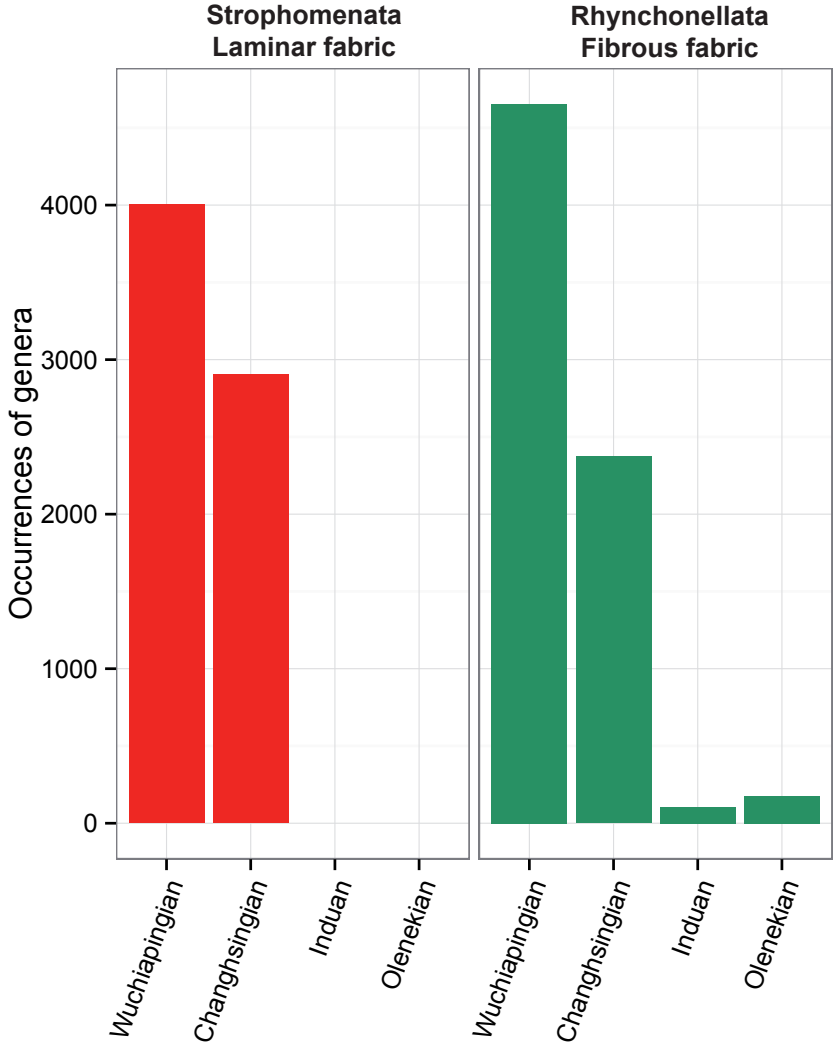

Figure 4.1A. Bar chart summarizing the number of generic occurrences based on the type of secondary fabric through the Late Permian and the Early Triassic obtained from the OccPD (see Appendix B for details).

of morphological details at high resolution (e. g. Williams 1968, MacKinnon 1974, Angiolini 1999), interpreting the patterns of the bottleneck in terms of shell fabric may be useful to better understand the extinction process, its causes, consequences and mechanisms. In fact, a first evidence is that some of the groups with fibrous fabric survived; on the contrary, those with a laminar shell became extinct. This fact, coupled with the deep differences in geochemical composition, gives the suggestion that, for some reasons, the crisis was more selective on some biological properties born by Strophomenata.

To better understand the pattern, I analyzed the number of genera occurrences. Since the occurrence is the "presence" of a fossil in a stratigraphic horizon, its study may be informative in terms of distribution of the taxon during

Stage	Occurrences of new genera	
	Strophomenata Laminar fabric	Rhynchonellata Fibrous fabric
Wuchiapingian	386	387
Changhsingian	203	261

Table 4.3. Number of new occurences for new genera of brachiopod appearing during the Upper Permian. The data are obtained form OccPD (see Appendix B).

Stage	Number of taxa			
	Strophomenata Laminar fabric		Rhynchonellata Fibrous fabric	
	Families	Genera	Families	Genera
Wuchiapingian	25	172	43	147
Changhsingian	25 (1)	152 (43)	39 (5)	140 (38)
Induan	0	0	14 (3)	23 (9)
Olenekian	0	0	16 (5)	22 (16)

Table 4.4. Number of families and genera with laminar or fibrous fabric found in different stages. The number in brackets represents the new taxa in the considered stage.

the different stages of the Upper Permian. The data from OccPD (see Appendix B) tell something very interesting about the biological history of brachiopods: the number of occurrences of brachiopods with fibrous fabric decreases more than that of genera with laminar fabric in the two stages of the Upper Permian (Fig. 4.1A and B). This strongly disagrees with the general idea that Strophomenata (Productida) decline in the Changhsingian (Curry and Brunton 2007): it is only the number of laminar taxa that is reduced, but in term of number of occurrences, they become more widespread than the coeval sister taxon, the Rhynchonellata. On the other hand, the number of occurrences of new genera is higher for taxa with fibrous fabric both in percentage and absolute number (Table 4.2). If we consider that a single occurrence may be interpreted as a defined environment in terms of temporal and spatial location, it is evident that the new genera of Rhynchonellata were able to occupy a more elevated number of environments than the Strophomenata. In addition brachiopods with fibrous fabric evolve a larger number of new lineage, as highlighted by the presence of 5 new families in the Changhsingian (Table 4.3). The new lineages with fibrous fabric represent about the 11% of generic occurrences; the new ones with laminar fabric represent about the 7%. Four of the five new fami-

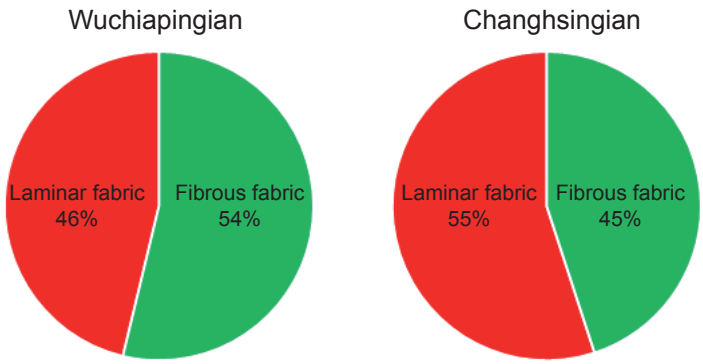

Figure 4.2. Pie charts of genera occurrence in the two stages of Upper Permian respectively. The probability to found genera with fibrous fabric rather than those with laminar fabric is higher in the Changhsingian.

lies belong to orders which possess a punctated fabric (3 to Terebratulida, 1 to Spiriferinida) and the fifth family (Retziidae) also bears punctation despite the fact that it is assigned to an order that is impuctated (Alvarez and Rong Jia 2002). This can be interpreted as a change in the ratio between inorganic and organic content in the brachiopod shell, with the latter increasing in case of endopunctation; as a consequence it appears that, during the Changhsingian, species with and higher organic content in the shell were favored compared to those with a lower organic content. This is in agreement with the fact that the organic-rich Strophomenata (see chapter 3), despite their reduction, suffered, in general, less than the Rhynchonellata. The laminar groups, even if characterized by the appearance of a new family only, the Pulsiidae, which counts only 6 generic occurrences, became more widespread than Rhynchonellata in the Changhsingian (Fig 4.1) and the probability to find one of the two groups occurrences is reversed in the two stages (Fig. 4.2). The shell features could be an interesting tool to interpret adaptation at the end Permian environmental changes, but other factors have to be taken in account. Indeed the two groups have some important ecological differences and the change in distribution may also be related to an environmental change rather than to a some physiological features of the biomineralization.

4.1.2 Detailed analysis of the stratigraphic distribution of Upper Permian brachiopods

To better describe the pattern of brachiopod distribution during the Late Permian based on shell fabric type, I considered the bed-by-bed occurrences of species along several stratigraphic successions. The data were taken in part from material collected during field activity and in part from available literature (see Table 2.1). For every bed/horizon, the stratigraphic distance from the PTB was calculated and information about age, lithology, depositional environment and paleolatitude was given. Here below, a description of the statistical analyses performed on these data is provided.

Statistical results. A general linear model for binomial response variable was

Terms	Df	Deviance Resid.	Df	Resid. Dev	Pr(>Chi)
NULL			30	118,106	
age	1	11,42	29	106,686	<0.0001
environment	3	6,22	26	100,466	0,101
lithology	2	8,069	24	92,397	0,018
paleolatitude	4	69,732	20	22,666	<0.0001
age:environment	3	6,525	17	16,141	0,089
age:lithology	2	0,761	15	15,38	0,684
environment:lithology	4	9,53	11	5,85	0,049
age:paleolatitude	3	2,551	8	3,299	0,466
environment:paleolatitude	1	0	7	3,299	0,100
lithology:paleolatitude	4	1,499	3	1,8	0,827
age:environment:lithology	1	0,789	2	1,012	0,375
age:environment:paleolatitude	0	0	2	1,012	
age:lithology:paleolatitude	2	1,012	0	0	0,603
environment:lithology:paleolatitude	0	0	0	0	
age:environment:lithology:paleolatitude	0	0	0	0	

Table 4.5. Summary results of the anova test for the logistic regression between number of occurrences per classes (Strophomenata/Rhynchonellata, binomial dependent variable) and the categorical predictors (age, environment, lithology and paleolatitude) for the saturated model. The chi-square test reveal a significative differences in the number of occurrences of the two classes between age and paleolatitude

applied to the OccB (Appendix B) data in order to esteem the significance of the factors responsible of the change in high rank taxonomic composition. In this model the response variable is the type of secondary fabric (laminar vs. fibrous) which is indicative of different biomineralization mechanisms. Two separate statistical models have been performed: the first one to test the effects of age, lithology, environment, and paleolatitude and the second one to see if there is a significant correlation between the distance from PTB and a turnover in taxonomic composition. The second model was performed separately on every single stratigraphic section considered, because it is almost impossible to correlate exactly the stratigraphic horizons among different localities. In fact,

the distances in meters from the PTB are not comparable because of differences in sedimentation rates and the biostratigraphic control is not so finely tuned (at a scale of hundred thousands of years) to allow a precise correlation among the selected sections. The statistical analysis of OccB (Table 4.5) shows that, in the saturated model, the main significant effect are related to age and paleolatitude; other factor had an order of magnitude almost not significant compared to that of the main effect and interaction effects are negligible.

The logistic regression between PTB distances and the dependent variable (laminar/fibrous) has resulted significant in some sections: Elikah, Mangol Quarry and Mangol Restaurant (Northern Iran), Main Valley (Nortwestern Iran), Meishan, Gyanyima, Dongpan (South China) (see Table 2.1 for their location and references). Shaiwa (South China) is very close to the significant level of 0.05%. A complete summary of the trends observed in the sections is available in Appendix B (PTBD statistics). Note that the sections Hazro and The Çürük Dag (Turkey) were not analyzed because they contain only species with laminar fabric

Descriptive results. Since the statistical analysis of the correlation between type of secretion mechanism and the distance from PTB shows that there is not an homogeneous and ubiquitous trend, a detailed description is required to better interpret the observed trends.

In the Dolomites, Italy (Figs 4.3, 4.4, 4.5), there is no significant shift from one group to the other up to the boundary, in none of the sections. However, in the upper part of the Sass the Putia, Bulla and Tesero Road sections, it is easier to find occurrences of species of Orthotetida which are characterized by a laminar, fabric such as *Streptorhynchus* sp., *Ombonia* sp. or *Orthothetina* sp. (Posenato 2009, 2011).

In Iran, the very richly fossiliferous beds of the Ali Bashi Mountains, Julfa (Northwestern Iran) and of the Alborz Mountains (Northern Iran) show an interesting pattern of brachiopods associations, if considered from a biomineralization point of view. In the Alborz sections, there are generally more occur-

rences of taxa with laminar fabric than those with a fibrous fabric (Angiolini and Carabelli 2010); in particular in the Elikah sections (fig 4.6), during the Changhsingian, there is a clear change in the dominant fauna, which shifts from Rhynchonellata to Strophomenata. In the lower part there are species belonging to genera *Araxathyris* and *Permophricodothyris*; in the upper part species of *Spinomarginifera* rule. A similar trend is observed in the Changhsingian part of the Mangol sections (Figs 4.8, 4.9). In the Bear Gully and Abredan sections none trend is evident, but the laminar taxa are more abundant (Fig. 4.7, 4.10). However, in all the Alborz sections the brachiopods disappear well before the PTB. On the contrary, in Julfa (Main Valley, Ali Bashi1-3 and Zal sections), the brachiopods are present up to the Boundary Clay, which contains the PTB (Garbelli *et al.* 2014b). In the Main Valley section (Ghaderi *et al.* 2014) (Fig. 4.11), the trend is different if compared to the one recorded in the Alborz Mountains. In the Wuchiapingian Lower Julfa beds, there is a slight dominance of species belonging to genera of Productida and Orthotetida, in particular *Spinomarginifera* and *Orthothetina*. Going through the Upper Julfa beds to the Changhsingian Ali Bashi Formation, the occurrences of Rhynchonellata species become dominant, as underscored by the phyletic line *Araxathyris-Transcaucasathyris*. Remarkable is also the presences of the genera *Acosarina* and *Paracrurithyris,* characterized by a fibrous secondary layer; the latter the last taxon was recovered in the Boundary Clay (Garbelli *et al.* 2014b).

In Kuristyk, Southeastern Pamir, Tajikistan (Angiolini *et al.* in press) the Wuchiapingian part of the section is dominated by taxa of Rhynchonellata (Fig 4.12). Unfortunately, no consistent brachiopod assemblage has been recovered from the Changhsingian part of the succession to further test the pattern.

Upper Permian brachiopods are extremely abundant in South China, as testified by the numerous papers published on their taxonomy (e. g. Shen et Archbold 2002, Chen *et al.* 2009) and this provides a good ground where to test the pattern of brachiopod fabric distribution. At Meishan Section C (Fig. 4.13), the laminar Orthotetida (*Derbya*, *Orthothetina*) and Productida (*Spinomarginifera*,

Neochonetes, *Cathaysia*, *Haydenella*, *Edriosteges*) are the dominant and most diverse groups (Li and Shen 2008). Numerous brachiopods are present in the Wuchiapingian part of the section (Lungtan Formation and Lower part of the Changhsing Formation), but they decline both in number and diversity during the Changhsingian (units 7-8-9-10-11-12-13 of the Changhsing Formation, fig. 2 in Li and Shen 2008). During this decline the Rhynchonellata disappear from this fossil association. The occurrence pattern at Dongpan and Shaiwa sections (Figs. 4.15, 2.16) is partially similar to that observed in Meishan (He *et al.* 2005, 2007, Chen *et al.* 2009).

The Çürük Dag section in Turkey is exclusively characterized by the occurrence of taxa with a laminar fabric both in the Wuchiapingian and in the Changhsingian part of the section: *Spinomarginifera*, *Orthothetina*, *Alatorthotetina* (Angiolini *et al.* 2007).

At Gyanyima (Fig. 4.17), the brachiopods assemblage is extremely differentiated, with 24 different species of brachiopods (Shen *et al.* 2010). The succession is Changhsingian (Wang *et al.* 2010, Garbelli *et al.* submitted), and the evolution of the brachiopods fauna shows a clear turnover, with a shift from a dominance of Rhynchonellata, to the dominance of the Strophomenata. Up to unit 7 (see fig. 2 in Shen *et al.* 2010) Rhynchonellata rule, with species of the genera *Permophricodothyris*, *Neospirifer*, *Martinia*, *Enteletes*. In units 8 and 9 there are many horizons in which *Costiferina* and other productida are the only group present. Noteworthy, in the horizon 9-23, many genera with fibrous fabric were found.

The analyzed sections from peri-Gondwanan regions (Shen *et al.* 2006), show differential patterns of taxonomic turnover. At Selong Xishan section (Fig. 4.18; Shen *et al.* 2000, 2001), Rhynchonellata species dominate in the upper part of the section. Here, brachiopods were recovered also from the mass extinction horizon and they show either fibrous and a laminar fabric: *Spiriferella*, *Bullarina*, *Cleiothyridina*, *Martinia*, *Hustedia*, *Stenoscisma*, and an indetermined species of Ambocoeliidae for the fibrous; *Tethychonetes* for the laminar.

(Shen *et al.* 2006). At Qubu and Tulong no trend is evident, but brachiopods in these sections disappear well before the PTB (Figs 4.19, 4.20). The brachiopod faunas of these two sections share many species with laminar fabric, as *Retimarginifera xizangensis*, *Biplatyconcha grandis* and *Costiferina indica*. Instead, the richly fossiliferous assemblages from Salt Range (Fig. 4.21) show a greater number of Strophomenata with the genera *Derbya*, *Costiferina*, *Marginifera*, *Megasteges*, *Spinomarginifera, Hustedia, Chonetella, Richtofenia, Orthothetina* and *Linoproductus* (Shen *et al.* 2006), with brachiopods having been found also in the extinction interval. In Kashmir the situation is similar, with a dominanceer of species with laminar fabric over the the fibrous ones (Fig. 4.22).

4.2 Discussion on the taxonomic turnover during the Late Permian: a change of biomineralization style?

4.2.1 The pattern of change in brachiopods composition

The statistical analyses of the data of OccPD and OccB highlight an important change in terms of taxonomic composition from the Wuchiapingian to the Changhsingian stage which could have had important implications for the end Permian environmental changes. One interesting feature is that brachiopods of latest Permian age represented by faunas of lower diversity than older ones (Angiolini *et al.* 2007). This observation is confirmed by the drop in the number of genera occurrences, in general agreement with the diminished number of taxa at familiar and generic level (Fig. 2.1, Table 4.4).

However, some important aspects connected with the number of generic occurrences have to be underscored. First of all, despite the general decline in the Changhsingian compared to the Wuchiapingian stages, the two main classes of Rhynchonelliformea behave differently: the Strophomenata loose more genera (n=63) than the Rhynchonellata (n=47). In addition, in front of a similar number of new genera found in the Changhsingian (table 2.1, Strophomenata n=43, Rhynchonellata n=38), the occurrences of Strophomenata exceed those of Rhynchonellata, becaming the most widespread class in this

time interval.

This agrees with what observed in the OccB dataset, where there is a general change that benefits the Strophomenata species occurrences in the Changhsingian horizon of the investigated sections. In fact the OccB could be considered as a subsample of OccPD, but with greater stratigraphic detail.

It is noteworthy that the statistical analysis of regression between PTB distance and the log.odds of the fabric type reveals that in several sections (see PTBD statistics, Appendix B) the association between distance from the extinction horizon and the composition change (Strophomenata vs. Rhynchonellata) is significant. In six of the eight sections in which there is a significant shift from laminar taxa to fibrous taxa, the shift is in favor of Strophomenata up to the PTB (i.e. Elikah, Mangol Restaurant, Meishan C, Gyanyima, Dongpan, Shaiwa sections). In some sections there is not a significant trend, but the taxa with laminar fabric seem to be more widespread, such as in Dolomites, Salt Range, Kashmir, Turkey or Pamir. In the Perigondwanan sections the situation is more difficult to interpret due to the complexity and articulation of the region itself.

Another important evidence is that, in the succession where the brachiopods disappear before the PTB, the faunas are dominated by taxa belonging to Strophomenata. In the few sections where the brachiopods are found in the extinction interval, they mostly belong to Rhynchonellata. For example, in the Main Valley section and in the Ali Bashi 1 section (Figs 1-2 in Appendix A), the most widespread taxon in the *Paratirolites* limestone is the genus *Transacaucasathyris*, coupled with *Acosarina* and rare *Spinomarginifera,* whereas the last survivor in the Boundary Clay is a species of *Paracrurithyris* (Ghaderi *et al.* 2014, Garbelli *et al.* 2014b). However, the brachiopod distribution in Salt Range and Kashmir is different, recording a dominance of taxa with laminar fabric right in the extinction interval.

Summing up, a certain amount of turnover in favor of Strophomenata is evident in the Changhsingian , even if most of these taxa have difficulties to

cross the extinction inverval and reach the PTB; on the other hand, even if Rhynchonellata seem less widespread, some of their genera are able to reach the PTB frequently dominating the extinction interval with species such as Paracrurithyris (He *et al.* 2012).

4.2.2 Possible factors controlling the change

The distribution of brachiopods with laminar fabric vs. those with fibrous fabric seems to suggest that the pattern of faunal change at the end of the Permian is related to the biomineralization processes forming the calcitic shell. This understanding could constrain the type of environmental changes that paved the way to the end Permian mass extinction. However, many complex and iterating factors could have contributed to the change in taxonomic composition of the brachiopod faunas, such as environmental preferences or ecological strategy.

The statistic analysis of OCCB reveals that lithology is a significant factor in controlling faunal composition. Because lithology is indicative of the type of substrate which is one of the factors that strongly control brachiopod distribution (Richardson 1997), the lifestyle of brachiopods itself could explain the significant results obtained. In fact the main representative group of the Strophomenata in this time interval, the Productidina, has a lifestyle which is mainly seminfaunal (Muir-Wood and Cooper 1960, Rudwick 1970, Grant 1971, 1976, Brunton 1972, 1984, 1987); whereas Rhynchonellata are mainly epifaunal, pedunculate or free-living (Rudwick 1970, Grant 1976). The second order of Strophomenata in abundance, the Orthothetida, frequently shows an epifaunal lifestyle, attached by pedicle threads and stabilized by penetration of an elongate umbo (Grant 1976, Angiolini and Carabelli 2010). As a consequence, concavo convex spiny seminfaunal Productida generally occur on soft bottom substrate with low energy, below the normal wave base. Pedunculate Rhynchonellata and Orthotetida species can live more frequently in higher energy environments, where a firm attachment to the substrate is required (Angiolini and Carabelli 2010, Ghaderi *et al.* 2014). Orthothetida, in particular with their

pedicle threads strategy can live both on hard and soft substrates, and are well adapted also to microbialites (Posenato 2009).

However, not always the observed changes in high rank taxonomic composition coincide with an environmental change favoring a certain groups. For example a significant shift in favor of Strophomenata taxa is present in sections which do not record any change in bathymetry or lithology in favour of their presence, such as Gyanyima, Shaiwa Dongpan, Elikah, and Mangol. In the Changhsingian part of these successions, the number of species with laminar fabric invariably increases more than that of species with fibrous fabric, notwithstanding the type of substrate or the sea level change involved. In fact, Gyanyima has been deposited in shallow, turbolent waters, Shaiwa in quiet deep waters, Dongpan records a marine regression, whereas Elikah and Mangol records a shallowing followed by a marine transgression. Consequently, the type of substrate and hydrodynamic conditions cannot explain the faunal turnover observed and the dominance of Chonetida and Productida in these regions.

Latitude is a significant factor controlling the number of high rank taxon occurrences and it explains more deviance than the stratigraphic position; this may be expected because Strophomenata, in particular the Productida, seem to prefer warm tropical water in the Permian as result by the significant difference in taxonomic composition of the paleolatitudes.

The stratigraphic position in term of stage is significant to explain the high rank taxonomic composition. In particular the stratigraphic position, despite it represents only one degree of freedom in the model, explains a certain amount of the variance in the model (see table 4.5). The effect of the stratigraphic position is evident also by the results of the logistic regression between PTB distance and class (fabric) composition: where the regression is significant, usually the taxa with laminar fabric become the rulers. In general, we can affirm that a big change is evident in the Changhsingian, during which it seems that taxa with laminar fabric proliferate in several sections. However, this abundance

is not coupled with an increase in taxonomic diversity, as only a new family of Strophomenata appears in the Changhisingian. On the contrary, even if the total occurrences of taxa with fibrous fabric seem to be reduced, the Rhynchonellata are able to evolve a higher number of families than the Strophomenata: five new families belonging to the former appear in the Changhsingian stage. Moreover, the occurrence of new genera is about 30% higher in the Rhynchonellata than in the Strophomenata. This shows that the Rhynchonellata were able to diversify more than the Strophomenata. On the contrary the latter, mainly represented by Productida, shows very specialized taxa, which, holding over since the Wuchiapingian, increased in abundance during the Changhsingian, before the extinction. In many successions, when Productida are present, they tend to dominate with high number of individuals. This happens more rarely with the Rhynchonellata. However, the Strophomenata, did not pass the crisis, whereas the Rhynchonellata did it.

The reason may be related to the ecological and biological differences among the two groups, which constrained the selective extinction of brachiopod taxa; in fact, it is known that some taxa of Rhynchonellata were capable to tolerate disparate environmental conditions and colonize several settings, such as, for instance deep water environments with low nutrients and possibly low oxygen, lending credit to the hypothesis of Vörös (2005) that brachiopod flourished in the bathyal and abyssal zones during the late Paleozoic golden age of the phylum.

What could have driven this pattern is still unclear. I will discuss a possible mechanism after the next chapter, where I will illustrate some important features of biomineralization in Permian brachiopod taxa.

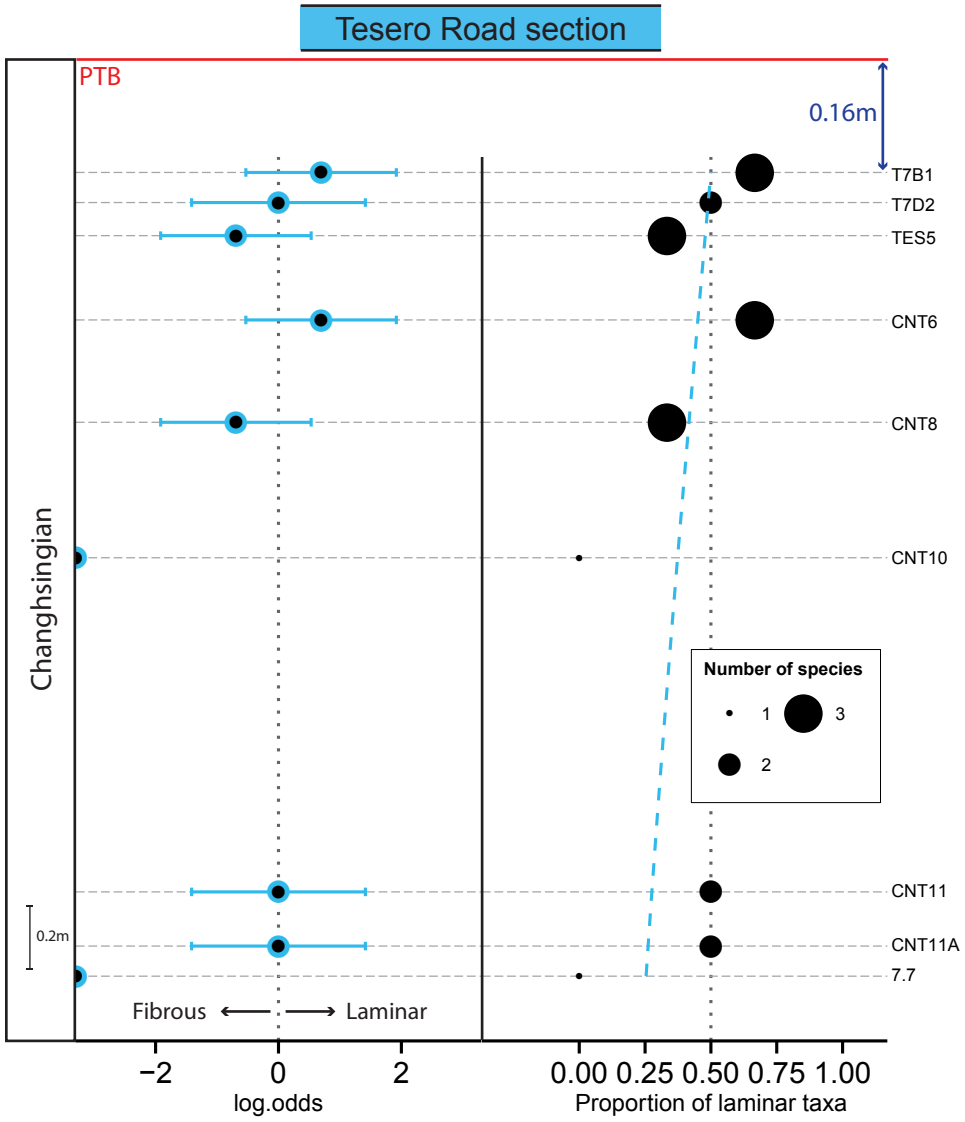
Tesero Road section
PTB
0.16m
T7B1
T7D2
TES5
CNT6
CNT8
CNT10
CNT11
CNT11A
7.7
Changhsingian
0.2m
Fibrous
Laminar
Number of species
1
2
3
−2
0
2
log.odds
0.00 0.25 0.50 0.75 1.00
Proportion of laminar taxa

Figure 4.3

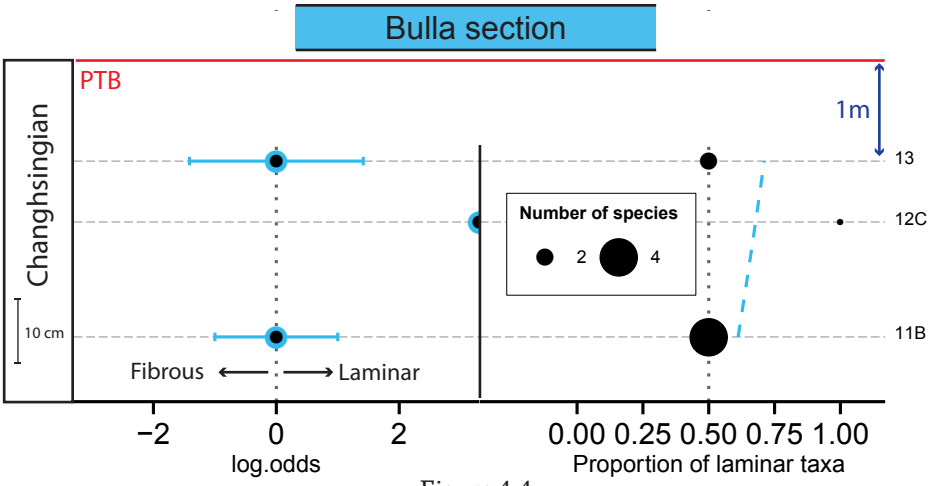

Figure 4.4

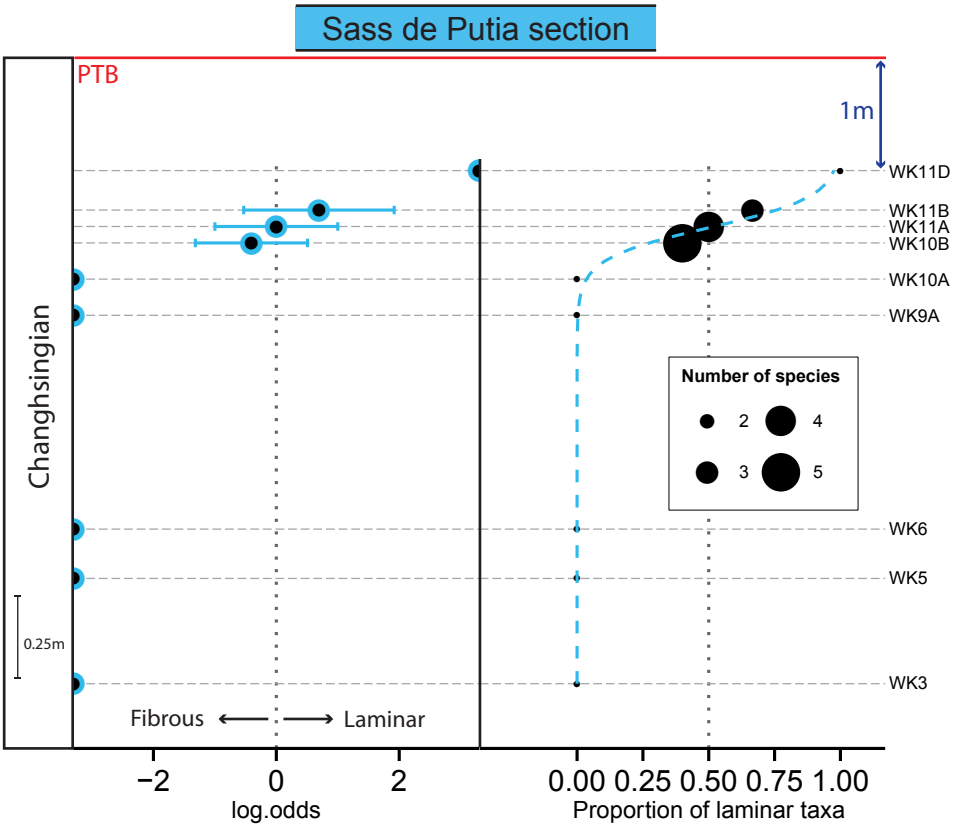

Figure 4.5

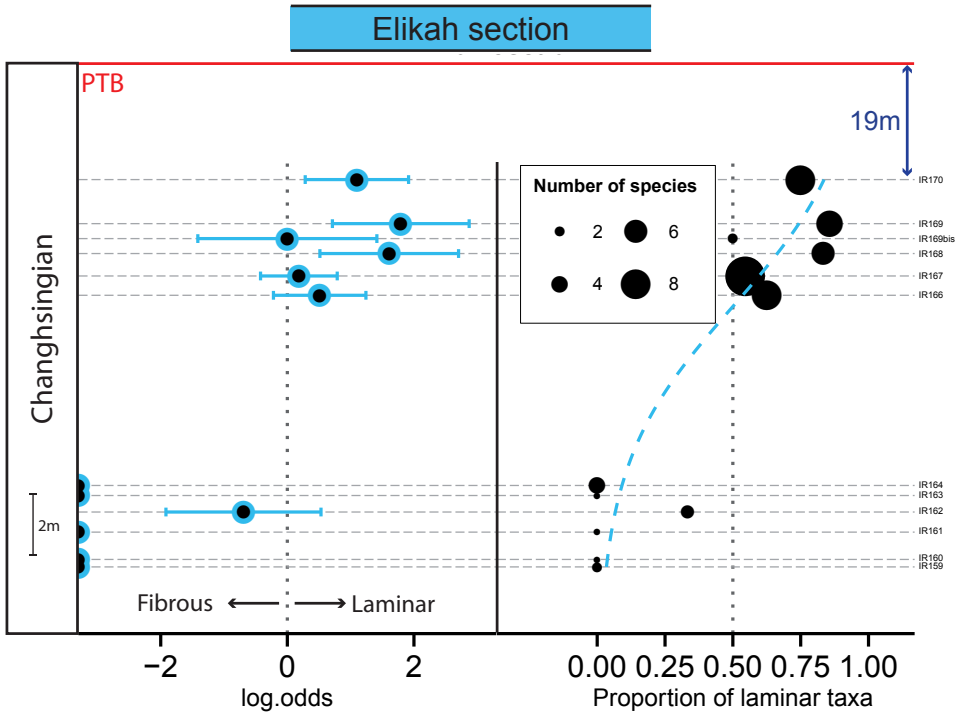
Elikah section
PTB
19m
Changhsingian
2m
Number of species
2
4
6
8
IR170
IR169
IR169bis
IR168
IR167
IR166
IR164
IR163
IR162
IR161
IR160
IR159
Fibrous
Laminar
−2
0
2
log.odds
0.00 0.25 0.50 0.75 1.00
Proportion of laminar taxa

Figure 4.6

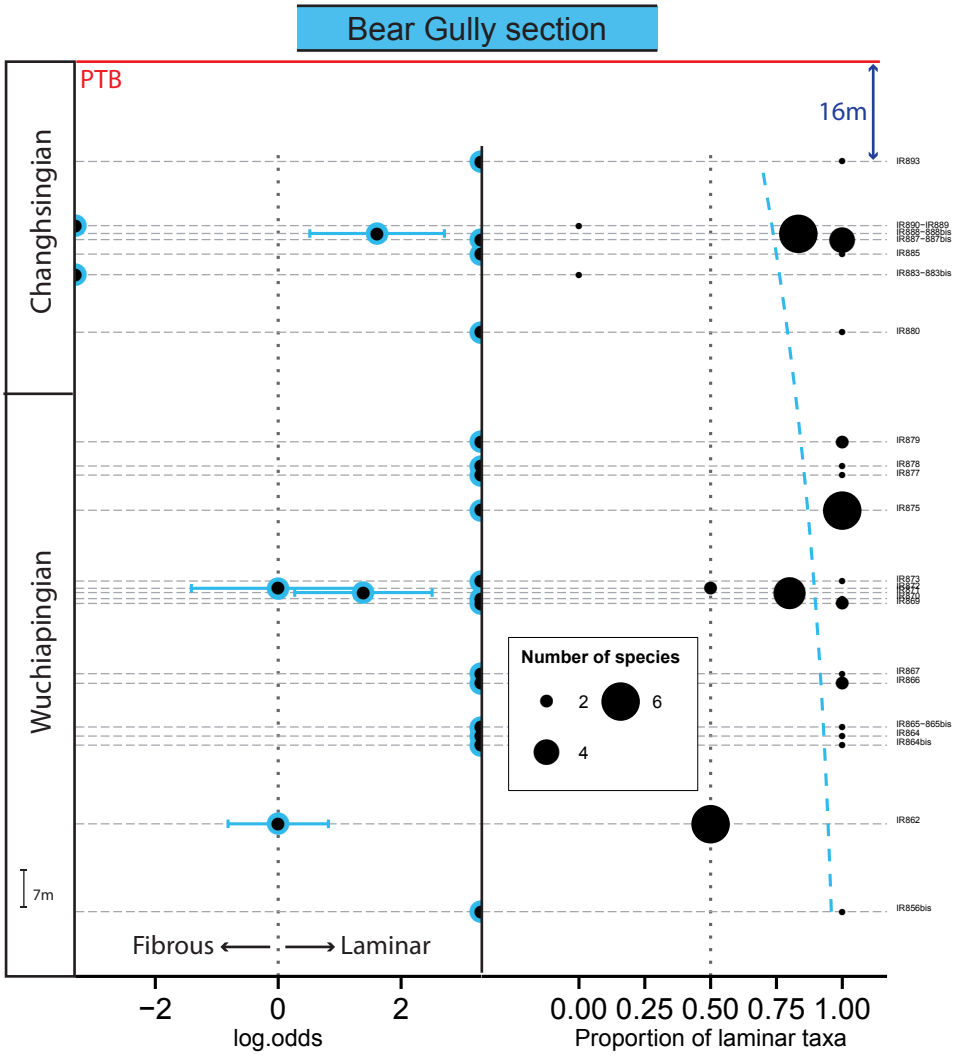
Bear Gully section
PTB
16m
Changhsingian
Wuchiapingian
7m
IR893
IR890–IR889
IR885
IR883–883bis
IR880
IR879
IR878
IR877
IR875
IR867
IR866
IR865–865bis
IR864
IR864bis
IR862
IR856bis
Number of species
2
4
6
Fibrous
Laminar
−2
0
2
log.odds
0.00 0.25 0.50 0.75 1.00
Proportion of laminar taxa

Figure 4.7

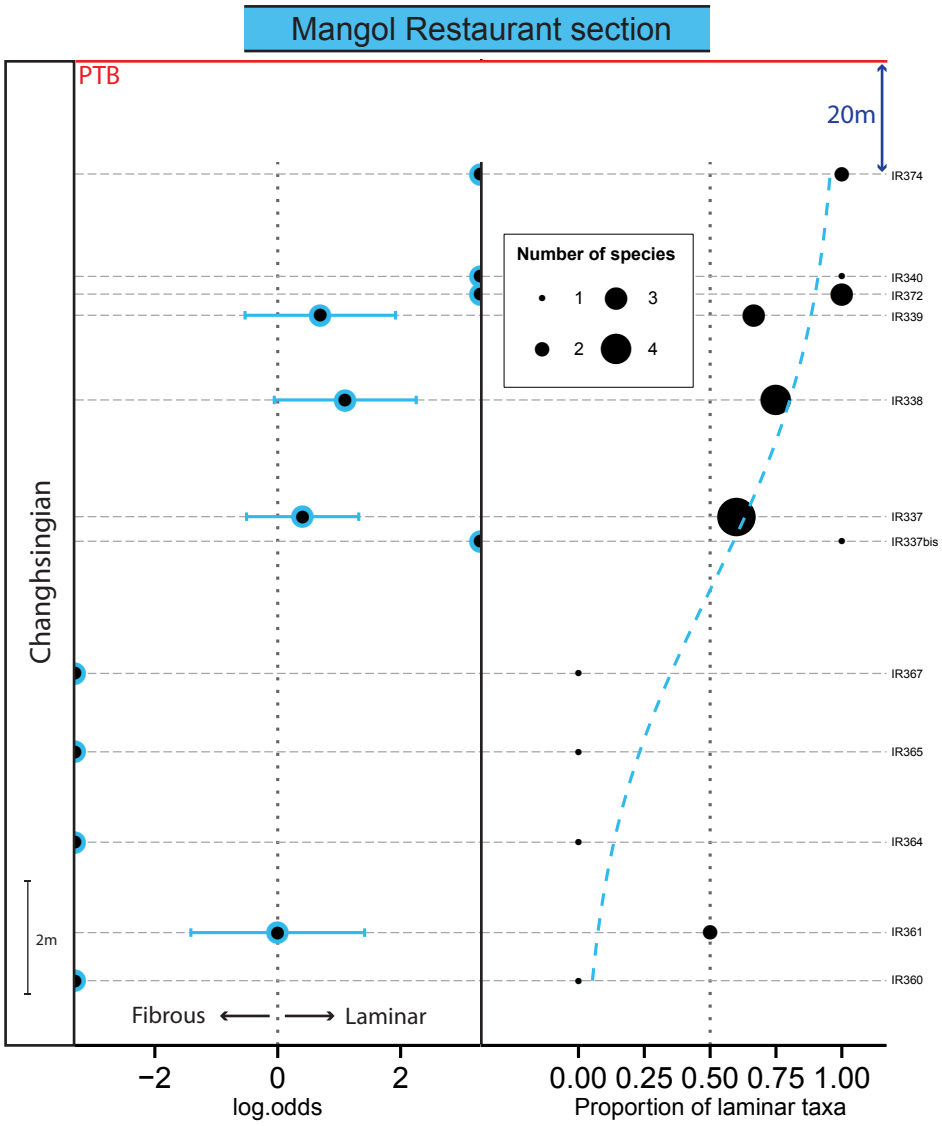
Mangol Restaurant section
PTB
20m
Changhsingian
2m
IR374
IR340
IR372
IR339
IR338
IR337
IR337bis
IR367
IR365
IR364
IR361
IR360
Number of species
1
2
3
4
Fibrous
Laminar
−2
0
2
log.odds
0.00 0.25 0.50 0.75 1.00
Proportion of laminar taxa

Figure 4.8

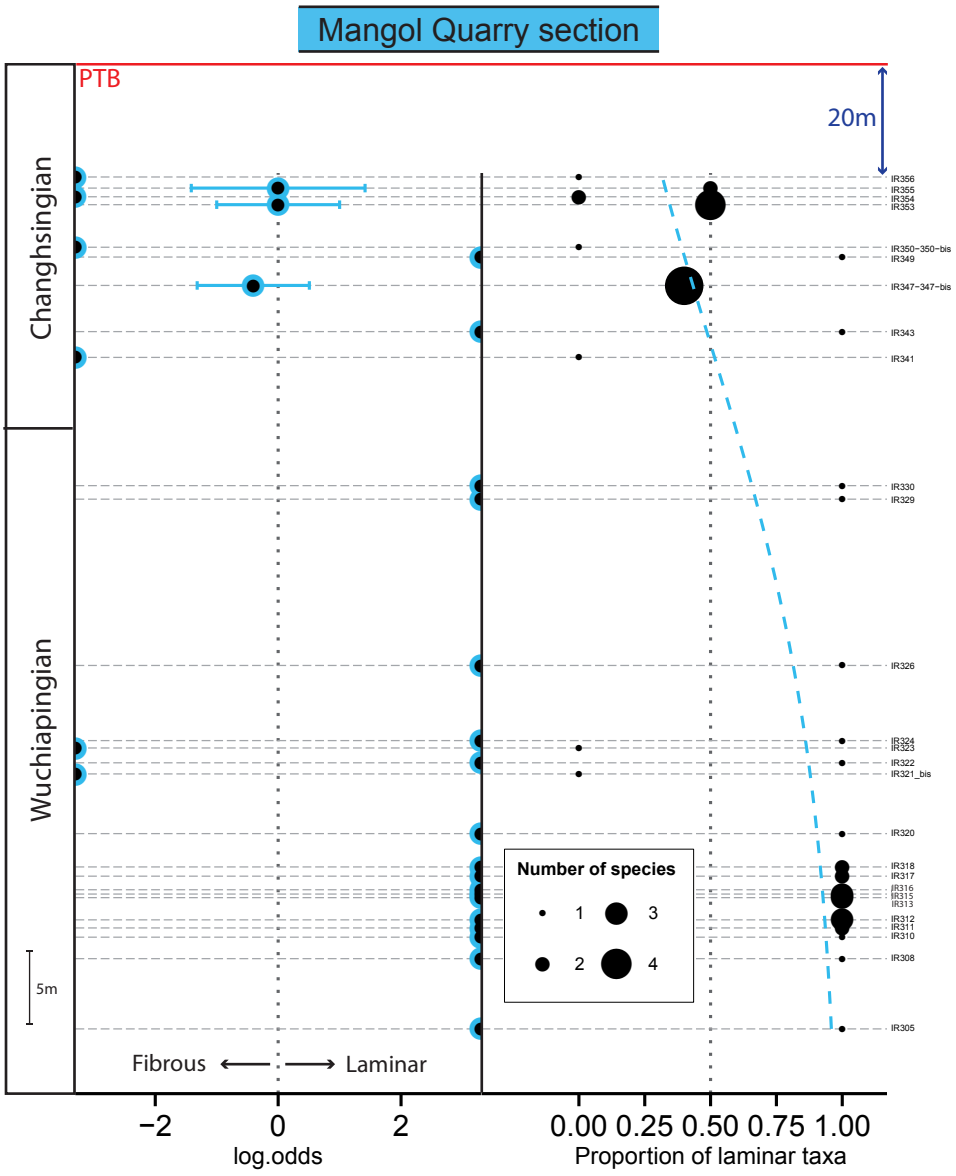
Mangol Quarry section
PTB
20m
Changhsingian
Wuchiapingian
IR356
IR355
IR354
IR353
IR350–350–bis
IR349
IR347–347–bis
IR343
IR341
IR330
IR329
IR326
IR324
IR323
IR322
IR321_bis
IR320
IR318
IR317
IR316
IR315
IR313
IR312
IR311
IR310
IR308
IR305
Number of species
1
2
3
4
5m
Fibrous
Laminar
−2
0
2
log.odds
0.00 0.25 0.50 0.75 1.00
Proportion of laminar taxa

Figure 4.9

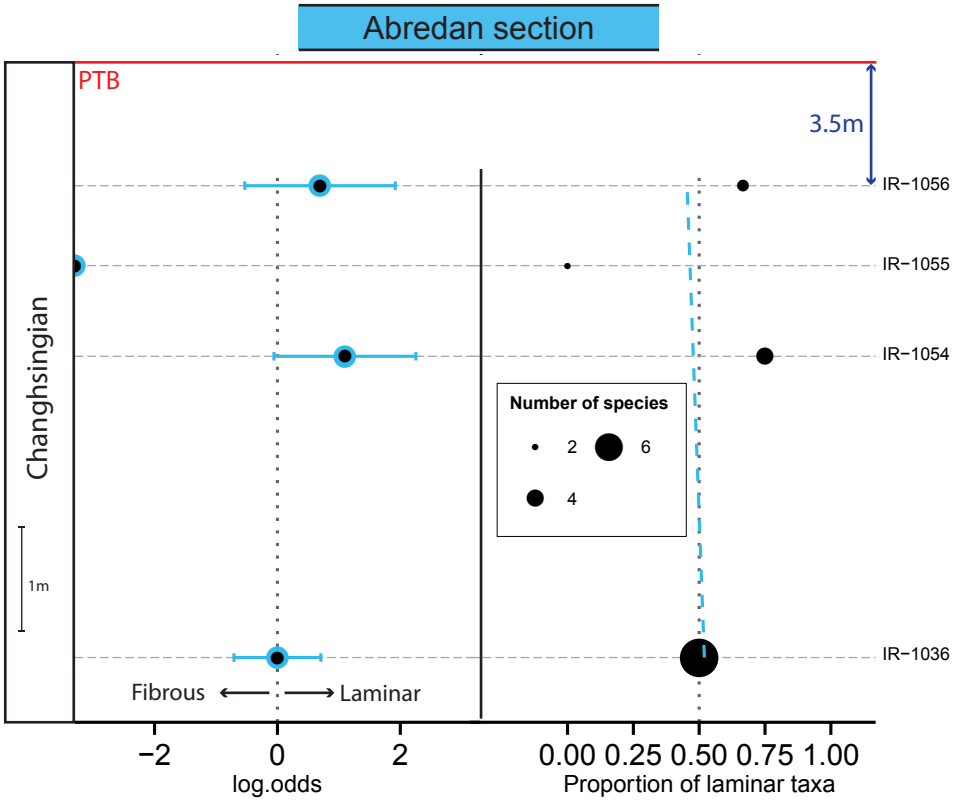

Figure 4.10

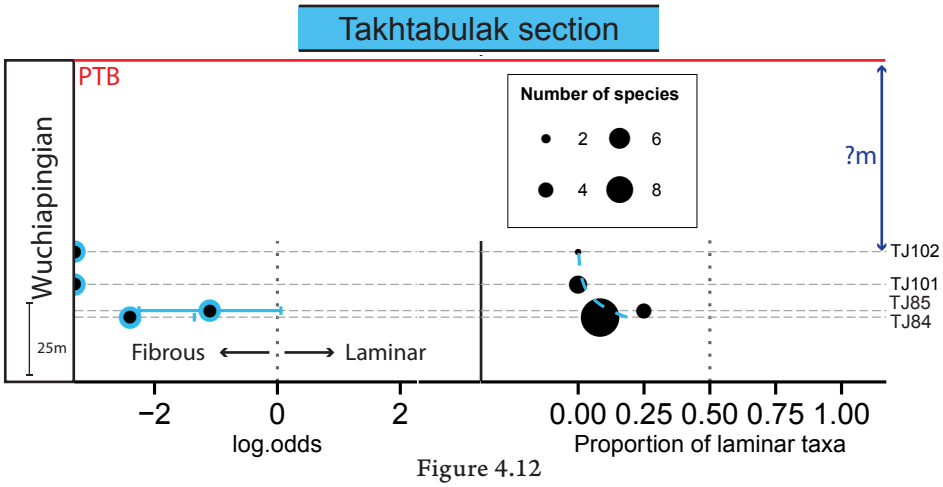

Figure 4.12

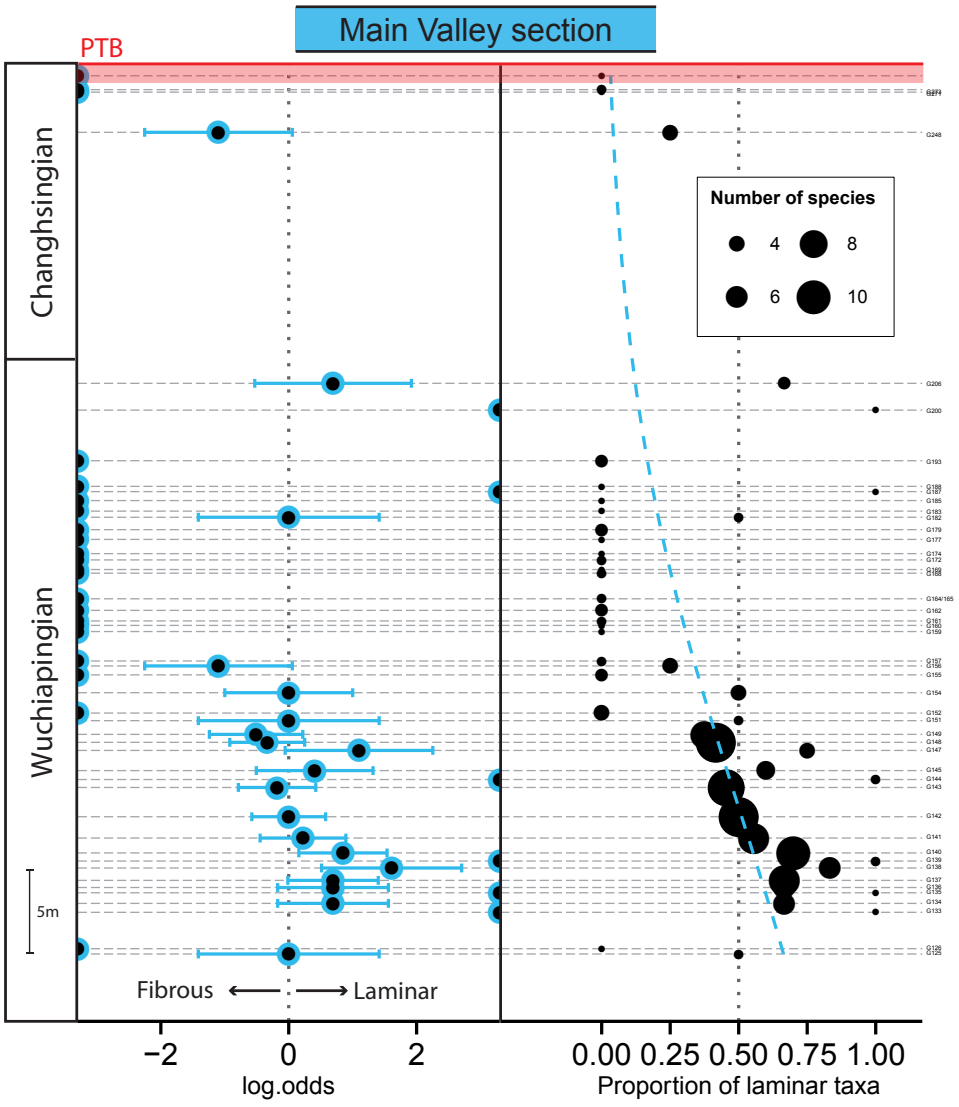
Main Valley section
PTB
Changhsingian
Wuchiapingian
5m
Number of species
4
6
8
10
Fibrous
Laminar
−2
0
2
log.odds
0.00 0.25 0.50 0.75 1.00
Proportion of laminar taxa

Figure 4.11

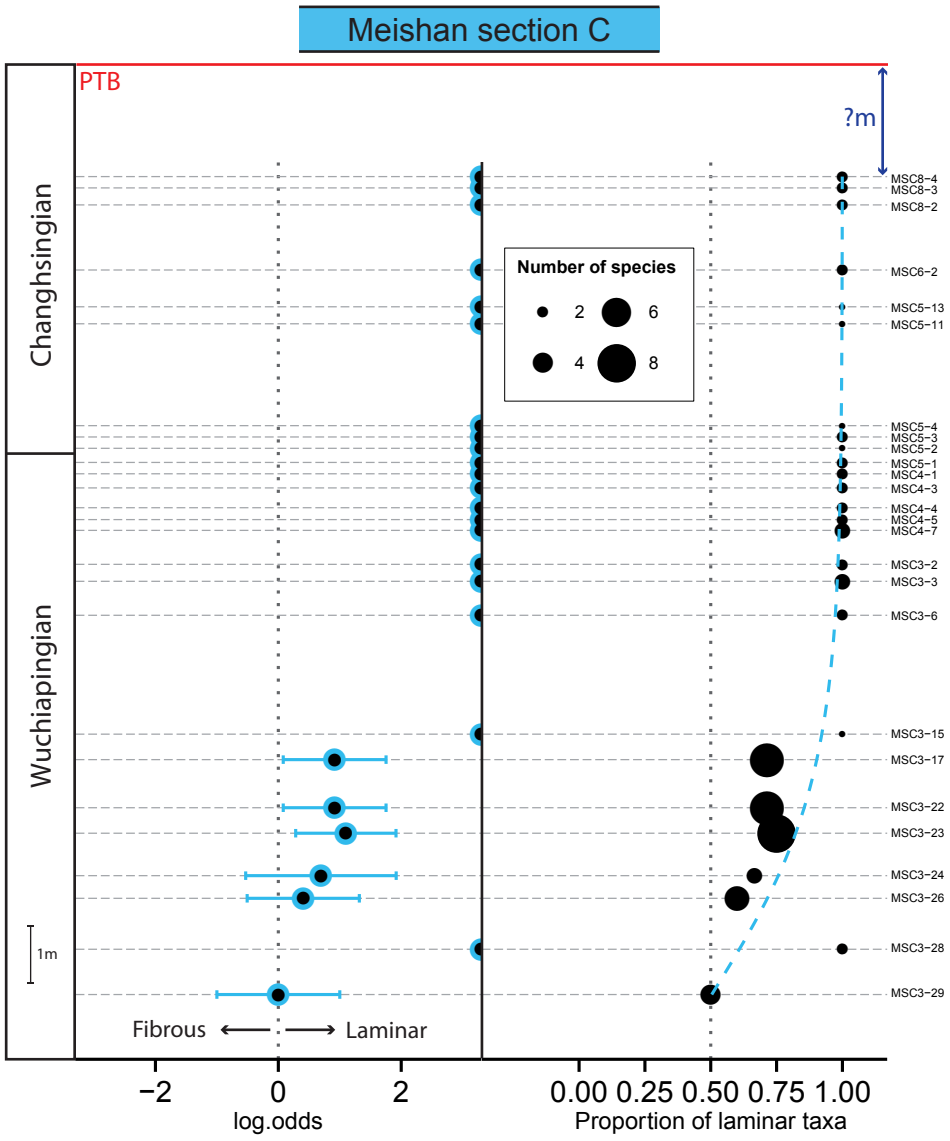
Meishan section C
PTB
?m
Changhsingian
Wuchiapingian
1m
Number of species
2
4
6
8
MSC8−4
MSC8−3
MSC8−2
MSC6−2
MSC5−13
MSC5−11
MSC5−4
MSC5−3
MSC5−2
MSC5−1
MSC4−1
MSC4−3
MSC4−4
MSC4−5
MSC4−7
MSC3−2
MSC3−3
MSC3−6
MSC3−15
MSC3−17
MSC3−22
MSC3−23
MSC3−24
MSC3−26
MSC3−28
MSC3−29
Fibrous
Laminar
−2
0
2
log.odds
0.00 0.25 0.50 0.75 1.00
Proportion of laminar taxa

Figure 4.13

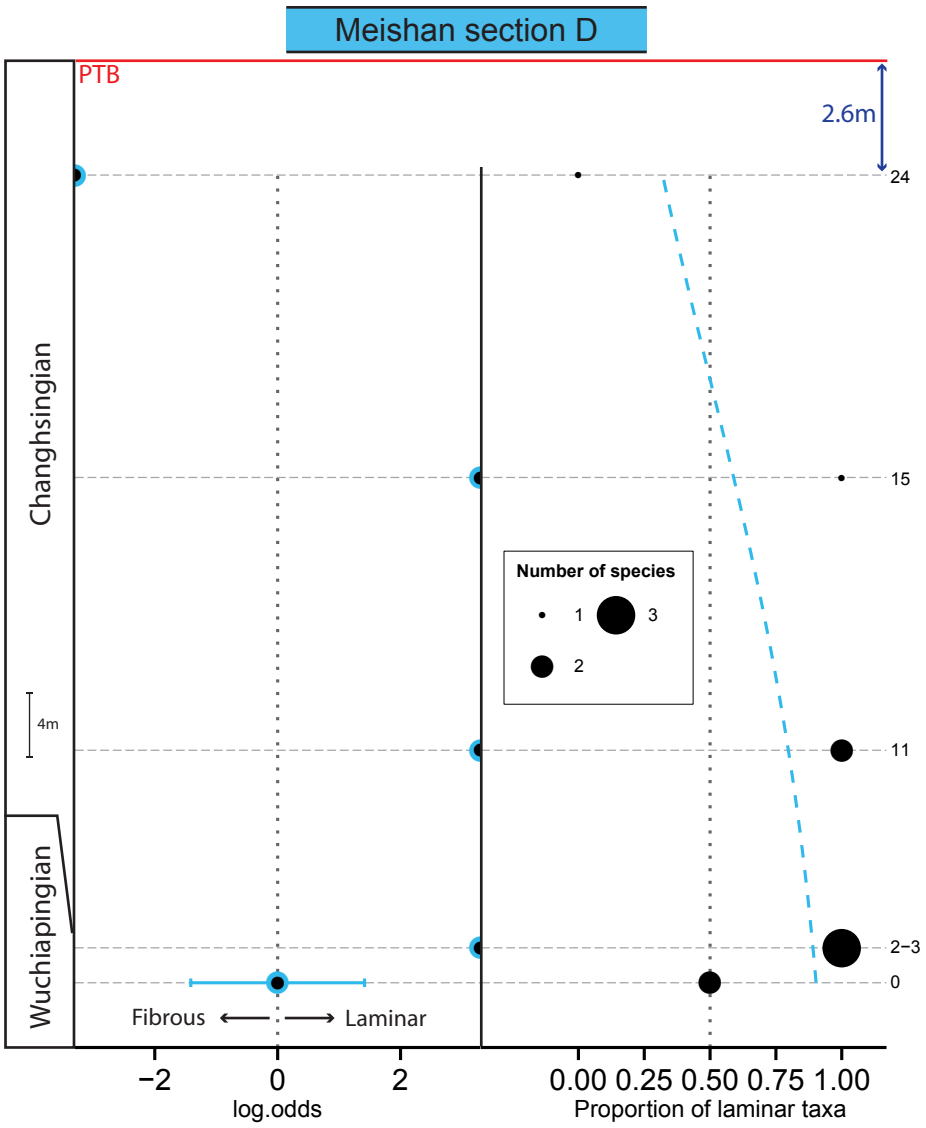
Meishan section D
PTB
2.6m
24
15
11
2–3
0
Changhsingian
Wuchiapingian
4m
Number of species
1
2
3
Fibrous
Laminar
−2
0
2
log.odds
0.00 0.25 0.50 0.75 1.00
Proportion of laminar taxa

Figure 4.14

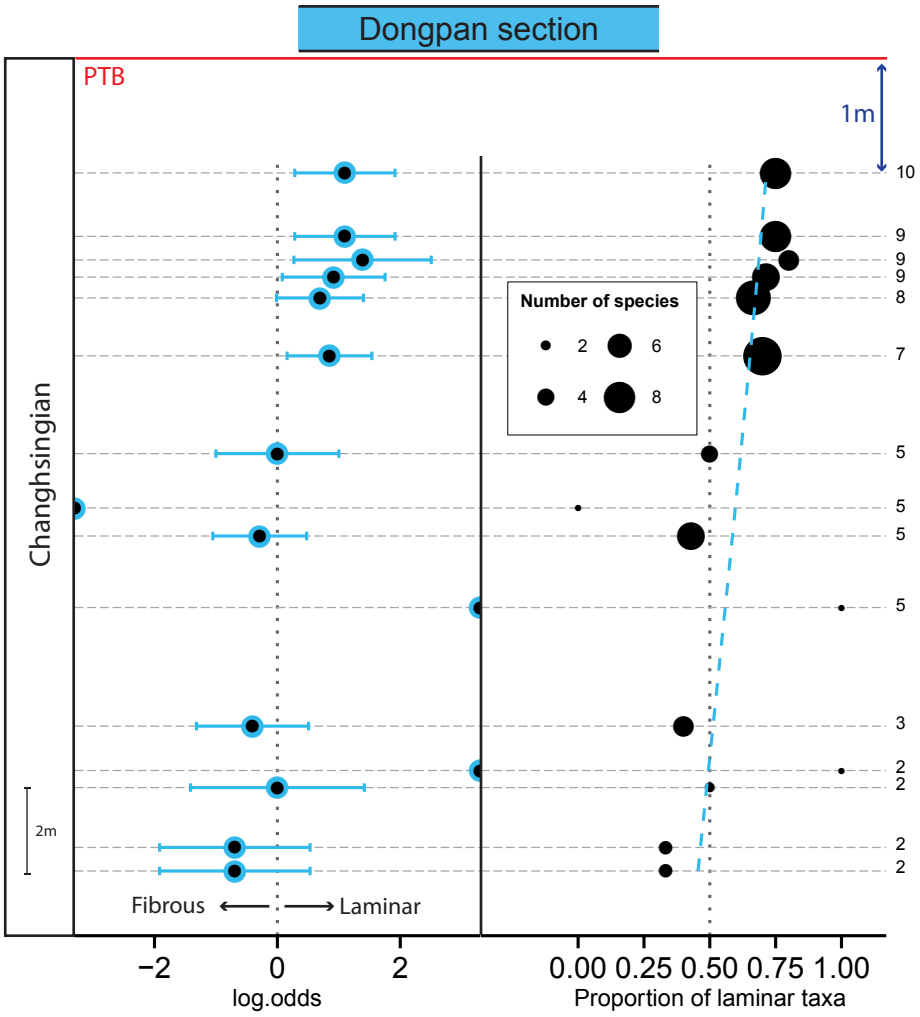
Dongpan section
PTB
1m
Changhsingian
2m
Number of species
2
4
6
8
10
9
9
9
8
7
5
5
5
5
3
2
2
2
2
Fibrous
Laminar
−2
0
2
log.odds
0.00 0.25 0.50 0.75 1.00
Proportion of laminar taxa

Figure 4.15

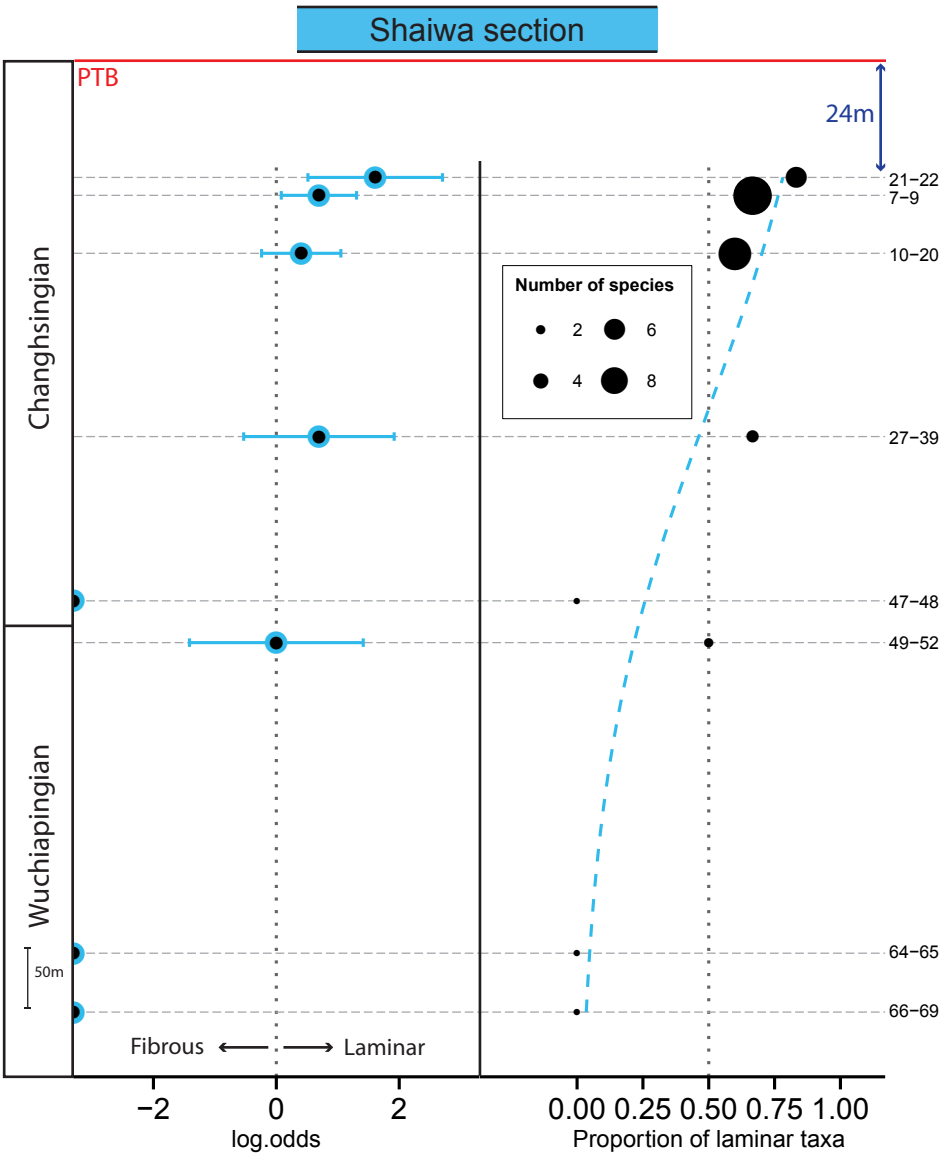
Shaiwa section
PTB
24m
Changhsingian
Wuchiapingian
50m
21–22
7–9
10–20
27–39
47–48
49–52
64–65
66–69
Number of species
2
4
6
8
Fibrous
Laminar
−2
0
2
log.odds
0.00 0.25 0.50 0.75 1.00
Proportion of laminar taxa

Figure 4.16

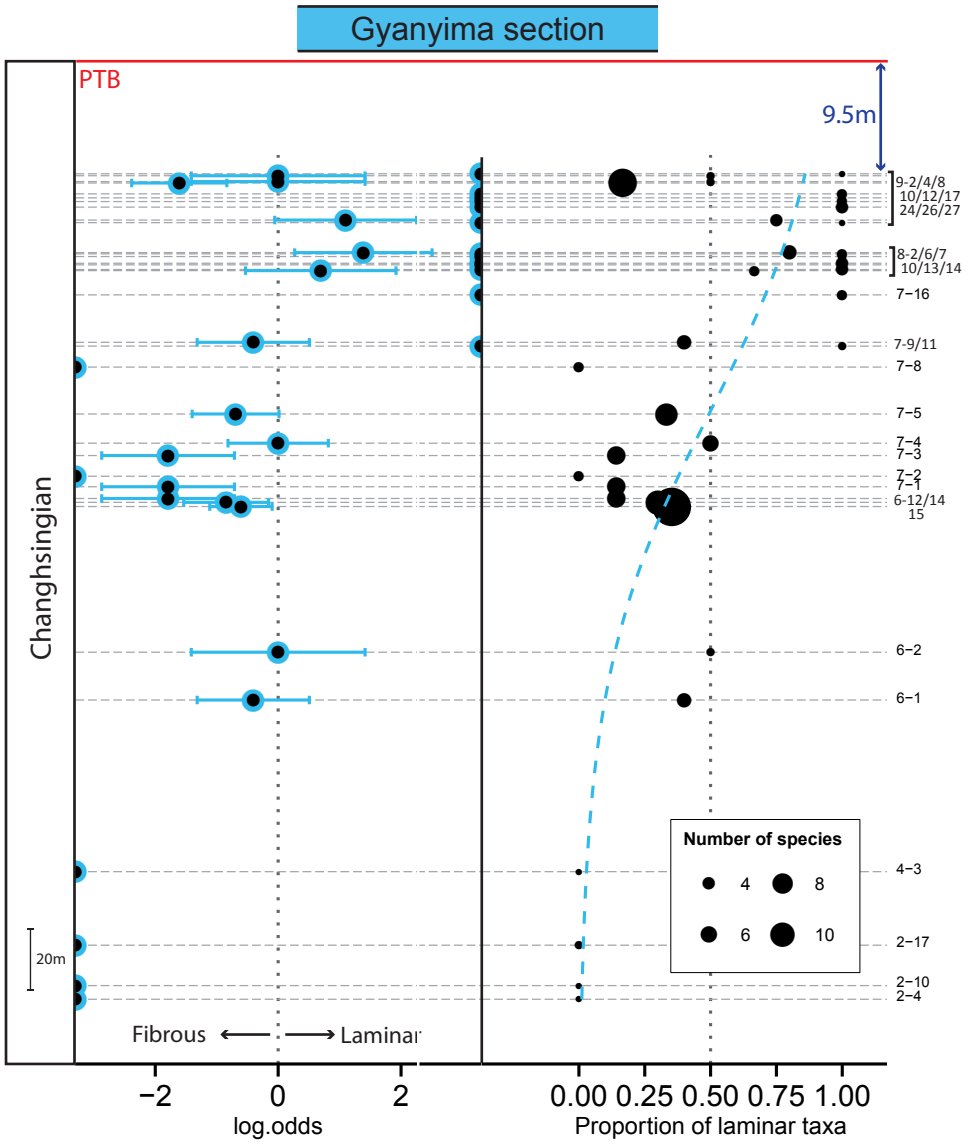
Gyanyima section
PTB
9.5m
Changhsingian
20m
9-2/4/8
10/12/17
24/26/27
8-2/6/7
10/13/14
7–16
7-9/11
7–8
7–5
7–4
7–3
7–2
7–1
6-12/14
15
6–2
6–1
4–3
2–17
2–10
2–4
Number of species
4
6
8
10
Fibrous
Laminar
−2
0
2
log.odds
0.00 0.25 0.50 0.75 1.00
Proportion of laminar taxa

Figure 4.17

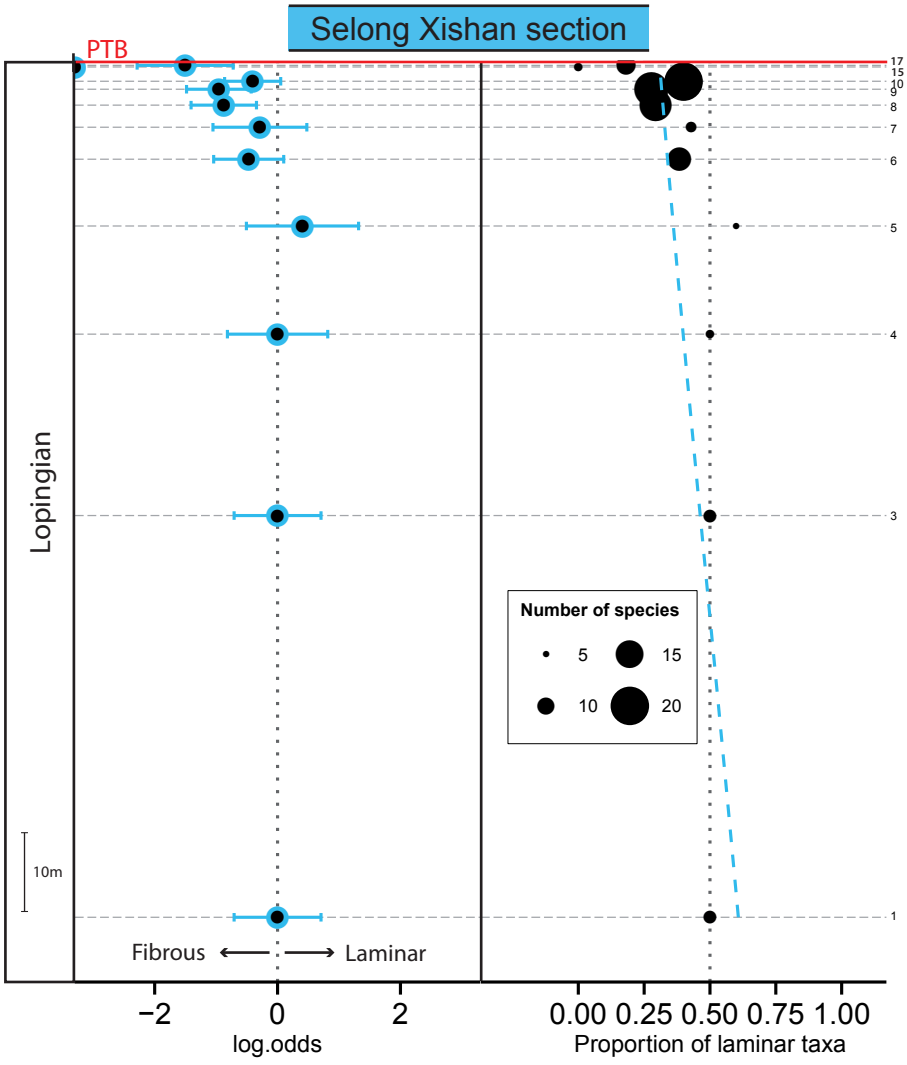
Selong Xishan section
PTB
Lopingian
10m
Fibrous
Laminar
log.odds
Proportion of laminar taxa
Number of species
5
10
15
20
17
15
10
9
8
7
6
5
4
3
1

Figure 4.18

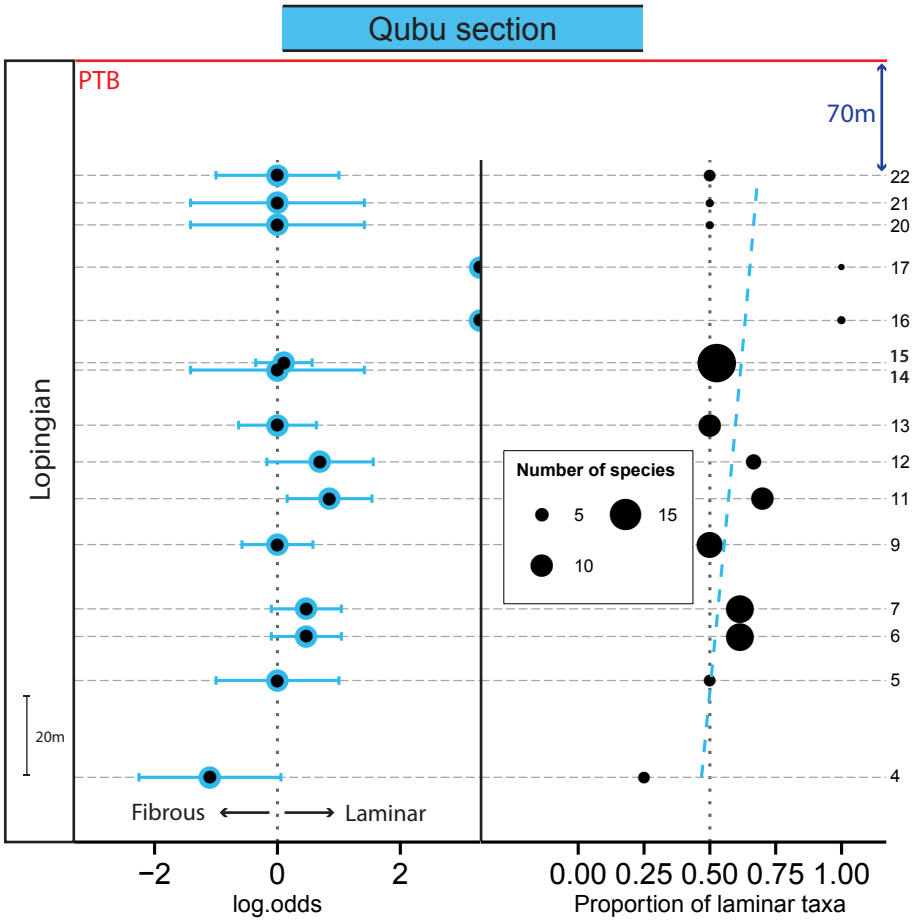
Qubu section
PTB
70m
Lopingian
20m
22
21
20
17
16
15
14
13
12
11
9
7
6
5
4
Number of species
5
10
15
Fibrous
Laminar
−2
0
2
log.odds
0.00 0.25 0.50 0.75 1.00
Proportion of laminar taxa

Figure 4.19

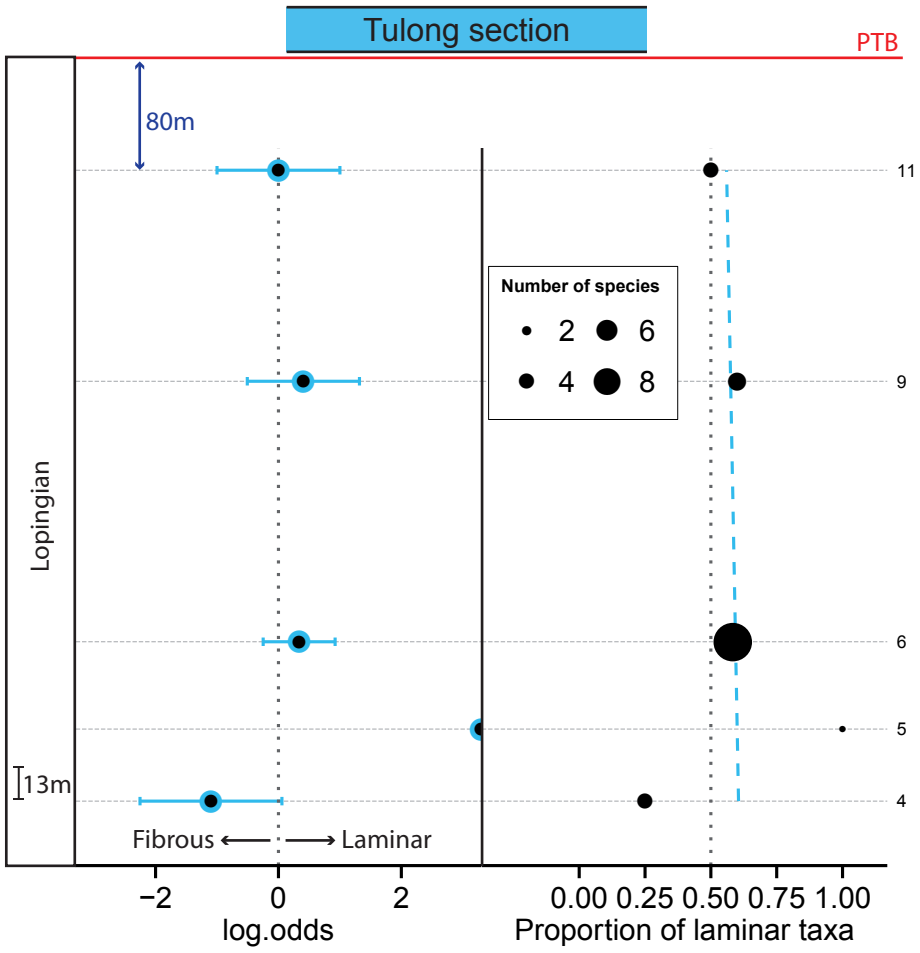
Tulong section
PTB
80m
Lopingian
13m
Fibrous ⟵ ⟶ Laminar
Number of species
2
4
6
8
11
9
6
5
4
−2
0
2
log.odds
0.00 0.25 0.50 0.75 1.00
Proportion of laminar taxa

Figure 4.20

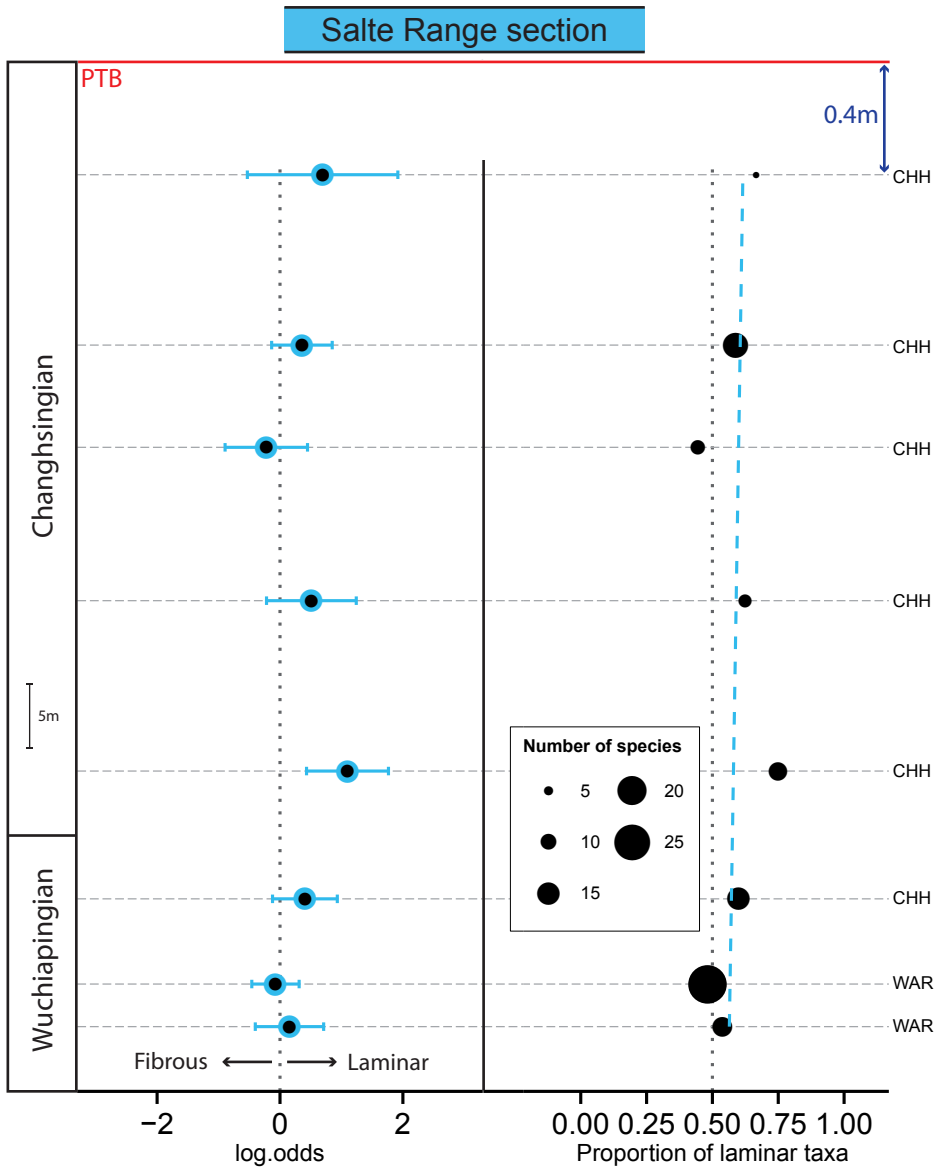
Salte Range section
PTB
0.4m
CHH
CHH
CHH
CHH
CHH
CHH
WAR
WAR
Changhsingian
Wuchiapingian
5m
Number of species
5
10
15
20
25
Fibrous
Laminar
−2
0
2
log.odds
0.00 0.25 0.50 0.75 1.00
Proportion of laminar taxa

Figure 4.21

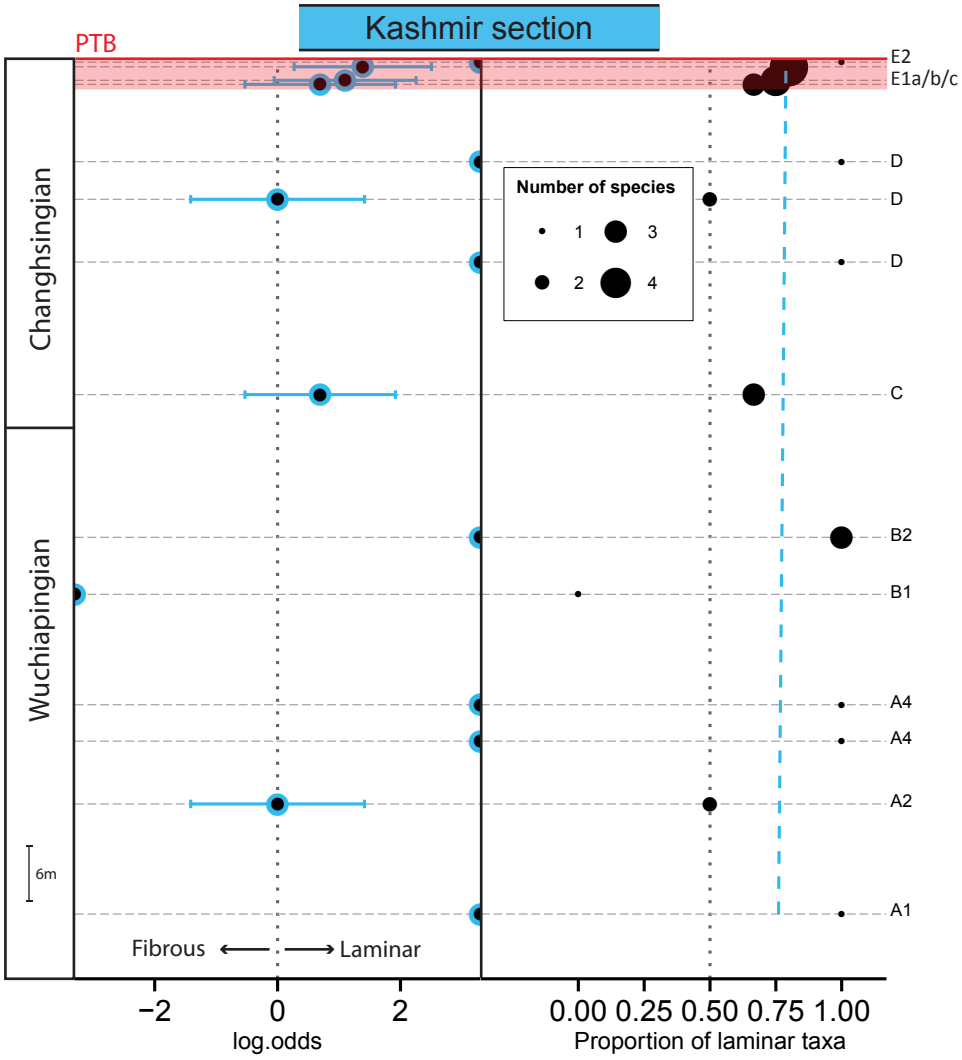
Kashmir section
PTB
E2
E1a/b/c
Changhsingian
Wuchiapingian
D
D
D
C
B2
B1
A4
A4
A2
A1
Number of species
1
2
3
4
6m
Fibrous
Laminar
−2
0
2
log.odds
0.00 0.25 0.50 0.75 1.00
Proportion of laminar taxa

Figure 4.22

Chapter 5
Shell fabric of Upper Permian brachiopods

In this part I describe the shell ultrastructure, micromorphology and fabric of several brachiopod taxa collected along Upper Permian successions of palaeoequatorial to subtropical-temperate palaeolatitudes (Fig. 2.1, paragraph 2.2). Part of the analyzed fossil material has been sampled by the writer during two field expeditions, performed in North Iran and South China, in September 2013 and March 2014 respectively. The other studied material was already present in the collections of Dipartimento di Scienze della Terra "A. Desio" of the University of Milano. In addition, prof. Shen Shuzhong, Academy of Sciences, Nanjing, had kindly provided some brachiopods from the collection of the NIGPAS, where I had performed some preliminary studies.

The data presented here are a synopsis of extensive shell ultrastructure investigations performed on material from:

1. Nesen Formation, Alborz Mountains, northern Iran
2. Julfa Formation, Ali Bashi Formation and Boundary Clay, Ali Bashi Mountains, northwestern Iran
3. Selong Group, southern Tibet
4. Gyanyima Formation, southwestern Tibet
5. Bulla Member, Dolomites, Northern Italy
6. Gomaniibrik Formation, Hazro, Turkey
7. Changhsing Limestone and Dalong Formation, South China

For further details see Materials and Methods chapter (paragraphs 2.1 and 2.2).

It must be noted that the ultrastructure of the material from the Nesen Formation (northern Iran) is not treated here in terms of description and preserva-

tion, because it has been already extensively studied during my master degree thesis (Garbelli, 2011). This material has been reviewed here from a different perspective and some new data were collected to obtain additional information. In particular I attempted a new approach based on the size of structural units of fabric (laminae and fibers).

5.1 Ultrastructure, micromorphology and shell fabric of Upper Permian brachiopods: descriptive results

5.1.1 Bellerophon Formation, southern Alps

Four specimens of species of *Comelicania* from the Bulla Member (fig. 4 in Posenato 2009, the sepciemens were courteously provided by Renato Posenato, Università di Ferrara) were sectioned. The specimens usually show a thick shell in which a fibrous secondary layer and an inner prismatic one can be observed (Plate 1, Fig. A). The fibrous secondary layer reaches about 500 μm in thickness. The fibers have a mean width of 15 μm in cross section, bearing a keel and saddle outline (Plate 1, Figs B, C). The prismatic tertiary layer can be thicker than 2 mm and usually shows very well organized fine growth bands (Plate 2, Figs A, B, C). In the tertiary layer there are some interruptions in the accretion of the prisms, which could be probably related to suspension of the growth, possibly annual (Plate 2, Figs B, C). Sometimes prisms show local dissolution (Table 2, Fig. D). Despite the very good morphostructural preservation, the cathodoluminescence analyses showed a differential pattern. Two samples retained a homogeneous non luminescent prismatic layer (Plate 3, Figs A, B). One sample is rather altered, in particular it is characterized by a luminescent fibrous layer and a prismatic layer with a net of luminescent lines, caused by microfractures injected by diagenetic fluids (Plate 3, Figs C, D). The fourth sample shows a differential preservation with some non luminescent regions both in the fibrous and prismatic layer (Plate 3, Fig. E); in other parts many luminescent microfractures are present, crossing the prisms (Plate 3, Fig. F).

5.1.2 Julfa and Ali Bashi formations, northwestern Iran

For the stratigraphic log of the sections see Appendix A (Figs 1, 2, 3 and 4). The taxonomic composition of the brachiopod assemblages from the Julfa and Ali Bashi formations is very similar to that of the Nesen Formation of the Alborz Mountains (compare Ghaderi *et al.*, 2014 to Angiolini and Carabelli 2010). Unfortunately, in the succession of the Alborz Mountains, brachiopods have their last occurrence well before the PTB, whereas in the Ali Bashi Mountains they not only occur in the upper Changhsingian *Paratirolites* Limestone at the top of the Ali Bashi Formation, but they are also present in the Boundary Clay, which represents the extinction interval and contains the PTB (Garbelli *et al.*, 2014b). In the Changhsingian Ali Bashi Formation and Boundary Clay, the most widespread genera are *Transcaucasathyris* and *Paracruruthyris*, with a few occurrences of *Haydenella*, *Acosarina* and *Spinomarginifera*.

Haydenella kiangsiensis shows a shell composed entirely of a laminar secondary layer (Plate 4, Fig. A). Laminae are composed by laths/blades (Plate 4, Figs B, C) and they are deflected to form pseudopunctae which can originate endospines (Plate 4, Fig. D). No tertiary layer has been found, as already observed for species of the same genus collected in the Nesen Formation.

The species of *Spinomarginifera* here analyzed come from the Wuchiapingian Julfa Formation. The shell succession comprises a laminar secondary layer and a prismatic tertiary layer (Plate 5, Fig. A, Plate 6, Figs A, D). The laminae are cross bladed (Plate 5, Fig. B) and the secondary shell is crossed by pseudopunctae with taleolae (Plate 5, Fig. C, Plate 6, Fig. B). The spines are hollow tubular, crossing the shell with a diameter of about 50 μm (Plate 5, Fig. D). The most important feature here observed is the tertiary layer which can be abundantly present (Plate 5, Fig. A, Plate 6, Figs A, D); on the other hand in conspecific specimens of the Nesen Formation a prismatic layer was observed only in correspondence of muscle scars (Garbelli *et al.*, 2012). The transition from the secondary to the tertiary layer is marked by a local change in the direction of the growth vector (Plate 6, Fig. C). It is noteworthy that the species of genus

Spinomarginifera here analyzed are able to reverse the secretion mechanism, from prismatic tertiary to laminar secondary, as shown by the occurrence of repetitive alternation of the two types of fabric (Plate 5, Fig. A, Plate 6, Fig. A, D).

Acosarina minuta shows the occurrence of the outer primary layer, which is thicker than 10 μm and recrystallized (Palte 7, Figs A, B). The secondary layer is fibrous and crossed by punctae. The fibers show keel and saddle outline (Plate 7, Figs A, C, D). No prismatic layer was observed.

The species of *Transcaucasathyris* have a well preserved shell composed of an outer fibrous secondary layer and an inner prismatic one (Plate 8, Fig. A). The primary layer has never been observed. The fibrous layer has a fabric that is not completely homogeneous and the shape and orientation of fibers vary from its outer part inwardly (Plate 8, Fig. B, Plate 9, Fig. A). The outermost fibers are slightly flat and show the typical keel and saddle outline (Plate 8, Fig. C, Plate 9, Fig. C). The innermost fibers become more squared or diamond shaped in cross section (Plate 8, Fig. D, Plate 9, Fig. D). The fibers often show fine growth banding (Plate 8, Fig. B, Plate 9, Fig. B, D). The prismatic layer is well developed and it increases in thickness towards the umbonal region (Plate 8 Fig. A, Plate 10, Fig. A). The prisms of many specimens show very fine growth banding which may be diurnal and, at high magnification, prismatic subunits are visible (Plate 10, Figs B, C, D).

Paracrurithyris pygmaea has a preserved shell composed only of a fibrous secondary layer, with flat fibers showing growth banding (Plate 11, Figs A, B, C). Most of the shells do not show a good morphostructural preservation at ultrastructural scale (Plate 11, Fig. D).

In general, most of the specimens of the Julfa and Ali Bashi formations have a very well preserved shell, which is not luminescent irrespectively of the type of fabric and thickness of the shell. For example both thin laminar *Spinomarginifera* (Plate 12, Figs A, B) and thick fibrous *Transcaucasathyris* (Plate 12, Figs C, D) species have non luminescent shells. However, the specimens from the Boundary Clay, which mostly belong to *P. pygmaea*, are invariably luminescent,

even if they are sometimes included in a not luminescent matrix (Plate 12, Figs E, F).

5.1.3 Changhsing and Dalong formations, South China

Brachiopods collected from several sections have been analyzed: Shangsi, Zhongliang Hill, Beifengjing and Daijaigou sections (Figs 5-9 in Appendix A). Several productid taxa were recovered: *Cathaysia*, *Paryphella*, *Haydenella* and *Spinomarginifera* were the most common. All the species of these genera bear a shell composed of a cross bladed laminar secondary fabric, which is indistinguishable at specific level (comparing figure A of Plate 13, 14, 15 and 16). No specimen has been found to possess a tertiary prismatic layer. Laminae may be grouped into packages of blades with their longitudinal axis parallel oriented. Packages of laminae with blade axis orientation approximately perpendicular to each other regularly alternate in the secondary layer. Perpendicular orientation of the blade axis was observed in all four taxa (Plate 13, Figs A, C; Plate 14, Fig. C; Plate 15, Fig. A; Plate 16, Figs A, D). Pseudopunctae have a taleola and form endospines (Plate 13, Fig. D; Plate 14, Fig. B; Plate 15, Figs C, D; Plate 16, Fig. C). Section of spines crossing the shell were observed in *Paryphella* and *Spinomarginifera* (Plate 15, Fig. C, Plate 16, Fig. B). All the show a laminar fabric with an highly porous structure. The mean thickness of the laminae is comprised between 0.25 and 0.35 μm.

The specimens of species of *Transcaucasathyris* have a similar fabric of the congeneric species from the Julfa and Ali Bashi formations in term of shell succession, in particular for the type of secondary fibrous layer (Plate 17, Figs A, C). However, the specimens show the preservation of the outermost primary layer, which is recrystallized (Plate 17, Figs A, B). On the contrary, the prismatic layer is usually altered by dissolution and only trace of it are observable (Plate 17, Fig. D).

The shell structure of *Paracrurithyris pygmaea* entirely consists of a secondary fibrous layer in both valves (Plate 18, Fig. A). The fibers have a keel and saddle outlines and an average maximum width in cross section comprised be-

tween 10 and 20 μm (Plate 18, Fig. B). An interesting feature is that fibers may be organized in groups with their longitudinal axis sub-parallel to each others. Packages of fibers may show different orientation as a result of different direction of growth (Plate 18, Fig. C). The investigated specimen of *Paraspiriferina alpha* show a relatively thin shell composed of an outermost primary layer and an inner fibrous secondary layer (Plate 19, Fig. A). The fibers are relatively small with a width in cross section less than 10 μm (Plate 19, Fig. B). The shell is strongly punctate (Plate 19, Figs C, D).

The analyzed specimens of *Acosarina minuta* show a similar structure to congeneric species that have been collected from other localities both in shell fabric and in the type of morphological preservation (Plate 20). Another Orthida, a species of *Peltichia*, has a shell entirely composed of a fibrous secondary layer which is thicker than 3 mm (Plate 21, Fig. A). The fibers are relatively small, with a width greater than 10 μm and the punctation is very fine and hard to detect due to the reduced size of the punctae (Plate 21, Fig. B, C). The secondary layer shows numerous change in the direction growth of the fibers (Plate 21, Fig. D). The rhynchonellida *Hustedia* sp. has a shell composed of a recrystallized primary layer and an inner fibrous layer (Plate 22, Fig. A). The fibers are small and shell is entirely crossed by pseudopunctae (Plate 22, Figs B, C, D).

In general, the morphological preservation of the brachiopod shells is very good as proven by many specimens preserving the primary layer and the outline of the fibers despite the fact that the shells are very thin and small. This is confirmed by the cathodoluminescence analysis of some selected specimens, which are invariably non luminescent, expect for some slightly luminescent areas, irrespectively of the level of luminescence of the matrix (Plate 23, Figs A, B, C, D).

5.1.4 Gomaniibrik Formation, Hazro, Turkey

From this succession only taxa with laminar fabric have been analyzed. Several species of *Spinomarginifera* are present: *S. helica*, *S. spinosocostata* and *S.*

sulcata. *S. helica* has a shell fabric similar to the one previously described for the specimens of the Julfa Formation of northwestern Iran: secondary cross bladed laminae with pseudopunctae and a prismatic tertiary layer (Table 24, Figs A, B, C, D). Specimens preserve spines in their proximal and distal parts and the alternation of secondary and tertiary layers is well developed (Table 25, Figs A, B, C). Noteworthy the prisms show well organized bands of growth, otherwise rarely observable in this genus (Table 25, Fig. D). In *S. spinoscostata* the same feautures are observed (Table 26, Figs A, B). The investigated specimens of *S. sulcata* do not have a prismatic layer, but only a laminar secondary one (Table 26, Figs C, D). The thickness of the laminae is consistent in all the species, with the mean value ranging from 0.24 to 0.34 μm (see Appendix C).

Alatorthotetina sp. has a shell composed only of a laminar secondary layer, with very well organized laminae, regularly crossed by pseudopunctae without taleolae (Plate 27, Figs A, B, C, D). The pseudopunctae are formed by inwardly inflected laminae. The outer ornamentation of costellae is produced by laminae which are outwardly deflected to form radial crests (Plate 27, Fig. A). The average thickness of the laminae ranges from 0.39 to 0.53 μm (see Appendix C).

The cathodoluminescence analysis of the shell material from this locality shows that there is a general good preservation, as grasped by the micromorphological observation. In fact the shells are non luminescent, irrespectively of fabric, even if they are thin (Plate 28, Figs A, B, C, D). Sometimes it is possible to observe localized alteration due to microborings or a complete alteration related to diagenetic fluid permeating the entire shells (Plate 28, Figs E, F respectively).

5.1.5 Gyanyima Formation, southwestern Tibet

Many taxa were analyzed from this section, which is very fossiliferous (fig. 2 in Shen *et al.*, 2010). Unfortunately, some specimens are not enough preserved to provide good material for a description of the shell succession.

For the genus *Costiferina*, three different species have been investigated: *C. subcostatus*, *C. indica* and *C. spiralis*. The specimens show a rather thick shell

(Plate 29, Fig. A) reaching more than 2 mm of thickness. These shells are completely formed by a cross bladed laminar secondary layer (Plate 29, Figs A, B). The thickness of the laminae ranges from 0.45 to 0.75 μm. The shell is crossed by pseudopunctae with taleolae, and by spine channels (Plate 29, Figs C, D).

Also *Richthofenia lawrenciana* shows quite a thick shell composed only of secondary laminar layer (Plate 30, Fig. A). The most impressive feature is the richness of small pseudopunctae crossing the shell walls, which have a different size (Plate 30, Figs B, D). The laminae are about 500 nm thick (Plate 30, Fig. C).

The species of *Permophricodothyris* shows the typical features already observed in *P. ovata* and *P. iranica* from the Nesen Formation of northern Iran: a secondary fibrous and a well developed tertiary layers (Plate 31, Fig. A); fibers have keel and saddle outlines (Plate 31, Fig. B) and tertiary prisms show very fine growth bands (Plate 31, Fig. C). Several intercalations of secondary and tertiary layer are present (Plate 31, Fig. D). Another spiriferida, *Neospirifer* sp., presents a shell composed of a fibrous secondary layer and an inner prismatic one (Plate 32, Fig. A). Fibers are long elements with a spatulate termination (Plate 32, Figs B, C). In some cases it has been possible to detect bands of accretion on the fibers (Plate 32, Fig. D). A common feature of these two genera of Spiriferida is the relative small thickness of the secondary layer compared to the prismatic one. *Stenoscisma* sp. (Plate 33) and *Martinia* sp. (Plate 34, Figs C, D) show a similar structure to the one of the previous two species, but they seem to have a greater ratio of the thickness between secondary and prismatic layer, if compared to species of *Permophricodothyris*. In *Alphaneospirifer anshuanensis,* no prismatic layer was observed (Plate 34, Figs A, B).

The terebratulida *Notothyris* sp. has a shell succession composed of a fibrous secondary and a prismatic tertiary layer (Plate 35, Figs A, C). The secondary layer is crossed by punctae and the prisms show organized bands of growth (Plate 35, Figs B, D).

The cathodoluminescence analysis shows that generally, the shells are non luminescent, a clear index of good preservation. This type of preservation is ir-

respective of the type of fabric, being laminar or fibrous, with or without punctae (Plate 36, Figs A, C, D). However, some multilayered shells may have the outermost part slightly luminescent, but the inner part remains dull (Table 36, Fig. E). The laminar shells may have a luminescent pattern, more variable due to their more porous fabric, being more permeable to the diagenetic fluids (Table 36, Fig. B). Some shells may be in part dolomitized in the upper part (Unit 9) of the Gyanyima Formation (Table 36, Fig. F).

5.1.6 Selong Xishan section, southwestern Tibet

I analyzed the specimens of species of three genera, kindly provided by prof. Shen Shuzhong, Nanjing Academy of Sciences (see fig. 4 in Shen *et al.* 2006). The species of *Retimarginifera* has a shell composed of a laminar secondary layer, which is thicker than 2 mm (Plate 37, Fig. A). The laminae are cross bladed and the shell is crossed by pseudopunctae with taleolae (Plate 37, Fig. B, C, D).

The preservation of *Neospirifer* sp. in this section shows that the shell is similar to the ones of species of the same genus coming from Gyanyima, but the ratio of the thickness of the secondary to the tertiary layer is greater in some specimens (Table 38, Figs A, B). The tertiary prisms show fine growth banding (Table 38, Fig. D). The species of *Spiriferella* has a similar shell structure, but preserves the primary layer in some specimens (Table 39, Figs. A, B). The fibers can reach 20 μm in width and their outline is keel and saddle (Table 39, Fig. C). Noteworthy, the fibers show changes in the direction of growth (Table 39, Fig. D). The luminescence of the specimens from this locality is highly variable. Some prismatic layers are non luminescent, even if a few fractures with diagenetic infilling may be present (Table 40, Figs A, B). In other cases alteration is stronger, as shown by very luminescent secondary layers or by enhanced web of luminescent fractures in the prismatic layers (Table 40, Fig. C). Processes of silicification have been observed in the prismatic layers of a few specimens (Table 40, Figs E, F).

5.2 Study of the size of the fabric structural units in a stratigraphic perspective

In several species of nine genera collected along different sections, the size of the structural units composing their shell fabric has been measured. The measurements were obtained as explained in paragraph 2.1.3 and they mainly concern the thickness of the laminae of the laminar secondary layer and the width of the fibers of the fibrous secondary layer, both measured in cross section.

A total of 93 specimens has been measured, 67 belonging to taxa of Strophomenata and 26 belonging to taxa of Rhynchonellata (Appendix C). The average number of measures taken for each specimen of Strophomenata taxa is 55 (min = 18, max = 204). In the case of Strophomenata, which have a laminar secondary layer, the acquired measure was the thickness of each single lamina. In the case of Rhynchonellata, the width of each fiber has been measured in cross section according to the methodology illustrated in Fig. 2.1. In a few specimens the area of the section of the fiber has also been calculated (see Table 3 in Appendix C). The average number of fibers measured for each specimens is 65 (min = 5, max= 264)

The measures and their relative statistics (mean and standard deviation) have been performed on species belonging the following genera:

8. Spinomarginifera, Tyloplecta and *Permophricodothyris* from the Nesen Formation, northern Iran;

9. Spinomarginifera from the Julfa Formation, northwestern Iran;

10. Alatorthotetina and *Spinomarginifera* from the Gomaniibrik Formation, Turkey;

11. Costiferina and *Permorphricodothyris* from the Gyanyima Formation, Tibet;

12. Haydenella, *Paryphella*, *Cathaysia*, *Spinomarginifera* and *Paracrurithyris* from the sections of South China.

Genera have been used instead of single species as they are the most objective taxonomic units for this kind of study, given the large time dimension and

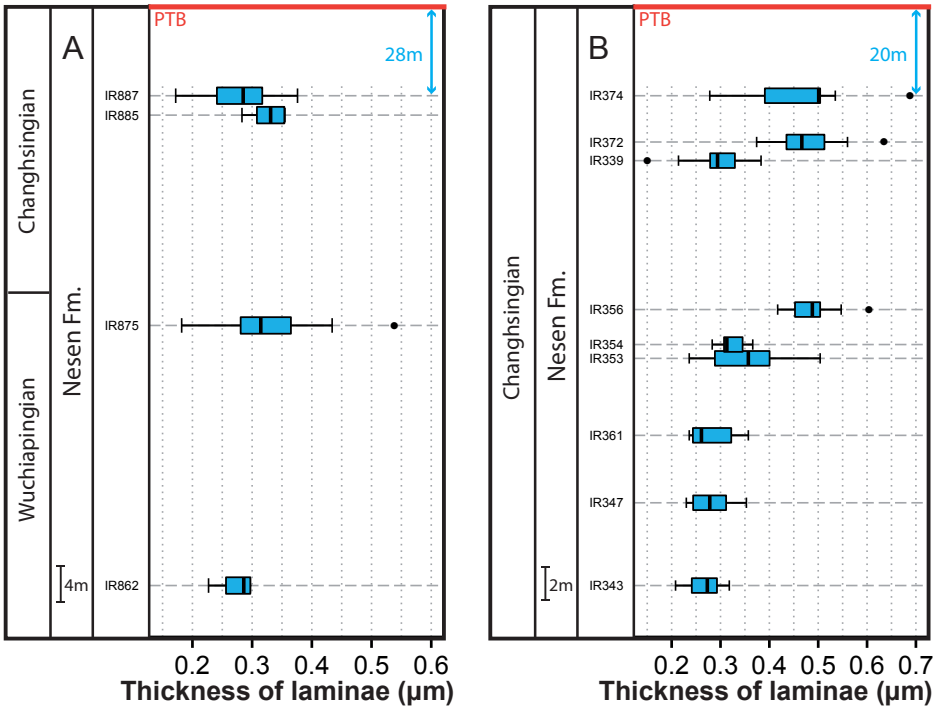

Figure 5.1. Box plot representing the thickness of laminae in *Spinomarginifera* from the Nesen Fomation, northern Iran; (A) Bear Gully section and (B) Mangol composite section (Mangol Quarry and Mangol Restaurant); see Angiolini and Carabelli (2010), fig.4 and fig. 5 respectively.

the incompleteness of the fossil record. The genus is also the taxonomic unit used in similar researches on extant brachiopods (e.g. Watson *et al.*, 2012). In fact when available, the record of different species in the same genus was almost overlapping, as was the case for the species of Spinomarginifera from Iran.

5.2.1 Nothern Iran

In the Nesen formation of the Alborz Mountains, northern Iran, *T. persica* and *T. yangtzeensis* have been recovered from the lower member of the Nesen Formation, which is early to middle Wuchiapingian in age. The three specimens collected in situ (IR329-5, IR867-4, IR871-7) have similar mean thickness of the laminae ranging from 0.32 to 0.39 µm. The specimens collected in the talus at the base of the section (IR314) show quite a large variability, span-

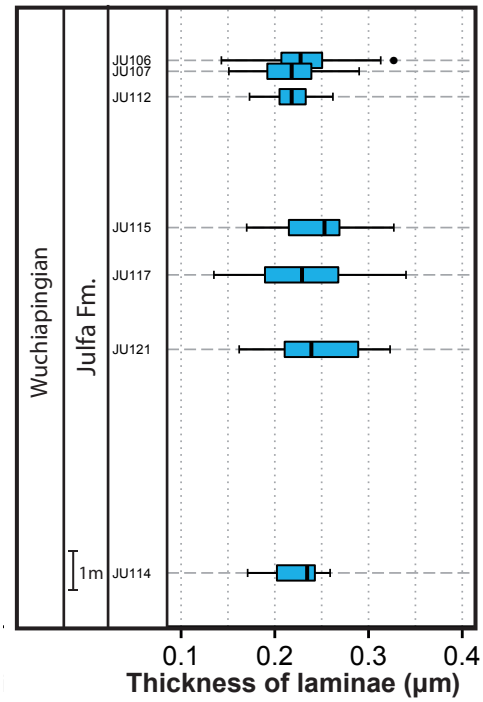

Figure 5.2. Box plot representing the thickness of laminae in species of *Spinomarginifera* from the Julfa Formation; see Figs 1-4 in Appendix A

ning from a mean of 0.24 to more than 0.40 µm in thickness. The specimens of *Spinomarginifera* in the Bear Gully section (fig. 4 in Angiolini and Carabelli, 2010) show most of the laminae having a thickness comprised between 0.25 and 0.35 µm, with some oscillations in the mean values, but no evident trend of thickness increase or decrease (Fig. 5.1a). Along the Mangol sections (Quarry and Restaurant, Fig. 5.1b; fig. 5 in Angiolini and Carabelli, 2010), the specimens show an increasing trend in the thickness of laminae, from 0.25-0.3 µm up to 0.4-0.5 µm.

The specimens of the species of *Spinomarginifera* of the Wuchiapingian Julfa Formation from the Main Valley section of the Ali Bashi Mountains, northwestern Iran (see Figs 1-4 in Appendix A) show the laminae having a thickness comprised between slightly less than 0.2 to 0.3 µm (Fig. 5.2a). No clear trend is evident along the stratigraphic succession. Here, the species of *Spino-*

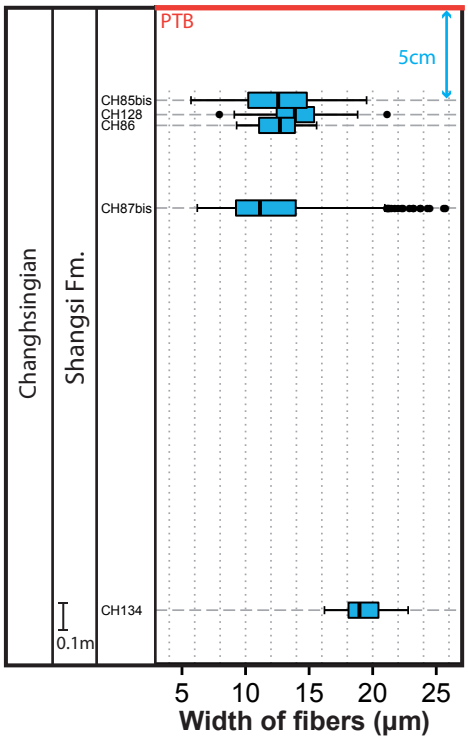

Figure 5.3. Box plot representing the width of fibers of *Paracrurithyris pygmaea* from the Shangsi composite section, Dalong Formation; see Figs 5 and 6 in Appendix A.

marginifera are characterized by a secondary layer with the thinnest laminae of all investigated conspecific specimens, with the thickness reaching values lower than 0.15 µm. Among the Rhynchonellata, the fibers of two specimens of *Permophricodothyris iranica* (IR164-3 and IR367-2) show a mean fiber width of 10 and 16 µm respectively.

5.2.2 South China

In South China, at Zhongliang Hill section, two specimens of *Paryphella* (CH4-3, CH5-9) have a mean laminar thickness equal to 0.36 µm, very similar to the specimens CH136-2 from the Shangsi section 1, which occupies a lower stratigraphic position (compare section in Figs 5, 6 and 9 in Appendix A).

Two specimens of *Spinomarginifera* from the Daijaigou section and horizon

CH71 which is very close to the PTB, have mean thickness of laminae equal to 0.3 µm. The two specimens of *Cathaysia* show a different average size, with the specimens in the lower horizon (CH71) assessed at 0.24, the one in the higher horizon has a thickness of the laminae of 0.31 µm (see Appendix C). For *P. pygmaea* a large amount of measurements is available from the Shangsi sections and the size shows a slight decline up to the PTB (Fig. 5.3). The fibers of the stratigraphical lowest specimens (CH134-7) have a mean width in cross section equal to 20 µm. The numerous specimens of the upper horizons show a mean value of 13 µm in beds CH87bis, CH86 and CH128. The lower mean value is reached by the two specimens from CH85bis, showing a mean value lower than 12 µm.

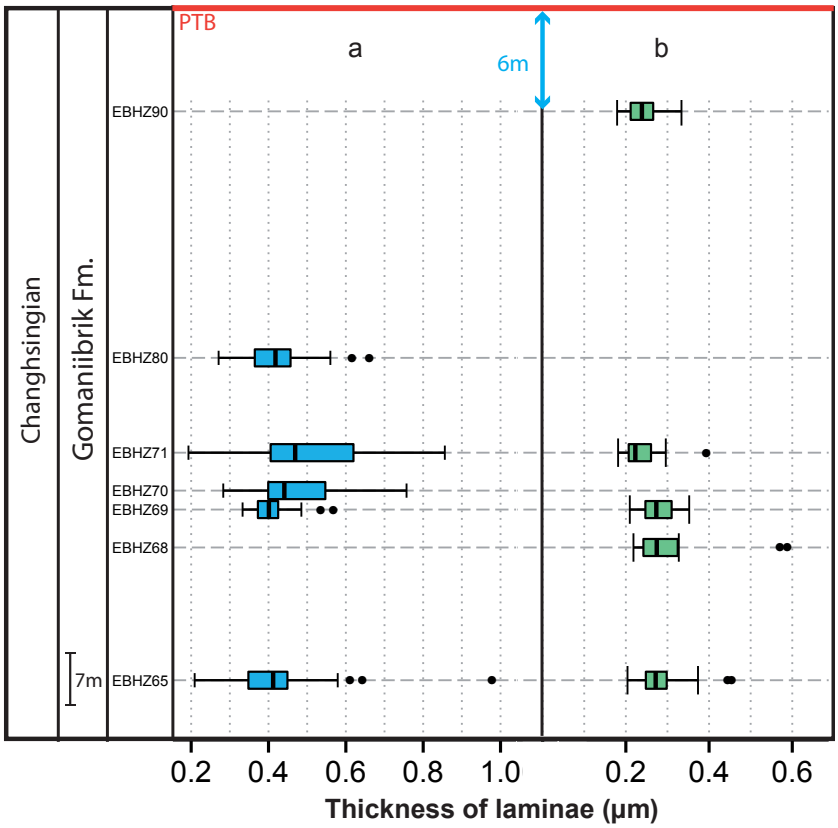

Figure 5.4 Box plot representing the thickness of laminae in species of *Alatorthotetina* (a) and *Spinomarginifera* (b) in the Gomaniibrik Formation, Turkey.

5.2.3 Turkey

In the Gomaniibrik Formation of the Hazro section, specimens of *Alatorthotetina* sp. record the maximum thickness of the laminae in bed EBHZ71, to return upward to background values (Fig. 5.4a). Overall, the thickness of the laminae in this species is comprised between 0.35 and 0.6 µm. Along the same section, specimens of species of *Spinomarginifera* have the thickness of the laminae varying between 0.2 and 0.35 µm, with the minimum thickness reached by specimens from bed EBHZ71. No clear trend is evident (Fig. 5.4b)

5.2.4 Tibet

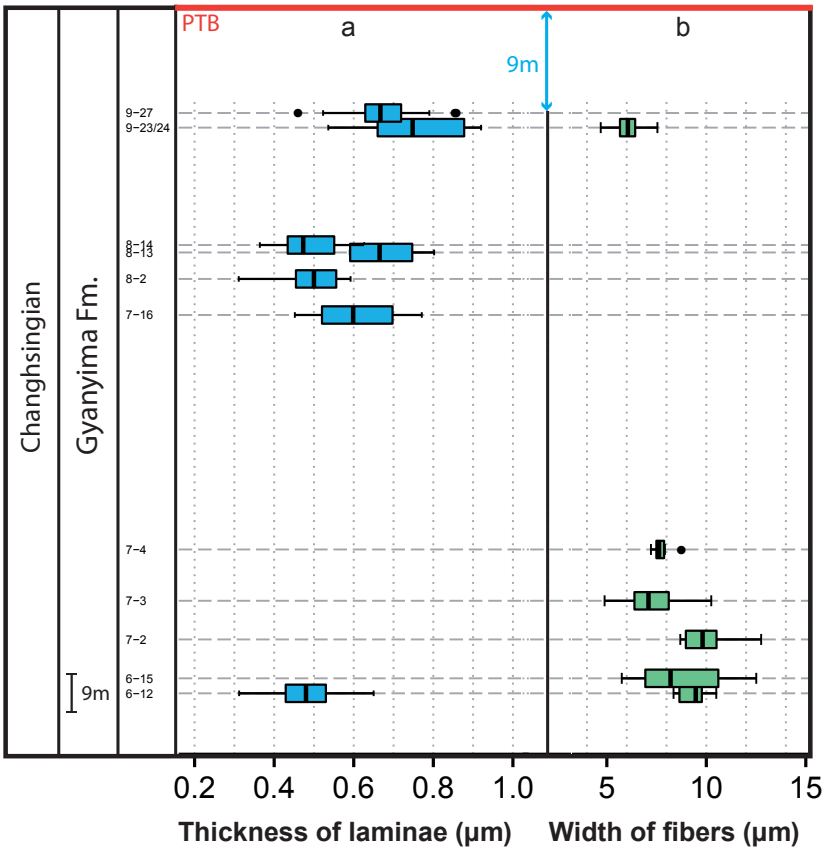

Figure 5.5. Box plot representing the thickness of laminae in species of *Costiferina* (a) and the width of the fibers in *Permophricodothyris* sp. (b) in the Gyanyima Formation (see fig. 2 in Shen *et al.*, 2010).

The specimens of the species of *Costiferina* in the Gyanyima section have laminae with a thickness ranging from more than 0.4 up to 0.8 μm. Even if there is a certain amount of oscillations in the size of the laminae, a clear trend of increasing thickness is present up to the PTB (Fig. 5.5a). Opposite is instead the trend recorded by the change in size of the fibers of species of *Permophricodothyris*, which show a decrease in size, with lower values of the width of fibers in bed 9-24 (Fig. 5.5b)

5.3 Discussion on the patterns related to the types of fabric observed

5.3.1 The change in brachiopod shell biomineralization during the Late Permian

The taxa under investigation show the typical shell succession described by Williams (1968), composed of an outermost primary layer, an inner secondary and, eventually, a tertiary layer. The primary layer is not always present because it is just a few micrometers thin and it easily undergoes corrasion or dissolution. The two inner layers are thicker and more easily preserved. Even when diagenetic processes heavily altered the shell, traces of both secondary and tertiary layer can be observed (Plate 17, Fig. D).

Upper Permian brachiopods show a variety of shell fabrics, which differ not only by the morphostructure of the secondary layer (fibrous vs. laminar), but also by the reciprocal arrangement of the secondary and tertiary layers. From this point of view, it is possible to classify the shells in two main different types, based on the presence or absence of the prismatic tertiary layer.

Shells belonging to the first type (type1) are composed of three layers: primary (not always preserved, but originally secreted), secondary and tertiary layers. Both classes, Strophomenata and Rhynchonellata, comprise taxa with this type of shell. Among the Strophomenata, groups belonging to the order Productida, such as the genera *Spinomarginifera*, *Araxilevis* and *Typloplecta*, show this type of shell succession (Plate 5, Fig. A, Plate 6, Fig. A, B, Plate 24,

Fig. A, Plate 25, Fig. C, fig. 3A/B/C in Garbelli *et al*., 2012). Among the Rhynchonellata, representatives of the Spiriferida usually show this type of fabric, as the analyzed genera *Permophricodothyris*, *Spiriferella, Stenoscisma* and *Neospirifer* (Plate 31, 32, 33, 39; fig. 4F in Garbelli *et al*. 2012). Also the Athyridida, represented here by *Transcaucasathyris* (Plate 8, 9, 10) and *Comelicania* (Plate 1, 2) can produce this kind of shell succession. The Terebratulida, as *Notothyris* (Plate 35), have this type of shell too.

In all these orders, the shells become usually very thick, even in the small to medium sized taxa, such as *Transcaucasathyris, Spinomarginifera* and *Notothyris*. One common feature of these shells is that they usually show multiple intercalations of the secondary and tertiary layers .

A second group (type2) of shell successions includes those composed entirely by the secondary layer below the primary layer, without evidence of the occurrence of the prismatic tertiary layer. This group contains either very thick shells (type2a), usually belonging to large sized taxa, and thin shells of small sized taxa. Among the Rhynchonellata, only one taxon has been found with a thick a shell of this kind: *Peltichia* of the Order Orthida (Plate 21). Among the Strophomenata, there are many more groups characterized by a thick shell of this type: the Productida *Costiferina* (Plate 29) and *Richthofenia* (Plate 30), and the Orthotetida *Alatorthotetina* (Plate 27). For what concerns the thin shell (type2b), Rhynchonellata comprise a variety of taxa: the Orthida *Acosarina* (Plate 7, 20), the Athyridida *Hustedia* (Plate 22), the Spiriferinida *Paraspiriferina alpha* (Plate 19) and the Spiriferida *Paracrurithyris pygmaea* (Plate 11, 18). Thin shelled Strophomenata of this type are represented by the Productida *Cathaysia*, *Paryphella* and *Haydenella* (Plate 4, 13, 14, 15).

However, there are some exceptions to these general types, especially for what concerns the development of tertiary layer. For example, the species of *Spinomarginifera* from the Julfa and Gomaniibrik formations show a well developed prismatic tertiary layer (Plates 5, 6, 24, 25). On the other hand, of the numerous conspecific specimens investigated from the Nesen Formation, none

has shown a developed tertiary layer (fig. 2 in Garbelli et al, 2012). A preservation bias affecting the Nesen material is unlikely because there are no evidences of dissolution in the fossil shells. A species-specific can be excluded because I have investigated the same species in the different stratigraphic successions (i.e. *S. helica*, *S.spinosocostata*, *S.iranica*, *S. ciliata*). A third option is that these differences may be related to change in the shell secretory mechanism due to different environmental settings or to different stratigraphic positions with respect to the PTB. However, no substantial difference in environmental conditions and stratigraphic position has been observed between the specimens of the Nesen and Julfa formations so the question remain open. The capacity of shell to shift the type of secretion from secondary to tertiary fabric, requires further investigations, in the next future. In modern brachiopods, a species specific effect has been observed. In fact *Liothyrella uva* (Broderip 1833, Peck *et al.* 1997) has a two layered shell (primary + secondary), while the congeneric *L. neozelandica* is characterized by three layers (primary+secondary+tertiary) (Thomson 1918, Williams and Rowell 1965a and b, Chuang 1994, Williams 1997). In support of this, Watson *et al.* (2012) found that *L. uva* has less inorganic content than *L. neozelandica*, and related this change in shell inorganic content to the carbonate saturation of seawater. Even if it is difficult to explain the mechanism producing/evolving these differences in the type of succession produced by the shell, we can argue that there is a selective force causing these differences and acting on relatively long evolutionary time. This effect on shell fabric is difficult to be evaluated in short time laboratory experiments (i.e. Cross *et al.* 2015) which test the response of single organisms during their lifetime or even smaller interval. To be said that the very recent publication of Cross *et al.* 2015) considered a 7-months perturbation experiment a long term study. In fact, the features of a single shell are the product of a process of evolution lasted several millions of years under disparate environmental conditions. From this point of view, the analysis of shell types present in the geological record using different time resolutions, could provide important information of selective pressure

acting on the biomineralization of brachiopod shells.

In the case study under exam, considering the stratigraphic record of Upper Permian brachiopods, we can observe that usually the shells with type 1 fabric are mostly widespread in the Wuchiapingian or in the early to middle Changhsingian (i.e Angiolini and Carbelli, 2010; Ghaderi *et al.* 2014, Shen *et al.*, 2006, 2010); stratigraphically above toward the PTB, the taxa with this type of fabric tend to disappear, with a few exceptions. For example, in the *Paratirolites* Limestone of the Ali Bashi Mountains, species of *Transcaucasathyris* bears a three layered shell, but they are smaller and thinner if compared to the ones occurring stratigraphically below (in the Unnamed shaly Unit and Julfa Formation); at Selong Xishan, it is possible to find the type 1 shells of *Spiriferella* and *Neospirifer* close to the PTB, but here there may be some problems of reworking and/or condensation (Figs B and C in Plate 40; Shen *et al.*, 2006).

Except for these local occurrences, in general in the upper part of the Changhsingian close to the onset of the extinction, brachiopods are small sized and characterized by a two layered fabric, so they belong to group 2b, described above.

These small and thin shells have been previously considered adaptations to oligotrophic and low oxygen levels (He *et al.* 2012). However, they were found also in well or normally oxygenated conditions (Garbelli *et al.* 2014b). PTB small sized faunas (Lilliput effect of Urbanek 1993) have been considered the result of a protracted primary productivity collapse causing the mass extinction (Twichett *at al.* 2005); some authors report the occurrence of a Lilliput effect on brachiopods already in the late Changhsingian, well before the main pulse of the crisis (He *et al* 2007, 2010). On the other hand, type 2b shells can be considered as having a higher ratio of organic/inorganic content, which could be produced by exposition to low carbonate saturation levels during prolonged intervals of time, as it has been shown to happen in modern organisms (Watson *et al.* 2012). If the thin shell is a result of this kind of selective process, than the shell size reduction may be only a secondary effect caused by

structural reasons (some brachiopod species became small for the difficulty to precipitate carbonate due to the high cost for precipitating the carbonate shell) and not the product of a primary productivity collapse . In fact the collapse of productivity and the real dwarfism in primary producers is only present in the extinction interval, whereas the thin shelled organic rich brachiopods start to be widespread slightly before the extinction interval. That shell size reduction may be a species specific secondary effect is also supported by the fact that medium to large sized brachiopods with thick shells are found in several sections close to the boundary; however, these are entirely composed of secondary fabric (both laminar or fibrous, type 2a), such as *Peltichia* at Shangsi or *Costiferina* at Gyanyima. Despite their shell may be rather thick, it has a low ratio of inorganic ($CaCO_3$) content, if compared to species disappearing earlier, such as *Permopricodothiris* or *Tyloplecta*, equipped with a thick tertiary prismatic layer. So the strategy of Strophomenata and Rhynchonellata towards the PTB is to acquire a less inorganic rich type 2 fabric and eventually a smaller size, to counteract the lower carbonate saturation level of seawater.

The pattern of disappearance of brachiopods in the fossil record could have been attained because they are low buffered organisms and they are very sensitive to changes in chemical composition of seawater (Clapham and Payne 2011). If any subtle change has already began in late Changhsingian, they could have recorded it.

Another observation is that, close to the onset of the extinction, it is easy to find shells with fibrous fabric of type 2 and possessing punctae, which is a further indication of a high ratio of organic/inorganic content. This type of fabric could be better suited in case of nutrient collapse, because punctae are supposed to have the function (Williams 1997) of nutrient storage and this fact could lead to survival in settings with low nutrients.

In South China, close to the PTB, there are also numerous species with laminar secondary layer belonging to the genera *Haydenella*, *Cathaysia*, *Paryphella* and *Spinomarginifera* (Plate 13-16). These taxa have a cross bladed lami-

nar shell which was rich in organic matter during life as shown by the fabric itself. Remarkable is that the specimens of species of *Spinomarginifera* close to the PTB in the Daijaigou section do not show the presence of the prismatic layer. All these features support that the increase in shell organic content may be an adaptation to low carbonate saturation level in seawate,r rather than to low nutrient settings.

5.3.2 Change in the size of the structural elements in the fabric and their implications for understanding the evolution of biomineralization in brachiopods

As shown in the literature, the structural units of both laminar and fibrous fabric have different sizes and morphologies (e.g. McKinnon 1974, for the fibrous fabric; Williams and Brunton 1993, for the laminar fabric). In an evolutionary perspective, it may be important to understand the causes of this variability. For example, Brunton (1972) proposed the hypothesis that laminar fabric in chonetids may have evolved from a primitive ancestor with a fibrous-like fabric. In this context, through the reduction in size of structural elements, the cells of the mantle lost the membranes which enveloped the structural units, and these structural units started to be secreted collectively by the mantle. However, the observation of differences in the shells of modern brachiopods and the consideration of the factors producing these differences (Watson *et al.* 2012, Goetz *et al.* 2009), suggest a link between fabric evolution and change in the environmental conditions. Similarly, in some extant bivalves, it has been assessed that the size of the structural units of aragonitic shells is correlated to environmental factors (Olson *et al.* 2012a, 2012b). This could represent an example of the fact that small variations could be caused by the environmental pressure, producing, in the long term, macro-evolutionary trends originating different shell fabrics.

In the case of the uppermost Permian brachiopods, some selective pressures were highlighted in the previous chapters, but other clues are provided by the detailed study of the shell fabric. A first evident trend is that, at the end of the

Permian, the occurring brachiopod taxa have very small structural units of the fabric: the blade/laths of laminae in the Strophomenata, which are normally small, or small-sized fibers in the Rhynchonellata. In particular, the Rhynchonellata species still present in the extinction interval have very small fibers, also less than 10 μm in width, smaller than those of species disappearing well before the PTB. This is the case of *Hustedia* (Plate 22), *P. pygmaea* (Plate 18), *P.alpha* (Plate 19). In these species, the width of fibers could drop below 4 μm, a size very close to that of blades/laths in some laminar species (e.g. Williams and Brunton 1993, Brunton 1972) and quite atypical for the class. It is interesting to note that in the two Changhsingian spiriferid taxa in which I have measured the size of the fibers in several stratigraphic horizons, a trend of fiber size reduction toward the PTB has been observed (Figs 5.3, 5.5b). The mechanism causing this width decrease is unclear, but we can affirm that this trend shows a certain reduction in the biomineralization activity of these taxa.

Brachiopods with a laminar secondary layer seem to behave differently. The trend in *Alatorthotetina* sp. show oscillations in the mean values with a significant increase of laminar thickness in the horizon EBHZ71(Fig. 5.4a). In two instances, also some species of Productida seem to show an increase of laminar thickness, as it is the case for *Costiferina* and *Spinomarginifera* (Figs 3.4a, 3.1b). Compared to the trend observed on *Alatorthotetina* sp., the change in productid taxa is observed just before the onset of the extinction interval.

For what concerns *Spinomarginifera*, the data from the Wuchiapingian Nesen and Julfa formations do not show any increase or decrease in laminar thickness (Figs 5.1a, 5.2), with a mean value similar to that observed stratigraphically above, at the base of the Changhsingan in the Mangol and Bear Gully sections (Fig. 5.1a, b). Noteworthy, at the top of the Mangol sections, the values of laminar thickness increase up to 30%, if compared to background values (Fig. 5.1b). However, in the Changhsingian Goniimbrick Formation, species of *Spinomarginifera* do not show any pattern of increase (Fig. 5.4b). In fact, the mean values of the thickness are assessed on the background values,

comprised between 0.2 and 0.35 μm. The same happened for the *Spinomarginifera* at Daijaigou section, which are very close to the PTB (see Appendix C). However, as said above, specimens of species of *Spinomarginifera* close to the PTB in the Daijaigou section of South China are characterized by the absence of the inorganic-rich prismatic layer. This seems to suggest that the record of the specie *Spinomarginifera* is rather complex and may respond to decrease carbonate saturation, both by increasing the thickness of the laminae as the allied Costiferina does, or suppressing the secretion of the prismatic layer. However, a local effect or a possible individual variability rather than a global cause may be responsible of the trendobserved in the Mangol sections. .

The case of the species of *Costiferina* in the Gyanyima section, Tibet, remains intriguing, because the increase in the thickness of the laminae is very large, with mean values shifting from 0.5 μm to 0.7 μm up to the PTB (Fig. 5.5a); this means a thickening of about 40%. In addition, this seems contemporaneous to the changes observed in *Permophricodothyris* and to a changes in physical conditions of seawater, which shows an increase in temperature (Garbelli *et al.* submitted). If these changes in metric are true, we can confidently assess that certain taxa of the Strophomenata and the Rhynchonellata have a different response to the end Permian changes and that further detailed investigations are required. Future applications, may result in a new tool to investigate environmental changes in deep time, also where geochemical analyses are difficult to perform.

5.4 Plates

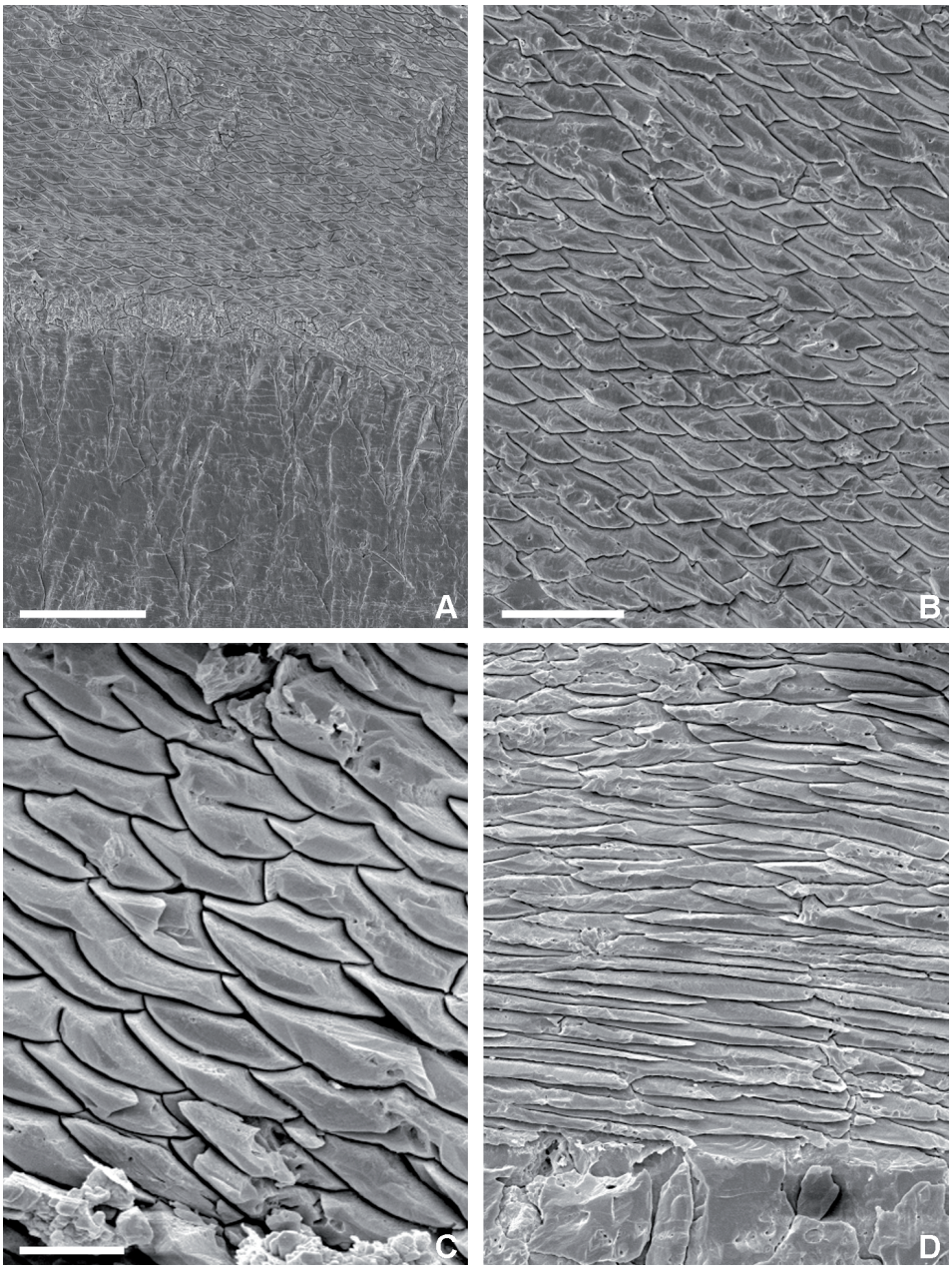

Plate 1. *Comelicania* sp., (A) Specimen VB9A-1, secondary fibrous (f) and tertiary prismatic (p) layer, scale bar 100 μm; (B) details of A showing the secondary fabric texture in cross section, scale bar 30 μm; (C) Specimen VB9B-1, secondary layer fibers in cross section showing keel and saddle outline, scale bar 50 μm; (D) secondary fibers (f) in longitudinal section with transition to the tertiary prismatic layer (p), scale bar 30 μm.

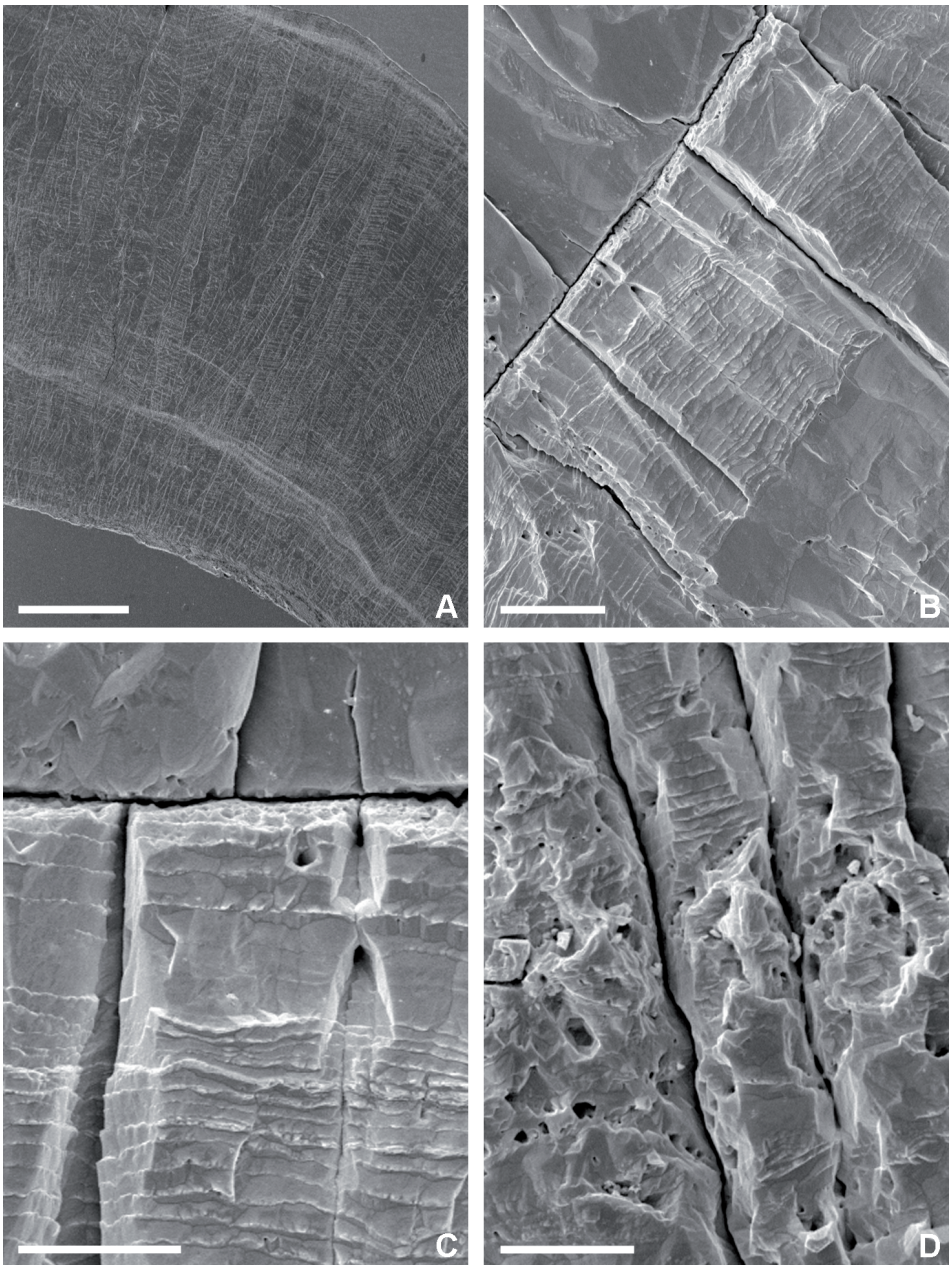

Plate 2. *Comelicania* sp., (A) Specimen PK-5-6-1, thick tertiary prismatic layer with evident growth line due to interruption of calcite secretion, scale bar 500 μm; (B) Specimen VB9B-2, details of prisms of the tertiary layer showing evident thin growth banding (a) and large interruption of the growth (d), scale bar 20 μm; (C) details of B in which it is evident the interruption of secretion (arrow) causing the formation of a major growth line, scale bar 10 μm; (D) Specimen VB9A-1, details of growth line in the prisms in which it is evident dissolution, scale bar 10 μm

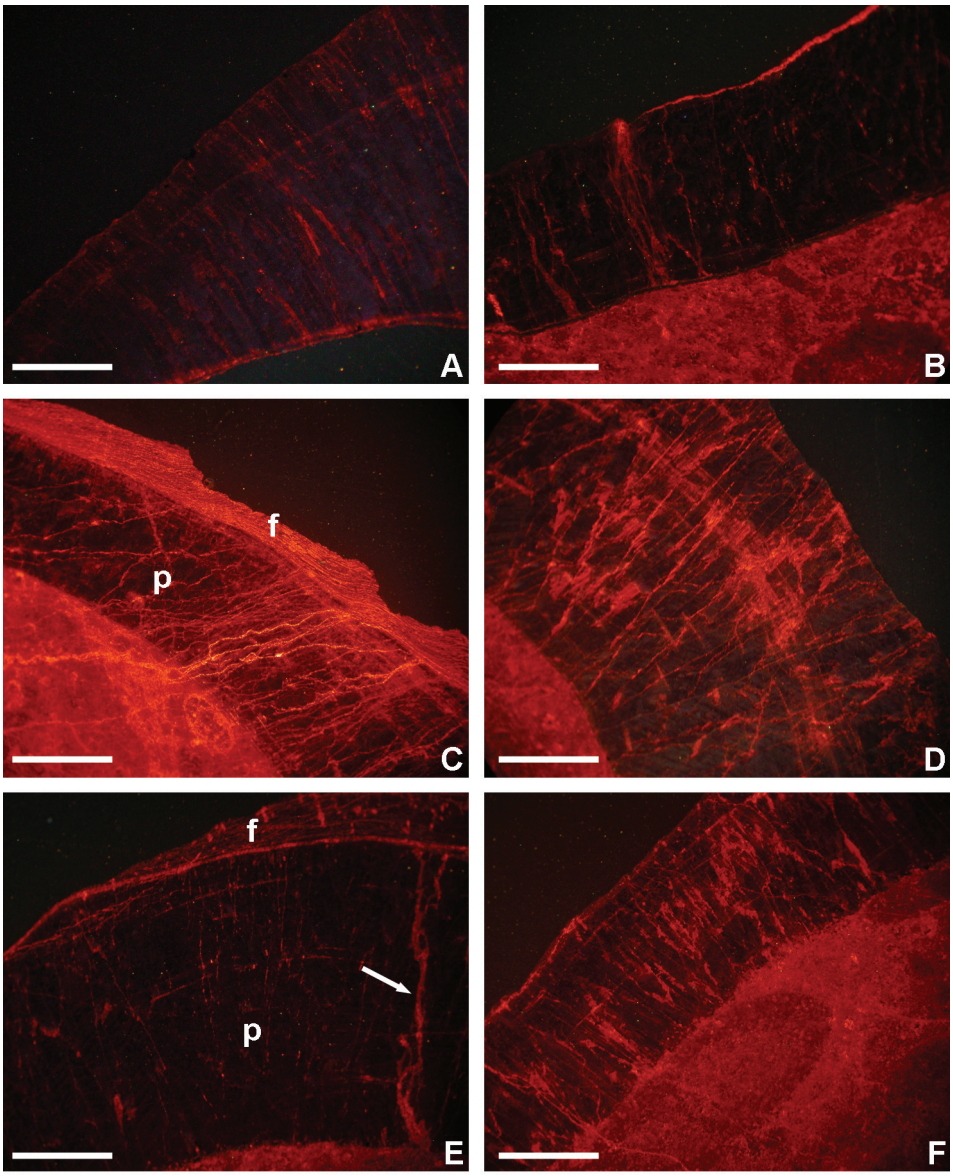

Plate 3. *Comelicania* sp., (A) specimen VB9B-1, non luminescent tertiary prismatic layer, scale bar 800 µm; (B) specimen VB9B-2, , non luminescent tertiary prismatic layer with some thinc slightly luminescent fracture filled by diagenetic fluids, scale bar 600 µm; (C) specimen PK56-1, very luminescent secondary layer (f) with non luminescent tertiary layer (p) in which are evident numerous fracture filled by diagenetic fluids, scale bar 600 µm; (D) specimen PK56-1, non luminescent tertiary layer in which are evident numerous fracture filled by diagenetic fluids, scale bar 400 µm, scale bar 250 µm; (E) specimen VB9A1, the shell illustrating a non luminescent fibrous (f) and prismatic layers (p) with a fracture (f), scale bar 400 µm; (F) specimen VB9A1, a different part of the shell that is more altered by fractures filled by diagenetic fluids, scale bar 900 µm.

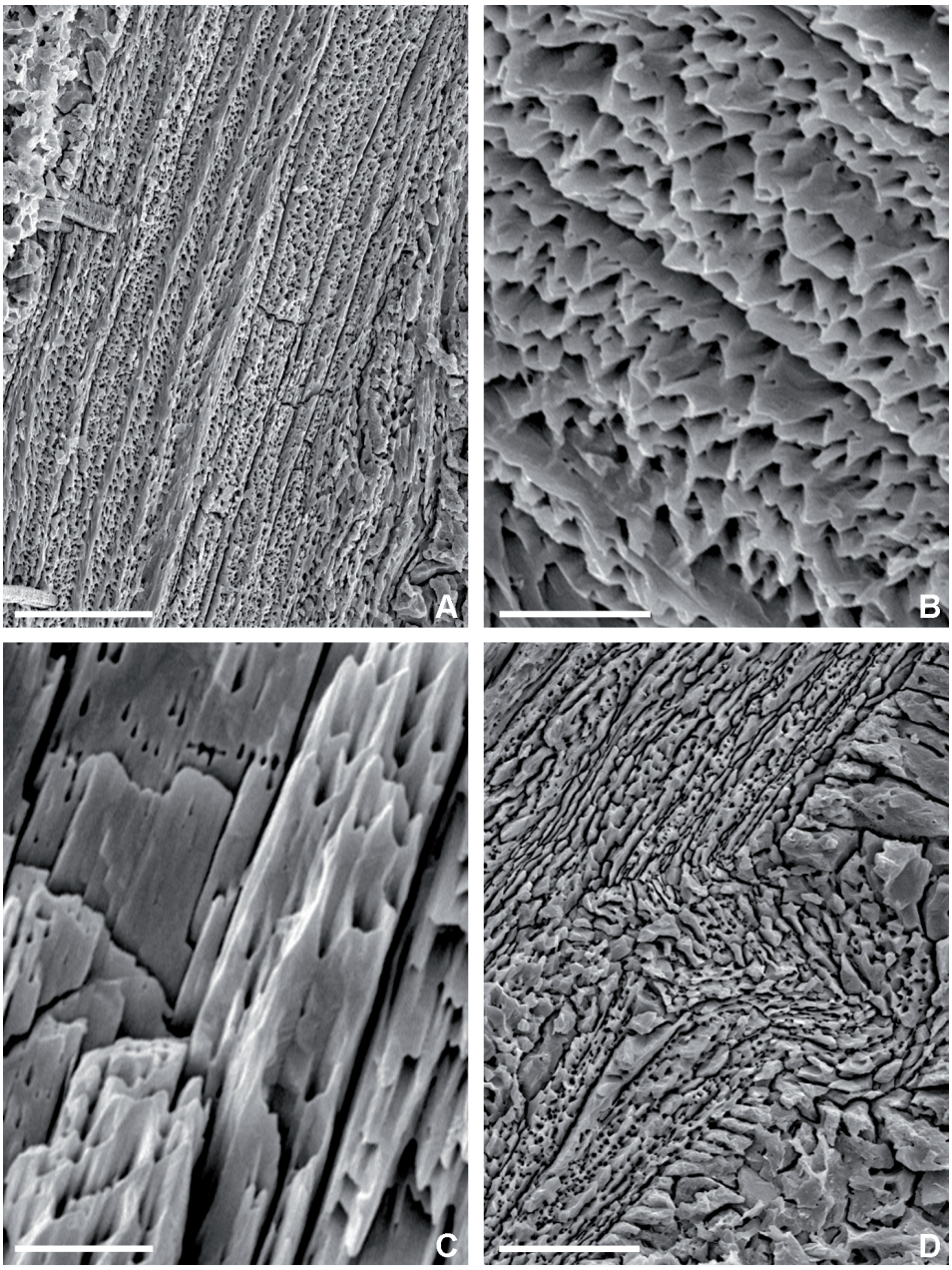

Plate 4. *Haydenella kiangsiensis*, (A) specimen JU129-4, shell composed entirely of secondary layer laminae, scale bar 25 μm; (B) details of (A) with cross section of the laminae in, where the single structural units (blades/laths) are observable, scale bar 6 μm; (C) specimen JU129-1, longitudinal section of a set of laminae in, scale bar 4 μm; (D) specimen JU129-4, pseudopuncta which forms an endospine protruding from the inner valve surface, scale bar 15 μm.

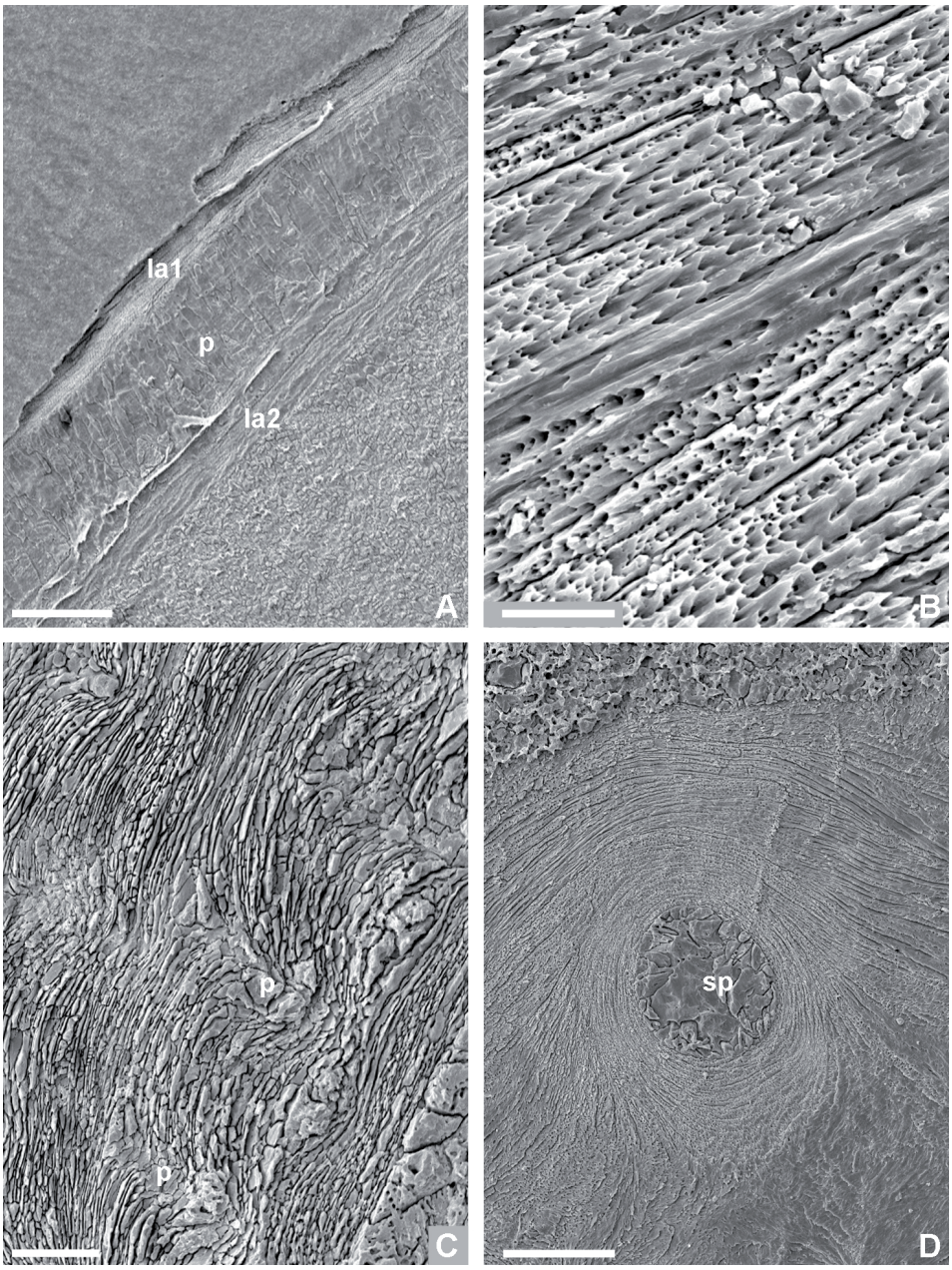

Plate 5. *Spinomarginifera spinosocostata*, (A) specimen JU1-3, shell composed of an outer secondary laminar layer (la1), an intermediate prismatic (p) and and inner laminar layer (la2), scale bar 50 µm; (B) details of (A) showing the cross bladed laminar layer, scale bar 8 µm; (C) specimen JU121-4, secondary laminar layer crossed by pseudopunctae (p) which deflected laminae inwardly, scale bar 12 µm; (D) specimen JU1-3, cross section of a spine channel (sp) filled by diagenetic calcite, scale bar 60 µm.

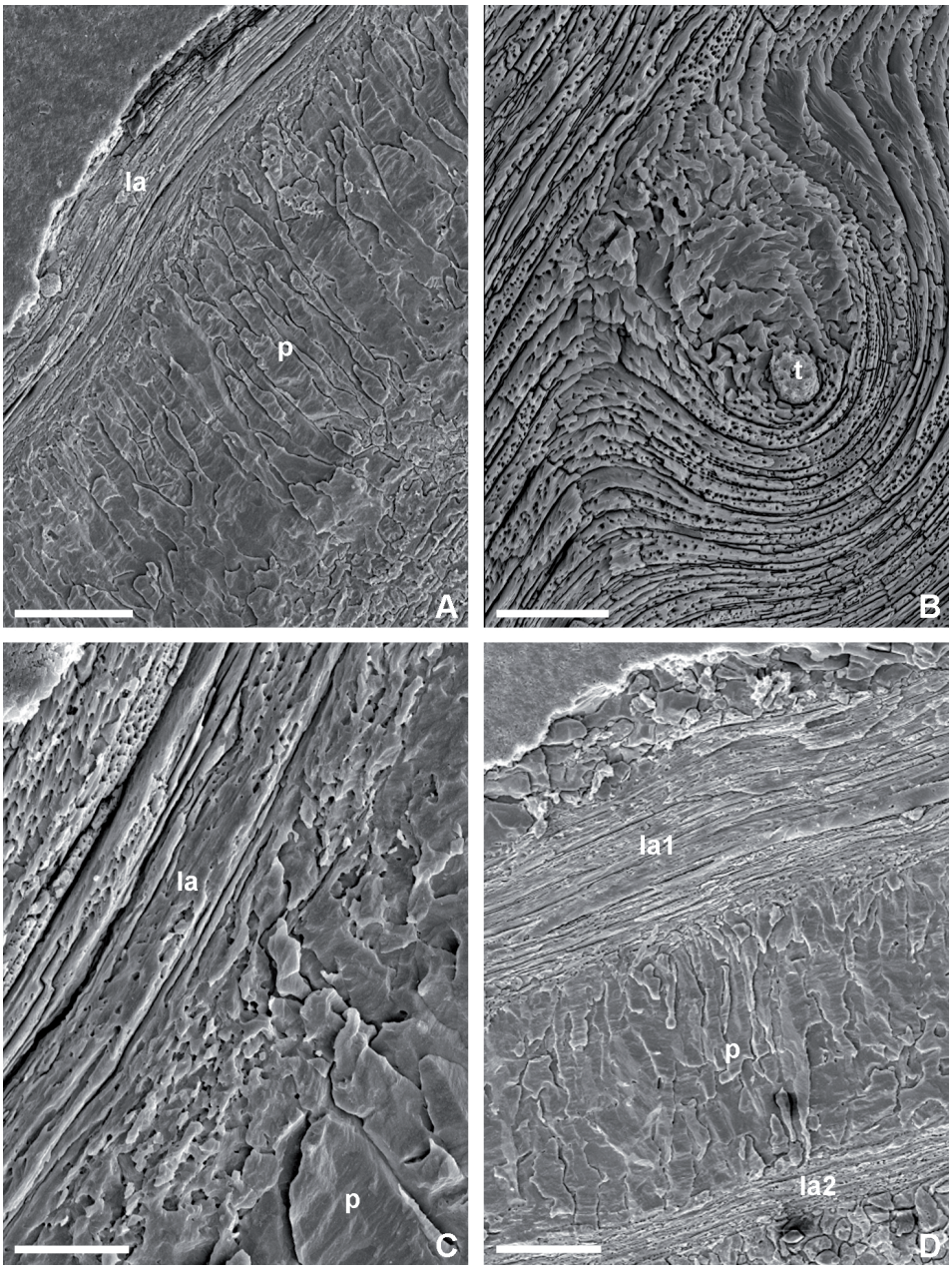

Plate 6. *Spinomarginifera iranica*, (A) specimen JU1-4, shell composed of secondary laminar (la) and tertiary prismatic (p) layers, scale bar 50 μm; (B) specimen JU115-1, secondary laminar layer crossed by a pseudopuncta with an inner rod of calcite called taleola (t), scale bar 15 μm; (C) specimen JU1-4, transition from the secondary laminar layer (la) to the tertiary prismatic one (p), scale bar 15 μm; (D) specimen JU1-3, shell with alternation of secondary laminar layer (la1, la2), tertiary prismatic layer (p), scale bar 40 μm.

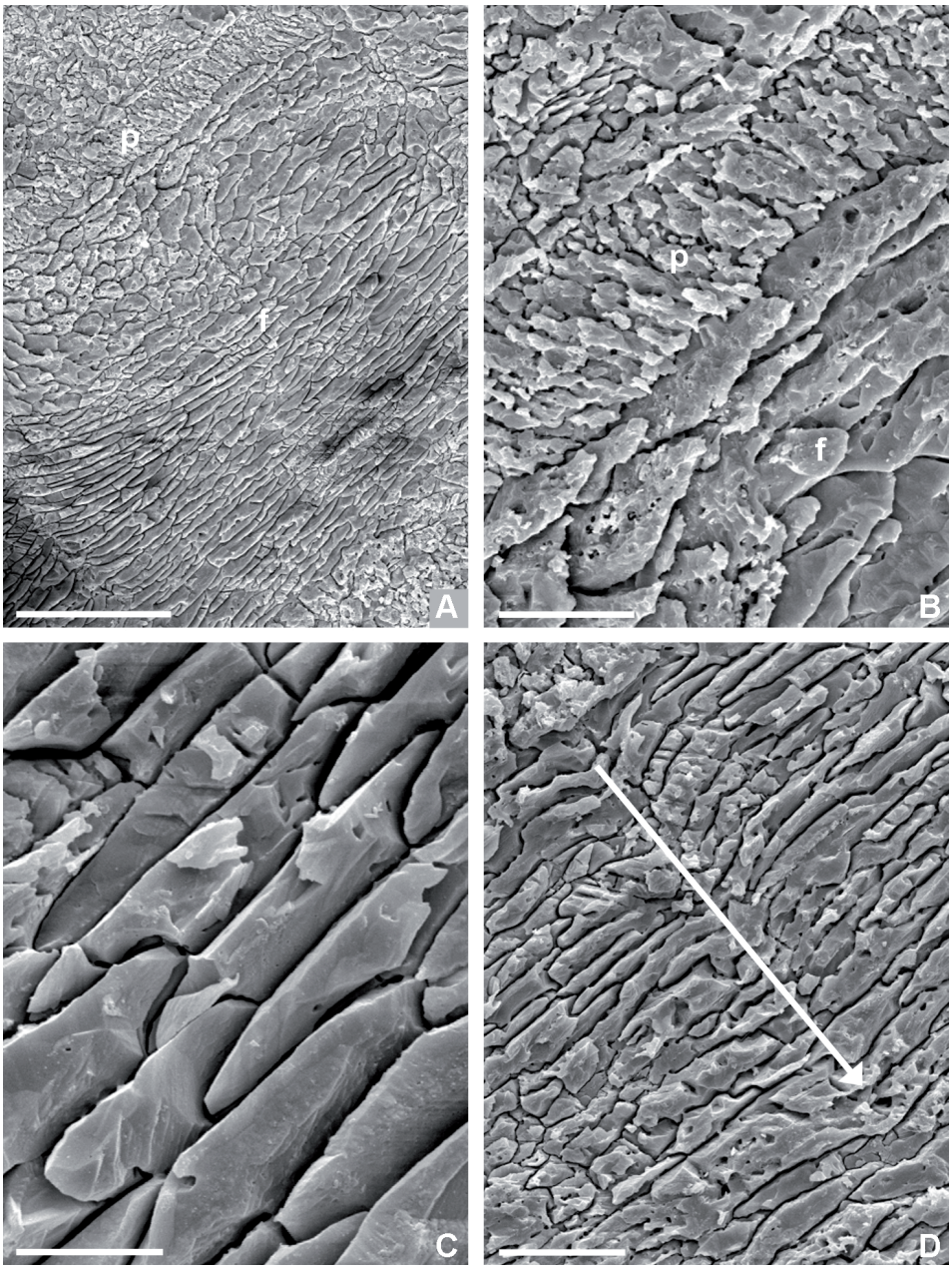

Plate 7. *Acosarina minuta*, (A) specimen JU77-2, shell composed of a recristallyzed outer primary layer (p) and a secondary fibrous one (f), scale bar 50 μm; (B) details of (A) showing the primary layer and the outer part of the secondary layer, scale bar 10 μm; (C) cross section of the secondary fibers with a keel and saddle outline, scale bar 5 μm; (D) puncta crossing the secondary shell which deflected the fibers outwardly, scale bar 12 μm.

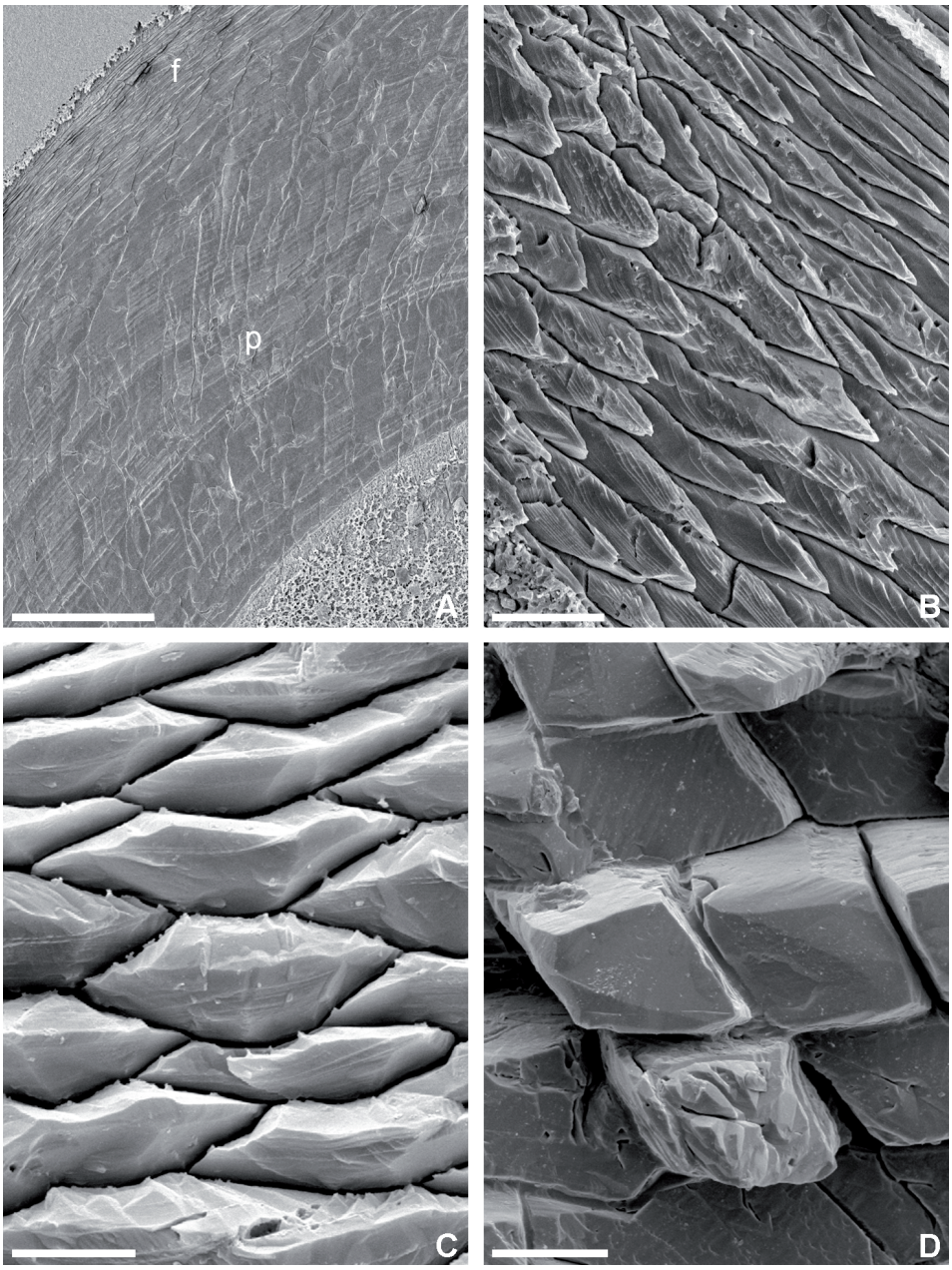

Plate 8. *Transcaucasathyris araxensis*, (A) specimen JU10-4, secondary fibrous (f) and tertiary prismatic (p) layers, scale bar 250 μm; (B) specimen JU136-1, secondary fibers with evident accretion bands, scale bar 20 μm; (C) specimen JU129-1, cross section of secondary fibers with poorly developed keel and saddle outline, bar 10 μm; (D) specimen JU89-1, cross section of diamond shape secondary fibers in the inner secondary layer, scale bar 20 μm.

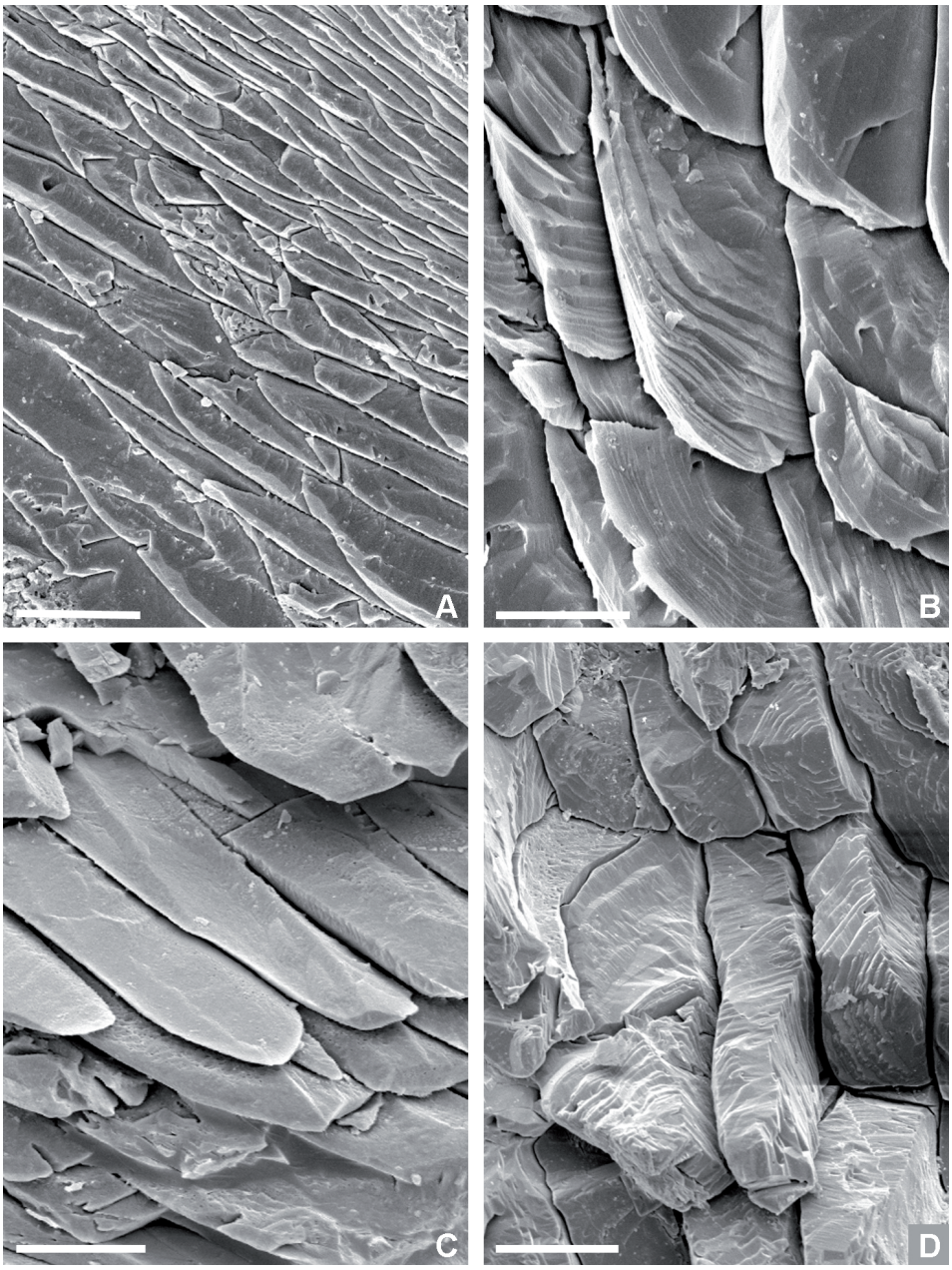

Plate 9. *Transcaucasathyris araxensis*, (A) specimen JU10-4, secondary fibrous layer, scale bar 25 μm; (B) specimen JU136-1, details of bands of growth in the secondary fibers, scale bar 10 μm. *Transcaucasathyris* sp., (C) specimen JU10-1, spatulate termination of secondary fibers, bar 10 μm; (D) specimen JU129-1 , accretion bands on the diamond shape secondary fibers of the inner secondary layer, scale bar 25 μm.

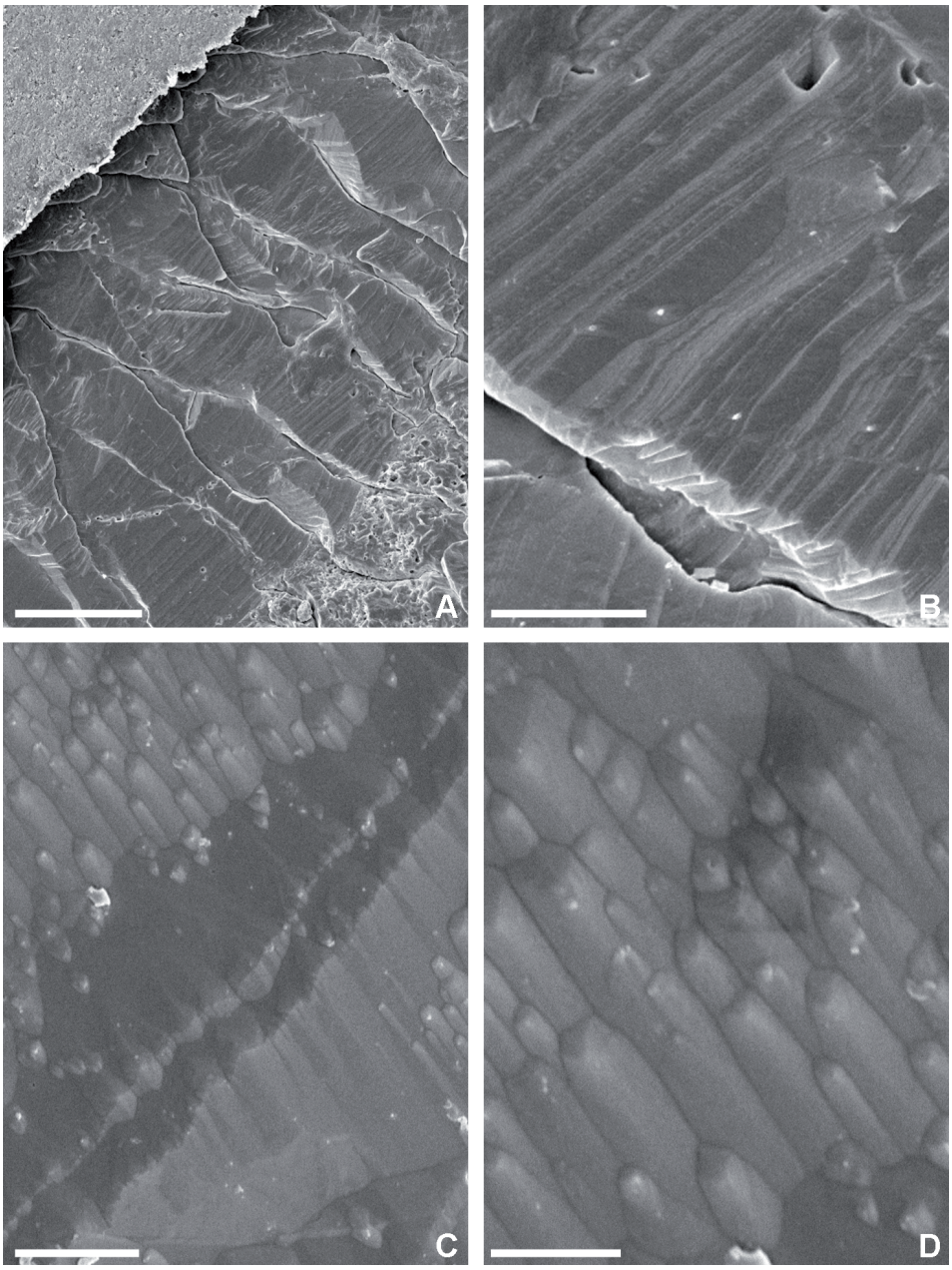

Plate 10. T*ranscaucasathyris* sp., (A) specimen JU140-1, prismatic tertiary layer, scale bar 50 μm; (B) details of A showing growth banding, scale bar 10 μm. *Transcaucasathyris araxensis*, (C) specimen JU136-1, high resolution image of a prism in the tertiary layer in which are evident subunits with elongated prismatic shape, scale bar 5 μm; (D) magnification of C, scale bar 2.5 μm.

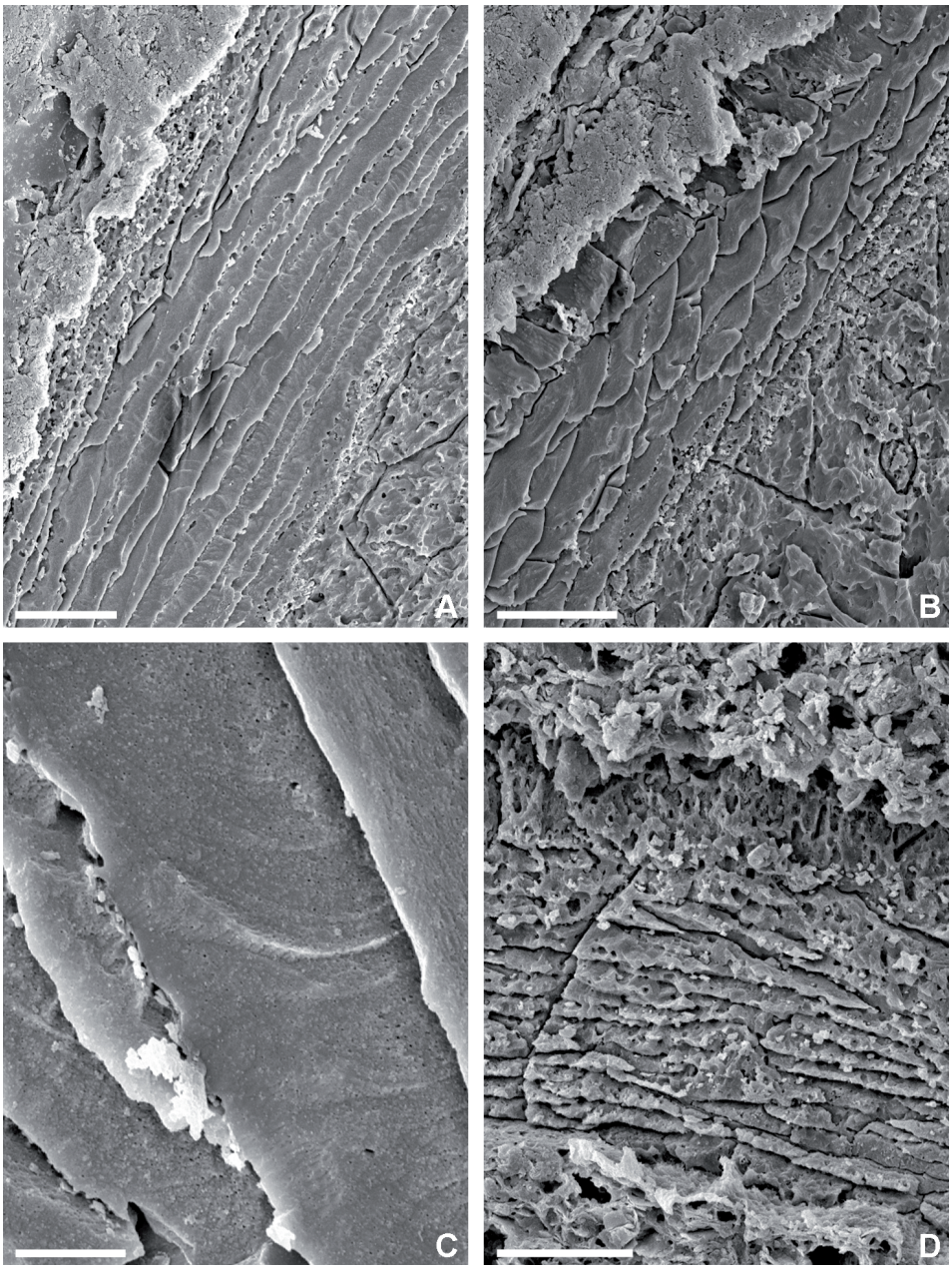

Plate 11. *Paracrurithyris pygmaea*, (A) specimen JU148-5, shell composed of fibers of the secondary layer in longitudinal section, scale bar 25 μm; (B) secondary fibers in oblique-transverse section, scale bar 25 μm; (C) details of a fiber showing growth banding, scale bar 4 μm. *Paracrurithyris* sp., (D) specimen JU172-3, shell composed of secondary fibers which are morphologically altered, scale bar 20 μm.

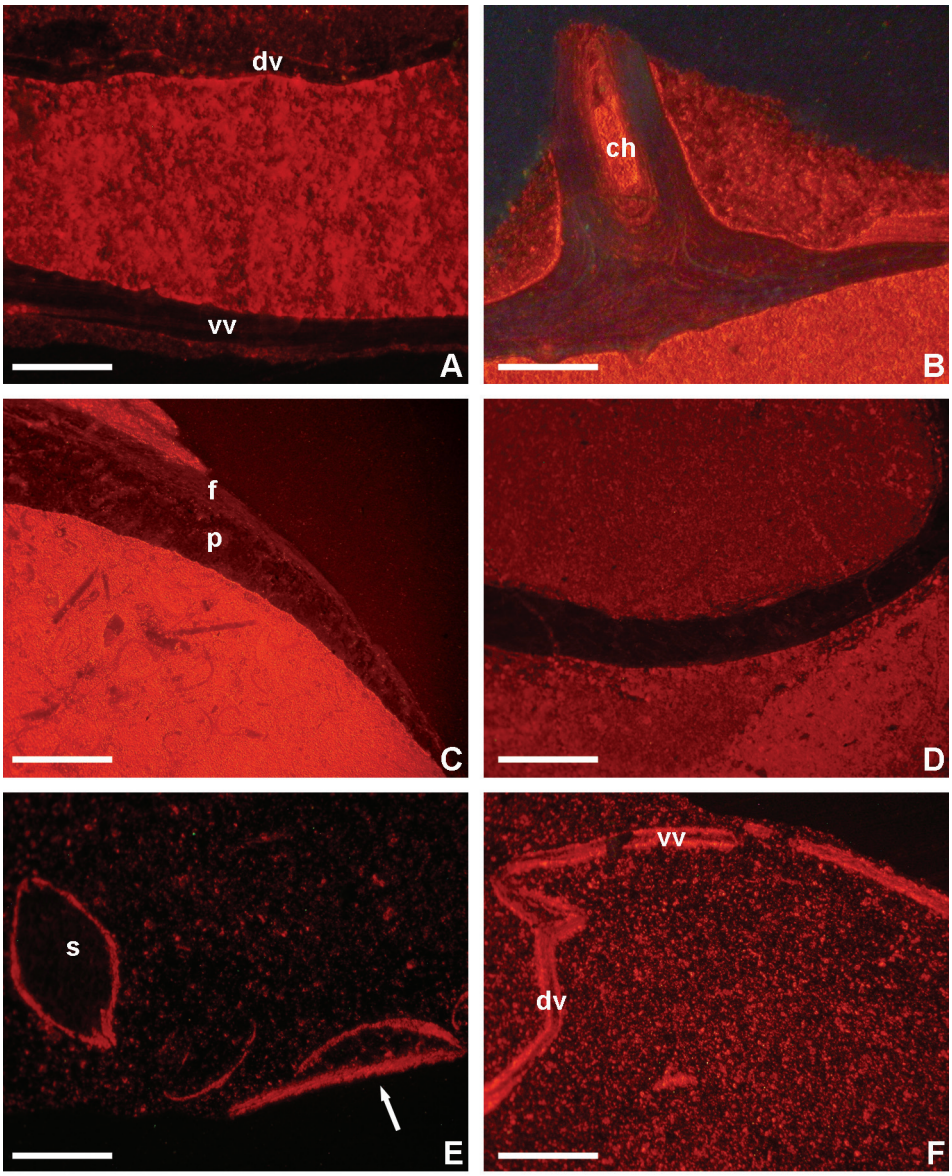

Plate 12. (A) *Spinomarginifera* sp., specimen JU115-1, non luminescent ventral (vv) and dorsal (dv) valves composed ofsecondary layer, scale bar 500 μm; (B) *Spinomarginifera* sp., specimen JU117-1, non luminescent shell crossed by a spine channel (ch) filled by luminescent diagenetic calcite, scale bar 350 μm; (C) *Transcaucasathyris araxensis*, specimen JU136-1, secondary fibrous (f) and tertiary prismatic (p) layers which are to slightly luminescent, scale bar 700 μm; (D) *Transcaucasathyris* sp., specimen JU139-3, completely non luminescent shell wall; scale bar 600 μm; (E) P. pygmaea, JU172-8, dorsal luminescent valve (arrow); in the matrix, an undetermined small brachiopods is present, which is luminescent too, scale bar 150 μm; (F) *Haydenella kiangsiensis*, specimen JU172-4, very luminescent ventral (vv) and dorsal (dv) valves, scale bar 200 μm.

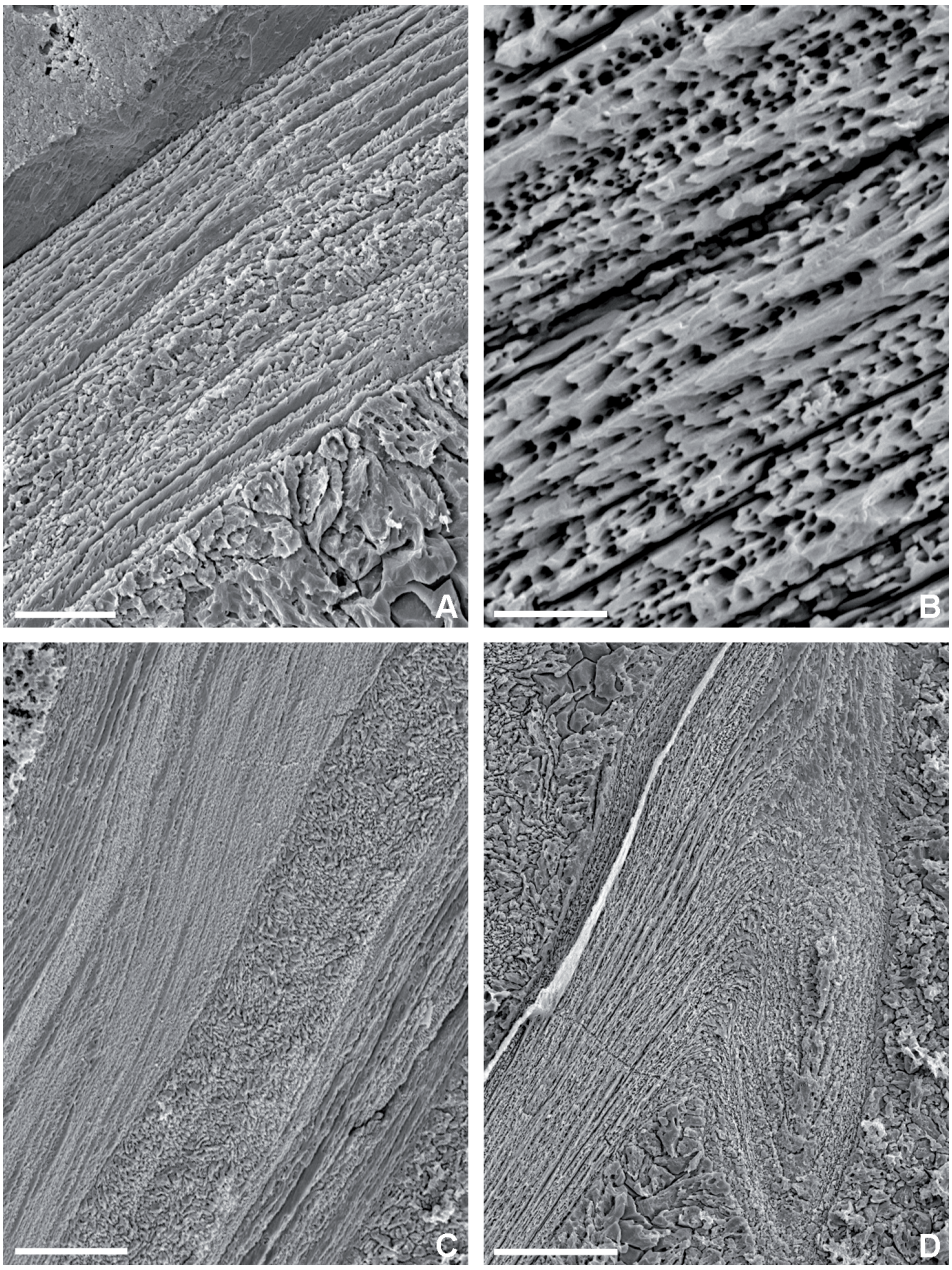

Plate 13. *Haydenella* sp., (A/C) specimen CH4-5 shell composed of secondary cross bladed laminae, scale bar 25 µm and 60 µm respectively ; (B) specimen CH4-5, details of secondary laminae in cross section showing interstitial spaces between structural units, scale bar 5 µm; (D) specimen CH40-5, pseudopunctae formed by inwardly deflected laminae protruding in the inner shell to form an endospine, scale bar 50 µm.

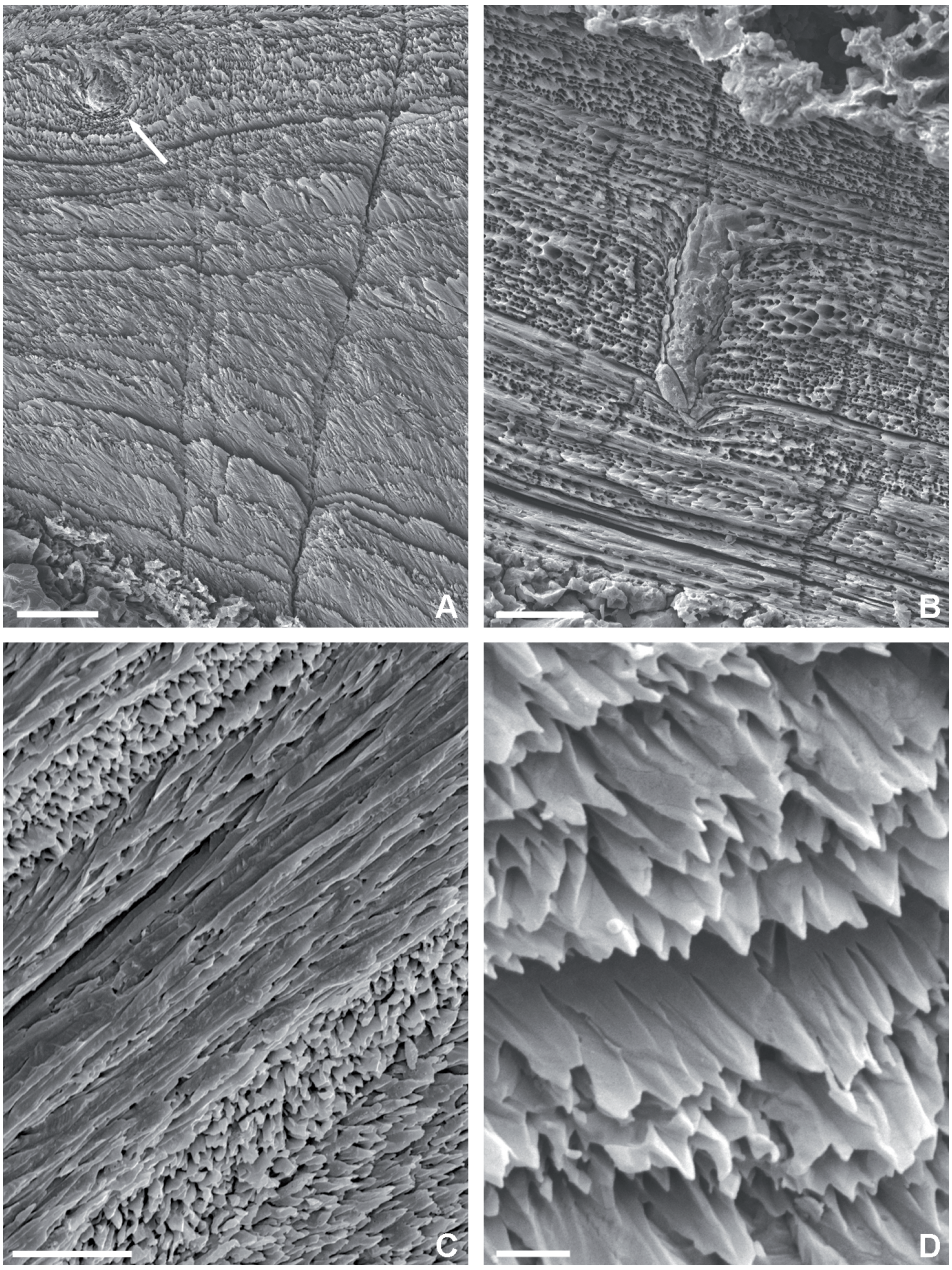

Plate 14. *Cathaysia* sp., (A) specimen CH71-8, shell composed of cross bladed laminae of the secondary layer with pseudopunctae (arrow), scale bar 30 μm; (B) specimen CH71-8, details of pseudopuncta showing the inner core of microgranular calcite, called taleola, scale bar 15 μm; (C) specimen CH4-8, packages of laminae with the principal axis of structural units oriented in orthogonal direction, scale bar 10 μm; (D) specimen CH71-8, details of the laminae composed of aligned blades/laths, scale bar 2 μm.

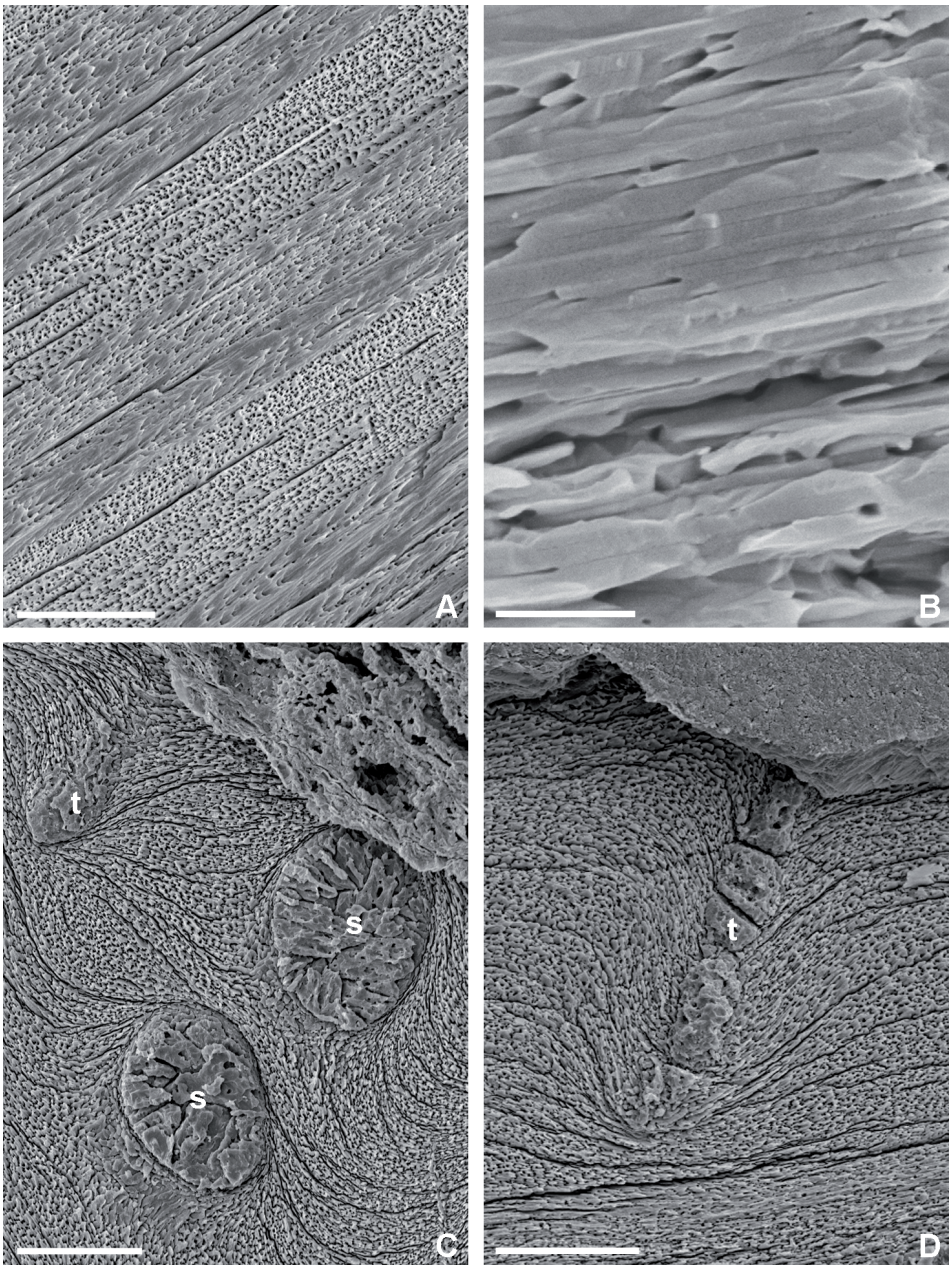

Plate 15. *Paryphella* sp., (A) specimen CH136-2, shell wall composed of a secondary laminar layer which is cross bladed with packages of laminae orthogonally oriented, scale bar 15 μm; Pariphella sulcatifera, (B) specimen CH4-3, details of laminae in longitudinal section, scale bar 3 μm; (C) specimen CH5-9, shell crossed by spine channels (s) in the posterior part of the shell and a pseudopuncta with taleola (t), scale bar 40 μm; (D) specimen CH5-9, pseudopuncta deflecting the laminae inwardly, scale bar 40 μm.

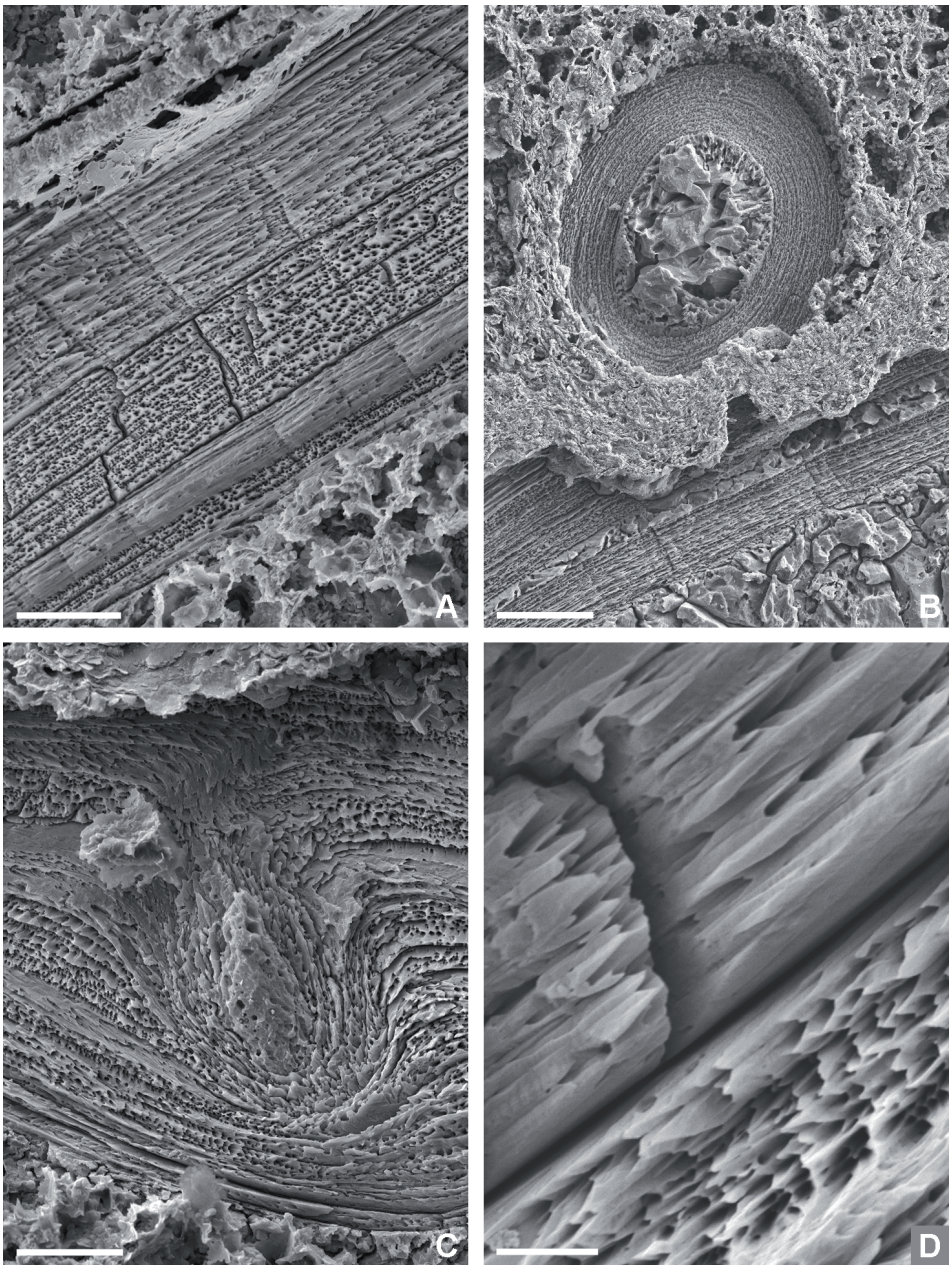

Plate 16. *Spinomarginifera* sp., (A) specimen CH71-3, shell wall composed of laminar secondary layer which is cross bladed, scale bar 20 μm; (B) specimen CH71-17, cross section of a spine in the proximal part of the shell wall, with the spine channel filled by diagenetic calcite, scale bar 50 μm; (C) specimen CH71-3, pseudopuncta crossing the shell and deflecting the laminae inwardly, scale bar 20 μm; (D) specimen CH71-17, details of longitudinal and cross sections of the cross bladed laminae, scale bar 3 μm.

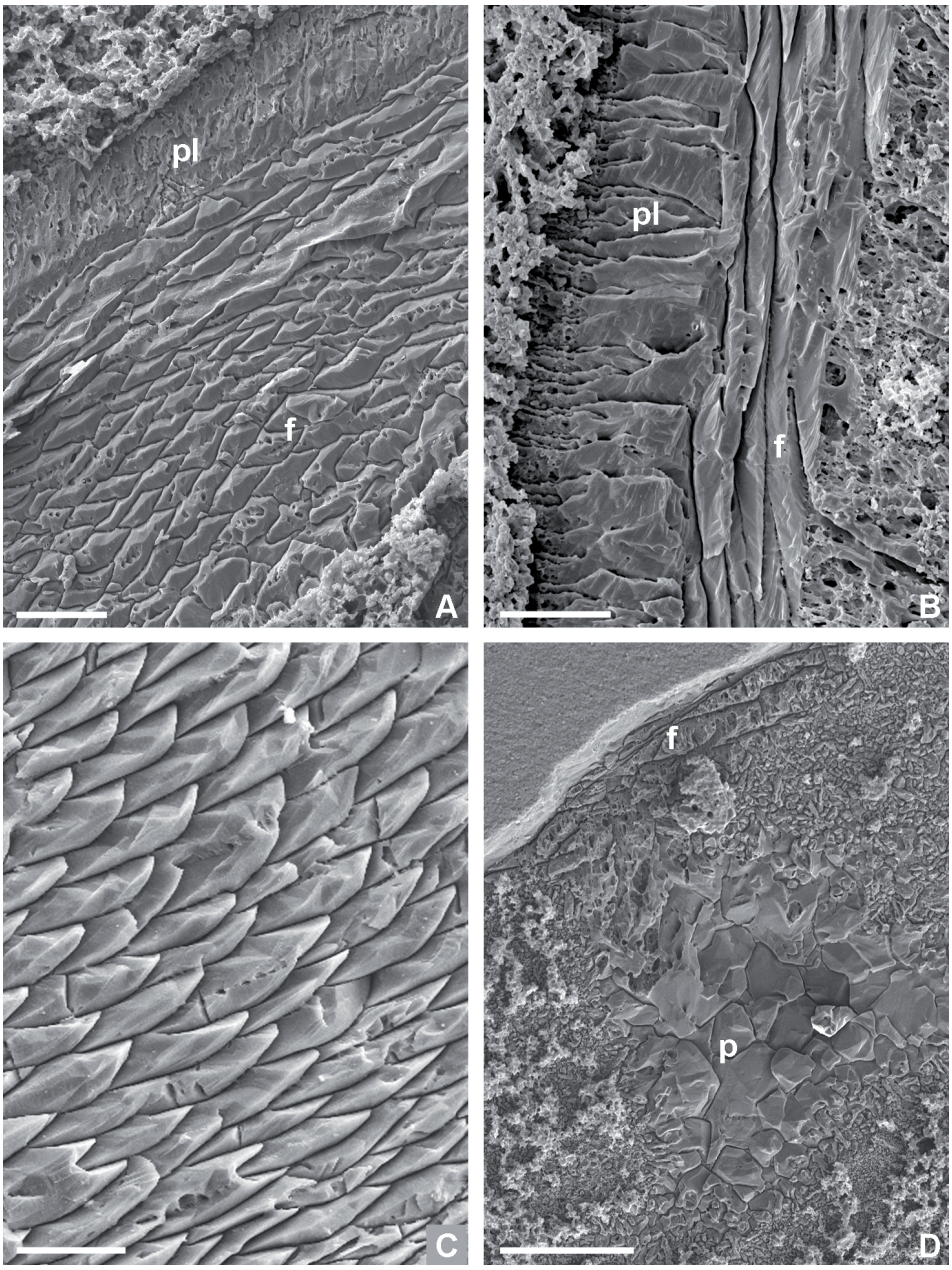

Plate 17. *Transcaucasathyris* sp., (A) specimen CH4bis-3, shell composed of a primary outermost layer(p) and an inner fibrous layer (f), scale bar 40 μm; (B) specimen CH30-4, details of the transition from the primary layer (pl) to the secondary one (f), scale bar 30 μm; (C) specimen CH4bis-3, fibers in cross section showing a keel and saddle outline, scale bar 15 μm; (D) specimen CH4bis-3, remains of the fibrous secondary layer (f) and the prismatic tertiary ones? (p), scale bar 100 μm.

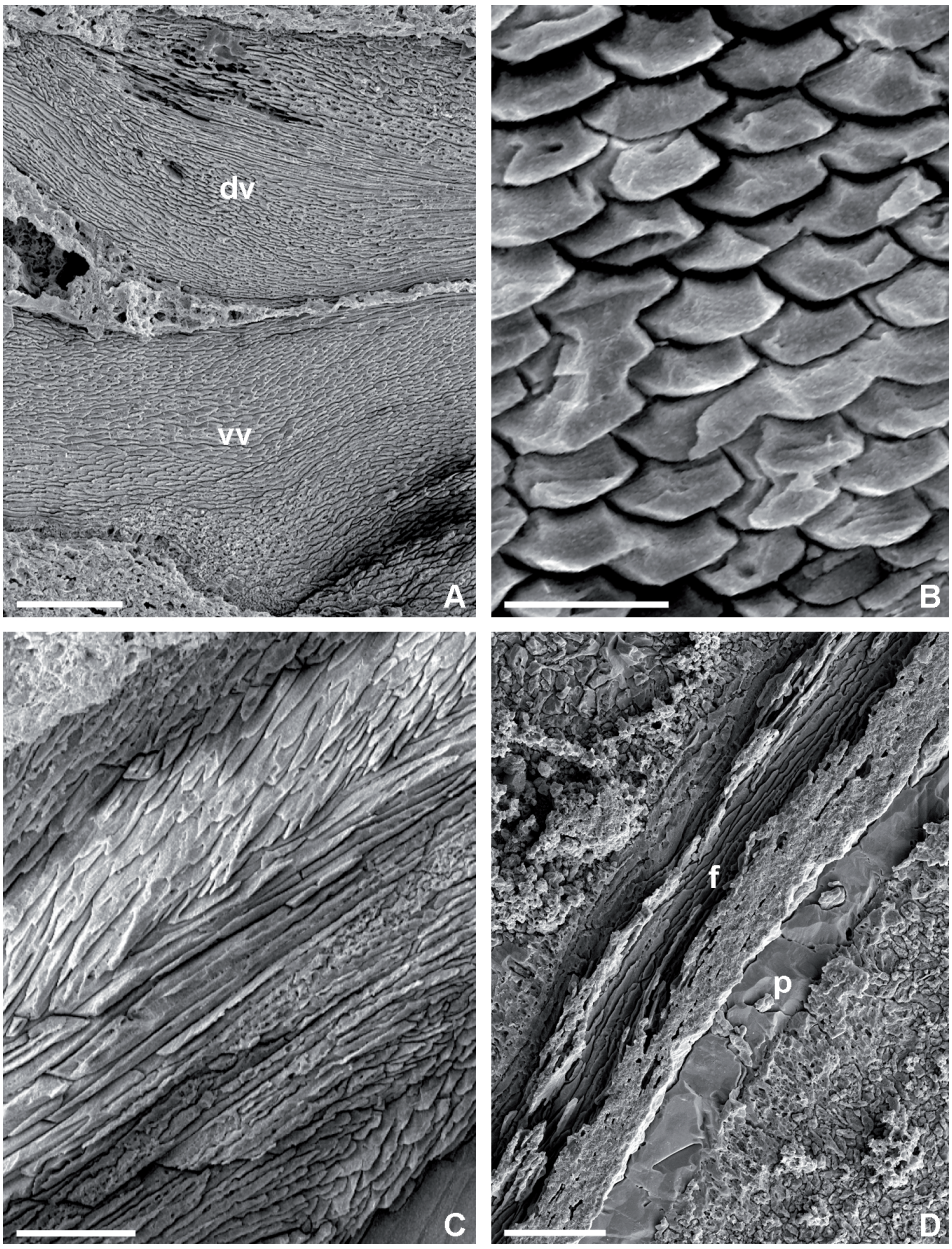

Plate 18. *Paracrurithyris pygmaea*, (A) specimen CH85bis-4, ventral (vv) and dorsal (dv) valves entirely composed of secondary fibrous layer, scale bar 50 µm; (B) specimen CH87bis-4, details of secondary fiber in cross section with keel and saddle outlines, scale bar 10 µm; (C) specimen CH87bis-40, section of the secondary layer in which the fibers are organized in differently oriented packages, scale bar 30 µm; (D) CH30-11 , shell composed of a fibrous secondary (f) and a thin prismatic tertiary (p) layers, scale bar 40 µm.

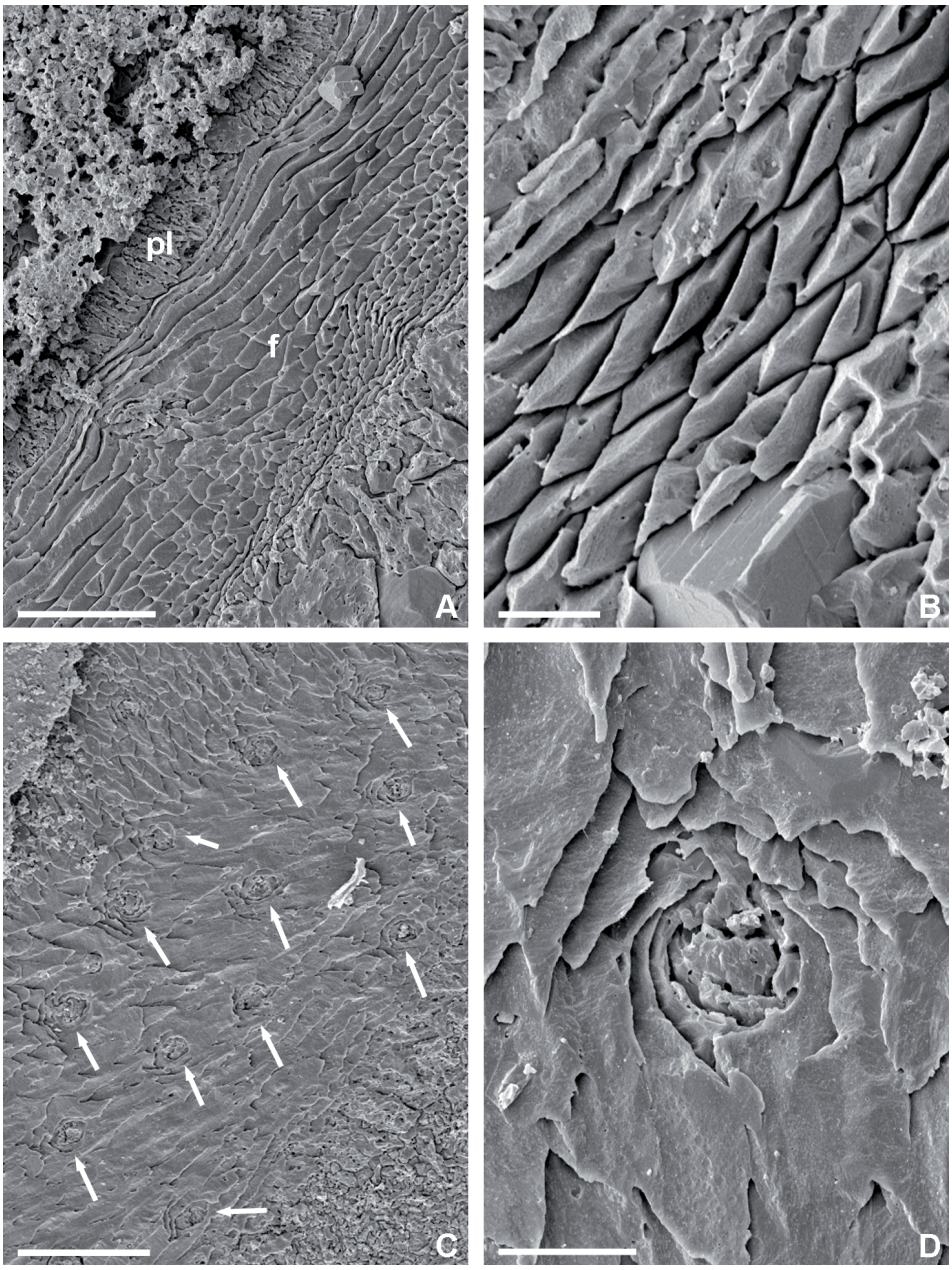

Plate 19. *Paraspiriferina alpha*, (A) specimen CH12-3, shell composed of a primary outermost layer(p) and an inner fibrous layer (f), scale bar 50 μm; (B) specimen CH12-3, detail of secondary layer showing fibers in cross section with a keel and saddle outline , scale bar 3 μm; (C) specimen CH12-3, secondary layer crossed by numerous punctae (arrows) in a roughly planar section , scale bar 40 μm; (D) details of C, scale bar 15 μm.

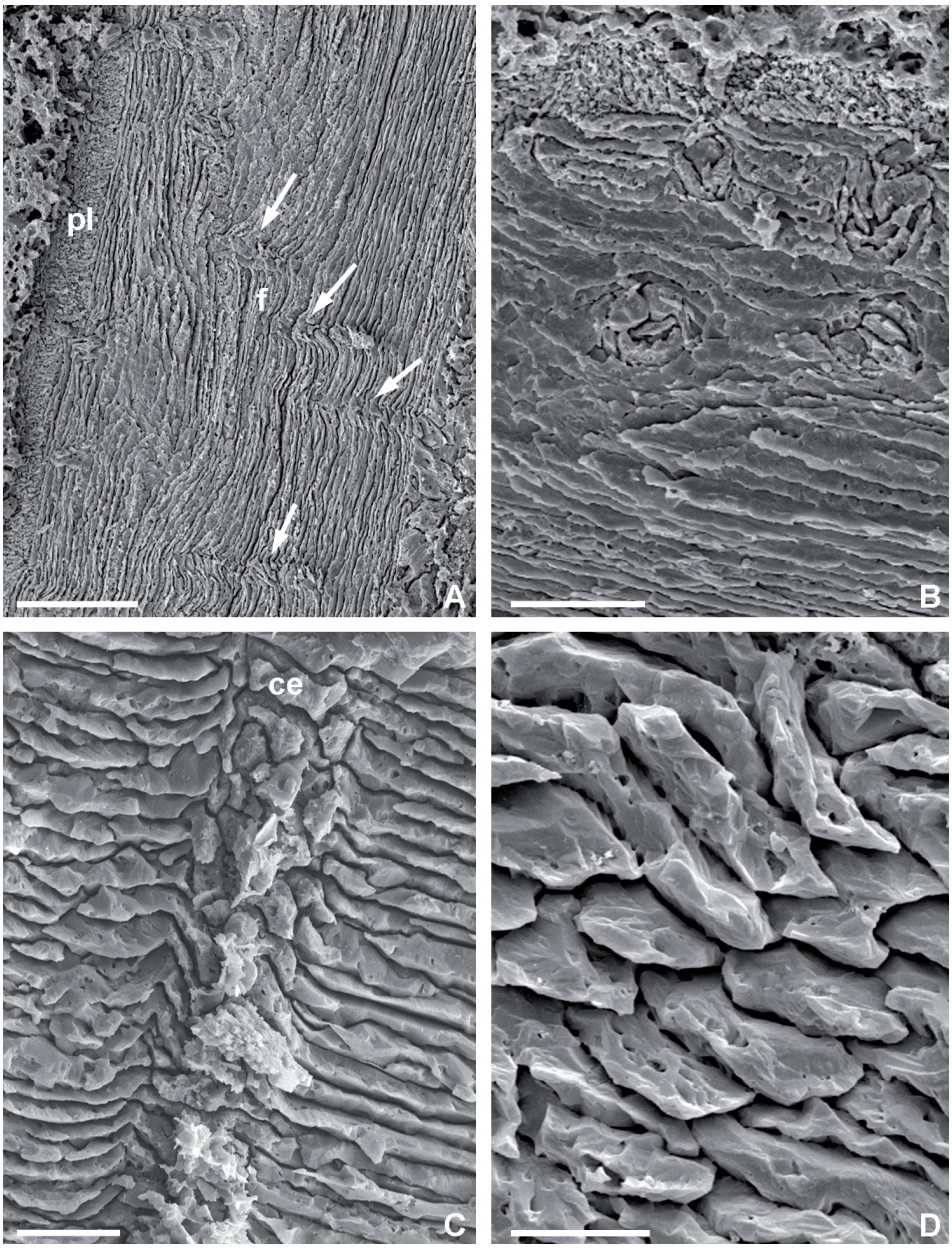

Plate 20. *Acosarina minuta*, (A) specimen CH72-11, shell composed of an outermost recrystallized primary layer (p) and a fibrous secondary layer (f) crossed by punctae (arrows), scale bar 50 µm; (B) specimen CH72-11, cross-section of the punctae, scale bar 30 µm. *Acosarina* sp., (C) specimen CH2bis-1, transverse section of a puncta filled by cement (ce), scale bar 10 µm. *Acosarina minuta*, (D) specimen CH72-11, details of the fibers which do not show a well defined outline, scale bar 10 µm.

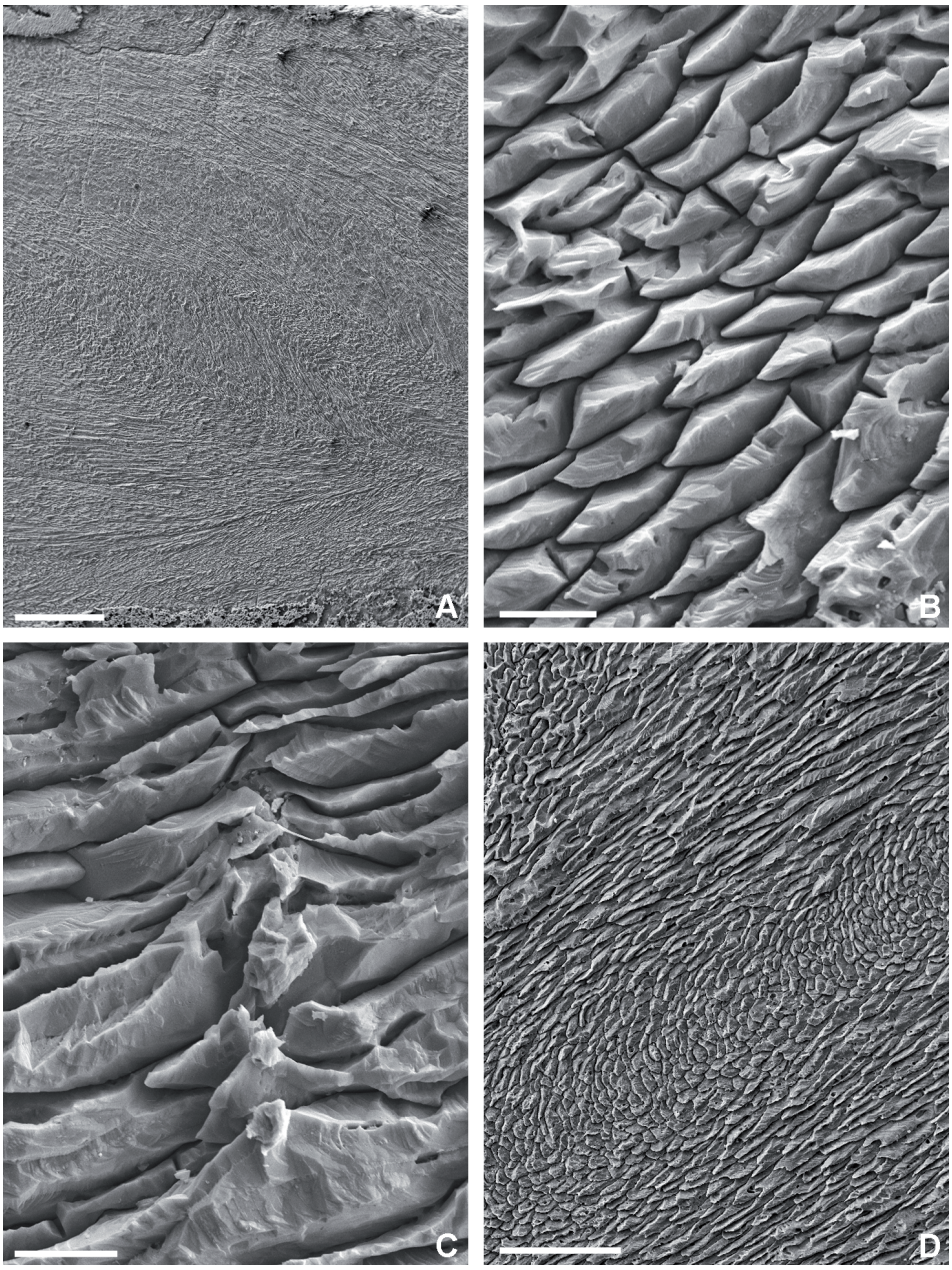

Plate 21. *Peltichia* sp., (A) specimen CH60-1, very thick shell composed entirely of a fibrous secondary layer, scale bar 300 μm; (B) specimen CH60-1, details of the secondary layer showing fibers in cross section with a keel and saddle outline, scale bar 10 μm; (C) specimen CH60-1, fibers outwardly deflected by a puncta, scale bar 5 μm; (D) changes in grow direction of the fibers, scale bar 100 μm.

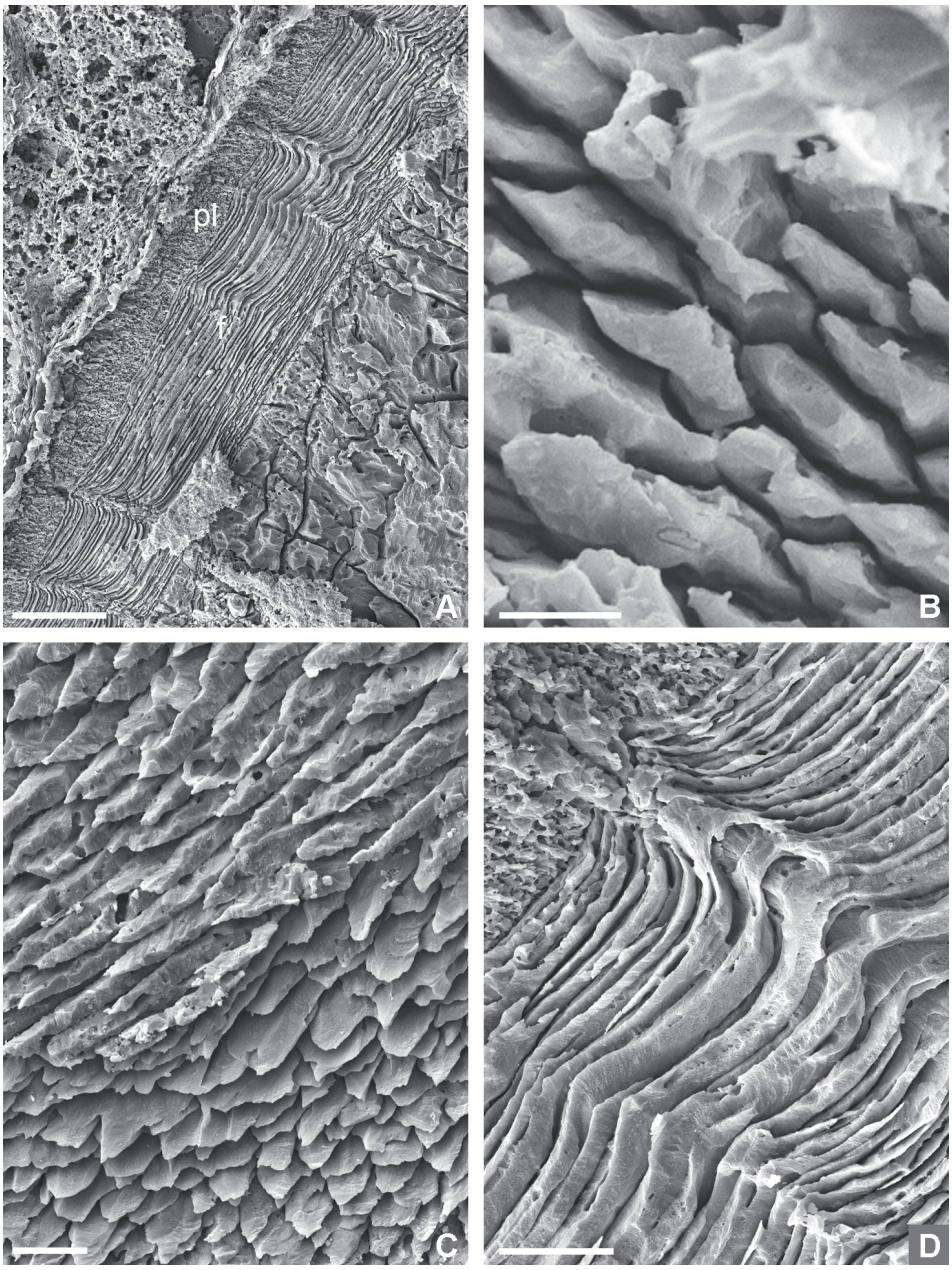

Plate 22. *Hustedia* sp., (A) specimen CH60-15 shell composed of an outermost recrystallized primary layer (pl) and a secondary fibrous layer (f) crossed by punctae (arrows), scale bar 60 μm; (B) specimen CH60-15, details of secondary fibers in cross section with keel and saddle outlines, scale bar 4 μm; (C) specimen CH60-15, fibers with spatulate termination, scale bar 10 μm; (D) specimen CH60-15, puncta crossing the outer secondary layer, deflecting the fibers outwardly and penetrating into the inner part of the primary layer, scale bar 15 μm.

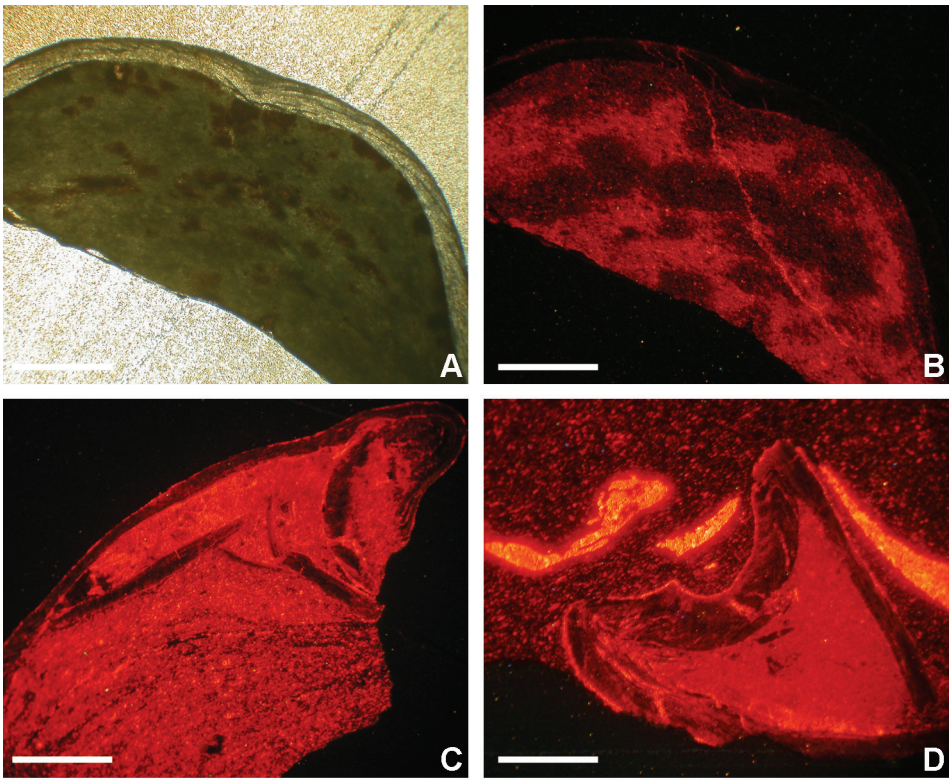

Plate 23. (A-B) *Paracrurithyris pygmaea*, specimen CH86-1, non luminescent shell filled by a slightly luminescent matrix, scale bar 450 µm; (C) *Paracrurithyris pygmaea*, specimen CH85bis-20, non luminescent shell which is fragmented inside a luminescent matrix, scale bar 600 µm; (D) *Paracrurithyris pygmaea*, specimen CH86bis-20, non luminescent to slightly luminescent shell; luminescent cements are present in the rock matrix which is otherwise coarse not luminescent, scale bar 300 µm.

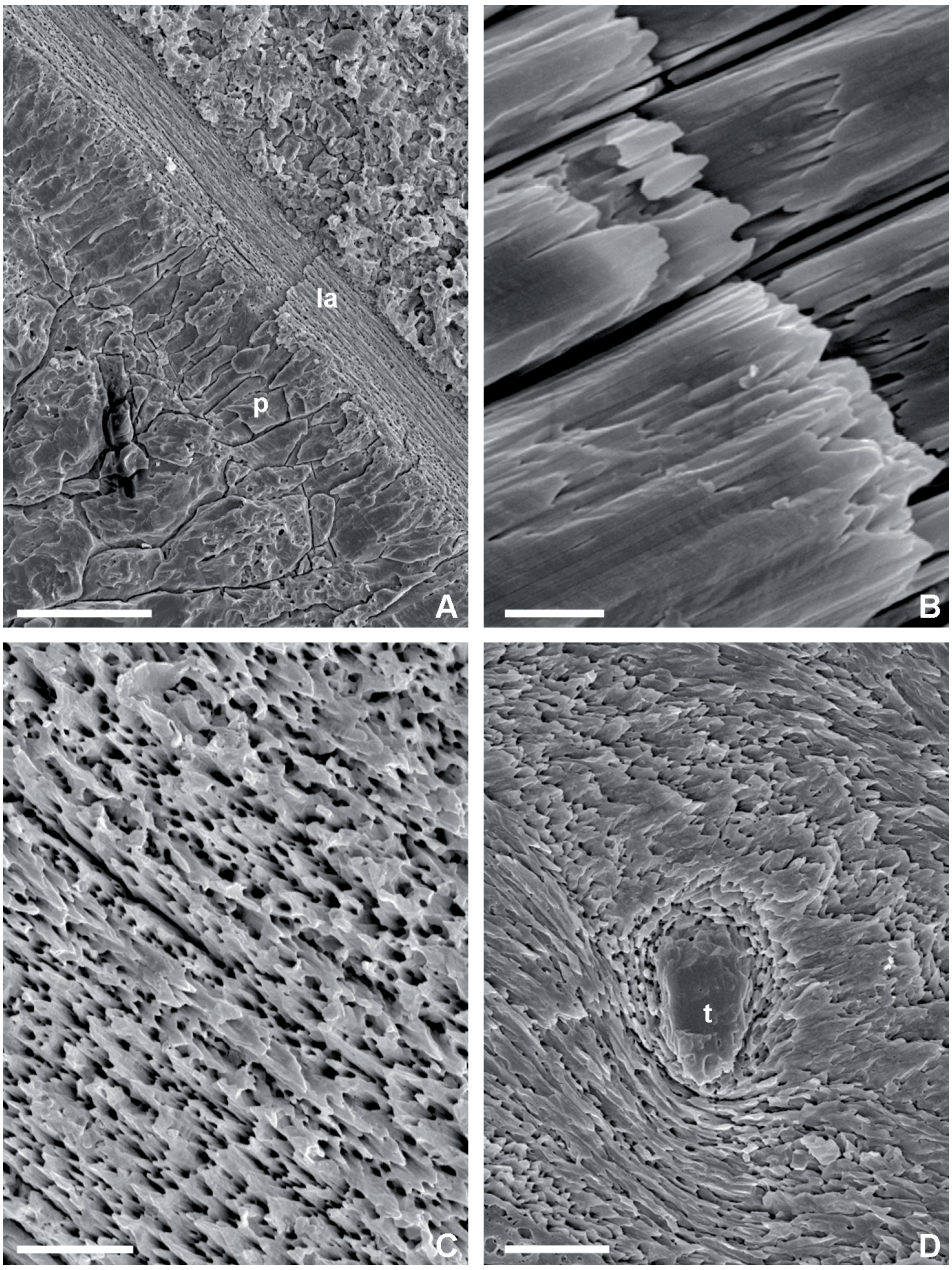

Plate 24 *Spinomarginifera helica*, (A) specimen EBHZ15-15, laminar secondary (la) and prismatic tertiary (p) layer, scale bar 50 µm; (B) specimen EBHZ71-10, laminae of the secondary layer in longitudinal section, scale bar 2 µm; (C) specimen EBHZ69-4, laminae of the secondary layer in cross section, scale bar 5 µm; (D) specimen EBHZ65-3, pseudopuncta crossing the secondary layer and producing an inward inflection of the laminae around an inner core of calcite, the taleola (t), scale bar 10 µm.

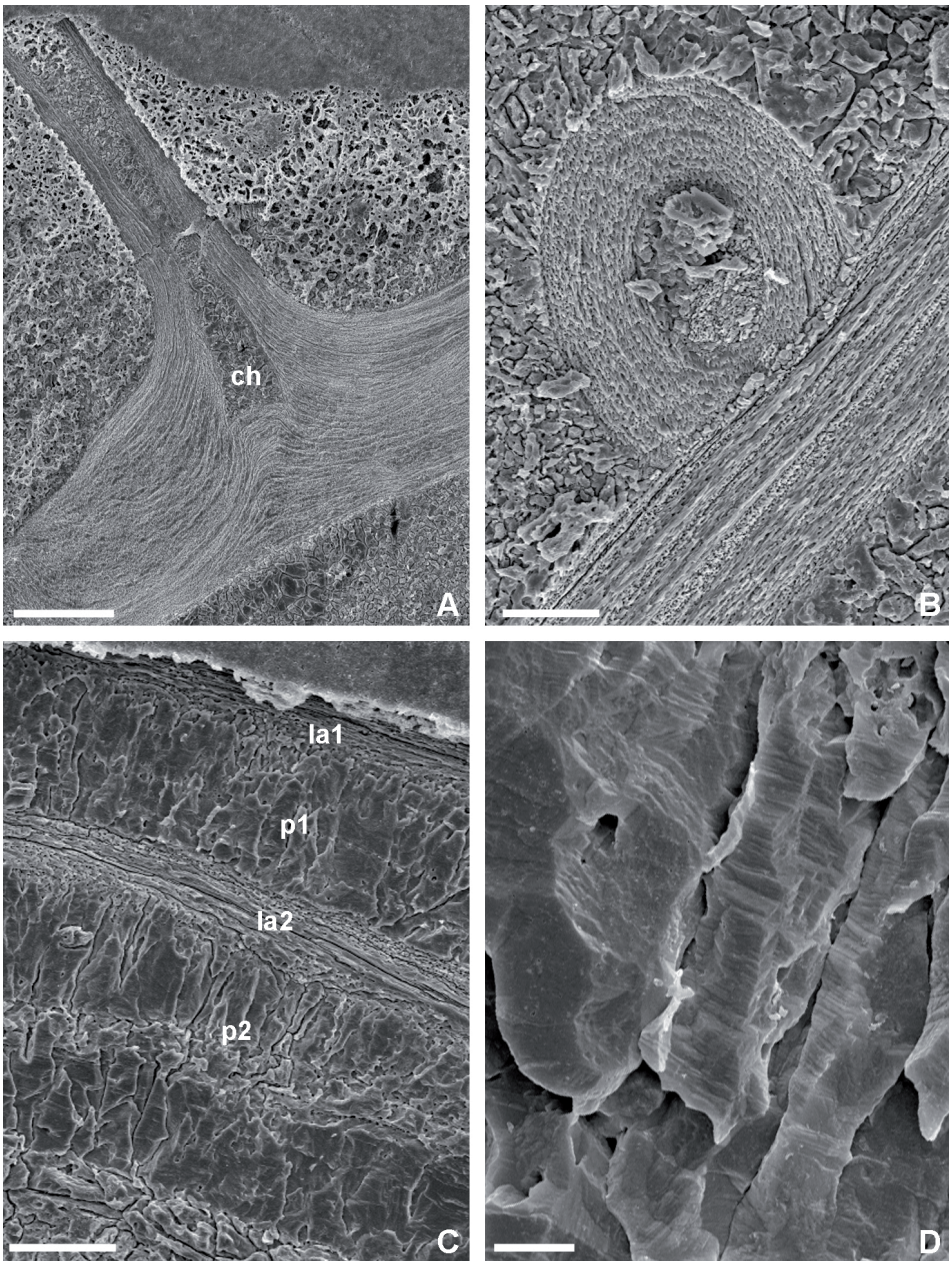

Plate 25. *Spinomarginifera helica*, (A) specimen EBHZ71-10, longitudinal section of distal part of a spine composed of laminar secondary layer with a channel (ch) filled by secondary calcite, scale bar 100 µm; (B) specimen EBHZ71-10, cross section of spine, scale bar 25 µm; (C) specimen EBHZ15-15, alternation of laminar secondary (la1, la2) and prismatic tertiary (p1, p2) layers, scale bar 40 µm; (D) details of C illustrating bands of growth in the prismatic layer, scale bar 20 µm.

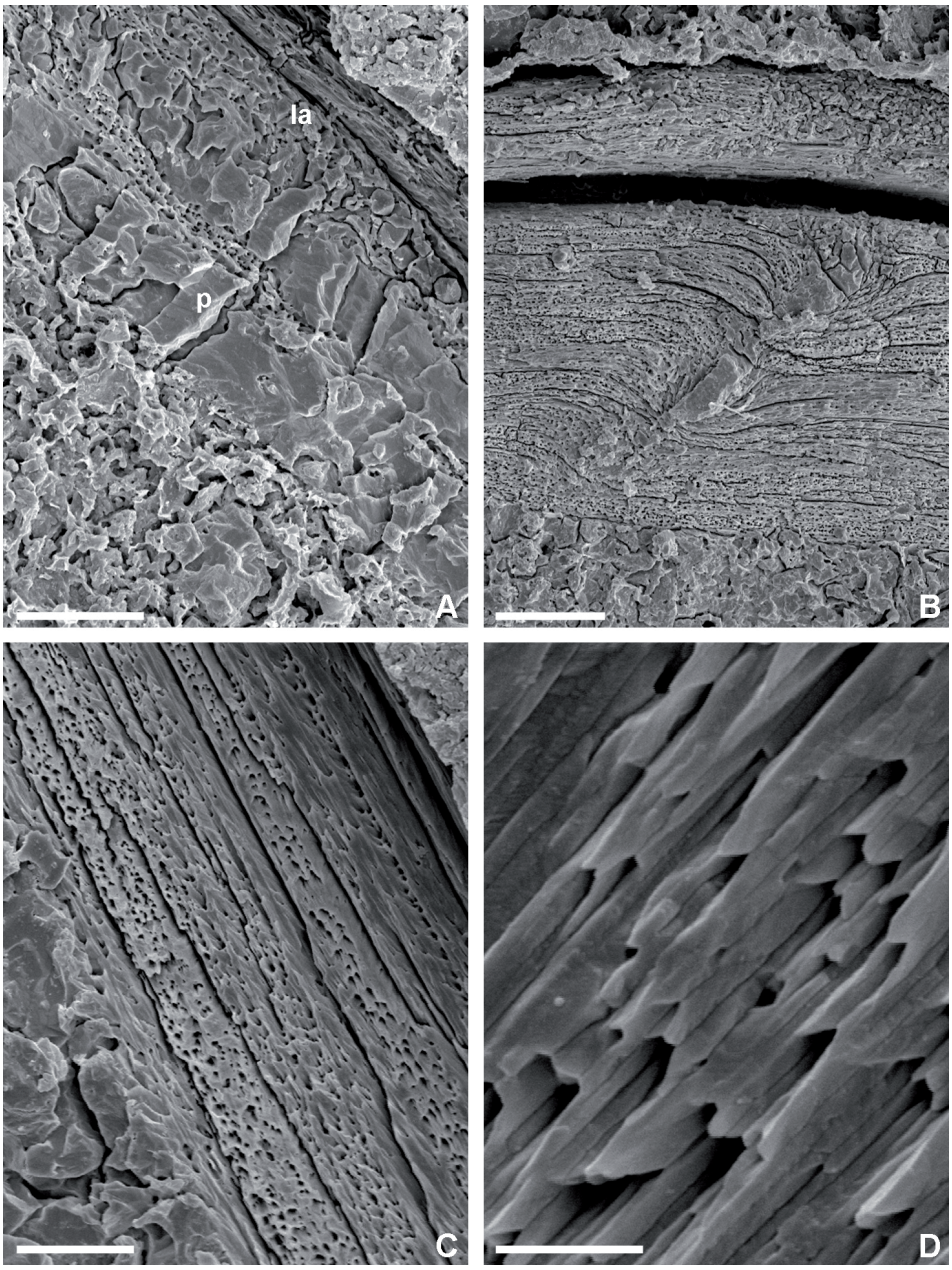

Plate 26. *Spinomarginifera spinosocostata*, (A) specimen EBHZ65-33, laminar secondary layer(la) and prismatic tertiary (p) layer, scale bar 20 μm; (B) specimen EBHZ65-33, pseudopuncta crossing the secondary shell, scale bar 25 μm; (C) *Spinomarginifera sulcata* specimen EBH65-27, secondary layer showing the typical cross bladed organization with packages of differently oriented laminae, scale bar 10 μm; (D) details of C illustrating the laminae in longitudinal section, scale bar 2 μm.

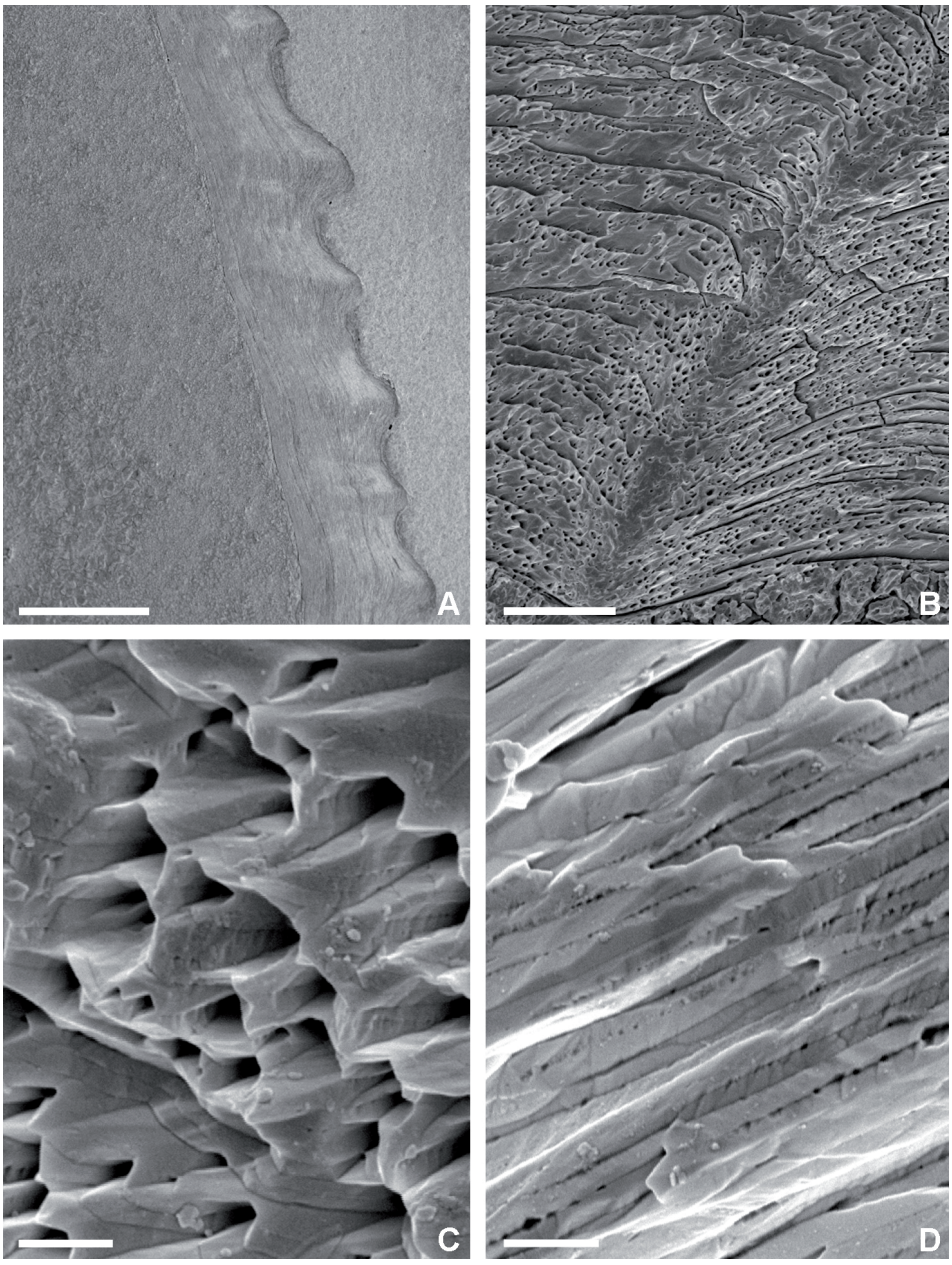

Plate 27. *Alatorthotetina* sp., (A) specimen EBHZ80-16, shell entirely composed of laminae that are folded, producing the external ornamentation of costellae, scale bar 500 μm; (B) specimen EBHZ65-12, pseudopuncta crossing the secondary shell an deflecting the laminae inwardly, scale bar 20 μm; (C) specimen EBH65-12, cross section of secondary layer laminae, scale bar 2 μm; (D) specimen EBH70-8, longitudinal section of secondary layer laminae, scale bar 2 μm.

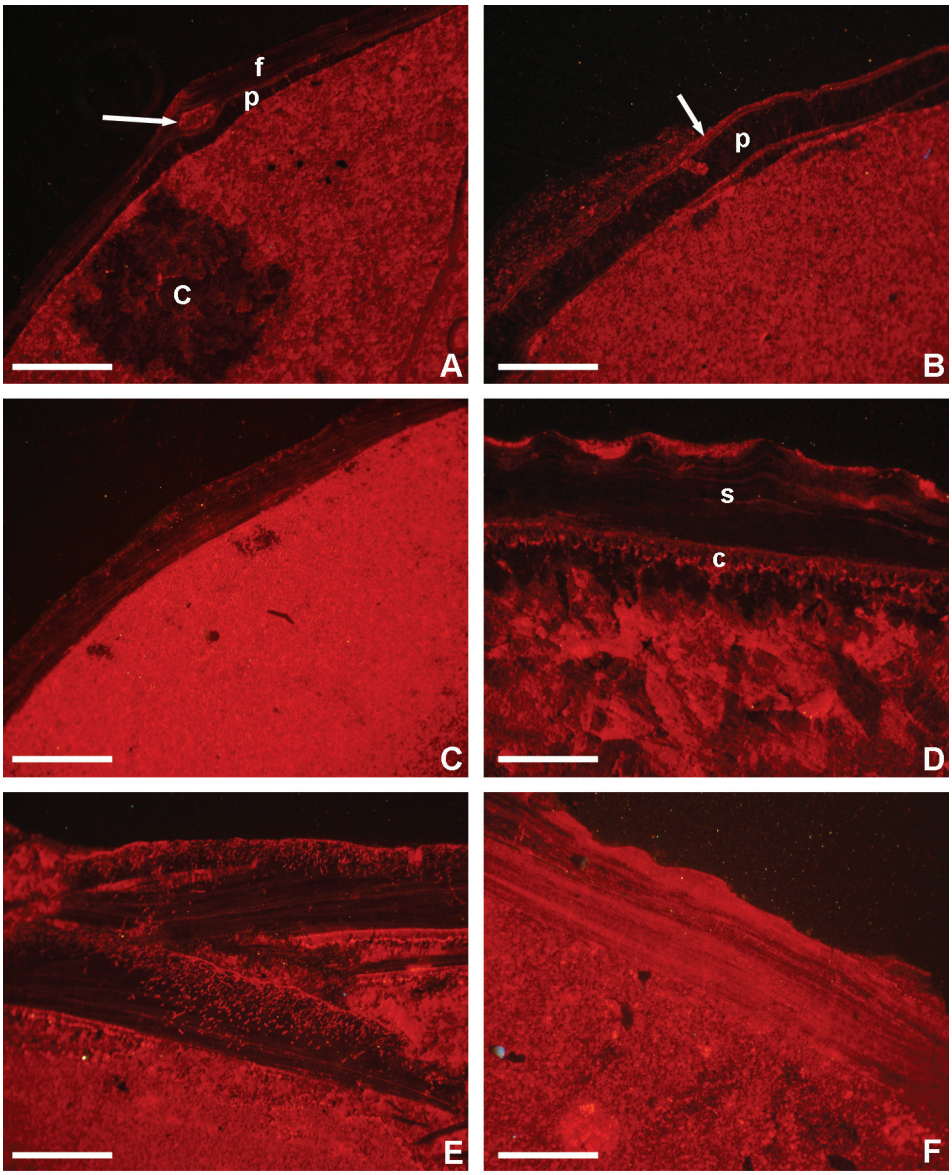

Plate 28. (A) *Spinomarginifera helica*, specimen EBHZ71-10, non luminescent secondary (f) and tertiary (p) layers with a spine channel filled by secondary luminescent calcite (arrow); matrix with not luminescent cement (c), scale bar 500 μm; (B) *Spinomarginifera helica*, specimen EBHZ68-2, luminescent outer laminar secondary layer (arrow) and not luminescent inner prismatic layer (p), scale bar 600 μm; (C) *Alatorthotetina* sp., specimen EBHZ70-6, shell mostly not luminescent with a few luminescent thin bands, scale bar 1 mm; (D) *Alatorthotetina* sp., specimen EBHZ65-9, non luminescent shell (s) filled by calcite cements, scale bar 800 μm; (E) *Alatorthotetina* sp., specimen EBHZ90-3, fractured non luminescent shell with micro-boring filled by luminescent diagenetic calcite, scale bar 1 mm; (F) *Alatorthotetina* sp., specimen EBHZ80-5, shell mostly luminescent, scale bar 1 mm.

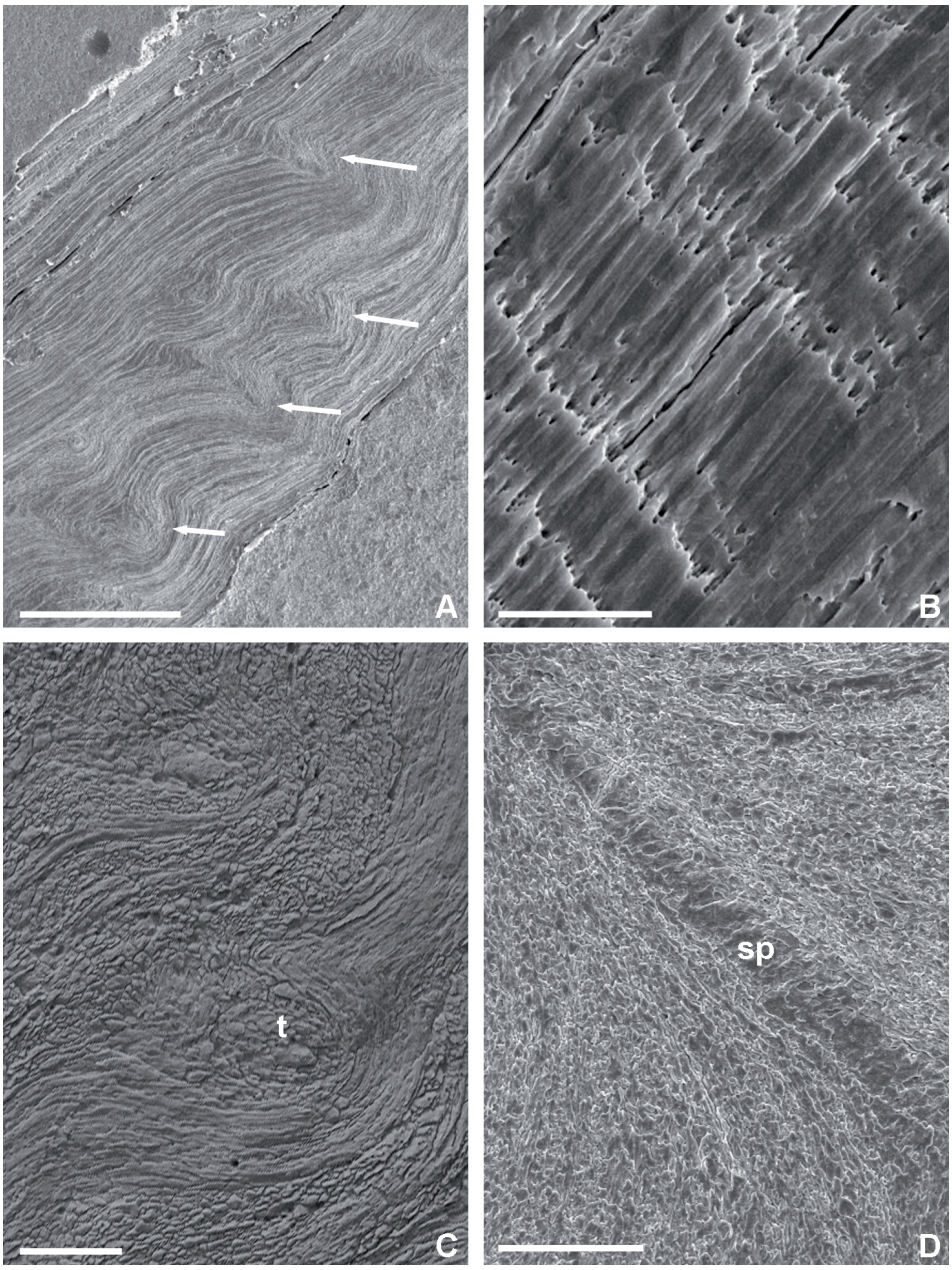

Plate 29. *Costiferina indica*, (A) specimen GY74 (horizon 7-16), shell wall composed of laminar secondary layer crossed by numerous large pseudopunctae (arrows), scale bar 400 µm; (B) details of the laminae in longitudinal section, scale bar 30 µm; *Costiferina spiralis*, (C) specimen GY13 (horizon 7-5), a pseudopuncta with taleola (t) crossing the secondary layer, scale bar 40 µm; *Costiferina subcostatus*, (D) specimen GY86 (horizon 9-27), channel of a spine (sp) which deflect laminae inwardly and it is filled by secondary calcite, scale bar 80 µm.

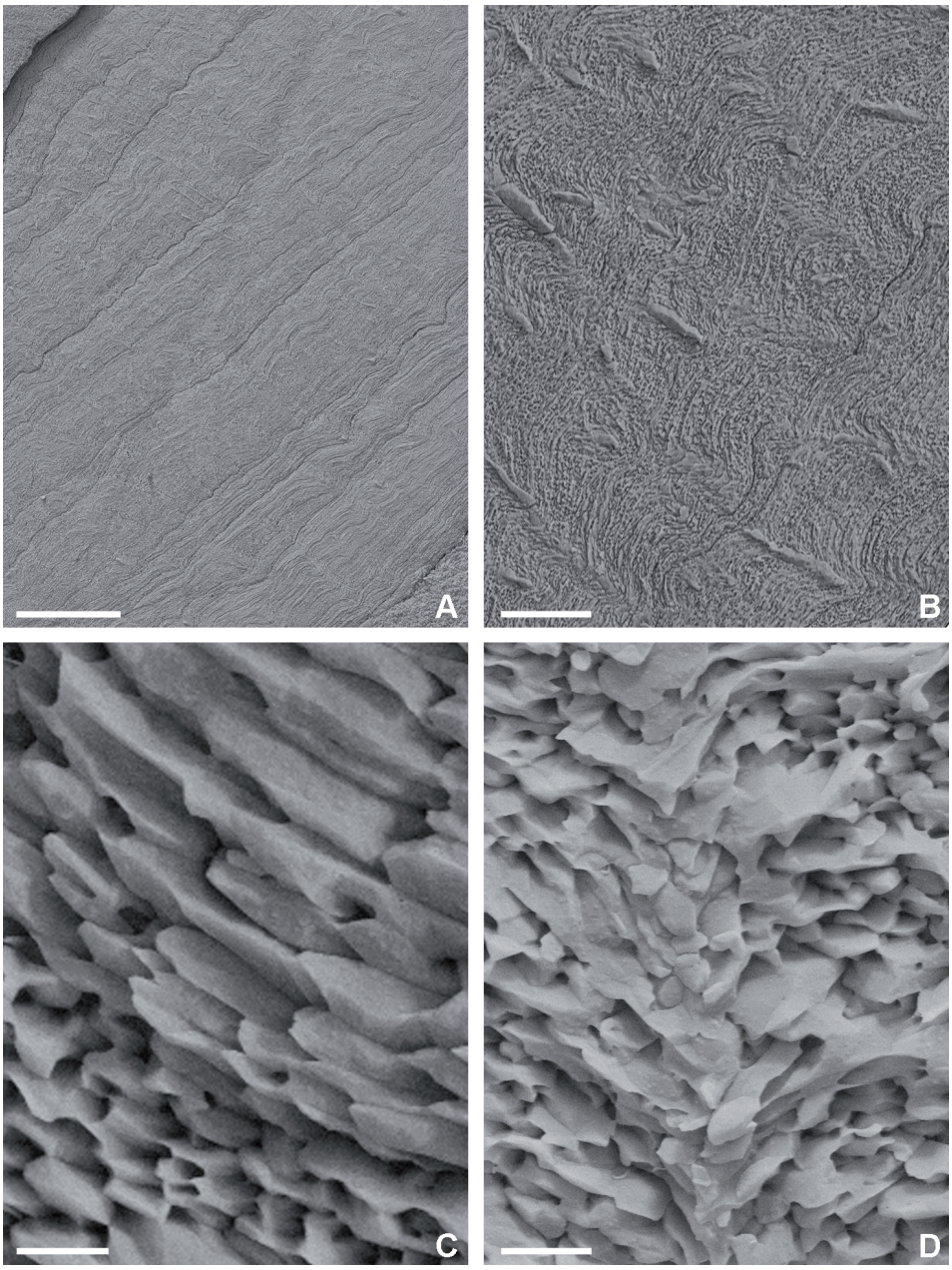

Plate 30. *Richtofenia lawrenciana*. (A) specimen GY52 (horizon 6-12), thick shell of secondary layer laminae, scale bar 200 μm; (B) details of A with laminar fabric crossed by numerous pseudopunctae, scale bar 40 μm; (C) details of A showing laminae composed by laths/blades placed side by side, scale bar 2 μm; (D) specimen GY61 (horizon 6-12), details of pseudopuncta which deflects the laminae inwardly, scale bar 4 μm.

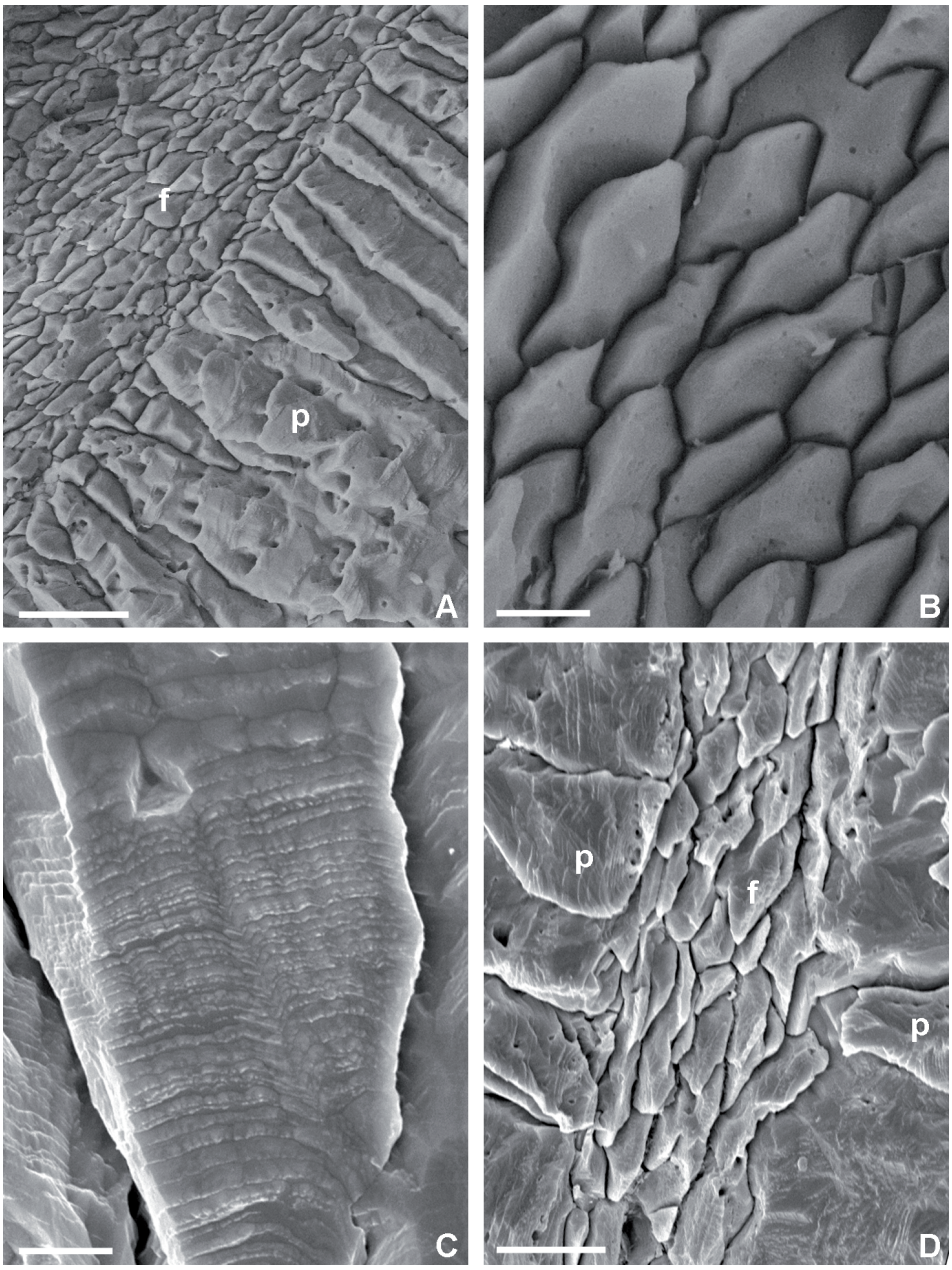

Plate 31. *Permophricodothyris* sp., (A) specimen GY57 (horizon 7-3), secondary fibrous (f) and tertiary prismatic (p) layers, scale bar 20 μm; (B) cross section of fibers with keel and saddle outline, scale bar 4 μm; (C), specimen GY84 (horizon 9-24), details of prismatic layer with growth bands, scale bar 5 μm; (D) specimen 5 (horizon 6-12), secondary layer (f) with coarse fibers intercalated between to levels with prismatic fabric (p), scale bar 10 μm.

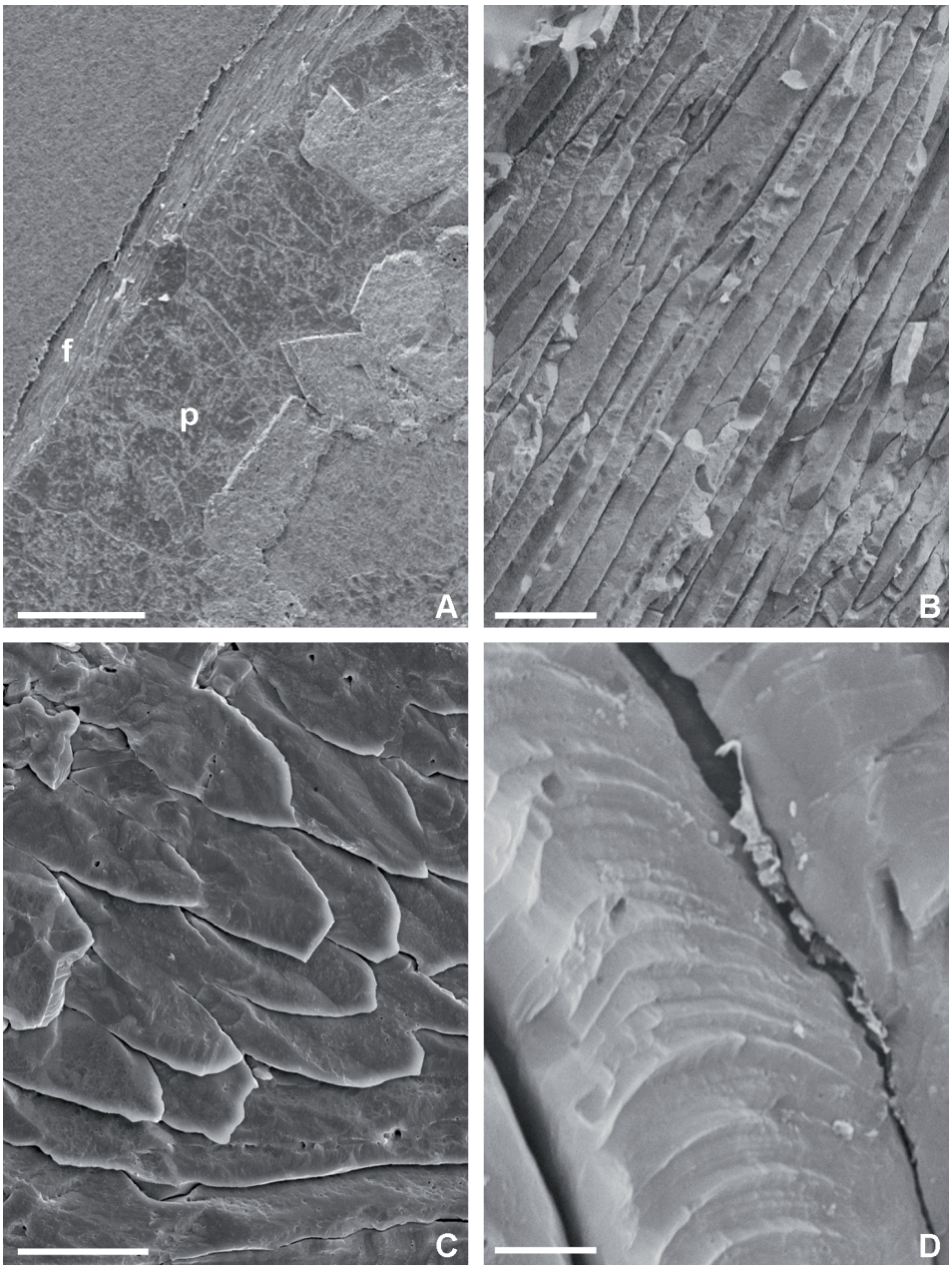

Plate 32. *Neospirifer* sp., (A) specimen GY81 (horizon 9-23), shell wall composed of a fibrous secondary layer (f) and a tertiary prismatic one (p), scale bar 300 μm; (B) specimen 8 (horizon 6-15), fibers of the secondary layer in longitudinal section, scale bar 15 μm; (C) specimen GY73 (horizon 7-4), spatulated termination of the secondary fibers, scale bar 20 μm; (D) specimen 2 (horizon 6-1), high magnification details of fibers showing growth bands, scale bar 3 μm.

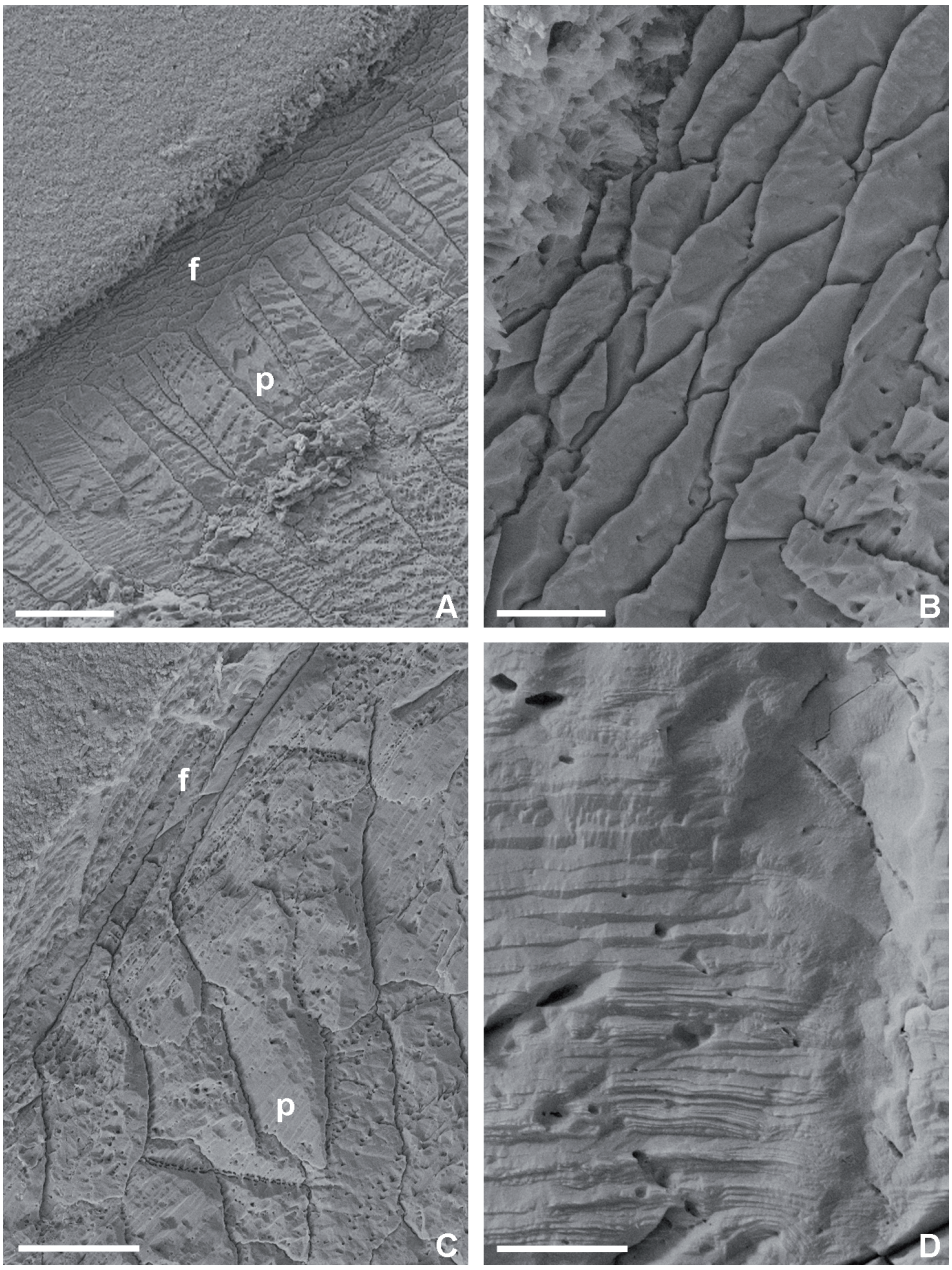

Plate 33. *Stenoscisma* sp., (A) specimen GY48 (horizon 9-23), shell composed of a fibrous secondary layer (f) and a prismatic tertiary one (p), scale bar 100 μm; (B) details of (A) showing the secondary layer in cross section, scale bar 15 μm; (B) longitudinal section of the shell showing the transition between the secondary and tertiary layers, scale bar 60 μm; (C) specimen GY17 (horizon 9-23), details of the prismatic layer showing growth bands, scale bar 10 μm.

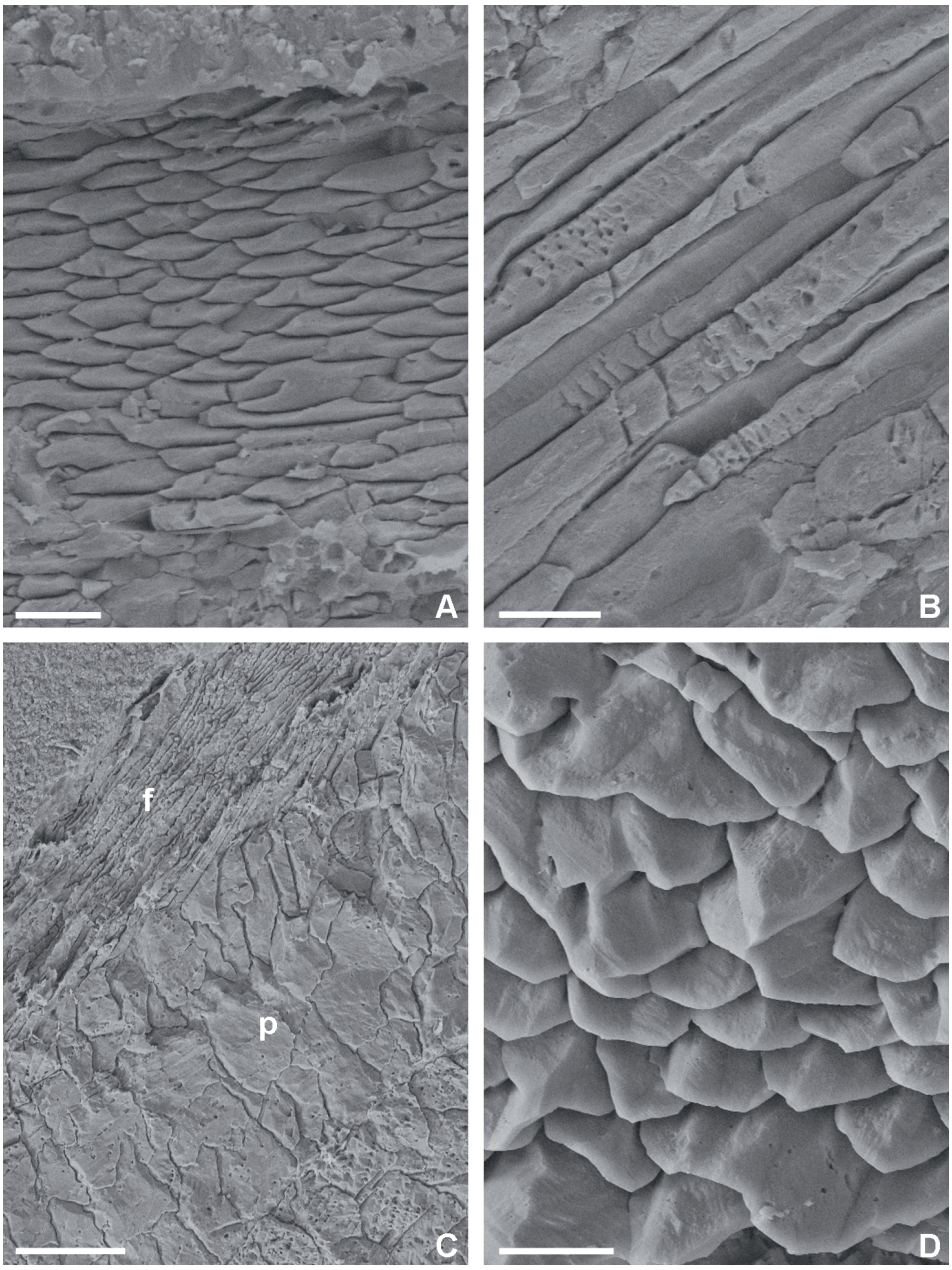

Plate 34. *Alphaneospirifer anshunensis*, (A) specimen GY12 (horizon 7-5), cross section of secondary layer composed by fibres with keel and saddle outline, scale bar 10 μm; (B) fibers in longitudinal section, scale bar 10 μm. *Martinia* sp. (C) specimen GY59 (horizon 6-12), shell composed of a fibrous secondary layer (f) and a tertiary prismatic one (p), scale bar 80 μm; (D) spatulated termination of the secondary fibers, scale bar 10 μm.

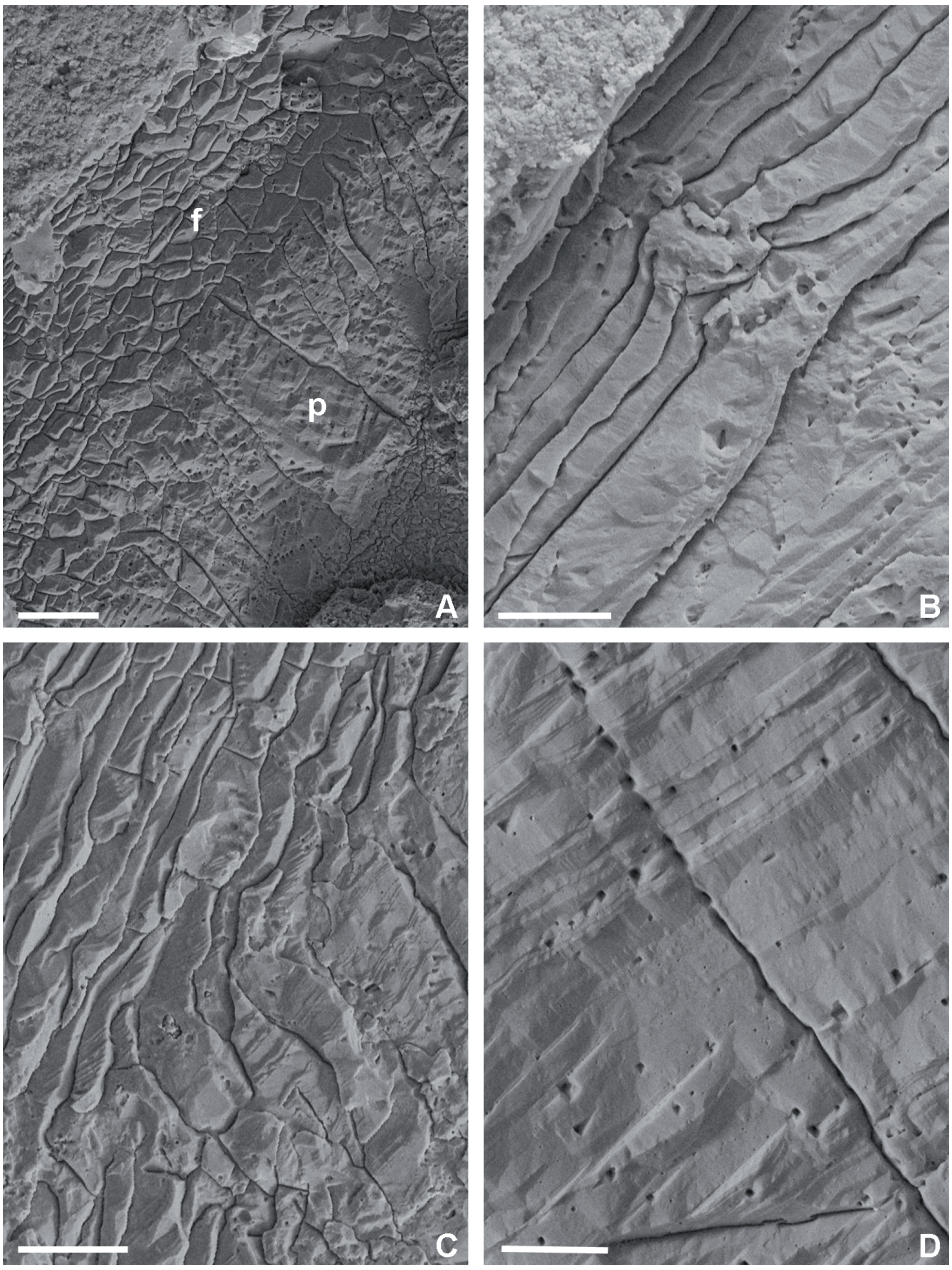

Plate 35. *Notothyris* sp., (A) specimen GY42 (horizon 9-23), shell composed by a fibrous secondary layer (f) and a tertiary prismatic one (p), scale bar 50 μm; (B) specimen GY47 (horizon 9-23), details of a puncta crossing the secondary fibrous layer and deflecting the fibers outwardly, scale bar 20 μm; (C) specimen GY39 (horizon 9-23), transition from the fibrous secondary to the prismatic tertiary layer, scale bar 40 μm; (D) details of C showing diurnal growth bands in the prismatic layer, scale bar 10 μm.

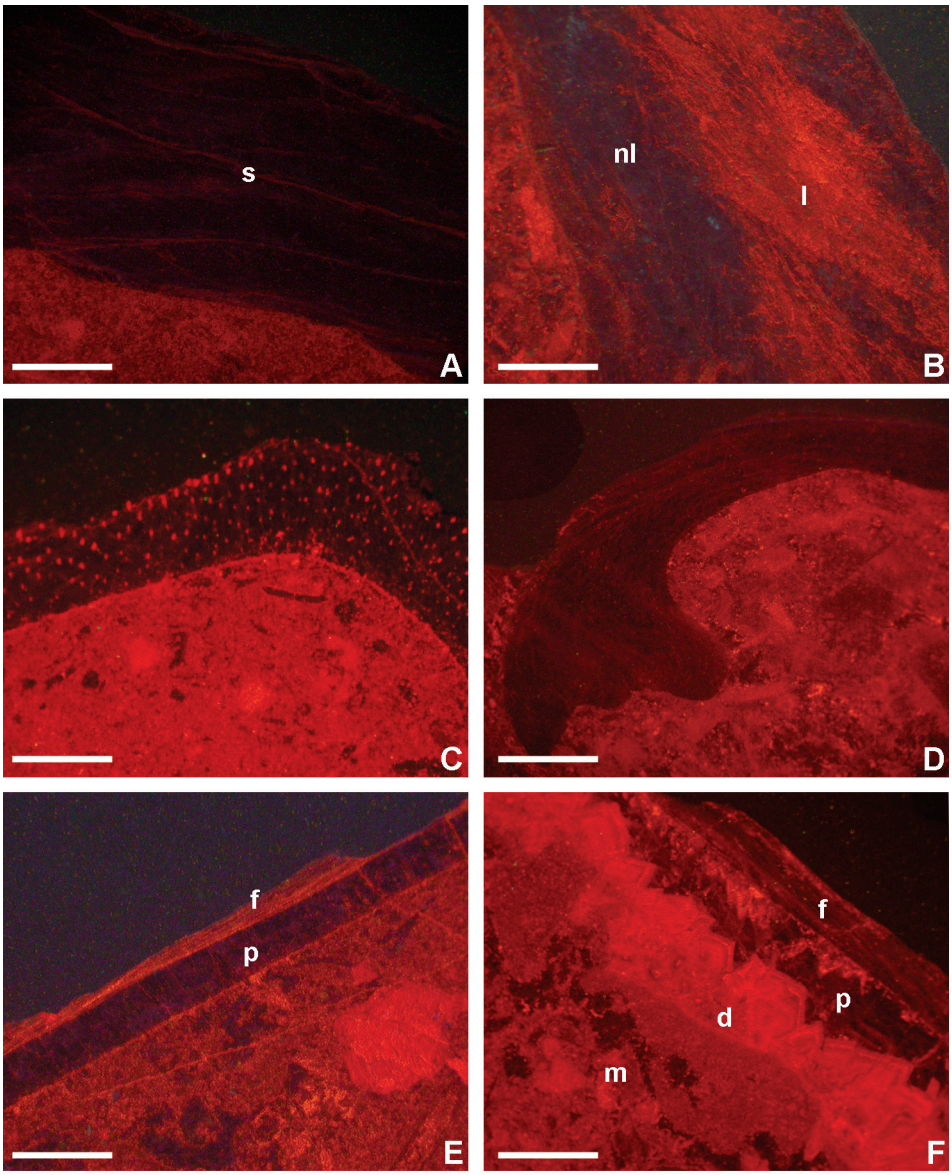

Plate 36. (A) *Costiferina indica*, specimen 75 (horizon 8-2), non luminescent secondary layer, scale bar 400 µm; (B) *Costiferina* sp., specimen 40 (horizon 6-12), differential preservation of the laminar shell with a non luminescent part (nl) and a luminescent one (l), scale bar 450 µm; (C) *Notothyris* sp., specimen 58 (horizon 9-23), non luminescent shell crossed by numerous punctae filled by diagenetic luminescent calcite, scale bar 500 µm; (D) *Neospirifer* sp., specimen 67 (horizon 6-12), slightly to non luminescent secondary layer in the umbonal region, scale bar 250 µm; (E) *Permophricodothyris* sp., specimen 83 (horizon 9-23), slightly luminescent secondary fibrous layer (f) and non luminescent prismatic tertiary layer (p), scale bar 400 µm; (F) *Neospirifer* sp., specimen 81 (horizon 9-23), slightly luminescent fibrous secondary layer (f) and non luminescent prismatic tertiary layer (p) partially dolomitized (d), scale bar 500 µm.

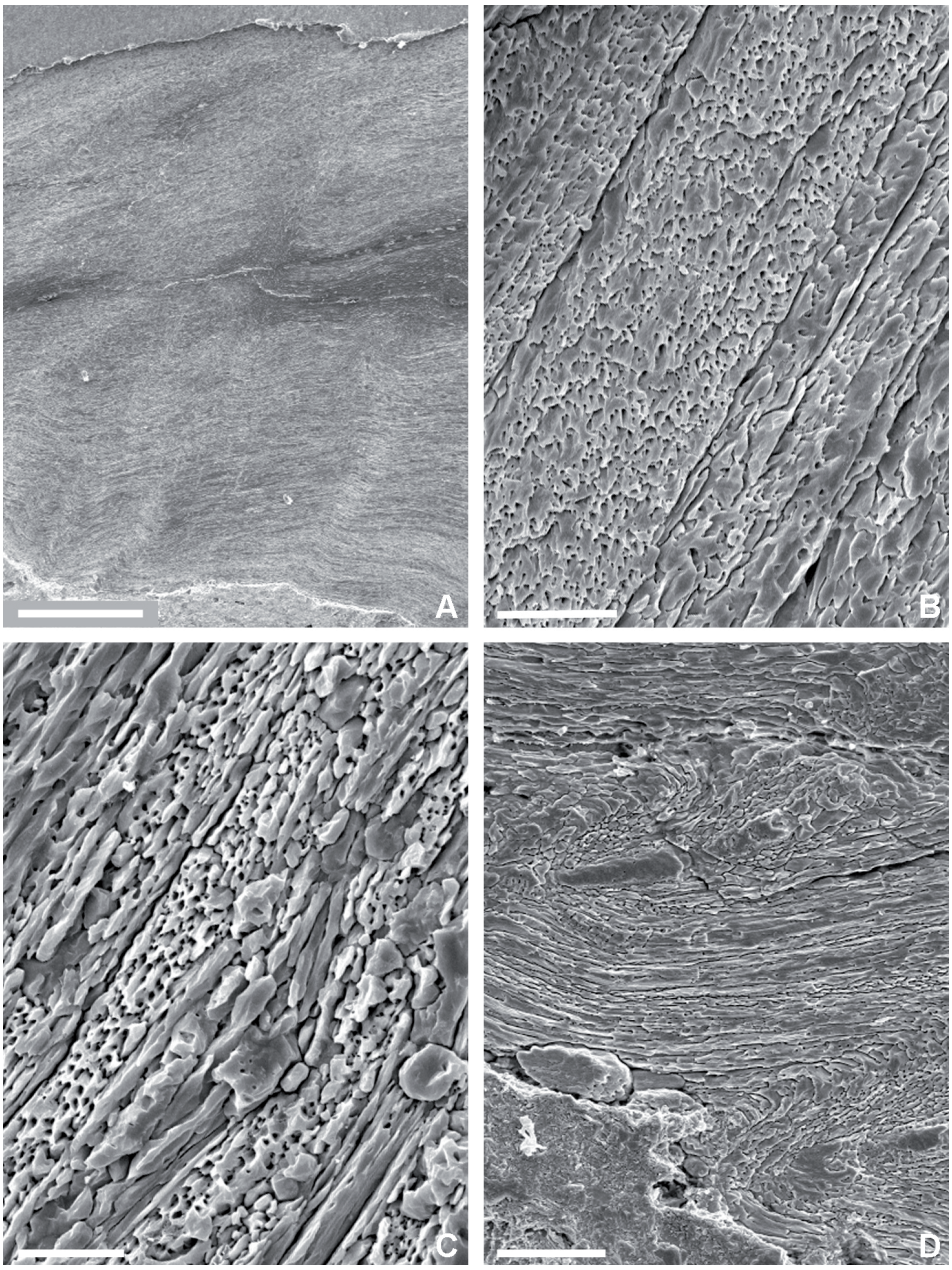

Plate 37. *Retimarginifera s*p., (A) specimen NL-3, shell entirely composed of a laminar secondary layer, scale bar 400 µm; (B) specimen NL-3, details of A with cross section of the laminae , scale bar 25 µm; (C) specimen NL-5, secondary layer with cross blade lamination and packages of laminae oriented in different direction, scale bar 10 µm; (D) specimen NL-4, large inclined pseudopuncta which produce an inward deflection of the laminae, scale bar 50 µm.

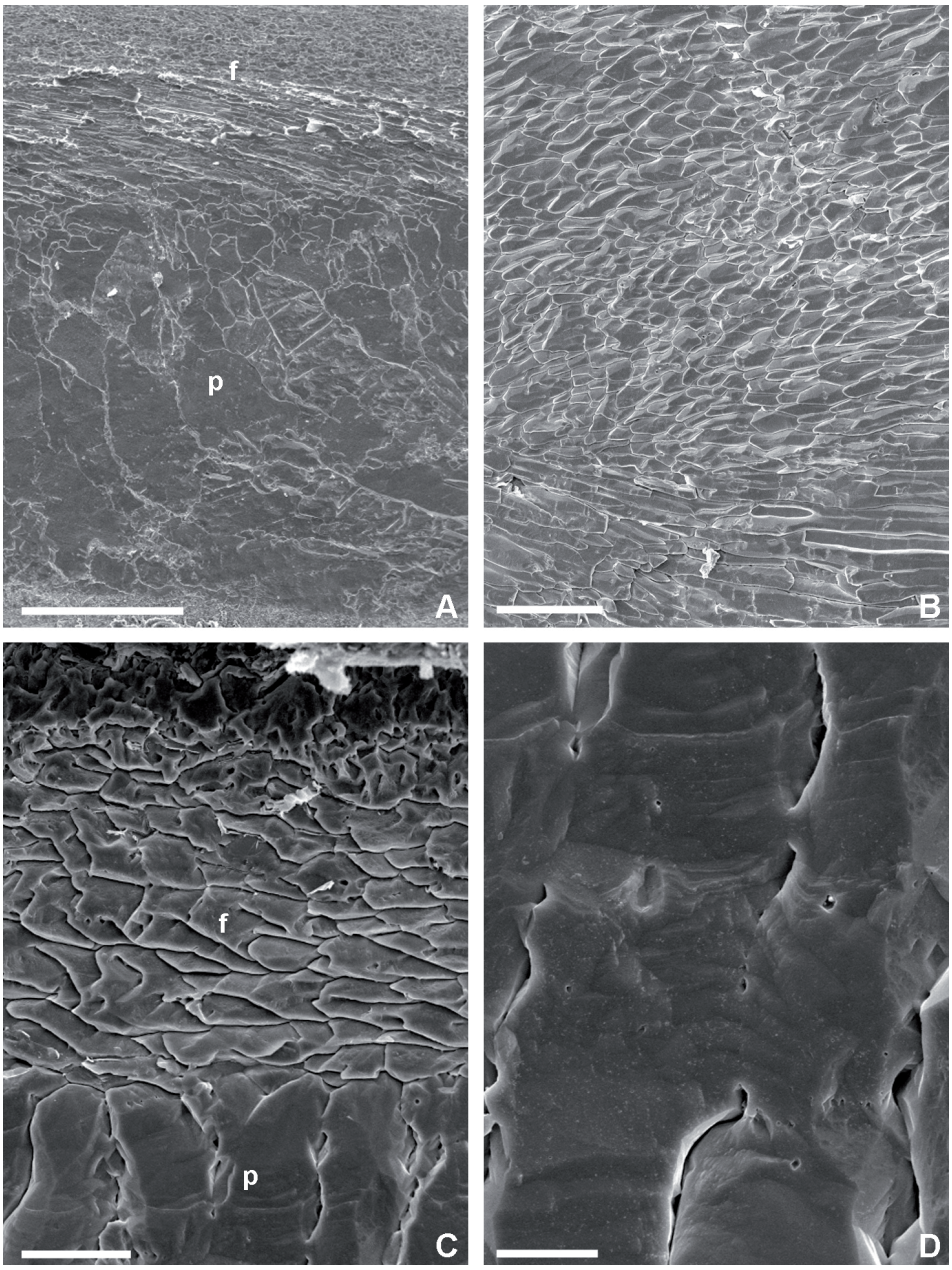

Plate 38. *Neospirifer* sp., (A) specimen NL-2c, secondary fibrous (f) and tertiary prismatic (p) layers, scale bar 500 μm; (B) specimen NL-20, secondary fibers with different direction of growth, scale bar 100 μm; (C) specimen NL-1b, transition between secondary fibrous (f) and tertiary prismatic (p) layers, scale bar 25 μm; (D) specimen NL-1b , details of a prism in the tertiary layer with some diurnal growth bands, scale bar 20 μm.

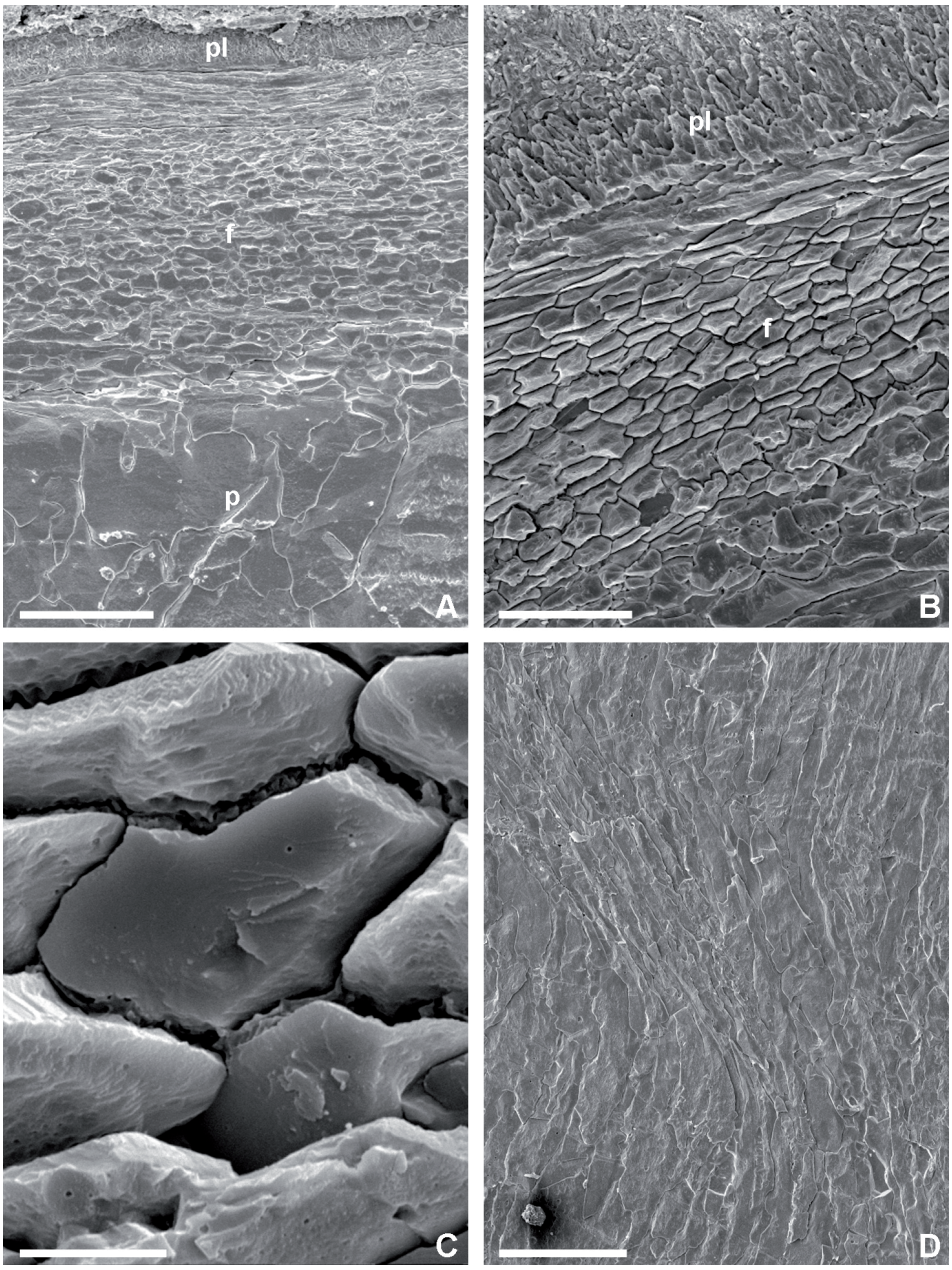

Plate 39. *Spiriferella* sp., (A) specimen NL-11, shell formed of an outermost recristallyzed primary layer (p) , an intermediate fibrous secondary (f) and an innermost tertiary prismatic (P) layers, scale bar 100 μm; (B) specimen NL-15, details of primary (p) and secondary (f) layers, scale bar 40 μm; (C) specimen NL-15, details of B that shows a fiber with a keel and saddle outline, scale bar 10 μm; (D) specimen NL-15 , change in orientation of the fibers in the secondary layer, scale bar 200 μm.

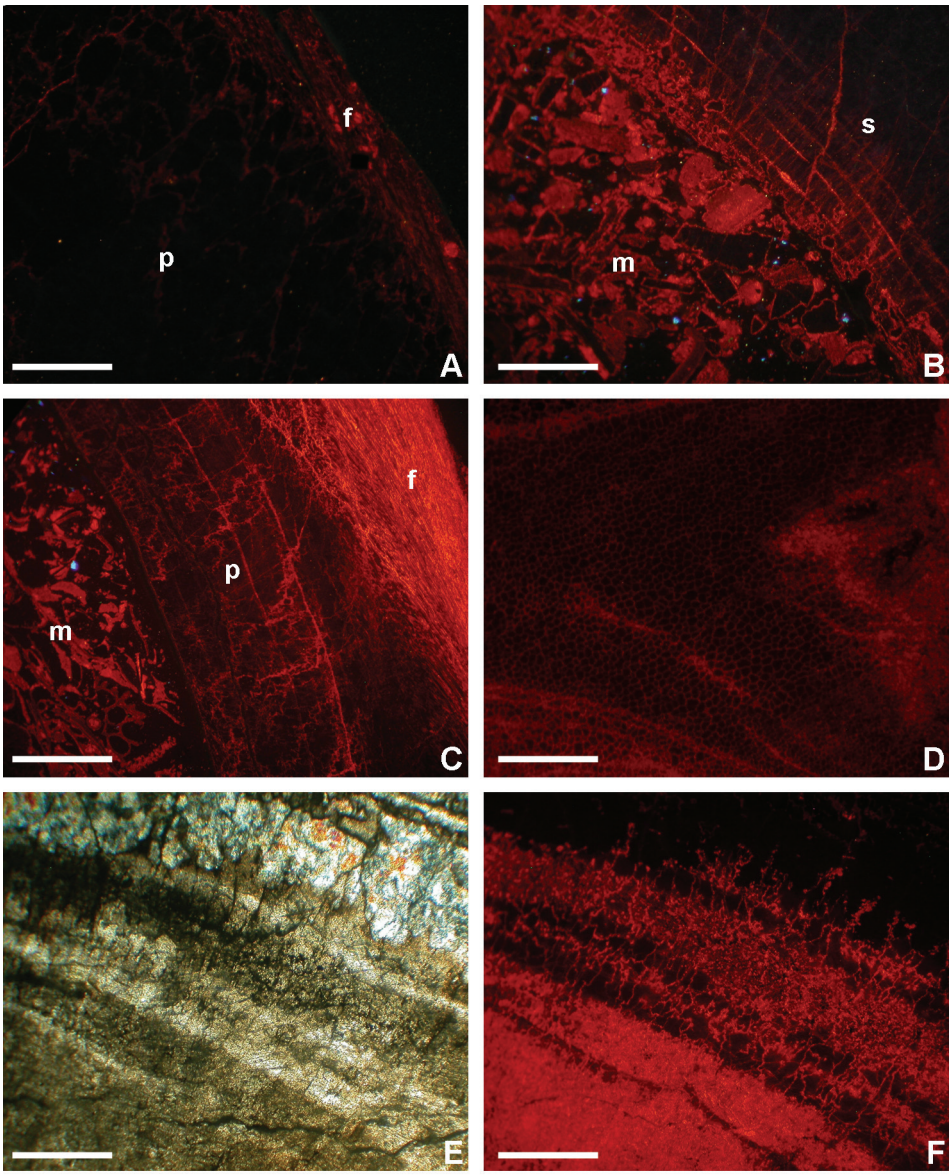

Plate 40. (A) *Neospirifer* sp., specimen NL-8, slightly luminescent secondary layer (f) and non luminescent tertiary layer, scale bar 800 µm; (B) *Neospirifer* sp., specimen NL-8, details of prismatic non luminescent layer (s) with slightky luminescent growth bands, scale bar 600 µm; (C) *Neospirifer* sp., specimen NL-7, very luminescent secondary layer (f) with non luminescent tertiary layer (p) in which are evident thin luminescent growth line and rock matrix (m); (D) *Neospirifer* sp., NL-26, fragment of secondary fibrous layer with non luminescent fibres cross by a luminescent network, scale bar 250 µm; (E/F) *Spiriferella* sp., specimen NL-21, prismatic layer in cross-polarized light and cathodoluminescence which show evidences of silicification, scale bar 500 µm.

Chapter 6
Conclusive remarks

The general aim of this research was to unravel the pattern of changes in the biomineralization of brachiopod shells during one of the most critical time intervals of the biotic evolution on Earth, which is the end of the Permian. This time interval witnessed major global changes in the Earth's geodynamics, climate, and seawater/atmosphere geochemistry, which culminated with the severest mass extinction of the Phanerozoic about 252 myr ago (e.g. Erwin 2006, Shen *et al.* 2011, Brand *et al.* 2012a, Burgess *et al.* 2014).

Through this research, two important conclusions were reached: the first concerning the paleobiological implications of the different biomineralization processes in brachiopods and the second related to the brachiopod response to the end Permian global environmental changes.

6.1 Biomineralization on fossils shell and its paleobiological meaning

This study has shown that the brachiopod classes of Strophomenata and Rhynchonellata have profound differences in terms of the structural and elemental composition of their shell. These differences are likely related to the biomineralization process responsible for the formation of the secondary layer (Garbelli *et al.* 2014a). In fact, Strophomenata shells were produced collectively by arrays of mantle cells of which secrete the organic membranes and control the precipitation of calcium carbonate; on the other hand, Rhynchonellata had and still have a discrete mechanism of biomineralization in which every single cell produce a structural unit (a fiber) of the fabric. The processes of biomineralization of the tertiary layer instead seems to have been similar in the two

classes and it involved a lower amount of organic matter, which is limited to ephemeral membranes separating the prisms.

Coupled with this, it has been found that the elemental content of Mg and Sr is higher in pristine shells of extinct Strophomenata than in those of Rhynchonellata and that the $\delta^{13}C$ composition of the two classes is significantly different, with, in general, the carbon isotope values of Strophomenata being more negative than those of co-occurring Rhynchonellata (Garbelli *et al.* 2014a, Garbelli *et al.* submitted). It is possible that brachiopod shell fabric and its relative organic matter content may be an important factor in shaping its isotopic and geochemical composition, but the precise mechanism remains unresolved.

An appealing interpretation could be that the higher Mg and Sr contents, the higher amount of organic matter and the microstructure variability in the species with laminar fabric (i.e. the Strophomenata) can be due to their greater potential in shaping and modifying their shell units, when compared to species with fibrous fabric (i.e. Rhynchonellata). This could have been achieved by addition of mismatched cations and organic material in the amorphous calcium carbonate (ACC), that promotes the initial stabilization of this highly disorganized phase. The ACC is anisotropic and can be more easily manipulated by organisms to form a specific shape (Addadi *et al.* 2003), promoting the diversity and plasticity of the laminar shells. These profound differences in the biomineralization processes between the two classes could have been one of the driving forces which produced the more distinctive and specialized shell shapes of the Strophomenata compared to the Rhynchonellata. It may also have been one of the trigger mechanisms of the different fate of the two classes during the end Permian extinction.

6.2 Brachiopods response to the end Permian global environmental changes

The study of the occurrences and stratigraphic distribution of brachiopods during the Late Permian highlighted that a big change occurred during the

Changhsingian, when taxa with laminar fabric proliferated more than those with fibrous fabric; however, this increase in abundance was not coupled with a concomitant increase in taxonomic diversity. On the contrary, even if the total occurrences of taxa with fibrous fabric became reduced in this time interval, the Rhynchonellata were able to evolve a higher number of new families than the Strophomenata. This taxonomic turnover was coupled with a change in the type of shell fabric in both classes: the taxa with thicker and higher carbonate content in the shell disappeared well before the PTB. Hence, at the end of the period, just before the extinction interval, brachiopods produced shells with higher organic content, irrespectively of their taxonomy; in particular, in the extinction interval, shells with a fabric consisting of small structural units (laths or blade or small fibers) were present. This is an indication of selective pressure for shells with low ratio of inorganic to organic content in the shell.

As outlined above, in several stratigraphic successions spanning the Late Permian-Early Triassic time interval, when taxa of the Strophomenata are present, they tend to dominate the assemblages with a high number of taxa. This happens more rarely with representatives of the Rhynchonellata. However, the Strophomenata did not pass the end Permian crisis, whereas the Rhynchonellata did it. Their different fate seems thus to be strictly related to their different shell fabric, showing that there was an evolutive response to the end Permian environmental changes, which was different in the two brachiopod classes.

The analyzed Strophomenata show a complex response, showing normal biomineralization activity and even proliferating during most of the Changhsingian, when they were the rulers of the benthic communities. The only anomaly found in this study is the increase in thickness of their secondary layer laminae observed along a few stratigraphic sections, which may be a clue to progressive difficulties to growth and reproduce in changing environmental conditions at the dawn of the extinction interval.

The analyzed Rhynchonellata show a different pattern of evolution; even though not abundant, they diversified more than the other class in the Chang-

hsingian and evolved a shell fabric made of small sized structural elements. In fact representatives of Rhynchonellata in the extinction interval are characterized by small and thin shells with small sized fibers, thus reducing the amount of inorganic content required to build the shell.. This shift mirrors the behavior of extant brachiopods living at different conditions of carbonate saturation of the seawater outlined by Watson *et al.* (2012), suggesting that producing a shell with a lower ratio of inorganic to organic content shell it is the successful strategy to cope with progressive ocean acidification in the long term (i.e. hundreds thousands of years).

In conclusion, the observed changes in brachiopod shell biomineralization are compatible with a change in the carbonate saturation state of seawater and thus with ocean acidification related to Siberian traps flood basalt volcanism (Knoll *et al.* 1996, Kump 2009, Clapham and Payne 2011, Hinojosa *et al.* 2012, Burgess *et al.* 2014). In fact, a general trend toward production of bLMCs with higher organic content is recorded up to the PTB in most brachiopod groups. This discourages the idea that the brachiopod small size reported before the extinction event may have been driven mainly by primary productivity collapse. It may have been more easily the result of changes in the physical and chemical composition of seawater, which corresponded to an increased energetic cost for carbonate precipitation in low buffered organisms such as brachiopods.

References

Addadi L., Raz S., Weiner S., 2003. Taking Advantage of Disorder: Amorphous Calcium Carbonate and its Roles in Biomineralization. *Advanced Materials*, 15(12), 959-970.

Afanasjeva G.A., 2010. Large extinctions of articulate brachiopods in the Paleozoic and their ecological and evolutionary consequences. *Paleontological Journal,* 44, 1200-1208.

Alvarez F., and Brunton C.H.C., 2001. Fundamental differences in external spine growth in brachiopods. BRACHIOPODS PAST AND PRESENT- Systematics Association Special Volume Series, 63, 108-118.

Alvarez F., and Rong J., 2002. Order Athyridida. 1475-1601. in KAESLER, R. (ed.) *Treatise on invertebrate paleontology. Part H. Brachiopoda (Revised)* 4. Geological Society of America, Boulder, and University of Kansas Press, Lawrence, 753 pp.

Angiolini L., 1993. Ultrastructure of some Permian and Triassic Spiriferida and Arthyridida (Brachiopoda). *Rivista italiana di paleontologia e stratigrafia*. 9(3), 283-306.

Angiolini L., Carabelli L., Nicora A., Crasquin-Soleau S., Marcoux J., Rettori R., 2007. Brachiopods and other fossils from the PermoTriassic boundary beds of the Antalya Nappes (SW Taurus, Turkey). *Geobios*, 40, 715-729.

Angiolini L., Darbyshire D.P.F., Stephenson M.H., Leng M.J., Brewer T.S., Berra F., Jadoul F., 2008. Lower Permian brachiopods from Oman: their potential as climatic proxies. *Earth and Environmental Science Transactions of the Royal Society of Edinburgh*, 98, 327-344.

Angiolini L., Jadoul F., Leng M.J., Stephenson M.H., Rushton J., Chenery S., Crippa G., 2009. How cold were the Early Permian glacial tropics? Testing sea surface temperature using the oxygen isotope composition of rigorously screened brachiopod shells. *Journal of the Geological Society*, 166, 933-945.

Angiolini L. and Carabelli L., 2010. Upper Permian brachiopods from the Nesen Formation, North Iran. *Special Papers in Palaeontology*, 84, 41-90.

Angiolini L., Stephenson M., Leng M.J., et al., 2012. Heterogeneity, cyclicity and diagenesis in a Mississippian brachiopod shell of palaeoequatorial Britain. *Terra Nova,* 24(1), 16-26.

Angiolini L., Zanchi A., Zanchetta S., Nicora A., Vuolo I., Berra F., Henderson C., Malaspina N., Rettori R., Vachard D., Vezzoli G., in press. From rift to drift in South Pamir (Tajikistan): Permian evolution. *Journal of Asian Earth Sciences of a Cimmerian terrane.*

Armstrong J.D., 1968. Microstructure of the shell of a Permian spiriferid brachiopod, *Australian Journal of Earth Sciences*, 15(2), 183-188.

Azmy K., Veizer J., Jin J., Copper P., Brand U., 2006. Paleobathymetry of a Silurian shelf based on brachiopod assemblages: an oxygen isotope test. *Canadian Journal of Earth Sciences*, 43, 281-293.

Barbin V., 2013. Application of cathodoluminescence microscopy to recent and past biological materials: a decade of progress. *Mineralogy and Petrology*, 107(3), 353-362.

Bates N.R., Brand U., 1991. Environmental and physiological influences on isotopic and elemental compositions of brachiopod shell calcite - implications for the isotopic evolution of Paleozoic oceans *Chemical Geology*, 94(1), 67-78.

Bengtson S., 1994. The advent of animal skeletons. In *Early Life on Earth. Nobel Symposium 84* (ed. S. Bengtson), pp. 412-25. New York: Columbia University Press.

Bengtson S., 2004. Early skeletal fossils. In *Neoproterozoic-Cambrian Biological Revolutions* (eds J. H. Lipps & B. M. Waggoner), pp. 67-77. The Paleontological Society Papers 10. The Paleontological Society.

Brand U. and Veizer J., 1980. Chemical diagenesis of a multicomponent carbonate system: 1, Trace elements. *Journal of Sedimentary Petrology,* 50, 1219-1236.

Brand U., Logan A., Hiller N., Richardson J., 2003. Geochemistry of modern brachiopods: applications and implications for oceanography and paleoceanography. *Chemical Geology* 198, 305-334.

Brand U., 2004. Carbon, oxygen and strontium isotopes in Paleozoic carbonate components: an evaluation of original seawater-chemistry proxies. *Chemical Geology* , 204(1-2), 23-44

Brand U., Webster G.D., Amy K., Logan A., 2007. Bathymetry and productivity of the southern Great Basin seaway, Nevada, USA: An evaluation of isotope and trace element chemistry in mid-Carboniferous and modern brachiopods. *Palaeogeography, Palaeoclimatology, Palaeoecology*, 256(3-4), 273-297.

Brand U., Logan A., Bitner M.A., Griesshaber E., Azmy K., Buhl D., 2011. What is the ideal proxy of Paleozoic seawater chemistry? *Memoirs of the Association of Australasian Palaeontologists*, 41, 9-24.

Brand U., Posenato R., Came R., Affek H., Angiolini L., Azmy, K., Farabegoli E., 2012. The end-Permian mass extinction: a rapid volcanic CO_2 and CH4-climatic catastrophe. *Chemical Geology* 322-323, 121-144.

Brand U., Azmy K., Bitner M.A., Logan A., Zuschin M., Came R., Ruggiero E., 2013. Oxygen isotopes and $MgCO_3$ in brachiopod calcite and a new paleotemperature equation. *Chemical Geology*, 359, 23-31.

Brayard A., et al., 2011. Transient metazoan reefs in the aftermath of the end-Permian mass extinction. *Nature Geoscience* 4, 693-697.

Bruckschen P., Oesmann S., Veizer J., 1999. Isotope stratigraphy of the European Carboniferous. Proxy signals for ocean chemistry, climate and tectonics. *Chemical Geology,* 161, 127-163.

Brunton C.H.C., 1972. The shell structure of Chonetacean brachiopods and their ancestors. *Bulletin of the British Museum (Natural History). Geology*, 21, 1-26.

Brunton C.H.C., 1984. Growth and shell shape in productacean brachiopods. *Bulletin of British Museum (Natural History), Geology,* 38, 273-281.

Brunton C.H.C., 1987. The palaeoecology of brachiopods and other faunas, of Lower Carboniferous (Asbian) limestones in West Fermanagh. *Irish Journal of Earth Sciences*, 8, 97-112

Buening N. and Spero H.J., 1996. Oxygen and carbon isotope analyses of the articulate brachiopod Laqueus californianus: A recorder of environmental changes in the subeuphotic zone. *Marine Biol*ogy, 127: 105-114.

Burgess, S.D., Bowring, S., Shen, S.-Z., 2014. High precision timeline for Earth's most severe extinction. *Proceedings of the National Academy of Sciences of the United States of America* 111, 3316-3321.

Carpenter S.J., Lohmann K.C., 1995. Delta-O-18 and delta-C-13 values of modern brachiopod shells. *Geochimica et Cosmochimica Acta*, 59(18), 3749-3764.

Chen Z.Q., Kaiho K., George A.D., Tong J., 2006. Survival brachiopod faunas of the end-Permian mass extinction from the Southern Alps (Italy) and South China. *Geological Magazine*, 143, 301-327.

Chen Z.Q. and Liao Z.T., 2007. Last Orthotetid brachiopods from the Uppermost Permian of South China. *Journal of Paleontology*, 81, 988- 1000.

Chen Z.Q., Shi G.R., Gao Y.Q., Tong J.N., Yang F.Q., Peng Y.Q., 2009. A late Changhsingian (latest Permian) deep-water brachiopod fauna from Guizhou, South China. *Alcheringa,* 33, 163-183.

Chuang S.H., 1994. Observations on the reproduction and development of *Liothyrella neozelanica* (Thomson 1918) (Terebratulacea, Articulata, Brachiopoda). *Journal of the Royal Society of New Zealand*, 24, 209-218.

Cross E.L.; Peck L.S., Harper, E.M., 2015. Ocean acidification does not impact shell growth or repair of the Antarctic brachiopod Liothyrella uva (Broderip, 1833) *Journal of Experimental Marine Biology and Ecology*, 462, 29-35

Curry G.B. and Fallick A.E., 2002. Use of stable oxygen isotope determinations from brachiopods in palaeoenvironmental reconstruction. *Palaeogeograohy Palaeoclimatology Palaeoecology*, 182, 133-143.

Curry G.B. and Brunton C.H.C., 2007. Stratigraphic distribution of Brachiopods. In: Selden, P.A. (Ed.), Treatise on Invertebrate Paleontology (Part H, Brachiopoda Revised): Geological Society of America. Supplement, vol. 6. University of Kansas Press, Boulder, CO, pp. 2901-3081 (Lawrence).

Cusack M. and Williams A., 2001. Evolutionary and diagenetic changes in the chemicostructure of the shell of cranioid brachiopods, *Palaeontology*, 44(5), 875- 903.

Cusack M., Dauphin Y., Chung P., Pérez-Huerta A., Cuif J.P., 2008. Multiscale structure of calcite fibres of the shell of the brachiopod Terebratulina retusa. *Journal of Structural Biology*, 164 (1), 96-100.

Cusack M., Chung P., Dauphin Y., Pérez-Huerta A., 2010. Brachiopod primary layer crystallography and nanostructure. *Special Papers In Palaeontology*, 84, 99-105.

Cusack M., Perez-Huerta A., EIMF, 2012. Brachiopods recording seawater temperature—a matter of class or maturation? *Chemical Geology,* 334, 139-143.

Dewing K., 2004. Shell structure and its bearing on the phylogeny of Late Ordovician- Early Silurian strophomenoid brachiopods from Anticosti Island, Quebec. *Journal of Paleontology*, 78 (2), 275-286.

Dove P.M., DeYoreo J.J., Weiner S., 2003. Biomineralization. Reviews in Mineralogy and Geochemistry, vol. 54. Mineralogical Society of America and Geochemical Society, Washington, D.C.

England J., Cusack M., Lee M.R., 2007.Magnesiumand sulphur in the calcite shells of two brachiopods, Terebratulina retusa and Novocrania anomala. *Lethaia,* 40, 2-10.

Erwin D.H., 1990. The End-Permian Mass Extinction. A*nnual Review of Ecology and Systematics,* 21, (1990) 69-91

Erwin D.H., 1993. The great Paleozoic crisis. Columbia University Press, New York.

Erwin D.H., 1994. The Permo-Triassic extinction. *Nature* 367, 231-236.

Erwin D.H., 2006. Extinction: how life on earth nearly ended 250 million years ago. Princeton University Press, Princeton, N.J.

Epstein S., Buchsbaum R., Lowenstam H.A., 1953. Revised carbonate-water isotopic temperature scale. *Geological Society of America Bulletin* 64, 1315-1325.

Fitzer S.C., Zhu W.,Tanner K.E.,Phoenix V.R.,Kamenos N.A.,Cusack M., 2014. Ocean acidification alters the material properties of Mytilus edulis shells. *Journal of the Royal Society,* 12(103).

Garbelli C., 2011. Brachiopodi del Permiano Superiore (260-251 Ma). Ultrastruttura e diagenesi della conchiglia. Thesis, pp. 133

Garbelli C., Angiolini L., Jadoul F., Brand U., 2012. Micromorphology and differential preservation of Upper Permian brachiopod low-Mg calcite. *Chemical Geology,* 299, 1-10.

Garbelli, C., Angiolini, L., Brand, U., Jadoul, F., 2014a. Brachiopod fabric, classes and biogeochemistry: Implications for the reconstruction and interpretation of seawater carbon-isotope curves and records. *Chemical Geology* 371, 60-67.

Garbelli C., Angiolini L., Shen S.Z., Crippa G.,Yuan D.X., Bahrammanesh M., Abbasi S., Birjandi M., 2014b. Additional brachiopod findings from the Lopingian succession of the Ali Bashi mountains, NW Iran. *Rivista Italiana di Stratigrafia e Paleontologia*,120(1), 119-126.

Garbelli C., Angiolini L., Brand U., Shen S.Z.,Jadoul F., Posenato R., Azmy K., Cao C.Q. Neotethys seawater chemistry and temperature at the dawn of the latest Permian extinction. *In revision.*

Gaspard D., 1982. Microstructure de Térébratules biplissées (Brachiopodes) du Cénomanien de la Sarthe (France). Affinités d'une des forms avec le genre *Sellithyris* Midd. *Annales de Paléontologie, Invertébrés*, 68 (1), 1-14.

Ghaderi A., Garbelli C., Angiolini L., Ashouri A.R., Korn D., Rettori R., Gharaie M.H.H., 2014. Faunal change near the end-Permian extinction: the brachiopods of the Ali Bashi mountains, NW Iran. *Rivista Italiana di Stratigrafia e Paleontologia*, 120(1), 27-59.

Goetz A.J., Griesshaber E., Neuser R.D., Lüter C., Hühner M., Harper E., Schmahl W.W., 2009. Calcite morphology, texture and hardness in the distinct layers of rhynchonelliform brachiopod shells. *European Journal of Mineralogy,* 21, 303-315.

Grant R.E., 1971. Brachiopods in the Permina reef environment of the west texas. Proceedings of the Noth Ameican Paleontological Convention, Chigago, 1969 (j) 1444-1481.

Grant R.E., 1976. Permian brachiopods from southern Thailand. *Journal of Paleontology,* 50, 1-269.

Grasby S.E., Sanei H., Beauchamp B., 2011. Catastrophic dispersion of coal fly ash into the oceans during the latest Permian extinction. Nature Geoscience. 4(2), 104-107.

Griesshaber E., Kelm K., Sehrbrock A. et al., 2009. Amorphous calcium carbonate in the shell material of the brachiopod Megerlia truncata. *European Journal of Mineralogy*, 21(4), 715-723.

Grossman E.H. and Ku T.L., 1986. Oxygen and carbon isotope fractionation in biogenic aragonite: temperature effects *Chemical Geology*, 59, 59-74.

Grossman E.L., Yancey T.E., Jones T.E., Bruckschen P., Chuvashov B., Mazzullo S.J., Mii H.S., 2008. Glaciation, aridification, and carbon sequestration in the Permo Carboniferous: the isotopic record from low latitude. *Palaeogeography, Palaeoclimatology, Palaeoecology*, 268, 222-233.

Grunt T.A., 1982. The shell microstructure of the brachiopod order Athyridida, *Paleontological Journal*, 4, 21-35.

Hardie L. A. and Stanley S. M. 1997. Secular biotic trends in skeletal secretion and sedimentary carbonate production resulting from oscillations in seawater chemistry driven by plate tectonics. *Eos (Transactions of the American Geophysical Union)* 78, S179.

Hahn S., Griesshaber E., Schmahl W.W., Neuser R.D., Ritter A.C., Hoffmann R., Buhl D., Niedermayr A., Geske A., Immenhauser A., 2014. Exploring aberrant bivalve shell ultrastructure and geochemistry as proxies for past sea water acidification. *Sedimentology*, 61, 1625-1658.

He W.H., Shen S.Z., Feng Q.I., Gu S.Z., 2005. A late Changhsingian (Late Permian) deep-water brachiopod fauna from the Talung Formation at the Dongpan Section, southern Guangxi, South China. *Journal of Paleontology*, 79 (5), 927-938.

He W.H., Shi G.R., Feng Q., Campi M.J., Gu S., Bu J., Peng Y., Meng Y., 2007. Brachiopod miniaturization and its possible causes during the Permian-Triassic crisis in deep water environments, South China. *Palaeogeography, Palaeoclimatology, Palaeoecology*, 252, 145-163.

He W.H., Twitchett R.J., Zhang Y. et al., 2010. Controls on body size during the Late Permian mass extinction event. *Geobiology*, 8(5), 391-402.

He W.H., Shi G.R., Zhang Y., Yang T.L., Teng F., Wu S.B., 2012. Systematics and palaeoecology of Changhsingian (Late Permian) Ambocoeliidae brachiopods from South China and implications for the end-Permian mass extinction. *Alcheringa*, 36, 515-530.

Hinojosa J.L., Brown S.T., Chen J., DePaolo D.J., Paytan A., Shen S.Z., Payne J.L., 2012. Evidence for end Permian ocean acidification from calcium isotopes in biogenic apatite. *Geology*, 40, 743-746.

Hönisch B., Ridgwell A., Schmidt D.N., Thomas E.,Gibbs S.J., Sluijs A., Zeebe R., Kump L., Martindale R.C., Greene S.E., et al., 2012. The geological record of ocean acidification. *Science*, 335, 1058-1063

Hosmer D.W. Jr., Lemeshow S., Sturdivant R.X.. Applied logistic regression-3rd Edition.

Jin Y.G., et al., 2000. Pattern of marine mass extinction near the Permian-Triassic boundary in South China. *Science* 289, 432-436.

Joachimski M.M., Lai X.L., Shen S.Z., Jiang H.S., Luo G.M., Chen B., Chen J., Sun Y.D., 2012. Climate warming in the latest Permian and the Permian-Triassic mass extinction. *Geology*, 40, 195-198.

Kidder D.L. and Worsley T.R., 2004. Causes and consequences of extreme Permo-Triassic warming to globally equable climate and relation to the Permo-Triassic extinction and recovery. Palaeogeography, Palaeoclimatology, Palaeoecology 203, 207-237.

Knoll A.H., Bambach R., Canfield D., Grotzinger J.P., 1996 Comparative Earth history and Late Permian mass extinction. Science 273, 452-457.

Knoll A.H., 2003. Biomineralization and evolutionary history. *Reviews in Mineralogy and Geochemistry*, 54, 329-356.

Knoll A. H., Bambach R.K., Payne J.L., Pruss S., Fischer W.W., 2007. Paleophysiology and end-Permian mass extinction. *Earth and Planetary Science Letters*, 256, 295-313.

Komarov V.N., 1991. Microstructure of the shell wall in Puncta trypa olgae Nalivkin (Atrypida, Brachiopoda), *Doklady Akademii Nauk*, 321(5), 1091-1094.

Korte C., Jasper T., Kozur H.W. et al., 2005. Delta(18)O and delta(13)C of Permian brachiopods: A record of seawater evolution and continental glaciation. *Palaeogeography Palaeoclimatology Palaeoecology*, 224 (4), 333-351.

Kouchinsky A., Bengtson S., Runnegar B. et al., 2012. Chronology of early Cambrian biomineralization. *Geological Magazine,* 149(2), 221-251.

Kozur H.W., 1998. Some aspects of the Permian-Triassic boundary (PTB) and the possible causes for the biotic crisis around this boundary. *Palaeogeography, Palaeoclimatology, Palaeoecology* 143, 227-272.

Labandeira C.C. and Sepkoski Jr. J.J., 1993. Insect diversity in the fossil record. *Science* 261, 310-315.

Lécuyer C., Reynard B., Martineau F. (2004) Stable isotope fractionation between mollusc shells and marine waters from Martinique Island. *Chemical Geology* 213: 293-305.

Li W.Z. and Shen S.Z., 2008. Lopingian (Late Permian) brachiopods around the Wuchiapingian-Changhsingian boundary at the Meishan sections C and D, Changxing, South China. *Geobios* 41, 307-320.

Lowenstam, H.A. 1961. Mineralogy, O^{18}/O^{16} ratios, and strontium and magnesium contents of recent and fossil brachiopods and their bearing on the history of the oceans. *Journal of Geology,* 69, 241-260.

Machel H.G., Mason R.A., Mariano A.N., Mucci, A., 1991. Causes and emission of luminescence in calcite and dolomite. In: Barker, C.E., Kopp, O.C. (Eds.), Luminescence Microscopy and spectroccopy: qualitative and quantitative applications. : Short Course, 25. Society for Sedimentary Geology, Tulsa, pp. 9-25.

Machel H.G., 2000. Application of cathodoluminescence to carbonate diagenesis. In: Pagel, M., Barbin, V., Blank, P., Ohnenstetter, D. (Eds.), Cathodoluminescence in Geosciences. Springer, New York, pp. 271-301.

MacKinnon D.I., 1974. The shell structure in spiriferide brachiopoda. *Bulletin of the British Museum (Natural History). Geology*, 5(3), 189-258.

Mann S., (2001) Biomineralization: Principles and Concepts in Bioinorganic Materials Chemistry. Vol 17. Oxford University Press, Oxford.

Maxwell W.D., 1992. Permian and early Triassic extinction of non-marine tetrapods. *Palaentology* 35, 571-583.

Mii H.S., Grossman E.L., Yancey T.E., Chuvashov B., Egorov A., 2001. Isotopic records of brachiopod shells from the Russian Platform — evidence for the onset of mid-Carboniferous glaciation. *Chemical Geology,* 175, 133-147.

Morrison J.O. and Brand U., 1986. Geochemistry of recent marine invertebrates. *Geoscience Canada*, 13: 237-253.

Muir-Wood H.M and Cooper G.A., 1960. Morphology, classification and life habits of the Productoidea (Brachiopoda). . *Geological Society of America Memoir*, 81(447), 135.

Muttoni G., Gaetani M., Kent D.V., Sciunnach D., Angiolini L., Berra F., Garzanti E., Mattei M., Zanchi A., 2009. Opening of the Neo-Tethys Ocean and the Pangea B to Pangea A transformation during the Permian. *GeoArabia* 14, 17-48.

Okumura T., Suzuki M., Nagasawa H., Kogure T., 2013. Microstructural control of calcitevia incorporation of intracrystalline organic molecules in shells. *Journal of Crystal Growth*, 381, 114-120.

Olson I.C., Kozdon R., Valley J.W. et al., 2012a. Mollusk Shell Nacre Ultrastructure Correlates with Environmental Temperature and Pressure. *Journal of the American Chemical Society,* 134(17), 7351-7358.

Olson I.C., Gilbert, Pupa U.P.A, 2012b. Aragonite crystal orientation in mollusk shell nacre may depend on temperature. The angle spread of crystalline aragonite tablets records the water temperature at which nacre was deposited by *Pinctada margaritifera. Faraday Discussion,* 159, 421-432.

Parkinson D., Curry G.B., Cusack M., Fallick A.E. 2005. Shell structure, patterns and trends of oxygen and carbon stable isotopes in modern brachiopod shells. *Chemical Geology*, 219, 193-235.

Parkinson D. and Cusack M. 2007. Stable oxygen isotopes in extant brachiopod shells: keys to deciphering ancient ocean environments. In *Treatise of Invertebrate Paleontology,* pp 2522-2531.

Peck S.L., Brockington S., Brey T., 1997. Growth and metabolism in the Antarctic Brachiopod *Liothyrella uva*. *Philosophical Transactions of the Royal Society B: Biological*, 352, 851-858.

Pérez-Huerta A. and Cusack M., 2008. Common crystal nucleationmechanism in shell formation of two morphologically distinct calcite brachiopods. *Zoology*, 111(1), 9-15.

Pérez-Huerta A., Cusack M., McDonald S., Marone F., Stampanoni M., MacKay S., 2009. Brachiopod punctae: a complexity in shell biomineralisation. *Journal of Structural Biology,* 167(1), 62-67.

Pérez-Huerta A., Dauphin Y., Cusack M., 2013. Biogenic calcite granules: are brachiopods different? *Micron*, 44, 395e403.

Pérez-Huerta A., 2013. Functional Morphology and Modifications on Spine Growth in the Productid Brachiopod *Heteralosia slocomi*. *Acta Palaeontologica Polonica*, 58(2), 383-390.

Popp B.N., Anderson T.F., Sandberg P.A., 1986. Brachiopods as indicators of original isotopic compositions in some Paleozoic limestones. *Geological Society of America Bulletin*, 97, 1262-1269.

Porter S.M., 2007. Seawater chemistry and early carbonate biomineralization. *Science* 316, 1302.

Posenato R., 2009. Survival patterns of macrobenthic marine assemblages during the end-Permian mass extinction in the western Tethys (Dolomites, Italy). *Palaeogeography, Palaeoclimatology, Palaeoecology*, 280, 150-167.

Posenato R., 2011. Latest changhsingian Orthotetid brachiopods in the Dolomites (Southern Alps, Italy): ecological opportunists at the peak of the end-Permian mass extinction. *Journal of Paleontology*, 85(1), 58-68.

Raup D.M., 1979. Size of the Permo-Triassic bottleneck and its evolutionary implications. *Science* 206, 217-218.

Racki G., Wignall P.B., 2005. Late Permian double-phased mass extinction and volcanism: an oceanographic perspective. In: Over, D.J., Morrow, J.R., Wignall P.B., (Eds.), Understanding Late Devonian and Permian-Triassic biotic and climatic events: towards an integrated approach. Elsevier, pp. 263-297.

Retallack G.J., 1995. Permian-Triassic life crisis on land. *Science* 267, 77-80.

Retallack G.J. and Jahren A.H., 2008. Methane release from igneous intrusions of coal during the Late Permian extinction events. *Journal of Geology*, 116, 1-20.

Retallack G.J. et al., 2011.Multiple Early Triassic greenhouse crises impeded recovery from Late Permian mass extinction. *Palaeogeography, Palaeoclimatology, Palaeoecology* 308, 233-251.

Retallack G.J., 2013. Permian and Triassic greenhouse crises. *Gondwana Research* 24, 90-103.

Richardson J.R., 1997. Ecology of articulated brachiopods. In: Kaesler R ed. - Colorado, Geological Society of America and University of Kansas. *Treatise of invertebrate paleontology, Brachiopoda (rev.)* Part H. Vol. 1, 441-462.

Rudwick M.J.S., 1970. Living and fossil brachiopods. Hutchinson and Co., London.

Schobben M., Joachimski M.M., Korn D., Leda L., Korte C., 2014. Palaeotethys seawater temperature rise and an intensified hydrological cycle following the end-Permian mass extinction. *Gondwana Research,* 26, 675-683.

Schone B.R., Fiebig J., Pfeiffer M., Gleb R., Hickson J., Johnson A L.A., Dreyer W. and Oschmann W.,2005. Climate records from a bivalved Methuselah (Arctica islandica, Mollusca; Iceland), *Palaeogeography. Palaeoclimatology. Palaeoecology*, 228, 130-148

Sepkoski J.J. Jr., 1992. A Compendium of Fossil Marine Families, second edition. *Milwaukee Publ. Mus. Contr. Biol. Geol.*, 83, 1-155.

Sepkoski J.J. Jr.,2002. A compendium of fossil marine animal genera, *Bulletins of American Paleontology*, 363, 1-563.

Shen S.Z., Archbold N.W., Shi G., Chen Z.Q., 2000. Permian brachiopods from the Selong Xishan Section, Xizang (Tibet), China, part 1: stratigraphy, Strophomenida, Productida and Rhynchonellida. *Geobios,* 33, 725-752.

Shen S.Z., Archbold N.W., Shi G., Chen Z.Q., 2001. Permian brachiopods from the Selong Xishan Section, Xizang (Tibet), China, part 2: palaeobiogeographical and palaeoecological implications, Spiriferida, Athyridida and Terebratulida. *Geobios,* 34,157-182.

Shen S.Z. and Archbold N.W., 2002. Chonetoidea (Brachiopoda) from the Lopingian (Late Permian) of South China. *Alcheringa*, 25, 327-349.

Shen S.Z., Cao C.Q., Henderson C.M., Wang X.D., Shi G.R., Wang Y., Wang W., 2006. End-Permian mass extinction pattern in the northern peri-Gondwanan region. *Palaeoworld*, 15(1), 3-30.

Shen S.Z., Cao C.Q., Zhang Y.C., Li W.Z., Shi G.R., Wang Y., Wu Y.S., Ueno K., Henderson C.M., Wang X.D., Zhang H., Wang X.J., Chen J., 2010. End-Permian mass extinction and palaeoenvironmental changes in Neotethys: evidence from an oceanic carbonate section in southwestern Tibet. *Global and Planetary Change*, 73, 3-14.

Shen, S. Z., Crowley J.L., Wang Y., Bowring S.A., Erwin D.H., Sadler P.M., Cao C.Q., Rothman D.H., Henderson C.M., Ramezani J., Zhang H., Shen Y.A., Wang X.A., Wang W., Mu L., Li W.Z., Tang Y.G., Liu W.L., Liu L.J., Zeng Y., Jiang Y.F. and Jin Y.G.. 2011. Calibrating the end-Permian mass extinction. *Science* 334, 1367-1372.

Simkiss K., Wilbur K.M. (1989) Biomineralization: Cell Biology and Mineral Deposition. Academic Press, New York.

Stanley S.M. and Hardie L.A. 1998. Secular oscillations in the carbonate mineralogy of reef-building and sedimentproducing organisms driven by tectonically forced shifts in seawater chemistry. Palaeogeography, Palaeoclimatology, *Palaeoecology,* 144, 3-19.

Svensen H., Planke S., Polozov A.G., Schmidbauer N., Corfu F., Podladchikov Y.Y., Jamtveit B., 2009. Siberian gas venting and the end-Permian environmental crisis. *Earth and Planetary Science Letters*, 277, 490-500.

Twitchett R.J., 2005. The Lilliput effect in the aftermath of the end-Permian extinction event. Albertiana 33, 79-81.

Urbanek A., 1993. Biotic crises in the history of upper Silurian graptoloids: a palaeobiological model. Historical Biology 7, 29-55.

Ushatinskaya G.T. and Zhuravlev A.Y., 1994 On the problem of skeletal mineralization (brachiopod implications) *Doklady Akademii Nauk*,337(2) 231-234

Vöros A., 2005. The smooth brachiopods of the Mediterranean Jurassic: Reffugees or invaders? *Palaeogeography, Palaeoclimatology, Palaeoecology*, 223, 222-242.

Wang Y., Ueno K., Zhang Y. et al., 2010. The Changhsingian foraminiferal fauna of a Neotethyan seamount: the Gyanyima Limestone along the Yarlung-Zangbo Suture in southern Tibet, China. Geological Journal, 45(2-3), 308-318.

Ward P.D. et al., 2005. Abrupt and gradual extinction among Late Permian vertebrates in the Karoo Basin, South Africa. Science 307, 709-714.

Watson S., Peck L.S., Tyler P.A. et al., 2012. Marine invertebrate skeleton size varies with latitude, temperature and carbonate saturation: implications for global change and ocean acidification. *Global Change Biology,* 18(10), 3026-303

White R.V., 2002. Earth's biggest 'whodunnit': unravelling the clues in the case of the end-Permian mass extinction. Philosophical Transactions of the Royal Society of London 360, 2963-2985.

Wignall P.B., 2007. The End-Permian mass extinction—how bad did it get? *Geobiology*, 5, 303-3.

Williams A., 1956. The calcareous shell of the Brachiopoda and its importance to their classification. *Biological Reviews,* 31, 243-287.

Williams A. and Rowell A.J., 1965a. Brachiopod anatomy. in ''Treatise on Invertebrate Paleontology'', R.C. Moore ed., part H. Geological Society of America and University of Kansas Press, New York and Lawrence, H6-H57.

Williams A. and Rowell A.J., 1965b. Brachiopod morphology. in ''Treatise on Invertebrate Paleontology'', R.C. Moore ed., part H. Geological Society of America and University of Kansas Press, New York and Lawrence, H57-H115.

Williams A., 1968. Evolution of the shell structure of articulate brachiopods. *Special Papers in Paleontology*, 2, 1-55.

Williams A., 1970. Origin of laminar-shelled articulate brachiopods. *Lethaia*, 3, 329-342.

Williams A. and Brunton C.H.C., 1993. *Role* of the *shell structure in the classification of the orthotetidine brachiopods*. *Palaeontology,* 36, 931-966.

Williams A., Carlson S.J., Brunton C.H.C., Holmer L.E., Popov L., 1996. A supra-ordinal classification of the Brachiopoda. *Philosophical Transactions: Biological Sciences* 351, 1171-1193.

Williams A., Brunton C.H.C., MacKinnon D.I., 1997. Morphology. In: Kaesler R ed. - Colorado, Geological Society of America and University of Kansas. *Treatise of invertebrate paleontology, Brachiopoda (rev.)* Part H. Vol. 1, 321-422.

Williams A., 1997. Shell structure. In: Kaesler, R.L. (Ed.), Treatise on Invertebrate Palaeontology (Part H, Brachiopoda Revised). Introduction. Geological Society of America, vol. 1. University of Kansas Press, Boulder, CO, pp. 267-320 (Lawrence).

Williams A. and Cusack M., 2007. Chemicostructural diversity of the brachiopod shell. In: Selden, P.A. (Ed.), Treatise on Invertebrate Paleontology (Part H, Brachiopoda Revised). Geological Society of America. Supplement, vol. 6. University of Kansas Press, Boulder, CO, pp. 2397-2521 (Lawrence).

Yamamoto K., Asami R., Iryu Y., 2013. Correlative relationships between carbon- and oxygen-isotope records in two cool-temperate brachiopod species off Otsuchi Bay, northeastern Japan. *Paleontological Research*, 17, 12-26.

Zhuravlev A.Y. and Wood R.A., 2008. Eve of biomineralization: Controls on skeletal mineralogy. *Geology*, 36, 923-926.

Zhuravlev A.Y. and Wood R.A., 2009. Controls on carbonate skeletal mineralogy: Global CO_2 evolution and mass extinctions. *Geology*, 37, 1123-1126.

Acknowledgements

Since I was a child, nature fascinated me, probably because I had the chance to grow up in a country village. During the high school, chemistry, earth science and biology were my favorite topics and, despite the few hours of classes, I spent several hours browsing old fashion books of natural science at the public library. During the years of university I discovered how wonderful Natural Science was and how much a single research topic may be complex. I was particularly influenced by the lessons of biological evolution and intrigued by the geobiological history of the planet Earth.

A key moment in my life was September 2009, when I started to work on my master degree under the supervision of Professor Lucia Angiolini. Since that moment she has been a great mentor for me.

Thanks to Professor Andrea Tintori for having supervised me during my doctorate.

Thanks to Professor Flavio Jadoul who has helped me a lot in interpreting the cathodoluminescence of brachiopod shells and for having reminded me that there is something else besides the organisms, that is their diagenetic history.

Thanks also to Professor Marco Ferraguti because he always encouraged me to study evolution and inspired me with his brilliant ideas.

A very special mention to professors Uwe Brand and Shen Shuzhong, for having supported me from different points of view. Their competences have enriched my research skills and activities, their eagerness and positive thinking make easier to conduct research.

Thanks to Doctor Cristina Lombardo for all the useful suggestions and good advices.

Thanks to Professor Renato Posenato who provided some brachiopod specimens for my research.

For the technical assistance, thanks to Curzio Malinverno, Agostino Rizzi and Andrea Risplendente for having granted all my requests.

Thanks to my classmates of the PhD course Alessia, Irene, Gaia and Giulia.

I want to remember all the people who dwelled office 56 during these years: Umberto, Laura, Matteo, Irene, Andrea, Claudia, Giovanni and Boris. I spent with you magnificent moments I will never forget!

Thanks to my family who has always supported me during my life itinerary.

…and who else if not her, the person close to me in the brightest and darkest moments of these three years. Thanks from the bottom of my heart to Marta, not only for the support she gave to me, but especially for the beautiful person she is.

Appendix A

Stratigraphic log of Main Valley section (Fig. 1, Modified from Ghaderi et al., 2014), and the Ali Bashi section 1 and 3 (Figs 2, 3) and the Zal section (Fig. 4) of Julfa and AliBashi formations in nortwestern Iran; Shangsi section 1 and 2 (Figs 5 and 6 respectively); of Dalong formation in South China Beifengjing section (Fig. 7), Daijaigou section (Fig. 8), Zhongliang hill section (Fig. 9) of Changhsing Formation in South China.

Note that for sample analyzed SEM the horizons have this correspondence: JU106=G134; JU112=G138, JU114=G142, JU115=G142B, JU117=G143, JU120=G144, JU121=G145B, JU129=G154, JU131=G154B, JU132=G156, JU133=G157, JU136=G187, JU141=G273; JU140 and JU139 are 30 and 60 cm below the PTB respectively.

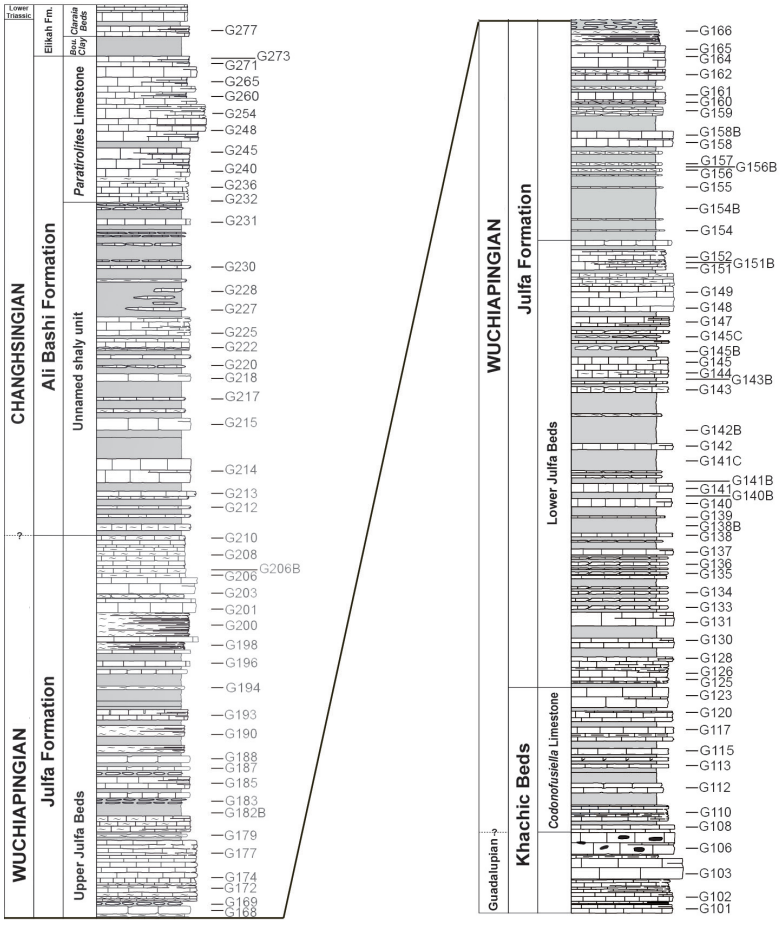

Figure 1 - Main Valley section, 38° 56’ 06.3”N 45° 31’ 17.7”E

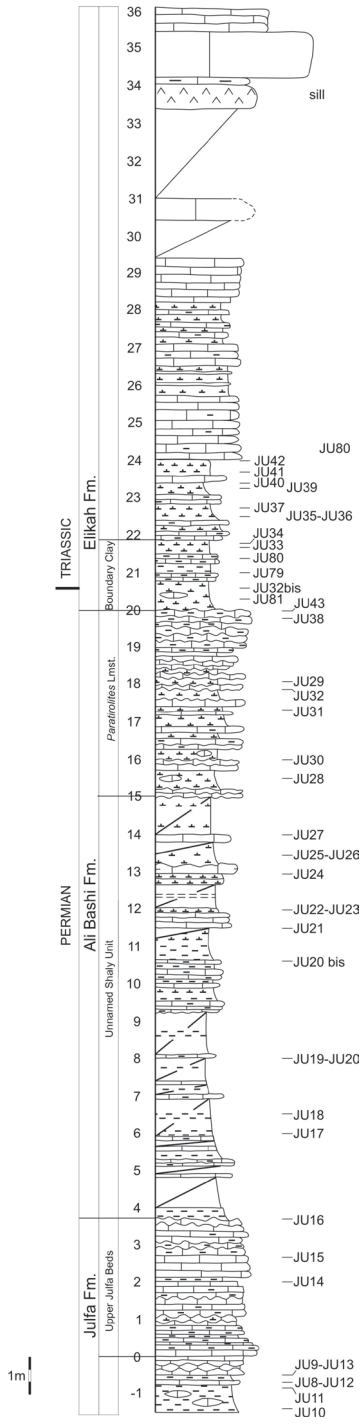

Figure 2 - Ali Bashi section 1, 38° 56’ 22.5”N 45° 31’ 13.0”E

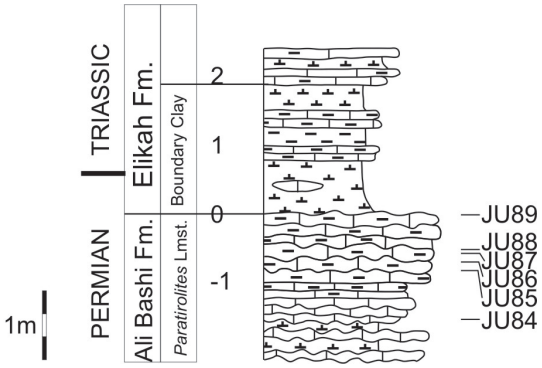

Figure 3 . Ali Bashi section 3, 38° 56’ 22.5”N 45° 31’ 13.0”E

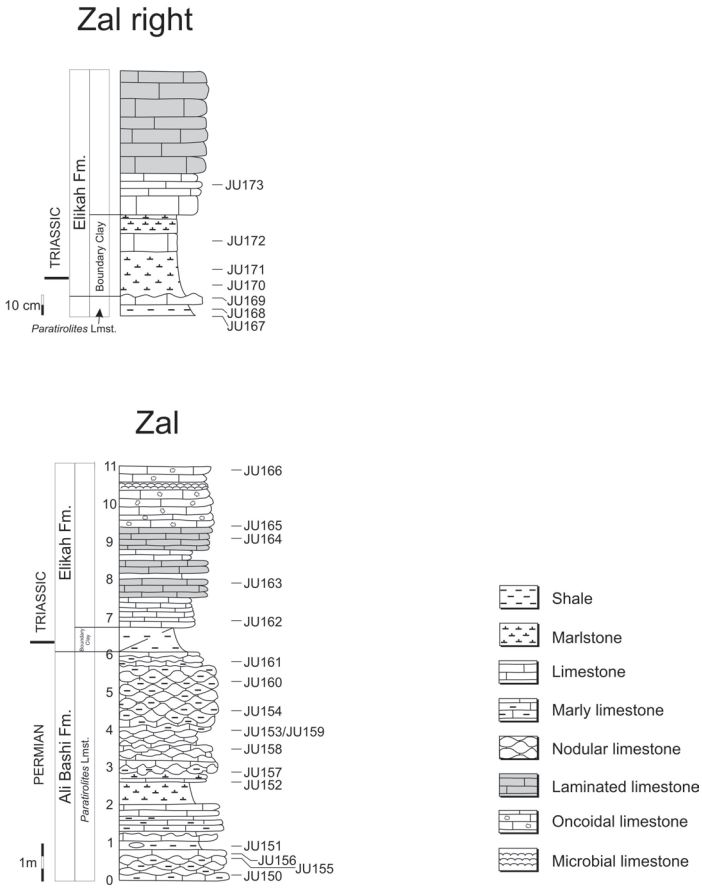

Figure 4 - Zal section, 38° 43’ 55.3”N 45° 34’ 54.7”E

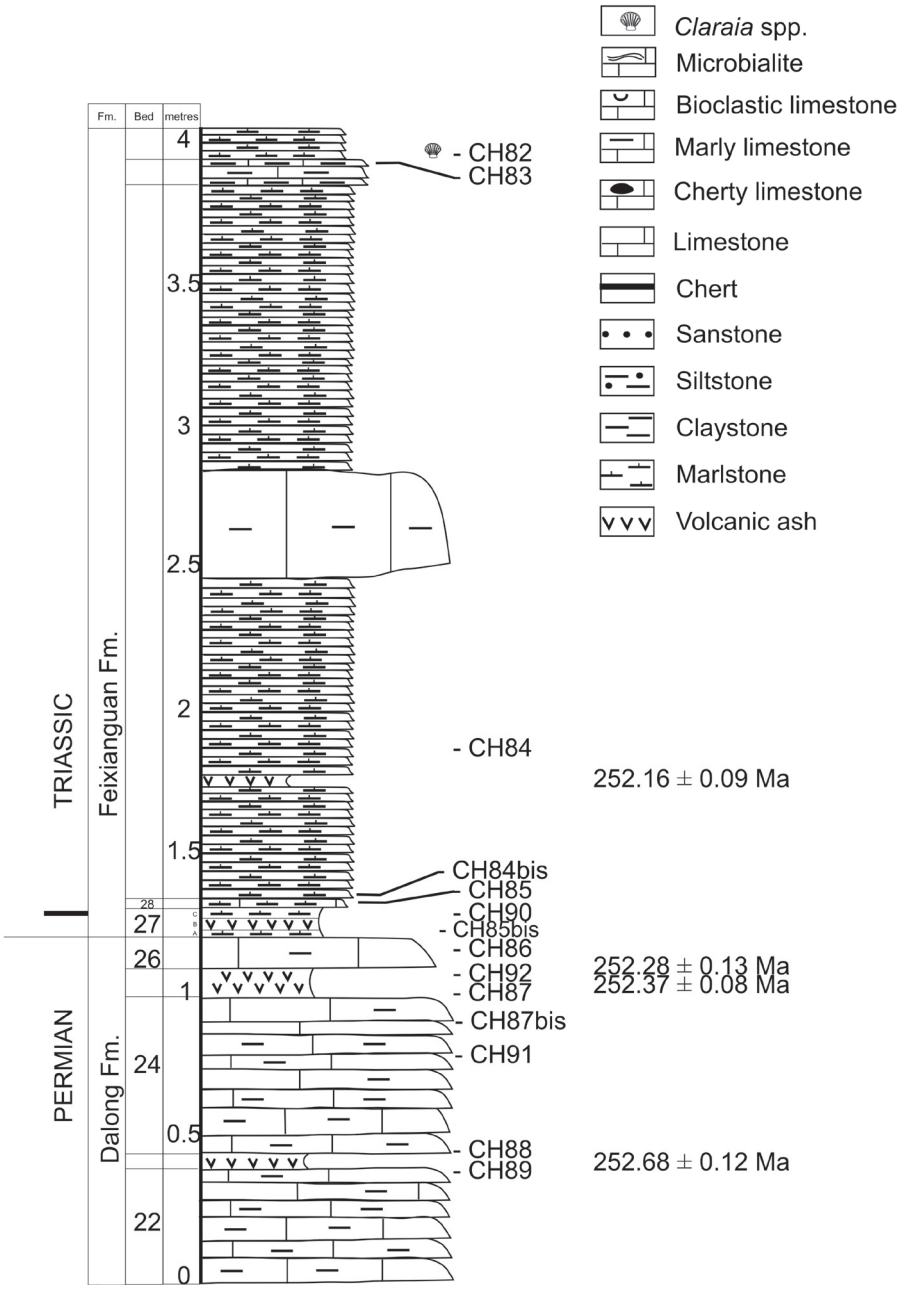

Figure 5 - Shangsi section 1, 32° 19’ 09.9”N 105° 27’ 17.3”E

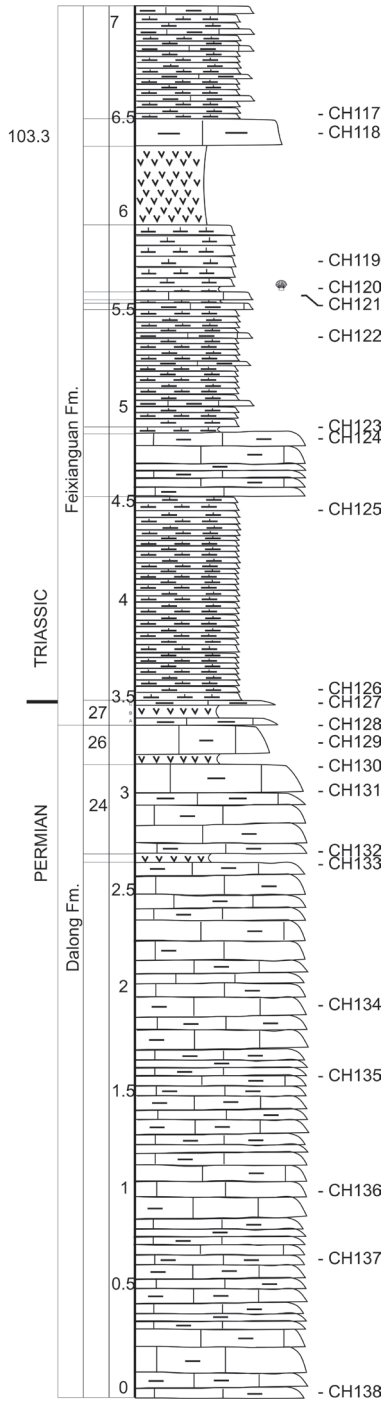

Figure 6 - Shangsi section 2, 32° 19’ 09.9”N 105° 27’ 17.3”E

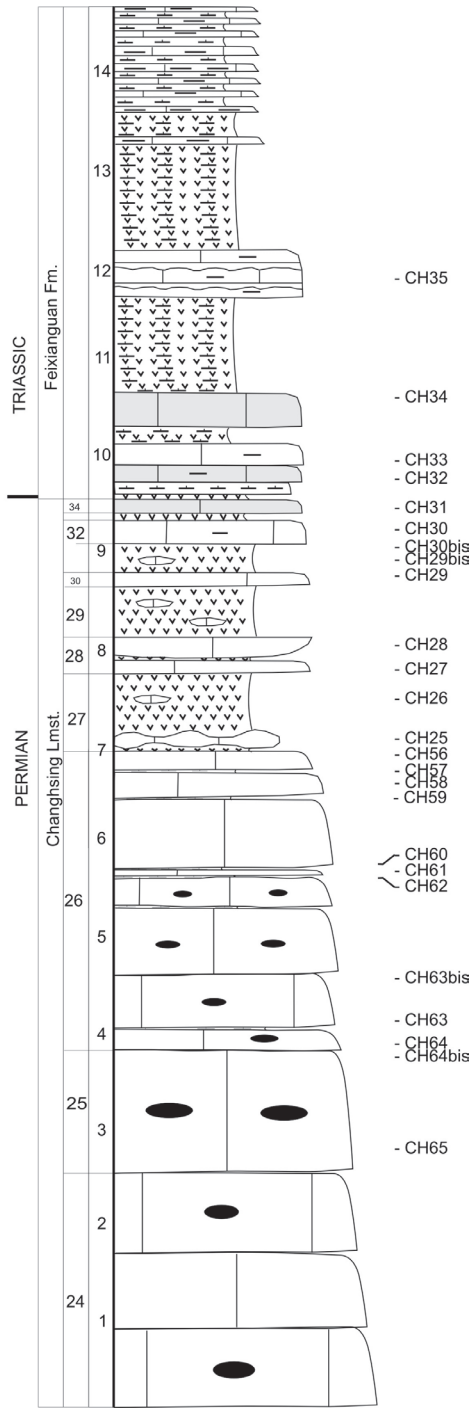

Figure 7 - Beifengjing section, 29° 30’ 16.1”N 106° 24’ 15.2”E

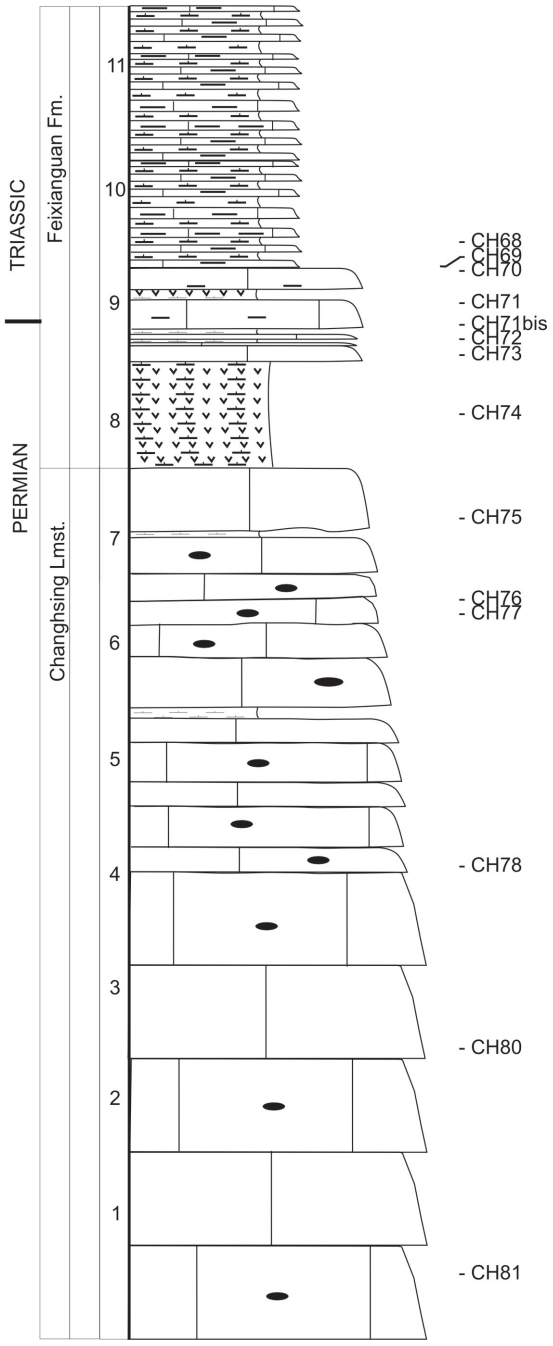

Figure 8 - Daijaigou section, 29° 54’ 29.5”N 106° 31’ 14.6”E

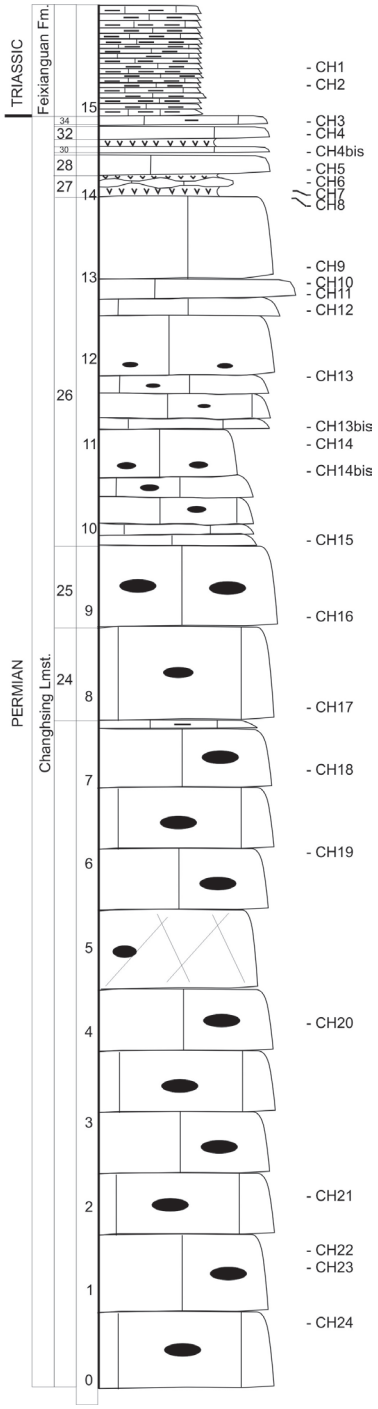

Figure 9 - Zhongliang hill section, 29° 30’ 20.2”N 106° 24’ 12.1”E

Appendix B

OccPD. Summary of the generic occurences in during Late Permian and Early Triassic, downloaded from the Paleobiology database.
W=Wuchiapingina, C=Changhsingian, I=Induan, O=Olenekian; NA = not present

Order	Family	Genus	W	C	I	O
Athyridida	Athyrididae	*Actinoconchus*	1	NA	NA	NA
Athyridida	Athyrididae	*Araxathyris*	161	130	3	NA
Athyridida	Athyrididae	*Athyris*	64	17	NA	NA
Athyridida	Athyrididae	*Bajtugania*	1	NA	NA	NA
Athyridida	Athyrididae	*Cleiothyridellina*	NA	26	NA	NA
Athyridida	Athyrididae	*Cleiothyridina*	476	72	NA	NA
Athyridida	Athyrididae	*Comelicania*	NA	27	NA	NA
Athyridida	Athyrididae	*Comelicothyris*	NA	13	NA	NA
Athyridida	Athyrididae	*Composita*	10	11	NA	NA
Athyridida	Athyrididae	*Gruntallina*	NA	6	NA	NA
Athyridida	Athyrididae	*Gruntea*	5	5	NA	NA
Athyridida	Athyrididae	*Himathyris*	5	NA	NA	NA
Athyridida	Athyrididae	*Janiceps*	6	26	NA	NA
Athyridida	Athyrididae	*Juxathyris*	33	60	1	NA
Athyridida	Athyrididae	*Mayangella*	3	NA	NA	NA
Athyridida	Athyrididae	*Pinegathyris*	4	NA	NA	NA
Athyridida	Athyrididae	*Rectambitus*	2	5	NA	NA
Athyridida	Athyrididae	*Septospirigerella*	NA	5	NA	NA
Athyridida	Athyrididae	*Spirigerella*	552	78	NA	NA
Athyridida	Athyrididae	*Tarimathyris*	NA	8	NA	NA
Athyridida	Athyrididae	*Tongzithyris*	1	8	NA	NA
Athyridida	Athyrididae	*Transcaucasathyris*	99	50	NA	NA
Athyridida	Athyrididae	*Xenosaria*	1	NA	NA	NA
Athyridida	Diplospirellidae	*Spirigerellina*	NA	NA	NA	5
Athyridida	Neoretziidae	*Hustedia*	88	43	NA	NA
Athyridida	Neoretziidae	*Hustedtiella*	NA	NA	NA	2
Athyridida	Retziidae	*Retzia*	NA	1	NA	NA
Orthida	Dalmanellidae	*Dalmanella*	NA	NA	NA	NA
Orthida	Enteletidae	*Camerenteletes*	NA	4	NA	NA
Orthida	Enteletidae	*Enteletella*	NA	2	NA	NA
Orthida	Enteletidae	*Enteletes*	57	61	NA	NA

Orthida	Enteletidae	*Enteletina*	12	1	NA	NA
Orthida	Enteletidae	*Enteletoides*	4	NA	NA	NA
Orthida	Enteletidae	*Peltichia*	25	79	NA	NA
Orthida	Orthidae	*Orthis*	3	NA	NA	NA
Orthida	Rhipidomellidae	*Rhipidomella*	6	8	NA	NA
Orthida	Schizophoriidae	*Acosarina*	93	101	2	NA
Orthida	Schizophoriidae	*Kotlaia*	1	7	4	NA
Orthida	Schizophoriidae	*Orthotichia*	34	19	2	NA
Orthida	Schizophoriidae	*Schizophoria*	3	3	NA	NA
Rhynchonellida	Allorhynchidae	*Allorhynchus*	7	2	NA	NA
Rhynchonellida	Allorhynchidae	*Gerassimovia*	1	6	NA	NA
Rhynchonellida	Allorhynchidae	*Pseudowellerella*	3	5	NA	NA
Rhynchonellida	Allorhynchidae	*Terebratuloidea*	125	13	4	NA
Rhynchonellida	Allorhynchidae	*Wairakiella*	2	7	NA	NA
Rhynchonellida	Lambdarinidae	*Lambdarina*	1	NA	NA	NA
Rhynchonellida	Norellidae	*Laevorhynchia*	NA	NA	1	NA
Rhynchonellida	Norellidae	*Meishanorhynchia*	NA	NA	5	NA
Rhynchonellida	Norellidae	*Paranorellina*	NA	NA	2	3
Rhynchonellida	Norellidae	*Piarorhynchella*	NA	NA	1	43
Rhynchonellida	Pontisiidae	*Lissorhynchia*	NA	2	NA	1
Rhynchonellida	Pontisiidae	*Neowellerella*	NA	2	2	NA
Rhynchonellida	Pontisiidae	*Prelissorhynchia*	32	130	7	NA
Rhynchonellida	Pontisiidae	*Wellerellina*	2	10	NA	NA
Rhynchonellida	Psilocamaridae	*Bicamella*	5	3	NA	NA
Rhynchonellida	Psilocamaridae	*Camarophorinella*	1	7	NA	NA
Rhynchonellida	Psilocamaridae	*Cyrolexis*	4	6	NA	NA
Rhynchonellida	Psilocamaridae	*Hybostenoscisma*	4	5	NA	NA
Rhynchonellida	Psilocamaridae	*Neopsilocamara*	1	1	NA	NA
Rhynchonellida	Psilocamaridae	*Psilocamara*	1	1	NA	NA
Rhynchonellida	Psilocamaridae	*Septacamarella*	4	NA	NA	NA
Rhynchonellida	Pugnacidae	*Pugnax*	8	2	NA	NA
Rhynchonellida	Rhynchonellidae	*Abrekia*	NA	NA	1	4
Rhynchonellida	Rhynchonellidae	*Rhynchonella*	1	NA	NA	3
Rhynchonellida	Rhynchoporidae	*Rhynchopora*	68	NA	NA	NA
Rhynchonellida	Rhynchotetradidae	*Rhynchotetra*	2	NA	NA	NA
Rhynchonellida	Stenoscismatidae	*Camarophoria*	12	NA	NA	NA

Rhynchonellida	Stenoscismatidae	*Coledium*	11	1	NA	NA
Rhynchonellida	Stenoscismatidae	*Stenoscisma*	262	16	NA	NA
Rhynchonellida	Wellerellidae	*Anchorhynchia*	9	38	NA	NA
Rhynchonellida	Wellerellidae	*Glyptorhynchia*	1	8	NA	NA
Rhynchonellida	Wellerellidae	*Plekonella*	10	8	NA	NA
Rhynchonellida	Wellerellidae	*Tautosia*	NA	4	NA	NA
Rhynchonellida	Wellerellidae	*Uncinunellina*	60	79	3	NA
Rhynchonellida	Wellerellidae	*Wellerella*	19	9	NA	NA
Spiriferida	Ambocoeliidae	*Attenuatella*	12	22	NA	NA
Spiriferida	Ambocoeliidae	*Cruricella*	1	5	NA	NA
Spiriferida	Ambocoeliidae	*Crurithyris*	21	37	6	NA
Spiriferida	Ambocoeliidae	*Orbicoelia*	7	96	31	NA
Spiriferida	Ambocoeliidae	*Paracrurithyris*	NA	77	15	NA
Spiriferida	Brachythyrididae	*Ella*	NA	1	NA	NA
Spiriferida	Brachythyrididae	*Pustuloplica*	1	1	NA	NA
Spiriferida	Choristitidae	*Alphaneospirifer*	1	16	NA	NA
Spiriferida	Choristitidae	*Brachythyrina*	NA	2	NA	NA
Spiriferida	Choristitidae	*Choristitella*	10	2	NA	NA
Spiriferida	Choristitidae	*Choristites*	1	NA	NA	NA
Spiriferida	Choristitidae	*Semibrachythyrina*	4	1	NA	NA
Spiriferida	Choristitidae	*Zhejiangospirifer*	1	NA	NA	NA
Spiriferida	Elythidae	*Bullarina*	3	8	NA	NA
Spiriferida	Elythidae	*Neophricadothyris*	4	NA	NA	NA
Spiriferida	Elythidae	*Permophricodothyris*	175	97	NA	NA
Spiriferida	Elythidae	*Phricodothyris*	44	23	NA	NA
Spiriferida	Elythidae	*Spirelytha*	NA	1	NA	NA
Spiriferida	Elythidae	*Squamularia*	23	26	NA	NA
Spiriferida	Ingelarellidae	*Ambikella*	3	16	NA	NA
Spiriferida	Ingelarellidae	*Ingelarella*	4	2	NA	NA
Spiriferida	Ingelarellidae	*Martiniopsis*	8	19	NA	NA
Spiriferida	Ingelarellidae	*Notospirifer*	6	7	NA	NA
Spiriferida	Ingelarellidae	*Tomiopsis*	11	6	NA	NA
Spiriferida	Martiniidae	*Jilinmartinia*	6	NA	NA	NA
Spiriferida	Martiniidae	*Ladoliplica*	NA	3	NA	NA
Spiriferida	Martiniidae	*Martinia*	147	73	4	NA

Spiriferida	Martiniidae	*Rallacosta*	1	NA	NA	NA
Spiriferida	Martiniidae	*Spinomartinia*	1	3	NA	NA
Spiriferida	Martiniidae	*Tiramnia*	7	2	NA	NA
Spiriferida	Paeckelmanellidae	*Odontospirifer*	7	NA	NA	NA
Spiriferida	Reticulariidae	*Bajkuria*	NA	3	NA	NA
Spiriferida	Reticulariidae	*Reticularia*	3	NA	NA	NA
Spiriferida	Reticulariidae	*Warrenella*	NA	NA	NA	1
Spiriferida	Spiriferellidae	*Alispiriferella*	3	NA	NA	NA
Spiriferida	Spiriferellidae	*Arcullina*	2	NA	NA	NA
Spiriferida	Spiriferellidae	*Elivina*	4	2	NA	NA
Spiriferida	Spiriferellidae	*Nakimusiella*	NA	5	NA	NA
Spiriferida	Spiriferellidae	*Spiriferella*	95	83	NA	NA
Spiriferida	Spiriferellidae	*Timaniella*	3	NA	NA	NA
Spiriferida	Spiriferellidae	*Tipispirifer*	NA	1	NA	NA
Spiriferida	Spiriferidae	*Eliva*	2	1	NA	NA
Spiriferida	Spiriferidae	*Latispirifer*	7	NA	NA	NA
Spiriferida	Spiriferidae	*Ovispirifer*	2	NA	NA	NA
Spiriferida	Spiriferidae	*Purdonella*	3	NA	NA	NA
Spiriferida	Spiriferidae	*Spirifer*	8	1	NA	NA
Spiriferida	Strophopleuridae	*Pteroplecta*	2	28	NA	NA
Spiriferida	Strophopleuridae	*Pterospirifer*	42	NA	NA	NA
Spiriferida	Strophopleuridae	*Spiriferinaella*	1	NA	NA	NA
Spiriferida	Trigonotretidae	*Aperispirifer*	NA	12	NA	NA
Spiriferida	Trigonotretidae	*Betaneospirifer*	37	52	NA	NA
Spiriferida	Trigonotretidae	*Blasispirifer*	12	2	NA	NA
Spiriferida	Trigonotretidae	*Cartorhium*	14	3	NA	NA
Spiriferida	Trigonotretidae	*Costatispirifer*	1	NA	NA	NA
Spiriferida	Trigonotretidae	*Crassispirifer*	1	1	NA	NA
Spiriferida	Trigonotretidae	*Fusispirifer*	13	8	NA	NA
Spiriferida	Trigonotretidae	*Gypospirifer*	1	NA	NA	NA
Spiriferida	Trigonotretidae	*Kaninospirifer*	37	NA	NA	NA
Spiriferida	Trigonotretidae	*Lepidospirifer*	NA	1	NA	NA
Spiriferida	Trigonotretidae	*Neospirifer*	145	29	NA	NA
Spiriferida	Trigonotretidae	*Occidalia*	2	NA	NA	NA
Spiriferida	Trigonotretidae	*Pondospirifer*	1	8	NA	NA

Spiriferida	Trigonotretidae	*Quadrospira*	9	3	NA	NA
Spiriferida	Trigonotretidae	*Transversaria*	5	12	NA	NA
Spiriferida	Trigonotretidae	*Trigonotreta*	7	4	NA	NA
Spiriferida	Trigonotretidae	*Wadispirifer*	8	4	NA	NA
Spiriferinida	Cyrtinidae	*Licharewina*	2	4	NA	NA
Spiriferinida	Laballidae	*Eolaballa*	NA	1	NA	NA
Spiriferinida	Lepismatinidae	*Lepismatina*	NA	NA	2	7
Spiriferinida	Licharewiidae	*Licharewia*	3	NA	NA	NA
Spiriferinida	Paraspiriferinidae	*Callispirina*	43	12	NA	NA
Spiriferinida	Paraspiriferinidae	*Paraspiriferina*	97	19	NA	NA
Spiriferinida	Paraspiriferinidae	*Yaonoiella*	NA	3	NA	NA
Spiriferinida	Pennospiriferinidae	*Xestotrema*	3	NA	NA	NA
Spiriferinida	Punctospiriferidae	*Lamnaespina*	4	NA	NA	NA
Spiriferinida	Punctospiriferidae	*Punctospirifer*	2	3	NA	NA
Spiriferinida	Reticulariinidae	*Gjelispinifera*	1	1	NA	NA
Spiriferinida	Reticulariinidae	*Reticulariina*	NA	8	NA	NA
Spiriferinida	Spiriferellinidae	*Crenispirifer*	24	22	NA	NA
Spiriferinida	Spiriferellinidae	*Pseudospiriferina*	NA	NA	NA	3
Spiriferinida	Spiriferellinidae	*Spiriferellina*	170	17	NA	NA
Spiriferinida	Spiriferellinidae	*Sulcispiriferina*	NA	4	NA	NA
Spiriferinida	Spiriferinidae	*Mentzelia*	6	NA	NA	1
Spiriferinida	Spiriferinidae	*Spiriferina*	29	NA	3	3
Spiriferinida	Syringothyrididae	*Permasyrinx*	NA	5	NA	NA
Spiriferinida	Syringothyrididae	*Petinospiriferina*	1	NA	NA	NA
Spiriferinida	Syringothyrididae	*Syrella*	NA	11	NA	NA
Spiriferinida	Syringothyrididae	*Syringothyris*	NA	3	NA	NA
Terebratulida	Angustothyrididae	*Rhaetina*	NA	NA	NA	2
Terebratulida	Antzeilleridae	*Antezeilleria*	NA	NA	NA	1
Terebratulida	Beecheriidae	*Beecheria*	1	NA	NA	NA
Terebratulida	Beecheriidae	*Hoskingia*	12	22	NA	NA
Terebratulida	Cranaenidae	*Girtyella*	NA	1	NA	NA
Terebratulida	Cryptonellidae	*Heterelasma*	NA	1	NA	NA
Terebratulida	Dielasmatidae	*Amygdalocosta*	3	3	NA	NA
Terebratulida	Dielasmatidae	*Dielasma*	104	30	NA	NA
Terebratulida	Dielasmatidae	*Dielasmina*	49	NA	NA	NA

Terebratulida	Dielasmatidae	*Fletcherina*	NA	NA	3	4
Terebratulida	Dielasmatidae	*Fletcherithyris*	4	NA	NA	3
Terebratulida	Dielasmatidae	*Whitspakia*	68	11	NA	NA
Terebratulida	Gillediidae	*Hemiptychina*	183	14	NA	NA
Terebratulida	Gillediidae	*Maorielasma*	5	7	NA	NA
Terebratulida	Gillediidae	*Omanilasma*	NA	1	NA	NA
Terebratulida	Gillediidae	*Sichuanothyris*	NA	1	NA	NA
Terebratulida	Gusarellidae	*Protogusarella*	NA	NA	NA	44
Terebratulida	Heterelasminidae	*Chuanyanella*	NA	4	NA	NA
Terebratulida	Heterelasminidae	*Gundarolasmina*	19	3	NA	NA
Terebratulida	Heterelasminidae	*Heterelasmina*	NA	4	NA	NA
Terebratulida	Heterelasminidae	*Mimaria*	NA	6	NA	NA
Terebratulida	Heterelasminidae	*Pseudolabaia*	3	7	NA	NA
Terebratulida	Heterelasminidae	*Qinglongia*	1	18	NA	NA
Terebratulida	Heterelasminidae	*Zhongliangshania*	NA	1	NA	NA
Terebratulida	Labaiidae	*Labaia*	NA	6	NA	NA
Terebratulida	Notothyrididae	*Cryptacanthia*	3	3	NA	NA
Terebratulida	Notothyrididae	*Gefonia*	7	8	NA	NA
Terebratulida	Notothyrididae	*Notothyrina*	1	5	NA	NA
Terebratulida	Notothyrididae	*Notothyris*	340	41	1	NA
Terebratulida	Notothyrididae	*Obnixia*	NA	NA	NA	31
Terebratulida	Notothyrididae	*Rostranteris*	3	5	NA	NA
Terebratulida	Pseudodielasmatidae	*Fredericksolasma*	9	3	NA	NA
Terebratulida	Pseudodielasmatidae	*Marinurnula*	5	2	NA	NA
Terebratulida	Zeilleriidae	*Periallus*	NA	NA	3	2
Terebratulida	Zugmayeriidae	*Portneufia*	NA	NA	NA	1
Orthotetida	Derbyiidae	*Derbyia*	202	111	NA	NA
Orthotetida	Derbyiidae	*Diplanus*	5	NA	NA	NA
Orthotetida	Meekellidae	*Alatorthotetina*	7	1	NA	NA
Orthotetida	Meekellidae	*Geyerella*	2	9	NA	NA
Orthotetida	Meekellidae	*Meekella*	93	88	NA	NA
Orthotetida	Meekellidae	*Meekellogeyerella*	NA	1	NA	NA
Orthotetida	Meekellidae	*Ombonia*	1	25	NA	NA
Orthotetida	Meekellidae	*Orthothetina*	149	214	NA	NA
Orthotetida	Meekellidae	*Paraorthotetina*	5	2	NA	NA

Orthotetida	Meekellidae	*Perigeyerella*	15	42	NA	NA
Orthotetida	Meekellidae	*Sicelia*	4	NA	NA	NA
Orthotetida	Orthotetidae	*Orthotetes*	3	4	NA	NA
Orthotetida	Pulsiidae	*Schellwienella*	NA	6	NA	NA
Orthotetida	Schuchertellidae	*Arctitreta*	20	5	NA	NA
Orthotetida	Schuchertellidae	*Erismatina*	NA	3	NA	NA
Orthotetida	Schuchertellidae	*Goniarina*	7	1	NA	NA
Orthotetida	Schuchertellidae	*Kiangsiella*	101	16	NA	NA
Orthotetida	Schuchertellidae	*Pseudostreptorhynchus*	2	3	NA	NA
Orthotetida	Schuchertellidae	*Schuchertella*	28	18	NA	NA
Orthotetida	Schuchertellidae	*Streptorhynchus*	100	35	NA	NA
Orthotetida	Schuchertellidae	*Teserina*	NA	4	NA	NA
Orthotetida	Schuchertellidae	*Tropidelasma*	3	15	NA	NA
Productida	Anopliidae	*Chonetina*	12	NA	NA	NA
Productida	Anopliidae	*Demonedys*	4	1	NA	NA
Productida	Anopliidae	*Glabrichonetina*	NA	1	NA	NA
Productida	Anopliidae	*Parvichonetes*	NA	1	NA	NA
Productida	Anopliidae	*Pygmochonetes*	NA	5	NA	NA
Productida	Anopliidae	*Tornquistia*	8	NA	NA	NA
Productida	Anopliidae	*Tschernovia*	NA	NA	NA	NA
Productida	Aulostegidae	*Aulosteges*	8	5	NA	NA
Productida	Aulostegidae	*Chonosteges*	1	NA	NA	NA
Productida	Aulostegidae	*Colemanosteges*	1	NA	NA	NA
Productida	Aulostegidae	*Costisteges*	NA	2	NA	NA
Productida	Aulostegidae	*Echinosteges*	1	NA	NA	NA
Productida	Aulostegidae	*Edriosteges*	47	26	NA	NA
Productida	Aulostegidae	*Glyptosteges*	NA	3	NA	NA
Productida	Aulostegidae	*Howseia*	6	NA	NA	NA
Productida	Aulostegidae	*Licharewiconcha*	NA	6	NA	NA
Productida	Aulostegidae	*Megasteges*	12	32	NA	NA
Productida	Aulostegidae	*Saeptathaerus*	6	9	NA	NA
Productida	Aulostegidae	*Strophalosiina*	4	11	NA	NA
Productida	Aulostegidae	*Taeniothaerus*	23	4	NA	NA
Productida	Aulostegidae	*Urushtenia*	1	6	NA	NA
Productida	Aulostegidae	*Urushtenoidea*	1	NA	NA	NA

Productida	Chonetidae	*Chonetes*	15	8	NA	NA
Productida	Cooperinidae	*Ceocypea*	5	NA	NA	NA
Productida	Cooperinidae	*Cooperina*	2	NA	NA	NA
Productida	Cooperinidae	*Epicelia*	3	NA	NA	NA
Productida	Cooperinidae	*Falafer*	7	4	NA	NA
Productida	Cyclacanthariidae	*Teguliferina*	1	NA	NA	NA
Productida	Echinoconchidae	*Chenxianoproductus*	6	11	NA	NA
Productida	Echinoconchidae	*Contraspina*	24	14	NA	NA
Productida	Echinoconchidae	*Echinoconchus*	1	1	NA	NA
Productida	Echinoconchidae	*Fostericoncha*	NA	5	NA	NA
Productida	Echinoconchidae	*Juresania*	10	3	NA	NA
Productida	Echinoconchidae	*Pustula*	NA	20	NA	NA
Productida	Echinoconchidae	*Vediproductus*	1	NA	NA	NA
Productida	Echinoconchidae	*Waagenoconcha*	151	20	NA	NA
Productida	Gemmellaroiidae	*Cyndalia*	5	NA	NA	NA
Productida	Gemmellaroiidae	*Tectarea*	NA	1	NA	NA
Productida	Hercosiidae	*Hercosia*	1	NA	NA	NA
Productida	Hercosiidae	*Neorichthofenia*	NA	2	NA	NA
Productida	Linoproductidae	*Anidanthus*	17	40	NA	NA
Productida	Linoproductidae	*Aurilinoproductus*	1	1	NA	NA
Productida	Linoproductidae	*Cancrinella*	7	3	NA	NA
Productida	Linoproductidae	*Cimmeriella*	1	NA	NA	NA
Productida	Linoproductidae	*Coolkilella*	3	8	NA	NA
Productida	Linoproductidae	*Fusiproductus*	3	8	NA	NA
Productida	Linoproductidae	*Kuvelousia*	14	NA	NA	NA
Productida	Linoproductidae	*Linoproductus*	130	39	NA	NA
Productida	Linoproductidae	*Megousia*	11	8	NA	NA
Productida	Linoproductidae	*Paucispinauria*	2	NA	NA	NA
Productida	Linoproductidae	*Platycancrinella*	NA	12	NA	NA
Productida	Linoproductidae	*Stepanoviella*	NA	5	NA	NA
Productida	Linoproductidae	*Terrakea*	2	6	NA	NA
Productida	Lyttoniidae	*Cardinocrania*	2	NA	NA	NA
Productida	Lyttoniidae	*Collemataria*	6	NA	NA	NA
Productida	Lyttoniidae	*Eolyttonia*	NA	5	NA	NA
Productida	Lyttoniidae	*Gubleria*	19	3	NA	NA

Productida	Lyttoniidae	*Keyserlingina*	9	13	NA	NA
Productida	Lyttoniidae	*Leptodus*	144	105	NA	NA
Productida	Lyttoniidae	*Loxophragmus*	NA	1	NA	NA
Productida	Lyttoniidae	*Matanoleptodus*	1	NA	NA	NA
Productida	Lyttoniidae	*Oldhamina*	73	109	NA	NA
Productida	Lyttoniidae	*Pararigbyella*	2	NA	NA	NA
Productida	Lyttoniidae	*Poikilosakos*	NA	NA	NA	NA
Productida	Lyttoniidae	*Spinolyttonia*	3	NA	NA	NA
Productida	Monticuliferidae	*Asperlinus*	25	1	NA	NA
Productida	Monticuliferidae	*Bandoproductus*	NA	2	NA	NA
Productida	Monticuliferidae	*Cancrinelloides*	1	NA	NA	NA
Productida	Monticuliferidae	*Chianella*	1	3	NA	NA
Productida	Monticuliferidae	*Chonopectoides*	NA	1	NA	NA
Productida	Monticuliferidae	*Compressoproductus*	51	39	NA	NA
Productida	Monticuliferidae	*Costatumulus*	28	23	NA	NA
Productida	Monticuliferidae	*Filiconcha*	6	NA	NA	NA
Productida	Monticuliferidae	*Magniplicatina*	2	1	NA	NA
Productida	Monticuliferidae	*Monticulifera*	NA	1	NA	NA
Productida	Monticuliferidae	*Nikitinia*	NA	4	NA	NA
Productida	Monticuliferidae	*Sarytchevinella*	23	5	NA	NA
Productida	Monticuliferidae	*Spitzbergenia*	15	NA	NA	NA
Productida	Monticuliferidae	*Striapustula*	3	NA	NA	NA
Productida	Monticuliferidae	*Striatifera*	NA	NA	NA	NA
Productida	Permianellidae	*Dicystoconcha*	1	NA	NA	NA
Productida	Permianellidae	*Laterispina*	NA	3	NA	NA
Productida	Permianellidae	*Permianella*	3	4	NA	NA
Productida	Productellidae	*Anemonaria*	32	NA	NA	NA
Productida	Productellidae	*Caricula*	NA	1	NA	NA
Productida	Productellidae	*Cathaysia*	68	88	NA	NA
Productida	Productellidae	*Caucasoproductus*	2	6	NA	NA
Productida	Productellidae	*Chaoiella*	1	NA	NA	NA
Productida	Productellidae	*Chonetella*	80	11	NA	NA
Productida	Productellidae	*Comuquia*	1	6	NA	NA
Productida	Productellidae	*Costispinifera*	3	2	NA	NA
Productida	Productellidae	*Dongpanoproductus*	NA	3	NA	NA

Productida	Productellidae	*Dorashamia*	3	NA	NA	NA
Productida	Productellidae	*Echinauriella*	NA	5	NA	NA
Productida	Productellidae	*Echinauris*	23	6	NA	NA
Productida	Productellidae	*Haydenella*	165	152	NA	NA
Productida	Productellidae	*Haydenoides*	3	2	NA	NA
Productida	Productellidae	*Huatangia*	NA	1	NA	NA
Productida	Productellidae	*Incisius*	1	3	NA	NA
Productida	Productellidae	*Jinomarginifera*	2	NA	NA	NA
Productida	Productellidae	*Krotovia*	14	1	NA	NA
Productida	Productellidae	*Labaella*	NA	7	NA	NA
Productida	Productellidae	*Lamnimargus*	23	11	NA	NA
Productida	Productellidae	*Lampangella*	NA	4	NA	NA
Productida	Productellidae	*Lazarevonia*	NA	27	NA	NA
Productida	Productellidae	*Lethamia*	3	1	NA	NA
Productida	Productellidae	*Liosotella*	20	2	NA	NA
Productida	Productellidae	*Marginifera*	208	49	NA	NA
Productida	Productellidae	*Neoplicatifera*	3	7	NA	NA
Productida	Productellidae	*Ogbinia*	5	1	NA	NA
Productida	Productellidae	*Parachonetella*	NA	4	NA	NA
Productida	Productellidae	*Paramarginifera*	5	1	NA	NA
Productida	Productellidae	*Paryphella*	13	62	NA	NA
Productida	Productellidae	*Plicatifera*	4	8	NA	NA
Productida	Productellidae	*Retimarginifera*	16	5	NA	NA
Productida	Productellidae	*Rugivestis*	2	NA	NA	NA
Productida	Productellidae	*Spinomarginifera*	248	347	NA	NA
Productida	Productellidae	*Tethysiella*	NA	6	NA	NA
Productida	Productellidae	*Transennatia*	143	34	NA	NA
Productida	Productidae	*Araxilevis*	21	NA	NA	NA
Productida	Productidae	*Bruntonia*	34	NA	NA	NA
Productida	Productidae	*Burovia*	3	NA	NA	NA
Productida	Productidae	*Buxtonia*	1	NA	NA	NA
Productida	Productidae	*Calliomarginatia*	2	NA	NA	NA
Productida	Productidae	*Costiferina*	204	18	NA	NA
Productida	Productidae	*Dasysaria*	NA	1	NA	NA
Productida	Productidae	*Dictyoclostus*	12	8	NA	NA

Productida	Productidae	*Eomarginifera*	NA	1	NA	NA
Productida	Productidae	*Horridonia*	61	1	NA	NA
Productida	Productidae	*Kochiproductus*	36	1	NA	NA
Productida	Productidae	*Liraplecta*	1	1	NA	NA
Productida	Productidae	*Niutoushania*	3	NA	NA	NA
Productida	Productidae	*Peniculauris*	NA	1	NA	NA
Productida	Productidae	*Pleurohorridonia*	17	NA	NA	NA
Productida	Productidae	*Productus*	16	18	NA	NA
Productida	Productidae	*Reticulatia*	4	1	NA	NA
Productida	Productidae	*Sowerbina*	1	1	NA	NA
Productida	Productidae	*Spyridiophora*	2	NA	NA	NA
Productida	Productidae	*Stereochia*	2	NA	NA	NA
Productida	Productidae	*Thamnosia*	1	NA	NA	NA
Productida	Productidae	*Thuleproductus*	3	NA	NA	NA
Productida	Productidae	*Tubaria*	2	NA	NA	NA
Productida	Productidae	*Tyloplecta*	103	52	NA	NA
Productida	Productidae	*Yakovlevia*	25	NA	NA	NA
Productida	Richthofeniidae	*Richthofenia*	62	22	NA	NA
Productida	Rugosochonetidae	*Capillomesolobus*	4	1	NA	NA
Productida	Rugosochonetidae	*Capillonia*	10	2	NA	NA
Productida	Rugosochonetidae	*Chonetinella*	14	12	NA	NA
Productida	Rugosochonetidae	*Dienerella*	NA	1	NA	NA
Productida	Rugosochonetidae	*Dyoros*	5	NA	NA	NA
Productida	Rugosochonetidae	*Fanichonetes*	1	6	NA	NA
Productida	Rugosochonetidae	*Fusichonetes*	2	17	NA	NA
Productida	Rugosochonetidae	*Kitakamichonetes*	1	NA	NA	NA
Productida	Rugosochonetidae	*Lissochonetes*	16	15	NA	NA
Productida	Rugosochonetidae	*Mesolobus*	1	NA	NA	NA
Productida	Rugosochonetidae	*Neochonetes*	75	176	NA	NA
Productida	Rugosochonetidae	*Plicochonetes*	NA	2	NA	NA
Productida	Rugosochonetidae	*Quinquenella*	7	1	NA	NA
Productida	Rugosochonetidae	*Rugaria*	NA	23	NA	NA
Productida	Rugosochonetidae	*Sandrella*	1	NA	NA	NA
Productida	Rugosochonetidae	*Subtilichonetes*	NA	1	NA	NA
Productida	Rugosochonetidae	*Sulcirugaria*	3	12	NA	NA

Productida	Rugosochonetidae	*Svalbardia*	13	NA	NA	NA
Productida	Rugosochonetidae	*Tenuichonetes*	NA	3	NA	NA
Productida	Rugosochonetidae	*Tethyochonetes*	80	154	NA	NA
Productida	Rugosochonetidae	*Waagenites*	71	9	NA	NA
Productida	Rugosochonetidae	*Waterhouseiella*	1	NA	NA	NA
Productida	Scacchinellidae	*Scacchinella*	1	9	NA	NA
Productida	Schrenkiellidae	*Permundaria*	2	1	NA	NA
Productida	Schrenkiellidae	*Schrenkiella*	NA	5	NA	NA
Productida	Schrenkiellidae	*Striatospica*	5	2	NA	NA
Productida	Sentosiidae	*Alatoproductus*	1	4	NA	NA
Productida	Strophalosiidae	*Biplatyconcha*	13	26	NA	NA
Productida	Strophalosiidae	*Craspedalosia*	48	NA	NA	NA
Productida	Strophalosiidae	*Dasyalosia*	19	NA	NA	NA
Productida	Strophalosiidae	*Echinalosia*	36	15	NA	NA
Productida	Strophalosiidae	*Etherilosia*	2	NA	NA	NA
Productida	Strophalosiidae	*Heteralosia*	1	2	NA	NA
Productida	Strophalosiidae	*Leptalosia*	1	NA	NA	NA
Productida	Strophalosiidae	*Lialosia*	NA	1	NA	NA
Productida	Strophalosiidae	*Licharewiella*	2	1	NA	NA
Productida	Strophalosiidae	*Liveringia*	3	NA	NA	NA
Productida	Strophalosiidae	*Marginalosia*	1	80	NA	NA
Productida	Strophalosiidae	*Notolosia*	4	NA	NA	NA
Productida	Strophalosiidae	*Orthothrix*	15	5	NA	NA
Productida	Strophalosiidae	*Strophalosia*	30	13	NA	NA
Productida	Strophalosiidae	*Truncatenia*	6	NA	NA	NA
Productida	Strophalosiidae	*Wyndhamia*	NA	3	NA	NA
Productida	Tschernyschewiidae	*Reedosepta*	5	NA	NA	NA
Productida	Tschernyschewiidae	*Tschernyschewia*	64	43	NA	NA

Appendix b - OccB dataset. PTBD is the distance from the Permian-Triassic boundary calculated in meters; stage: C = Changhsingian, W = Wuchiapingian, L = Lopingian; environment: IN = infralittoral, CI = circalittoral, BA = bathyal; sedimentation: CA = carbonate SI = silicicalstic CA-SI= mixed carbonate siliciclastic; paleolatitude: EQ = equatorial. Author: 1 = Angiolini and Carabelli, 2010; 2 = Posenato, 2009; 3 = Angiolini *et al.*, 2007; 4 = He *et al.*, 2005; 5 = He *et al.*, 2006; 6 = Shen *et al.*, 2010; 7 = Shen *et al.*, 2006; 8 = Ghaderi *et al.*, 2014; 9 = Garbelli *et al.*, 2014; 10 = Li and Shen, 2008; 11 = Wang *et al.*, 2004; 12 = Chen and Liao, 2009; 13 = Chen *et al.*, 2009; 14 = Wang *et al.*, 2004. Mangol Rest. = Mangol Restaurant

PTBD	Bed	ST	RH	Stage	Section	Formation	Environment	Sedimentation	Paleolatitude	Author
3.52	IR1056	2	1	C	Abredan	Nesen	IN	CA	EQ	1
4.26	IR1055	0	2	C	Abredan	Nesen	IN	CA	EQ	1
5.1	IR1054	3	1	C	Abredan	Nesen	IN	CA	EQ	1
7.89	IR1036	4	4	C	Abredan	Nesen	IN	CA	EQ	1
134	IR856bis	1	0	W	Bear-Gully	Nesen	CI	CA	EQ	1
120.19	IR862	3	3	W	Bear-Gully	Nesen	CI	CA	EQ	1
107.81	IR864bis	1	0	W	Bear-Gully	Nesen	CI	CA	EQ	1
106.38	IR864	1	0	W	Bear-Gully	Nesen	CI	CA	EQ	1
104.95	IR865-865bis	1	0	W	Bear-Gully	Nesen	CI	CA	EQ	1
98.09	IR866	2	0	W	Bear-Gully	Nesen	CI	CA	EQ	1
96.57	IR867	1	0	W	Bear-Gully	Nesen	CI	CA	EQ	1
85.52	IR869	2	0	W	Bear-Gully	Nesen	CI	CA	EQ	1
84.76	IR870	1	0	W	Bear-Gully	Nesen	CI	CA	EQ	1
83.81	IR871	4	1	W	Bear-Gully	Nesen	CI	CA	EQ	1
83.14	IR872	1	1	W	Bear-Gully	Nesen	CI	CA	EQ	1
82	IR873	1	0	W	Bear-Gully	Nesen	CI	CA	EQ	1
70.86	IR875	6	0	W	Bear-Gully	Nesen	CI	CA	EQ	1
65.33	IR877	1	0	W	Bear-Gully	Nesen	CI	CA	EQ	1
63.9	IR878	1	0	W	Bear-Gully	Nesen	CI	CA	EQ	1
60.09	IR879	2	0	W	Bear-Gully	Nesen	CI	CA	EQ	1
42.86	IR880	1	0	C	Bear-Gully	Nesen	IN	CA	EQ	1
33.81	IR883-883bis	0	1	C	Bear-Gully	Nesen	IN	CA	EQ	1
30.57	IR885	1	0	C	Bear-Gully	Nesen	IN	CA	EQ	1

28.29	IR887-887bis	4	0	C	Bear-Gully	Nesen	IN	CA	EQ	1
27.33	IR888-888bis	5	1	C	Bear-Gully	Nesen	IN	CA	EQ	1
26.09	IR890-IR889	0	1	C	Bear-Gully	Nesen	IN	CA	EQ	1
16	IR893	1	0	C	Bear-Gully	Nesen	IN	CA	EQ	1
1	13	1	1	C	Bulla	Werfen	IN	CA-SI	EQ	2
1.09	12C	1	0	C	Bulla	Werfen	IN	CA	EQ	2
1.26	11B	2	2	C	Bulla	Werfen	IN	CA	EQ	2
7.2	TK-46	1	0	C	Curuk-Dag	Pamucak	IN	CA	10S	3
6.14	TK-47	1	0	C	Curuk-Dag	Pamucak	IN	CA	10S	3
5.38	TK-48	1	0	C	Curuk-Dag	Pamucak	IN	CA	10S	3
4.52	TK-49	1	0	C	Curuk-Dag	Pamucak	IN	CA	10S	3
3.47	TK-49.1	1	0	C	Curuk-Dag	Pamucak	IN	CA	10S	3
9.23	TK-59.2	2	0	C	Curuk-Dag-left	Pamucak	IN	CA	10S	3
8.6	TK-59	3	0	C	Curuk-Dag-left	Pamucak	IN	CA	10S	3
17.5	TK-111	1	0	W	Curuk-southeast	Pamucak	CI	CA	10S	3
23.16	TK-112	1	0	W	Curuk-southeast	Pamucak	CI	CA	10S	3
23.56	TK-112bis	2	0	W	Curuk-southeast	Pamucak	CI	CA	10S	3
25.5	TK-113	1	0	W	Curuk-southeast	Pamucak	CI	CA	10S	3
35.5	TK-114	1	0	W	Curuk-southeast	Pamucak	CI	CA	10S	3
36.7	TK-115	1	0	W	Curuk-southeast	Pamucak	CI	CA	10S	3
39	TK-116	1	0	W	Curuk-southeast	Pamucak	CI	CA	10S	3
1.83	TK-138	5	0	W	Curuk-southeast	Pamucak	IN	CA	10S	3
1.054	10	6	2	C	Dongpan	Talung	IN	CA-SI	EQ	4. 5
1.499	9	6	2	C	Dongpan	Talung	IN	CA-SI	EQ	4. 5
1.647	9	4	1	C	Dongpan	Talung	IN	CA-SI	EQ	4. 5
1.788	9	5	2	C	Dongpan	Talung	IN	CA-SI	EQ	4. 5
1.944	8	6	3	C	Dongpan	Talung	IN	CA-SI	EQ	4. 5
2.319	7	7	3	C	Dongpan	Talung	CI	CA-SI	EQ	4. 5
3.006	5	2	2	C	Dongpan	Talung	BA	CA	EQ	4. 5
3.360	5	0	1	C	Dongpan	Talung	BA	CA	EQ	4. 5
3.560	5	3	4	C	Dongpan	Talung	BA	CA	EQ	4. 5
4.040	5	1	0	C	Dongpan	Talung	BA	CA	EQ	4. 5
5.190	3	2	3	C	Dongpan	Talung	BA	CA	EQ	4. 5
6.240	2	1	0	C	Dongpan	Talung	BA	CA	EQ	4. 5
6.640	2	1	1	C	Dongpan	Talung	BA	CA	EQ	4. 5
8.005	2	1	2	C	Dongpan	Talung	BA	CA	EQ	4. 5

8.610	2	1	2	C	Dongpan	Talung	BA	CA	EQ	4. 5
34.06	IR159	0	2	C	Elikah	Nesen	IN	CA	EQ	1
33.77	IR160	0	1	C	Elikah	Nesen	IN	CA	EQ	1
32.71	IR161	0	1	C	Elikah	Nesen	IN	CA	EQ	1
31.93	IR162	1	2	C	Elikah	Nesen	IN	CA	EQ	1
31.29	IR163	0	1	C	Elikah	Nesen	IN	CA	EQ	1
30.9	IR164	0	4	C	Elikah	Nesen	IN	CA	EQ	1
23.52	IR166	5	3	C	Elikah	Nesen	IN	CA	EQ	1
22.77	IR167	6	5	C	Elikah	Nesen	IN	CA	EQ	1
21.9	IR168	5	1	C	Elikah	Nesen	IN	CA	EQ	1
21.32	IR169bis	1	1	C	Elikah	Nesen	IN	CA	EQ	1
20.74	IR169	6	1	C	Elikah	Nesen	IN	CA	EQ	1
19.03	IR170	6	2	C	Elikah	Nesen	IN	CA	EQ	1
305.7	NA	0	1	C	Gyanyima	Gyanyima	IN	CA	35S	6
300.8	NA	0	1	C	Gyanyima	Gyanyima	IN	CA	35S	6
286.31	NA	0	2	C	Gyanyima	Gyanyima	IN	CA	35S	6
259.92	NA	0	1	C	Gyanyima	Gyanyima	IN	CA	35S	6
198.32	NA	2	3	C	Gyanyima	Gyanyima	IN	CA	35S	6
181.17	NA	1	1	C	Gyanyima	Gyanyima	IN	CA	35S	6
128.9	NA	6	11	C	Gyanyima	Gyanyima	IN	CA	35S	6
127.4	NA	3	6	C	Gyanyima	Gyanyima	IN	CA	35S	6
126	NA	1	6	C	Gyanyima	Gyanyima	IN	CA	35S	6
121.8	NA	1	6	C	Gyanyima	Gyanyima	IN	CA	35S	6
118.02	NA	0	3	C	Gyanyima	Gyanyima	IN	CA	35S	6
110.59	NA	1	6	C	Gyanyima	Gyanyima	IN	CA	35S	6
106.16	NA	3	3	C	Gyanyima	Gyanyima	IN	CA	35S	6
95.68	NA	3	6	C	Gyanyima	Gyanyima	IN	CA	35S	6
78.85	NA	0	3	C	Gyanyima	Gyanyima	IN	CA	35S	6
69.97	NA	2	3	C	Gyanyima	Gyanyima	IN	CA	35S	6
52.94	NA	3	0	C	Gyanyima	Gyanyima	IN	CA	35S	6
44.24	NA	2	1	C	Gyanyima	Gyanyima	IN	CA	35S	6
43.84	NA	4	0	C	Gyanyima	Gyanyima	IN	CA	35S	6
42.16	NA	1	0	C	Gyanyima	Gyanyima	IN	CA	35S	6
41.59	NA	4	0	C	Gyanyima	Gyanyima	IN	CA	35S	6
39.19	NA	2	0	C	Gyanyima	Gyanyima	IN	CA	35S	6
38.21	NA	3	0	C	Gyanyima	Gyanyima	IN	CA	35S	6
37.78	NA	4	1	C	Gyanyima	Gyanyima	IN	CA	35S	6
27.02	NA	1	0	C	Gyanyima	Gyanyima	IN	CA	35S	6

26.1	NA	3	1	C	Gyanyima	Gyanyima	IN	CA	35S	6
21.45	NA	4	0	C	Gyanyima	Gyanyima	IN	CA	35S	6
19.45	NA	3	0	C	Gyanyima	Gyanyima	IN	CA	35S	6
18.13	NA	1	0	C	Gyanyima	Gyanyima	IN	CA	35S	6
16.69	NA	3	0	C	Gyanyima	Gyanyima	IN	CA	35S	6
12.79	NA	2	10	C	Gyanyima	Gyanyima	IN	CA	35S	6
12.29	NA	1	1	C	Gyanyima	Gyanyima	IN	CA	35S	6
10.19	NA	1	1	C	Gyanyima	Gyanyima	IN	CA	35S	6
9.49	NA	1	0	C	Gyanyima	Gyanyima	IN	CA	35S	6
88.2	A1	1	0	W	Kashmir	Zewan	IN-CI	CA-SI	35S	7
76.8	A2	1	1	W	Kashmir	Zewan	IN-CI	CA-SI	35S	7
70.3	A4	1	0	W	Kashmir	Zewan	IN-CI	CA-SI	35S	7
66.53	A4	1	0	W	Kashmir	Zewan	IN-CI	CA-SI	35S	7
55.1	B1	0	1	W	Kashmir	Zewan	IN-CI	SI	35S	7
49.2	B2	3	0	W	Kashmir	Zewan	IN-CI	SI	35S	7
34.42	C	2	1	C	Kashmir	Zewan	IN-CI	CA-SI	35S	7
20.7	D	1	0	C	Kashmir	Zewan	IN	CA-SI	35S	7
14.2	D	1	1	C	Kashmir	Zewan	IN	CA-SI	35S	7
10.3	D	1	0	C	Kashmir	Zewan	IN	CA-SI	35S	7
2.3	E1	2	1	C	Kashmir	Zewan	IN-CI	CA-SI	35S	7
1.88	E1	3	1	C	Kashmir	Zewan	IN-CI	CA-SI	35S	7
0.48	E1	4	1	C	Kashmir	Zewan	IN-CI	CA-SI	35S	7
0	E2	1	0	C	Kashmir	Zewan	IN-CI	CA-SI	35S	7
53.61	G125	1	1	W	Main-Valley	Julfa	CI	CA	EQ	8. 9
53.29	G126	0	1	W	Main-Valley	Julfa	CI	CA	EQ	8. 9
51.09	G133	1	0	W	Main-Valley	Julfa	CI	CA	EQ	8. 9
50.55	G134	4	2	W	Main-Valley	Julfa	CI	CA	EQ	8. 9
49.91	G135	1	0	W	Main-Valley	Julfa	CI	CA	EQ	8. 9
49.59	G136	4	2	W	Main-Valley	Julfa	CI	CA	EQ	8. 9
49.16	G137	6	3	W	Main-Valley	Julfa	CI	CA	EQ	8. 9
48.41	G138	5	1	W	Main-Valley	Julfa	CI	CA	EQ	8. 9
47.99	G139	2	0	W	Main-Valley	Julfa	CI	CA	EQ	8. 9
47.5	G140	7	3	W	Main-Valley	Julfa	CI	CA	EQ	8. 9
46.6	G141	5	4	W	Main-Valley	Julfa	CI	CA	EQ	8. 9
45.31	G142	6	6	W	Main-Valley	Julfa	CI	CA	EQ	8. 9
43.54	G143	5	6	W	Main-Valley	Julfa	CI	CA	EQ	8. 9
43.06	G144	2	0	W	Main-Valley	Julfa	CI	CA	EQ	8. 9
42.52	G145	3	2	W	Main-Valley	Julfa	CI	CA	EQ	8. 9

41.3	G147	3	1	W	Main-Valley	Julfa	CI	CA	EQ	8. 9
40.81	G148	5	7	W	Main-Valley	Julfa	IN	CA	EQ	8. 9
40.33	G149	3	5	W	Main-Valley	Julfa	IN	CA	EQ	8. 9
39.5	G151	1	1	W	Main-Valley	Julfa	IN	CA	EQ	8. 9
39.04	G152	0	4	W	Main-Valley	Julfa	IN	CA	EQ	8. 9
37.81	G154	2	2	W	Main-Valley	Julfa	CI	CA	EQ	8. 9
36.73	G155	0	3	W	Main-Valley	Julfa	CI	CA	EQ	8. 9
36.19	G156	1	3	W	Main-Valley	Julfa	CI	CA	EQ	8. 9
35.89	G157	0	2	W	Main-Valley	Julfa	CI	CA	EQ	8. 9
34.11	G159	0	1	W	Main-Valley	Julfa	CI	CA-SI	EQ	8. 9
33.74	G160	0	1	W	Main-Valley	Julfa	CI	CA-SI	EQ	8. 9
33.47	G161	0	2	W	Main-Valley	Julfa	CI	CA	EQ	8. 9
32.83	G162	0	3	W	Main-Valley	Julfa	CI	CA	EQ	8. 9
32.13	G164/165	0	2	W	Main-Valley	Julfa	CI	CA	EQ	8. 9
30.58	G168	0	2	W	Main-Valley	Julfa	CI	CA	EQ	8. 9
30.36	G169	0	1	W	Main-Valley	Julfa	CI	CA-SI	EQ	8. 9
29.78	G172	0	2	W	Main-Valley	Julfa	IN	CA	EQ	8. 9
29.4	G174	0	1	W	Main-Valley	Julfa	IN	CA	EQ	8. 9
28.54	G177	0	1	W	Main-Valley	Julfa	IN	CA	EQ	8. 9
27.95	G179	0	3	W	Main-Valley	Julfa	IN	CA-SI	EQ	8. 9
27.2	G182	1	1	W	Main-Valley	Julfa	IN	CA-SI	EQ	8. 9
26.83	G183	0	1	W	Main-Valley	Julfa	CI	CA-SI	EQ	8. 9
26.19	G185	0	1	W	Main-Valley	Julfa	CI	CA	EQ	8. 9
25.65	G187	1	0	W	Main-Valley	Julfa	CI	CA	EQ	8. 9
25.33	G188	0	1	W	Main-Valley	Julfa	CI	CA	EQ	8. 9
23.78	G193	0	3	W	Main-Valley	Julfa	CI	CA	EQ	8. 9
20.72	G200	1	0	W	Main-Valley	Julfa	CI	CA-SI	EQ	8. 9
19.1	G206	2	1	W	Main-Valley	Julfa	CI	CA	EQ	8. 9
3.92	G248	1	3	C	Main-Valley	Julfa	BA	CA	EQ	8. 9
1.49	G271	0	1	C	Main-Valley	Julfa	BA	CA	EQ	8. 9
1.34	G273	0	2	C	Main-Valley	Julfa	BA	CA	EQ	8. 9
0.5	NA	0	1	C	Main-Valley	Julfa	BA	CA	EQ	8. 9
59.07	IR305	1	0	W	Mangol-Quarry	Nesen	CI	CA	EQ	1
54.20	IR308	1	0	W	Mangol-Quarry	Nesen	CI	CA	EQ	1
52.71	IR310	1	0	W	Mangol-Quarry	Nesen	CI	CA	EQ	1
52.07	IR311	2	0	W	Mangol-Quarry	Nesen	CI	CA	EQ	1
51.51	IR312	3	0	W	Mangol-Quarry	Nesen	CI	CA	EQ	1
49.97	IR313	3	0	W	Mangol-Quarry	Nesen	CI	CA	EQ	1

49.72	IR315	3	0	W	Mangol-Quarry	Nesen	CI	CA	EQ	1
49.42	IR316	1	0	W	Mangol-Quarry	Nesen	CI	CA	EQ	1
48.48	IR317	2	0	W	Mangol-Quarry	Nesen	CI	CA	EQ	1
47.84	IR318	2	0	W	Mangol-Quarry	Nesen	CI	CA	EQ	1
45.53	IR320	1	0	W	Mangol-Quarry	Nesen	CI	CA	EQ	1
41.39	IR321_bis	0	1	W	Mangol-Quarry	Nesen	CI	CA	EQ	1
40.62	IR322	1	0	W	Mangol-Quarry	Nesen	CI	CA	EQ	1
39.59	IR323	0	1	W	Mangol-Quarry	Nesen	CI	CA	EQ	1
39.08	IR324	1	0	W	Mangol-Quarry	Nesen	CI	CA	EQ	1
33.87	IR326	1	0	W	Mangol-Quarry	Nesen	CI	CA	EQ	1
22.34	IR329	1	0	W	Mangol-Quarry	Nesen	CI	CA	EQ	1
21.40	IR330	1	0	W	Mangol-Quarry	Nesen	CI	CA	EQ	1
12.51	IR341	0	1	C	Mangol-Quarry	Nesen	IN	CA	EQ	1
10.72	IR343	1	0	C	Mangol-Quarry	Nesen	IN	CA	EQ	1
7.52	IR347-347bis	2	3	C	Mangol-Quarry	Nesen	IN	CA	EQ	1
5.55	IR349	1	0	C	Mangol-Quarry	Nesen	IN	CA	EQ	1
4.87	IR350-350bis	0	1	C	Mangol-Quarry	Nesen	IN	CA	EQ	1
1.92	IR353	2	2	C	Mangol-Quarry	Nesen	IN	CA	EQ	1
1.37	IR354	0	2	C	Mangol-Quarry	Nesen	IN	CA	EQ	1
0.77	IR355	1	1	C	Mangol-Quarry	Nesen	IN	CA	EQ	1
0.00	IR356	0	1	C	Mangol-Quarry	Nesen	IN	CA	EQ	1
14.89	IR360	0	1	C	Mangol Rest.	Nesen	IN	CA	EQ	1
14.05	IR361	1	1	C	Mangol Rest.	Nesen	IN	CA	EQ	1
12.47	IR364	0	1	C	Mangol Rest.	Nesen	IN	CA	EQ	1
10.89	IR365	0	1	C	Mangol Rest.	Nesen	IN	CA	EQ	1
9.52	IR367	0	1	C	Mangol Rest.	Nesen	IN	CA	EQ	1
7.21	IR337bis	1	0	C	Mangol Rest.	Nesen	IN	CA	EQ	1
6.78	IR337	3	2	C	Mangol Rest.	Nesen	IN	CA	EQ	1
4.74	IR338	3	1	C	Mangol Rest.	Nesen	IN	CA	EQ	1
3.26	IR339	2	1	C	Mangol Rest.	Nesen	IN	CA	EQ	1
2.89	IR372	3	0	C	Mangol Rest.	Nesen	IN	CA	EQ	1
2.58	IR340	1	0	C	Mangol Rest.	Nesen	IN	CA	EQ	1
0.79	IR374	2	0	C	Mangol Rest.	Nesen	IN	CA	EQ	1
15.05	MSC3-29	2	2	W	Meishan C	Lungtan	IN	CA-SI	EQ	10
14.25	MSC3-28	2	0	W	Meishan C	Lungtan	IN	CA-SI	EQ	10
13.35	MSC3-26	3	2	W	Meishan C	Lungtan	IN	CA-SI	EQ	10
12.95	MSC3-24	2	1	W	Meishan C	Lungtan	IN	CA-SI	EQ	10

12.20	MSC3-23	6	2	W	Meishan C	Lungtan	IN	CA-SI	EQ	10
11.75	MSC3-22	5	2	W	Meishan C	Lungtan	IN	CA-SI	EQ	10
10.90	MSC3-17	5	2	W	Meishan C	Lungtan	IN	CA-SI	EQ	10
10.45	MSC3-15	1	0	W	Meishan C	Lungtan	IN	CA-SI	EQ	10
8.35	MSC3-6	2	0	W	Meishan C	Lungtan	IN	CA-SI	EQ	10
7.75	MSC3-3	3	0	W	Meishan C	Lungtan	IN	CA-SI	EQ	10
7.45	MSC3-2	2	0	W	Meishan C	Lungtan	IN	CA-SI	EQ	10
6.85	MSC4-7	3	0	W	Meishan C	Changhsing	IN	CA	EQ	10
6.75	MSC4-5	2	0	W	Meishan C	Changhsing	IN	CA	EQ	10
6.45	MSC4-4	2	0	W	Meishan C	Changhsing	IN	CA	EQ	10
6.10	MSC4-3	2	0	W	Meishan C	Changhsing	IN	CA	EQ	10
5.85	MSC4-1	2	0	W	Meishan C	Changhsing	IN	CA	EQ	10
5.65	MSC5-1	2	0	W	Meishan C	Changhsing	IN	CA	EQ	10
5.40	MSC5-2	1	0	C	Meishan C	Changhsing	CI	CA	EQ	10
5.20	MSC5-3	2	0	C	Meishan C	Changhsing	CI	CA	EQ	10
5.00	MSC5-4	1	0	C	Meishan C	Changhsing	CI	CA	EQ	10
3.20	MSC5-11	1	0	C	Meishan C	Changhsing	CI	CA	EQ	10
2.90	MSC5-13	1	0	C	Meishan C	Changhsing	CI	CA	EQ	10
2.25	MSC6-2	2	0	C	Meishan C	Changhsing	CI	CA	EQ	10
1.10	MSC8-2	2	0	C	Meishan C	Changhsing	CI	CA	EQ	10
0.80	MSC8-3	2	0	C	Meishan C	Changhsing	CI	CA	EQ	10
0.60	MSC8-4	2	0	C	Meishan C	Changhsing	CI	CA	EQ	10
49.72	1	1	1	W	Meishan D	Changhsing	IN	CA	EQ	11, 13
47.68	2-3	3	0	W	Meishan D	Changhsing	IN	CA	EQ	11, 13
36.15	11	2	0	C	Meishan D	Changhsing	CI	CA-SI	EQ	11, 13
20.23	15	1	0	C	Meishan D	Changhsing	CI	CA	EQ	11, 13
2.58	24	0	1	C	Meishan D	Changhsing	CI	CA	EQ	11, 13
237.7	4	1	3	L	Qubu	Quberga	IN	SI	45S	7
210.69	5	2	2	L	Qubu	Quberga	IN	CA-SI	45S	7
198.39	6	8	5	L	Qubu	Quberga	IN	CA-SI	45S	7
190.7	7	8	5	L	Qubu	Quberga	IN	CA-SI	45S	7
172.76	9	6	6	L	Qubu	Quberga	IN	CA-SI	45S	7
159.94	11	7	3	L	Qubu	Quberga	IN	CA-SI	45S	7
149.69	12	4	2	L	Qubu	Quberga	IN	SI	45S	7
139.44	13	5	5	L	Qubu	Quberga	IN	SI	45S	7
124.06	14	1	1	L	Qubu	Quberga	IN	CA-SI	45S	7
122.01	15	10	9	L	Qubu	Quberga	IN	CA	45S	7
110.22	16	2	0	L	Qubu	Quberga	IN	CA	45S	7

95.35	17	1	0	L	Qubu	Quberga	IN	SI	45S	7
83.56	20	1	1	L	Qubu	Quberga	IN	CA-SI	45S	7
77.41	21	1	1	L	Qubu	Quberga	IN	CA-SI	45S	7
69.72	22	2	2	C	Qubu	Quberga	IN	CA	45S	7
0.4	Chh	2	1	C	Salt-Range	Chhidru	IN	SI	35S	11. 12
10.5	Chh	10	7	C	Salt-Range	Chhidru	IN	CA	35S	11. 12
16.7	Chh	4	5	C	Salt-Range	Chhidru	IN	SI	35S	11. 12
25.6	Chh	5	3	C	Salt-Range	Chhidru	IN	CA	35S	11. 12
35.7	Chh	9	3	C	Salt-Range	Chhidru	IN	CA	35S	11. 12
43.6	War	9	6	W	Salt-Range	Wargal	IN	CA	35S	7
48.6	War	13	14	W	Salt-Range	Wargal	IN	CA	35S	7
51.3	War	7	6	W	Salt-Range	Wargal	IN	CA	35S	7
2.59	WK3	0	1	C	Sass-de-Putia	Bellerophon	IN	CA	EQ	2
2.27	WK5	0	1	C	Sass-de-Putia	Bellerophon	IN	CA	EQ	2
2.12	WK6	0	1	C	Sass-de-Putia	Bellerophon	IN	CA	EQ	2
1.47	WK9A	0	1	C	Sass-de-Putia	Bellerophon	IN	CA	EQ	2
1.36	WK10A	0	1	C	Sass-de-Putia	Bellerophon	IN	CA	EQ	2
1.25	WK10B	2	3	C	Sass-de-Putia	Bellerophon	IN	CA	EQ	2
1.2	WK11A	2	2	C	Sass-de-Putia	Werfen	IN	CA	EQ	2
1.15	WK11B	2	1	C	Sass-de-Putia	Werfen	IN	CA	EQ	2
1.03	WK11D	1	0	C	Sass-de-Putia	Werfen	IN	CA	EQ	2
107.13	1	4	4	L	Selong-Xishan	Selong-Group	IN	CA	45S	7
56.61	3	4	4	L	Selong-Xishan	Selong-Group	IN	CA	45S	7
33.8	4	3	3	L	Selong-Xishan	Selong-Group	IN	SI	45S	7
20.2	5	3	2	L	Selong-Xishan	Selong-Group	IN	SI	45S	7
11.8	6	5	8	L	Selong-Xishan	Selong-Group	IN	CA	45S	7
7.78	7	3	4	L	Selong-Xishan	Selong-Group	IN	SI	45S	7
5	8	5	12	L	Selong-Xishan	Selong-Group	IN	SI	45S	7
3	9	5	13	L	Selong-Xishan	Selong-Group	IN	CA	45S	7
2	10	8	12	L	Selong-Xishan	Selong-Group	IN	SI	45S	7
0.2	15	0	6	C	Selong-Xishan	Selong-Group	IN	CA	45S	7
0	17	2	9	C	Selong-Xishan	Selong-Group	IN	CA	45S	7
583.65	66-69	0	1	W	Shaiwa	Shaiwa-group	BA	SI	EQ	13
543.31	64-65	0	1	W	Shaiwa	Shaiwa-group	BA	SI	EQ	13
330.54	49-52	1	1	W	Shaiwa	Shaiwa-group	BA	SI	EQ	13
301.91	47-48	0	1	C	Shaiwa	Shaiwa-group	BA	SI	EQ	13
189.35	27-39	2	1	C	Shaiwa	Shaiwa-group	BA	SI	EQ	13
11.82	21-22	5	1	C	Shaiwa	Shaiwa-group	BA	CA-SI	EQ	13

63.80	10-20	6	4	C	Shaiwa	Shaiwa-group	BA	CA-SI	EQ	13
24.10	7-9	8	4	C	Shaiwa	Shaiwa-group	BA	CA-SI	EQ	13
65	TJ84	1	11	C	Takhtabulak	Takhtabulak	CI	CA-SI	10N	NA
65	TJ85	2	3	C	Takhtabulak	Takhtabulak	CI	CA-SI	10N	NA
62.5	TJ101	0	5	C	Takhtabulak	Takhtabulak	CI	CA-SI	10N	NA
60	TJ102	0	1	C	Takhtabulak	Takhtabulak	CI	CA-SI	10N	NA
2.83	7-7	0	1	C	Tesero	Bellerophon	IN	CA	EQ	2
0.16	CNT11A	1	1	C	Tesero	Werfen	IN	CA-SI	EQ	2
0.26	CNT11(?)	2	0	C	Tesero	Werfen	IN	CA-SI	EQ	2
0.37	CNT10	1	2	C	Tesero	Werfen	IN	CA-SI	EQ	2
0.65	CNT8	2	1	C	Tesero	Werfen	IN	CA-SI	EQ	2
0.99	CNT6	1	2	C	Tesero	Werfen	IN	CA-SI	EQ	2
1.44	Tes5	0	1	C	Tesero	Werfen	IN	CA	EQ	2
2.55	T7D2	1	1	C	Tesero	Werfen	IN	CA	EQ	2
2.73	T7B1	1	1	C	Tesero	Werfen	IN	CA	EQ	2
312	4	1	3	L	Tulong	Qubuerga	IN-CI	CA	45S	7
285.5	5	1	0	L	Tulong	Qubuerga	IN-CI	CA	45S	7
253.4	6	7	5	L	Tulong	Qubuerga	IN-CI	CA	45S	7
157.6	9	3	2	L	Tulong	Qubuerga	IN-CI	CA	45S	7
80	11	2	2	L	Tulong	Qubuerga	IN-CI	CA	45S	7
NA	NA	0	1	C	Well-H2	Changhsing	CI	CA	EQ	12
NA	NA	2	0	C	Well-H2	Changhsing	CI	CA-SI	EQ	12
NA	NA	1	0	W	Well-H2	Lungtan	IN	SI	EQ	12
NA	NA	4	0	W	Well-H2	Lungtan	IN	CA-SI	EQ	12
NA	NA	8	0	W	Well-H2	Lungtan	IN	CA-SI	EQ	12
NA	NA	5	2	W	Well-H2	Lungtan	IN	CA-SI	EQ	12

PTDB statistic -summary of the statistical results of the logistic regression analysis preformed on the OccB data

```
-------------------------------------------------------------------
ELIKAH *
Call:
glm(formula = cbind(ST, RH) ~ LPE, family = binomial(logit),
    data = A)
Deviance Residuals:
    Min       1Q   Median       3Q      Max
-1.0409  -0.5412  -0.4356   0.4163   1.1251
Coefficients:
            Estimate Std. Error z value Pr(>|z|)
(Intercept)  7.30443    2.23306   3.271  0.00107 **
LPE          0.29887    0.09606   3.111  0.00186 **
---
Signif. codes:  0 '***' 0.001 '**' 0.01 '*' 0.05 '.' 0.1 ' ' 1
(Dispersion parameter for binomial family taken to be 1)
    Null deviance: 21.7112  on 11  degrees of freedom
Residual deviance:  5.4481  on 10  degrees of freedom
AIC: 23.884
Number of Fisher Scoring iterations: 5
> 1-pchisq(5.4481,df=10)
[1] 0.8593082
-------------------------------------------------------------------
ABREDAN
Call:
glm(formula = cbind(ST, RH) ~ LPE, family = binomial(logit),
    data = A)
Deviance Residuals:
       1         2         3         4
 0.41813  -1.76880   0.88105  -0.08855
Coefficients:
            Estimate Std. Error z value Pr(>|z|)
(Intercept)  0.29766    1.68569   0.177    0.860
LPE          0.02979    0.26718   0.111    0.911
(Dispersion parameter for binomial family taken to be 1)
    Null deviance: 4.1000  on 3  degrees of freedom
Residual deviance: 4.0876  on 2  degrees of freedom
AIC: 14.029
Number of Fisher Scoring iterations: 4
> 1-pchisq(4.0876,df=2)
[1] 0.1295355
-------------------------------------------------------------------
BEAR GULLY
Call:
glm(formula = cbind(ST, RH) ~ LPE, family = binomial(logit),
    data = A)
Deviance Residuals:
    Min       1Q   Median       3Q      Max
-2.0299   0.1725   0.6114   0.6810   1.4517
Coefficients:
            Estimate Std. Error z value Pr(>|z|)
(Intercept) 2.083548   0.973464   2.140   0.0323 *
LPE         0.006113   0.011787   0.519   0.6040
---
Signif. codes:  0 '***' 0.001 '**' 0.01 '*' 0.05 '.' 0.1 ' ' 1
(Dispersion parameter for binomial family taken to be 1)
    Null deviance: 22.113  on 22  degrees of freedom
Residual deviance: 21.841  on 21  degrees of freedom
AIC: 33.162
Number of Fisher Scoring iterations: 4
> 1-pchisq(21.841,df=21)
[1] 0.4087216
-------------------------------------------------------------------
```

```
MANGOL QUARRY*
Call:
glm(formula = cbind(ST, RH) ~ LPE, family = binomial(logit),
    data = A)
Deviance Residuals:
    Min       1Q   Median       3Q      Max
-2.1937   0.0111   0.4468   0.5551   1.3359
Coefficients:
            Estimate Std. Error z value Pr(>|z|)
(Intercept) -0.77985    0.53985  -1.445  0.14858
LPE         -0.07469    0.02281  -3.274  0.00106 **
---
Signif. codes:  0 '***' 0.001 '**' 0.01 '*' 0.05 '.' 0.1 ' ' 1
(Dispersion parameter for binomial family taken to be 1)
    Null deviance: 39.056  on 26  degrees of freedom
Residual deviance: 22.333  on 25  degrees of freedom
AIC: 31.806
Number of Fisher Scoring iterations: 5
> 1-pchisq(22.333,df=25)
[1] 0.61645
------------------------------------------------------------------
MANGOL RESTAURANT*
Call:
glm(formula = cbind(ST, RH) ~ LPE, family = binomial(logit),
    data = A)
Deviance Residuals:
    Min       1Q   Median       3Q      Max
-1.0304  -0.7066  -0.1252   0.6559   1.2262
Coefficients:
            Estimate Std. Error z value Pr(>|z|)
(Intercept)   2.7716     1.0685   2.594  0.00949 **
LPE           0.3285     0.1418   2.317  0.02053 *
---
Signif. codes:  0 '***' 0.001 '**' 0.01 '*' 0.05 '.' 0.1 ' ' 1
(Dispersion parameter for binomial family taken to be 1)
    Null deviance: 14.8504  on 11  degrees of freedom
Residual deviance:  7.1298  on 10  degrees of freedom
AIC: 17.989
Number of Fisher Scoring iterations: 4
> 1-pchisq(7.1298,df=10)
[1] 0.7131369
------------------------------------------------------------------
BULLA
Call:
glm(formula = cbind(ST, RH) ~ LPE, family = binomial(logit),
    data = A)
Deviance Residuals:
      1        2        3
-0.3778   1.0131  -0.1391
Coefficients:
            Estimate Std. Error z value Pr(>|z|)
(Intercept)    2.069      7.717   0.268    0.789
LPE            1.532      6.593   0.232    0.816
(Dispersion parameter for binomial family taken to be 1)
    Null deviance: 1.2429  on 2  degrees of freedom
Residual deviance: 1.1884  on 1  degrees of freedom
AIC: 8.5364
Number of Fisher Scoring iterations: 3
> 1-pchisq(1.1884,df=1)
[1] 0.2756525
------------------------------------------------------------------SASS DE
PUTIA
Call:
glm(formula = cbind(ST, RH) ~ LPE, family = binomial(logit),
    data = A)
Deviance Residuals:
     Min        1Q    Median        3Q       Max
```

```
-0.39872  -0.16465  -0.00080  -0.00002   0.32502
Coefficients:
            Estimate Std. Error z value Pr(>|z|)
(Intercept)    19.79      13.46   1.470    0.141
LPE            16.38      11.10   1.476    0.140
(Dispersion parameter for binomial family taken to be 1)
    Null deviance: 7.96257  on 8  degrees of freedom
Residual deviance: 0.44554  on 7  degrees of freedom
AIC: 10.154
Number of Fisher Scoring iterations: 8
> 1-pchisq(0.44554,df=7)
[1] 0.9996225
-----------------------------------------------------------------
TESERO ROAD
Call:
glm(formula = cbind(ST, RH) ~ LPE, family = binomial(logit),
    data = A)
Deviance Residuals:
     Min        1Q    Median        3Q       Max
-1.05051  -0.58492  -0.02407   0.47482   0.65021
Coefficients:
            Estimate Std. Error z value Pr(>|z|)
(Intercept)   0.1090     0.6761   0.161    0.872
LPE           0.2882     0.4770   0.604    0.546
(Dispersion parameter for binomial family taken to be 1)
    Null deviance: 3.9314  on 8  degrees of freedom
Residual deviance: 3.5559  on 7  degrees of freedom
AIC: 18.202
Number of Fisher Scoring iterations: 3
> 1-pchisq(3.5559,df=7)
[1] 0.8292696
-----------------------------------------------------------------
MAIN VALLEY*
Call:
glm(formula = cbind(ST, RH) ~ LPE, family = binomial(logit),
    data = A)
Deviance Residuals:
    Min       1Q   Median       3Q      Max
-2.0546  -0.8658  -0.3173   0.6465   2.2364
Coefficients:
            Estimate Std. Error z value Pr(>|z|)
(Intercept) -3.60226    0.91312  -3.945 7.98e-05 ***
LPE         -0.08295    0.02150  -3.858 0.000115 ***
---
Signif. codes:  0 ‘***’ 0.001 ‘**’ 0.01 ‘*’ 0.05 ‘.’ 0.1 ‘ ’ 1
(Dispersion parameter for binomial family taken to be 1)
    Null deviance: 74.399  on 46  degrees of freedom
Residual deviance: 52.799  on 45  degrees of freedom
AIC: 97.393
Number of Fisher Scoring iterations: 5
> 1-pchisq(52.799,df=45)
[1] 0.1981435
-----------------------------------------------------------------
MEISHAN C*
Call:
glm(formula = cbind(ST, RH) ~ LPE, family = binomial(logit),
    data = A)
Deviance Residuals:
     Min        1Q    Median        3Q       Max
-0.92300   0.08089   0.17820   0.31088   1.55839
Coefficients:
            Estimate Std. Error z value Pr(>|z|)
(Intercept) 6.823796   2.166258   3.150  0.00163 **
LPE         0.004662   0.001741   2.678  0.00741 **
---
Signif. codes:  0 ‘***’ 0.001 ‘**’ 0.01 ‘*’ 0.05 ‘.’ 0.1 ‘ ’ 1
(Dispersion parameter for binomial family taken to be 1)
```

```
    Null deviance: 19.3822  on 25  degrees of freedom
Residual deviance:  5.1571  on 24  degrees of freedom
AIC: 21.772
Number of Fisher Scoring iterations: 6
> 1-pchisq(5.1571,df=24)
[1] 0.999983
------------------------------------------------------------------
MEISHAN D
Call:
glm(formula = cbind(ST, RH) ~ LPE, family = binomial(logit),
    data = A)
Deviance Residuals:
      1       2       3       4       5
-1.3764  0.8768  0.9599  0.9862 -0.9695
Coefficients:
            Estimate Std. Error z value Pr(>|z|)
(Intercept) -0.65389    1.86228  -0.351    0.725
LPE         -0.05545    0.05128  -1.081    0.280
(Dispersion parameter for binomial family taken to be 1)
    Null deviance: 6.7621  on 4  degrees of freedom
Residual deviance: 5.4973  on 3  degrees of freedom
AIC: 10.884
Number of Fisher Scoring iterations: 4
> 1-pchisq(5.4973,df=3)
[1] 0.1388002
------------------------------------------------------------------
DONGPAN*
Call:
glm(formula = cbind(ST, RH) ~ LPE, family = binomial(logit),
    data = A)
Deviance Residuals:
     Min        1Q    Median        3Q       Max
-1.29927  -0.15858  -0.03244   0.28239   1.34190
Coefficients:
            Estimate Std. Error z value Pr(>|z|)
(Intercept)   1.5123     0.5345   2.829  0.00467 **
LPE           0.3829     0.1761   2.174  0.02971 *
---
Signif. codes:  0 '***' 0.001 '**' 0.01 '*' 0.05 '.' 0.1 ' ' 1
(Dispersion parameter for binomial family taken to be 1)
    Null deviance: 10.8673  on 14  degrees of freedom
Residual deviance:  5.9077  on 13  degrees of freedom
AIC: 35.05
Number of Fisher Scoring iterations: 3
> 1-pchisq(5.9077,df=13)
[1] 0.9494477
------------------------------------------------------------------------
---------------
SHAIWA*
Call:
glm(formula = cbind(ST, RH) ~ LPE, family = binomial(logit),
    data = A)
Deviance Residuals:
    Min       1Q   Median       3Q      Max
-0.8840  -0.4301  -0.3615   0.6272   0.6480
Coefficients:
            Estimate Std. Error z value Pr(>|z|)
(Intercept) 1.038251   0.461211   2.251   0.0244 *
LPE         0.005884   0.003191   1.844   0.0652 .
---
Signif. codes:  0 '***' 0.001 '**' 0.01 '*' 0.05 '.' 0.1 ' ' 1
(Dispersion parameter for binomial family taken to be 1)
    Null deviance: 7.3789  on 7  degrees of freedom
Residual deviance: 2.6474  on 6  degrees of freedom
AIC: 17.112
Number of Fisher Scoring iterations: 4
> 1-pchisq(2.6474,df=6)
```

```
[1] 0.8516203
-----------------------------------------------------------------
GYANYIMA*
Call:
glm(formula = cbind(ST, RH) ~ LPE, family = binomial(logit),
    data = A)
Deviance Residuals:
    Min       1Q   Median       3Q      Max
-3.9338  -0.5320   0.3741   1.2935   1.9882
Coefficients:
            Estimate Std. Error z value Pr(>|z|)
(Intercept) 1.097113   0.339410   3.232  0.00123 **
LPE         0.014813   0.003563   4.158 3.21e-05 ***
---
Signif. codes:  0 '***' 0.001 '**' 0.01 '*' 0.05 '.' 0.1 ' ' 1
(Dispersion parameter for binomial family taken to be 1)
    Null deviance: 80.948  on 33  degrees of freedom
Residual deviance: 58.796  on 32  degrees of freedom
AIC: 95.066
Number of Fisher Scoring iterations: 4
> 1-pchisq(58.796,df=32)
[1] 0.002667933
-----------------------------------------------------------------
KASHMIR
Call:
glm(formula = cbind(ST, RH) ~ LPE, family = binomial(logit),
    data = A)
Deviance Residuals:
    Min       1Q   Median       3Q      Max
-1.6815  -0.3631   0.4763   0.7466   1.2920
Coefficients:
             Estimate Std. Error z value Pr(>|z|)
(Intercept) 1.1543865  0.5894129   1.959   0.0502 .
LPE         0.0003517  0.0151176   0.023   0.9814
---
Signif. codes:  0 '***' 0.001 '**' 0.01 '*' 0.05 '.' 0.1 ' ' 1
(Dispersion parameter for binomial family taken to be 1)
    Null deviance: 9.3685  on 13  degrees of freedom
Residual deviance: 9.3680  on 12  degrees of freedom
AIC: 22.896
Number of Fisher Scoring iterations: 4
> 1-pchisq(9.3680,df=12)
[1] 0.6712183
-----------------------------------------------------------------
SALT RANGE
Call:
glm(formula = cbind(ST, RH) ~ LPE, family = binomial(logit),
    data = A)
Deviance Residuals:
     Min        1Q    Median        3Q       Max
-0.88013  -0.23786   0.07286   0.28629   1.32739
Coefficients:
            Estimate Std. Error z value Pr(>|z|)
(Intercept)  0.44979    0.46898   0.959    0.338
LPE          0.05295    0.12544   0.422    0.673
(Dispersion parameter for binomial family taken to be 1)
    Null deviance: 3.4559  on 7  degrees of freedom
Residual deviance: 3.2770  on 6  degrees of freedom
AIC: 30.086
Number of Fisher Scoring iterations: 3
> 1-pchisq(3.277,df=6)
[1] 0.7733629
-----------------------------------------------------------------
QUBU
Call:
glm(formula = cbind(ST, RH) ~ LPE, family = binomial(logit),
    data = A)
```

```
Deviance Residuals:
    Min       1Q   Median       3Q      Max
-1.1683  -0.4144  -0.2263   0.4741   1.4654
Coefficients:
            Estimate Std. Error z value Pr(>|z|)
(Intercept) 0.508917   0.798567   0.637    0.524
LPE         0.001517   0.004925   0.308    0.758
(Dispersion parameter for binomial family taken to be 1)
    Null deviance: 7.0901  on 14  degrees of freedom
Residual deviance: 6.9951  on 13  degrees of freedom
AIC: 40.876
Number of Fisher Scoring iterations: 3
> 1-pchisq(6.9951,df=13)
[1] 0.9024039
------------------------------------------------------------------
SELONG XISHAN
Call:
glm(formula = cbind(ST, RH) ~ LPE, family = binomial(logit),
    data = A)
Deviance Residuals:
    Min       1Q   Median       3Q      Max
-2.1141  -0.4411   0.2587   0.5376   1.0919
Coefficients:
             Estimate Std. Error z value Pr(>|z|)
(Intercept) -0.797773   0.227805  -3.502 0.000462 ***
LPE         -0.010859   0.006631  -1.638 0.101505
---
Signif. codes:  0 ‘***’ 0.001 ‘**’ 0.01 ‘*’ 0.05 ‘.’ 0.1 ‘ ’ 1
(Dispersion parameter for binomial family taken to be 1)
    Null deviance: 11.1896  on 10  degrees of freedom
Residual deviance:  8.4698  on  9  degrees of freedom
AIC: 39.705
Number of Fisher Scoring iterations: 4
> 1-pchisq(8.4698,df=9)
[1] 0.4875803
------------------------------------------------------------------
TULONG
Call:
glm(formula = cbind(ST, RH) ~ LPE, family = binomial(logit),
    data = A)
Deviance Residuals:
      1       2       3       4       5
-1.0367  1.1546  0.4022  0.1749 -0.3624
Coefficients:
            Estimate Std. Error z value Pr(>|z|)
(Intercept) 0.483886   1.212045   0.399    0.690
LPE         0.001506   0.005225   0.288    0.773
(Dispersion parameter for binomial family taken to be 1)
    Null deviance: 2.8150  on 4  degrees of freedom
Residual deviance: 2.7315  on 3  degrees of freedom
AIC: 15.496
Number of Fisher Scoring iterations: 3
> 1-pchisq(2.7315,df=3)
[1] 0.4349007
------------------------------------------------------------------
```

Appendix C

Table 1. List of the specimens investigated using SEM. PR=primary layer recrystallized, L=laminar, F=fibrous, P=prismatic, NP=not present.

Section	*Taxon*	Specimen number	Pimary layer	Secondary layer	Tertiary layer
Bulla	*Comelicania* sp.	VB9B-1	NP	F	P
Bulla	*Comelicania* sp.	VB9B-2	NP	F	P
Bulla	*Comelicania* sp.	VB9A-1	NP	F	P
Bulla	*Comelicania* sp.	PK56-1	NP	F	P
Bulla	*Transcaucasathyris* sp.	JU10-1	NP	F	P
Bulla	*Transcaucasathyris* sp.	JU10-2	NP	F	P
Bulla	*Transcaucasathyris* sp.	JU10-3	NP	F	P
Bulla	*Transcaucasathyris araxensis*	JU10-4	NP	F	P
Ali Bashi 1	*Transcaucasathyris* sp.	JU10-1	NP	F	P
Ali Bashi 1	*Transcaucasathyris* sp.	JU10-2	NP	F	P
Ali Bashi 1	*Transcaucasathyris* sp.	JU10-3	NP	F	P
Ali Bashi 1	*Transcaqucasathyris araxensis*	JU10-4	NP	F	P
MainValley	*Spinomarginifera* sp.	Ju106-1	NP	L	P
MainValley	*Spinomarginifera* sp.	Ju106-2	NP	L	P
MainValley	*Spinomarginifera* sp.	Ju106-3	NP	L	P
MainValley	*Spinomarginifera* sp.	JU107-1	NP	L	P
MainValley	*Spinomarginifera* sp.	JU112-1	NP	L	P
MainValley	*Spinomarginifera* sp.	JU114-1	NP	L	P
MainValley	*Spinomarginifera* sp.	Ju115-1	NP	L	P
MainValley	*Spinomarginifera* sp.	JU117-1	NP	L	P
Detrito	*Spinomarginifera iranica*	JU1-2	NP	L	P
MainValley	*Spinomarginifera* sp.	JU120-1	NP	L	P
MainValley	*Spinomarginifera spinosocostata*	JU121-1	NP	L	P
MainValley	*Spinomarginifera spinosocostata*	JU121-2	NP	L	P
MainValley	*Transcaucasathyris araxensis*	JU129-1	NP	L	P
MainValley	*Haydenella kiangsiensis*	JU129-1	NP	L	NP
MainValley	*Haydenella kiangsiensis*	JU129-4	NP	L	NP
Detrito	*Spinomarginifera spinosocostata*	JU1-3	NP	L	P
MainValley	*Transcaucasathyris* sp.	JU131-2	NP	F	P
MainValley	*Transcaucasathyris* sp.	JU131-4	NP	F	P
MainValley	*Transcaucasathyris* sp.	JU132-1	NP	F	P
MainValley	*Transcaucasathyris* sp.	JU132-2	NP	F	P

MainValley	*Transcaucasathyris* sp.	JU133-2	NP	F	P
MainValley	*Ammonoids*	JU133-3	NP		
MainValley	*Transcaucasathyris* sp.	JU133-5	NP	F	P
MainValley	*Transcaucasathyris* sp.*?*	JU133-6	NP	F	P
MainValley	*Transcaucasathyris araxensis*	JU136-1	NP	F	P
MainValley	*Transcaucasathyris* sp.	JU139-3	NP	F	P
Detrito	*Spinomarginifer iranica*	JU1-4	NP	L	P
MainValley	*Transcaucasathyris* sp.	JU140-1	NP	F	P
MainValley	*Transcaucasathyris* sp.	JU140-2	NP	F	P
MainValley	*Transcaucasathyris* sp.	JU140-3	NP	F	P
MainValley	*Transcaucasathyris* sp.	JU140-4	NP	F	P
MainValley	*Transcaucasathyris* sp.	JU140-5	NP	F	P
MainValley	*Transcaucasathyris* sp.	JU140-6	NP	F	P
MainValley	*Transcaucasathyris* sp.	JU141-4	NP	F	P
Ali Bashi 1	*Paracrurithyris pygmaea*	JU148-2	NP	F	NP
Ali Bashi 1	*Paracrurithyris pygmaea*	JU148-5	NP	F	NP
Ali Bashi 1	*Paracrurithyris pygmaea*	JU148-8	NP	F	NP
Zal	*Transcaucasathyris* sp.	JU150-2	NP	F	P
Zal	*Transcaucasathyris* sp.	JU150-8	NP	F	P
Zal	*Transcaucasathyris* sp.	JU151-4	NP	F	P
Zal	*Transcaucasathyris* sp.	JU151-5	NP	F	P
Zal	*Transcaucasathyris* sp.*?*	JU152-1	NP	NP	P
Zal	*Transcaucasathyris* sp.	JU152-2	NP	F	P
Zal	*Transcaucasathyris* sp.	JU167-1	NP	F	P
Zal	*Unknow*	JU172-2	NP	NP	NP
Zal	*Paracrurithyris* sp.	JU172-3	NP	F	NP
Zal	*Paracrurithyris pygmaea*	JU172-4	NP	L	NP
Zal	*Paracrurithyris pygmaea*	JU172-5	NP	F	NP
Zal	*Paracrurithyris pygmaea*	JU172-6	NP	F	NP
Zal	*Paracrurithyris pygmaea*	JU172-7	NP	F	NP
Zal	*Paracrurithyris pygmaea*	JU172-8	NP	F	NP
Ali Bashi 1	*Transcaucasathyris* sp.	JU25-1	NP	F	P
Ali Bashi 1	*Transcaucasathyris* sp.	JU25-2	NP	F	P
Ali Bashi 1	*Transcaucasathyris* sp.	JU30-1	NP	F	P
Ali Bashi 1	*Transcaucasathyris* sp.	JU30-2	NP	F	P
Ali Bashi 1	*Transcaucasathyris* sp.	JU30-3	NP	F	P
Ali Bashi 1	*Transcaucasathyris* sp.	JU32-1	NP	F	P
Ali Bashi 1	*Paracrurithyris pygmaea*	JU75	NP	F	NP
Ali Bashi 1	*Paracrurithyris pygmaea*	JU75	NP	F	NP
Ali Bashi 1	*Transcaucasathyris* sp.	JU75	NP	F	P
Ali Bashi 1	*Transcaucasathyris* sp.	JU75	NP	F	P
Ali Bashi 1	*Transcaucasathyris* sp.	JU75	NP	F	P
Ali Bashi 1	*Acosarina minuta*	JU75-1	R	F	NP

Ali Bashi 1	*Transcaucasathyris* sp.	JU75-2	NP	F	P
Ali Bashi 1	*Transcaucasathyris* sp.	JU75-3	NP	F	P
Ali Bashi 1	*Transcaucasathyris* sp.	JU75-4	NP	F	P
Ali Bashi 1	*transcaucasa thyris*	JU76	NP	F	P
Ali Bashi 1	*Transcaucasathyris* sp.	JU76-1	NP	F	P
Ali Bashi 1	*Acosarina* sp.*?*	JU76-2	R	F	NP
Ali Bashi 1	*Transcaucasathyris* sp.	JU77-1	NP	F	P
Ali Bashi 1	*Acosarina minuta*	JU77-2	R	F	P
Ali Bashi 1	*Transcaucasathyris* sp.	JU77-3	NP	F	P
Ali Bashi 1	*Transcaucasathyris* sp.	JU77-4	NP	F	P
Ali Bashi 1	*Transcaucasathyris* sp.	JU78-1	NP	F	P
Ali Bashi 1	*Transcaucasathyris* sp.	JU78-2	NP	F	P
Ali Bashi 1	*Paracrurithyris pygmaea*	JU83-2	NP	F	P
Ali Bashi 3	*Transcaucasathyris* sp.	JU85-3	NP	F	P
Ali Bashi 3	*Transcaucasathyris* sp.	JU85-4	NP	F	P
Ali Bashi 1	*Spinomarginifera* sp.	JU85-7	NP	L	P
Ali Bashi 1	*Spinomarginifera* sp.	JU86	NP	L	P
Ali Bashi 3	*Transcaucasathyris araxensis*	JU89-1	NP	F	P
Gyanyima	*Acosarina minuta*	GY1(1-1)	NP	F	na
Gyanyima	*Neospirifer* sp.	GY2(6-1)	NP	F	P
Gyanyima	*Acosarina minuta*	GY3(6-1)	NP	F	NP
Gyanyima	*Stenoscisma gigantea*	GY4(6-1)	NP	NP	P
Gyanyima	*Permophricosothyris* sp.	GY5(6-12)	PR	F	P
Gyanyima	*Enteletes* sp.	GY6(6-12)	PR	F	P?
Gyanyima	*Dielasma* sp.	GY7(6-12)	NP	F	NP
Gyanyima	*Neospirifer* sp.	GY8(6-15)	NP	F	P
Gyanyima	*Permophricosothyris* sp.	GY9(6-15)	NP	F	P
Gyanyima	*Permophricosothyris* sp.	GY10(6-15)	NP	F	P
Gyanyima	*Martinia* sp.	GY11(7-5)	NP	NP	P
Gyanyima	*Alphaneospirifer anshunensis*	GY12(7-5)	NP	F	P?
Gyanyima	*Costiferina spiralis*	GY13(7-5)	NP	L	NP
Gyanyima	*Costiferina spiralis*	GY14(8-2)	NP	L	NP
Gyanyima	*Costiferina spiralis*	GY15(8-2)	NP	L	NP
Gyanyima	*Costiferina spiralis*	GY16(8-2)	NP	L	NP
Gyanyima	*Stenoscisma* sp.	GY17(9-23)	NP	F	P
Gyanyima	*Stenoscisma* sp.	GY18(9-23)	NP	F	P
Gyanyima	*Permophricosothyris* sp.	GY19(9-23)	PR	F	P
Gyanyima	*Hemiptychina* sp.	GY20(9-23)	NP	F	P
Gyanyima	*Araxathyris* sp.	GY21(9-23)	PR	F	P
Gyanyima	*Costiferina* sp.*?*	GY22(9-24)	NP	L	NP
Gyanyima	*Costiferina* sp.	GY23(9-24)	NP	L	NP
Gyanyima	*Costiferina* sp.	GY24(9-24)	NP	L	NP
Gyanyima	*Terebratudlida* sp.	GY25(6-12)	PR	F	NP

Gyanyima	*Transennatia gratiosa*	GY26(6-14)	NP	L	P?
Gyanyima	*Marginalosia* sp.*?*	GY27(9-17)	PR	L	NP
Gyanyima	*Marginalosia* sp.*?*	GY28(9-17)	NP	L	NP
Gyanyima	*Costatumulus sp*	GY29(9-17)	NP	L	NP
Gyanyima	*Permophricosothyris* sp.	GY30(6-12)	NP	NP	P
Gyanyima	*Permophricosothyris* sp.	GY31(6-12)	NP	F	P
Gyanyima	*Permophricosothyris* sp.	GY32(6-12)	NP	F	P
Gyanyima	*Permophricosothyris* sp.	GY33(7-1)	NP	no	P
Gyanyima	*Permophricosothyris* sp.	GY34(7-1)	NP	F	P
Gyanyima	*Permophricodothyris* sp.	GY35(7-1)	NP	F	P
Gyanyima	*Permophricosothyris* sp.	GY36(9-23)	NP	NP	P
Gyanyima	*Permophricodothyris* sp.	GY37(9-23)	NP	F	P
Gyanyima	*Permophricodothyris* sp.	GY38(9-23)	NP	F	P
Gyanyima	*Notothyris* sp.	GY39(9-23)	NP	F	P
Gyanyima	*Costiferina* sp.	GY40(6-12)	NP	L	NP
Gyanyima	*Acosarina* sp.	GY41(6-12)	NP	F	NP
Gyanyima	*Notothyris* sp.	GY42(9-23)	NP	F	P
Gyanyima	*Permophricodothyris* sp.	GY43(7-4)	NP	F	P
Gyanyima	*Permophricodothyris* sp.	GY44(7-4)	NP	F	P
Gyanyima	*Permophricodothyris* sp.	GY45(7-2?)	NP	F	NP
Gyanyima	*Permophricodothyris* sp.	GY46(7-2?)	NP	F	P
Gyanyima	*Notothyris sp*	GY47(9-23)	NP	F	P
Gyanyima	*Stenoscisma sp*	GY48(9-23)	NP	F	P
Gyanyima	*Alphaneospirifer sp*	GY49(9-23)	NP	F	NP
Gyanyima	*Martinia* sp.	GY50(9-23)	NP	F	P
Gyanyima	*Hemiptychina* sp.	GY51(9-23)	NP	F	P
Gyanyima	*Richthofenia lawrenciana*	GY52(6-12)	NP	L	NP
Gyanyima	*Notothyris* sp.	GY53(9-23)	NP	F	P
Gyanyima	*Permophricodothyris* sp.	GY54(7-4)	NP	NP	P
Gyanyima	*Permophricodothyris* sp.	GY55(6-1)	NP	NP	P
Gyanyima	*Dielasma* sp.	GY56(7-3)	NP	F	na
Gyanyima	*Permophricodothyris* sp.	GY57(7-3)	NP	F	P
Gyanyima	*Notothyris* sp.	GY58(9-23)	NP	F	P
Gyanyima	*Martinia* sp.	GY59(6-12)	NP	F	P
Gyanyima	*Stenoscisma* sp.	GY60(7-1)	NP	F	P
Gyanyima	*Richthofenia lawrenciana*	GY61(6-12)	NP	F	NP
Gyanyima	*Neospirifer* sp.	GY62(6-1)	PR	F	na
Gyanyima	*Costiferina subcostatus*	GY63(6-12)	NP	L	na
Gyanyima	*Permophricodothyris* sp.	GY64(6-12)	NP	NP	P
Gyanyima	*Permophricodothyris* sp.	GY65(6-12)	NP	NP	P
Gyanyima	*Permophricodothyris* sp.	GY66(6-12)	NP	F	P
Gyanyima	*Neospirifer* sp.	GY67(6-12)	NP	F	P
Gyanyima	*Permophricodothyris* sp.	GY70(6-15)	NP	F	P

Gyanyima	*Neospirifer* sp.	GY73(7-4)	NP	F	P
Gyanyima	*Costiferina indica*	GY74(7-16)	NP	L	NP
Gyanyima	*Costiferina indica*	GY75(8-2)	NP	L	NP
Gyanyima	*Costiferina indica*	GY76(8-2)	NP	L	NP
Gyanyima	*Costiferina indica*	GY77(8-13)	NP	L	NP
Gyanyima	*Costiferina indica*	GY78(8-14)	NP	L	NP
Gyanyima	*Costiferina indica*	GY79(8-14)	NP	L	NP
Gyanyima	*Neospirifer* sp.	GY80(9-23)	NP	F	na
Gyanyima	*Neospirifer* sp.	GY81(9-23)	NP	F	P
Gyanyima	*Permophricodothyris* sp.	GY83(9-23)	NP	F	P
Gyanyima	*Permophricodothyris* sp.	GY84(9-24)	NP	NP	P
Gyanyima	*Costiferina indica*	GY85(9-24)	NP	L	NP
Gyanyima	*Costiferina subcostatus*	GY86(9-27)	NP	L	na
Shangsi 1	*Paracrurithyris pygmaea*	CH87bis-40	NP	F	NP
Shangsi 2	*Paracrurithyris pygmaea*	CH128-14	NP	F	NP
Shangsi 1	*Paracrurithyris pygmaea*	CH87-bis-28	NP	F	NP
Shangsi 1	*Paracrurithyris pygmaea*	CH86-1	NP	F	NP
Shangsi 1	*Paracrurithyris pygmaea*	CH87bis-38	NP	F	NP
Shangsi 1	*Paracrurithyris pygmaea*	CH85bis-20	NP	F	NP
Shangsi 2	*Paracrurithyris pygmaea*	CH134-16	NP	F	NP
Shangsi 1	*Paracrurithyris pygmaea*	CH87bis-4	NP	F	NP
Shangsi 1	*Paracrurithyris pygmaea*	CH87bis-20	NP	F	NP
Shangsi 1	*Paracrurithyris pygmaea*	CH85bis-10	NP	F	NP
Shangsi 1	*Paracrurithyris pygmaea*	CH87bis-25	NP	F	NP
Shangsi 1	*Paracrurithyris pygmaea*	CH87bis-7	NP	F	NP
Shangsi 1	*Paracrurithyris pygmaea*	CH87bis-8	NP	F	NP
Shangsi 1	*Paracrurithyris pygmaea*	CH87bis-3	NP	F	NP
Shangsi 1	*Paracrurithyris pygmaea*	CH87bis-33	NP	F	NP
Shangsi 1	*Paracrurithyris pygmaea*	CH87bis-9	NP	F	NP
Shangsi 1	*Paracrurithyris pygmaea*	CH87bis-39	NP	F	NP
Shangsi 1	*Paracrurithyris pygmaea*	CH87bis-27	NP	F	NP
Shangsi 2	*Paracrurithyris pygmaea*	CH134-9	NP	F	NP
Shangsi 1	*Paracrurithyris pygmaea*	CH87bis-30	NP	F	NP
Shangsi 2	*Paracrurithyris pygmaea*	CH128-3	NP	F	NP
Shangsi 1	*Paracrurithyris pygmaea*	CH85bis-4	NP	F	NP
Shangsi 2	*Paryphella* sp.	CH136-2	NP	L	NP
Shangsi 2	*Paracrurithyris pygmaea*	CH136-5	NP	F	NP
Shangsi 2	*Paracrurithyris pygmaea*	CH131-2	NP	F	NP
Shangsi 1	*Paracrurithyris pygmaea*	CH85bis-11	NP	F	NP
Shangsi 2	*Paracrurithyris pygmaea*	CH136-4	NP	F	NP
Shangsi 2	*Paracrurithyris pygmaea*	CH136-5	NP	F	NP
Shangsi 2	*Paracrurithyris pygmaea*	CH128-11	NP	F	NP
Zhongliang hill	*Paraspiriferina alpha*	CH12-3	R	F	NP
Zhongliang hill	*Pariphella sulcatifera*	CH4-7	NP	F	NP

Zhongliang hill	*Acosarina* sp.	CH2bis-1	R	F	NP
Beifengjing	*Brachiopod?*	CH30-10	NP	NO	NP
Zhongliang hill	*Spinomarginifera* sp.*?*	CH6-9	NP	L	NP
Zhongliang hill	*Acosarina minuta*	CH5-7	R	F	NP
Zhongliang hill	*Bivalve-unknow*	CH4-2	NP	NP	na
Beifengjing	*Acosarina minuta*	CH30-3	NP	F	NP
Zhongliang hill	*Pariphella sulcatifera*	CH4-3	NP	L	NP
Beifengjing	*Brachiopod?*	CH34-8	NP	NO	NP
Zhongliang hill	*Acosarina* sp.	CH4bis-3	R	F	NP
Zhongliang hill	*P. pseudoutah?*	CH6-12	NP	F	NP
Zhongliang hill	*Cathaysia* sp.	CH4-8	NP	L	NP
Zhongliang hill	*Pariphella sulcatifera*	CH4-6	NP	L	NP
Zhongliang hill	*Pariphella sulcatifera*	CH5-9	NP	L	NP
Zhongliang hill	*Acosarina minuta*	CH6-6	NP	F	NP
Zhongliang hill	*Haydenella* sp.	CH4-5	NP	L	NP
Beifengjing	*Transcaucasathyris*	CH30-4	NP	F	P
Beifengjing	*Paracrurithyris pygmaea*	CH30-11	NP	F	NP
Daijaigou	*Spinomarginifera* sp.	CH71-3	NP	L	NP
Daijaigou	*Spinomarginifera* sp.	CH71-17	NP	L	NP
Daijaigou	*Cathaysia* sp.	CH71-4	NP	L	NP
Zhongliang hill	*Pariphella* sp.	CH6-5	NP	L	NP
Daijaigou	*Cathaysia* sp.*?*	CH71-8	NP	L	NP
Daijaigou	*Acosarina* sp.	CH71-14	R	F	NP
Beifengjing	*Peltichia* sp.	CH60-8	NP	F	NP
Beifengjing	*Paracrurithyris pygmaea*	CH30-11	NP	F	NP
Beifengjing	*Paracrurithyris pygmaea*	CH30-11	NP	F	P?
Daijaigou	*Paracrurithyris pygmaea*	CH72-5	NP	F	NP
Daijaigou	*Rhynchonellata*	CH72-6	NP	F	NP
Daijaigou	*Acosarina minuta*	CH72-11	R	L	NP
Daijaigou	*Strophomenata*	CH72-10	NP	L	NP
Daijaigou	*Cathaysia* sp.	CH72-13	NP	L	NP
Daijaigou	*Pariphella* sp.	CH72-4	NP	L	NP
Beifengjing	*Hustedia* sp.	CH60-15	R	F	NP
Beifengjing	*Hustedia* sp.	CH30-15	R	F	NP
Gomaniibrik	*Spinomarginifera helica*	EBHZ15-15	NP	L	P
Gomaniibrik	*Spinomarginifera sulcata*	EBHZ65-27	NP	L	NP
Gomaniibrik	*Spinomarginifera spinosocostata*	EBHZ69-1	NP	L	P
Gomaniibrik	*Spinomarginifera spinosocostata*	EBHZ65-33	NP	L	NP
Gomaniibrik	*Spinomarginifera helica*	EBHZ91-3	NP	L	NP
Gomaniibrik	*Spinomarginifera helica*	EBHZ91-4	NP	L	NP
Gomaniibrik	*Spinomarginifera helica*	EBHZ65_32	NP	L	NP
Gomaniibrik	*Spinomarginifera helica*	EBHZ65_31	NP	L	P
Gomaniibrik	*Spinomarginifera helica*	EBHZ68-1	NP	L	P
Gomaniibrik	*Spinomarginifera helica*	EBHZ68-2	NP	L	P

Gomaniibrik	*Spinomarginifera helica*	EBHZ69-2	NP	L	P
Gomaniibrik	*Spinomarginifera helica*	EBHZ69-4	NP	L	NP
Gomaniibrik	*Spinomarginifera helica*	EBHZ71-9	NP	L	P
Gomaniibrik	*Spinomarginifera helica*	EBHZ71-10	NP	L	P
Gomaniibrik	*Spinomarginifera helica*	EBHZ90-2	NP	L	NP
Gomaniibrik	*Spinomarginifera helica*	EBHZ90-3	NP	L	P
Gomaniibrik	*Alatorthotetina* sp.	EBHZ65-9	NP	L	NP
Gomaniibrik	*Alatorthotetina* sp.	EBHZ70-6	NP	L	NP
Gomaniibrik	*Alatorthotetina* sp.	EBHZ71-2	NP	L	NP
Gomaniibrik	*Alatorthotetina* sp.	EBHZ80-5	NP	L	NP
Gomaniibrik	*Alatorthotetina* sp.	EBHZ80-16	NP	L	NP
Gomaniibrik	*Alatorthotetina* sp.	EBHZ71-6	NP	L	NP
Gomaniibrik	*Alatorthotetina* sp.	EBHZ70-8	NP	L	NP
Gomaniibrik	*Alatorthotetina* sp.	EBHZ65-12	NP	L	NP
Gomaniibrik	*Alatorthotetina* sp.	EBHZ69-6	NP	L	NP
Selong Xishan	*Spiriferella* sp.	NL-11	PR	F	P
Selong Xishan	*Neospirifer* sp.	NL-13	NP	F	P
Selong Xishan	*Spiriferella* sp.	NL-15	NP	F	P
Selong Xishan	*Neospirifer* sp.	NL-20	NP	F	P
Selong Xishan	*Spiriferella* sp.	NL-25	NP	F	P
Selong Xishan	*Neospirifer* sp.	NL-7	NP	F	P
Selong Xishan	*Spiriferella* sp.	NL-21	NP	F	P
Selong Xishan	*Rhynchonella*	NL-26	NP	F	P
Selong Xishan	*Neospirifer* sp.	NL-2c	NP	L	P
Selong Xishan	*Retimarginifera* sp.	NL-3	NP	L	NP
Selong Xishan	*Spiriferella* sp.	NL-16	NP	F	P
Selong Xishan	*Spiriferella* sp.	NL-23	NP	F	P
Selong Xishan	*Spiriferella* sp.	NL-12	NP	F	P
Selong Xishan	*Spiriferella* sp.	NL-19	NP	F	P
Selong Xishan	*Neospirifer* sp.	NL-2b	NP	F	P
Selong Xishan	*Retimarginifera*	NL-5	NP	L	NP
Selong Xishan	*Neospirifer* sp.	NL-6	NP	F	P
Selong Xishan	*Bullarina* sp.	NL-10	NP	NP	NP
Selong Xishan	*Spiriferella* sp.	NL-14	NP	F	P
Selong Xishan	*Spiriferella* sp.	NL-17	NP	F	P
Selong Xishan	*Neospirifer* sp.	NL-22	NP	F	P
Selong Xishan	*Neospirifer* sp.	NL-1	NP	F	P
Selong Xishan	*Spiriferella* sp.	NL-2a	NP	F	P
Selong Xishan	*Spiriferella* sp.	NL-4	NP	F	P
Selong Xishan	*Spiriferella* sp.	NL-18	NP	F	P
Selong Xishan	*Neospirifer* sp.	NL-24	NP	F	P
Selong Xishan	*Spiriferella* sp.	NL-8	NP	F	P
Selong Xishan	*Neospirifer* sp.	NL-9	NP	F	P

Table 2. Mean, standard deviation (SD) and number of measures (N) for the thickness of laminae some of the specimens under investigation with SEM.

		Thickness of laminae (µm)		
Species	Specimen	Mean	SD	N
Spinomarginifera sp.	JU106-1	0.23	0.03	51
Spinomarginifera sp.	JU106-2	0.22	0.04	23
Spinomarginifera sp.	JU107-1	0.22	0.03	53
Spinomarginifera sp.	JU112-1	0.22	0.02	41
Spinomarginifera sp.	JU114-1	0.22	0.03	14
Spinomarginifera sp.	JU115-1	0.25	0.04	27
Spinomarginifera sp.	JU117-1	0.23	0.05	30
Spinomarginifera spinosocostata	JU121-1	0.25	0.05	13
Spinomarginifera spinosocostata	JU121-2	0.24	0.04	19
Spinomarginifera iranica	IR361-4	0.28	0.05	6
Spinomarginifera ciliata	IR358-10	0.28	0.01	6
Spinomarginifera iranica	IR357-2	0.24	0.04	11
Spinomarginifera pygmaea	IR357-3	0.33	0.04	14
Spinomarginifera helica	IR357-1	0.48	0.04	8
Spinomarginifera ciliata	IR356-1	0.49	0.06	10
Spinomarginifera ciliata	IR354-7	0.32	0.03	10
Spinomarginifera helica	IR353-5	0.35	0.09	7
Spinomarginifera spinosocostata	IR347-1	0.28	0.04	7
Spinomarginifera iranica	IR343-1	0.27	0.04	6
Spinomarginifera iranica	IR875-10	0.34	0.09	13
Spinomarginifera iranica	IR339-8	0.28	0.07	8
Spinomarginifera spinosocostata	IR887-2	0.28	0.06	11
Spinomarginifera iranica	IR885-2	0.33	0.03	5
Spinomarginifera helica	IR875-12	0.31	0.06	9
Spinomarginifera sp.	IR862-11	0.28	0.03	10
Spinomarginifera helica	IR374-6a	0.46	0.12	10
Spinomarginifera iranica	IR372-2	0.48	0.07	12
Spinomarginifera pygmaea	IR372-15	0.47	0.04	10
Spinomarginifera pygmaea	IR339-23	0.30	0.04	12
Spinomarginifera sulcata	EBHZ65-27	0.28	0.04	18
Spinomarginifera helica	EBHZ65-31	0.26	0.03	4
Spinomarginifera spinosocostata	EBHZ65-33	0.28	0.07	17
Spinomarginifera helica	EBHZ68-2	0.33	0.14	10
Spinomarginifera spinosocostata	EBHZ69-1	0.27	0.04	15
Spinomarginifera helica	EBHZ69-2	0.31	0.04	7
Spinomarginifera helica	EBHZ69-4	0.27	0.03	12
Spinomarginifera helica	EBHZ71-10	0.24	0.05	19
Spinomarginifera helica	EBHZ90-3	0.24	0.04	14

Costiferina subcostatus	GY62 (6-12)	0.49	0.10	13
Costiferina indica	GY79 (8-14)	0.49	0.07	17
Costiferina subcostatus	GY86 (9-27)	0.68	0.12	13
Costiferina indica	GY85 (9-24)	0.75	0.13	15
Costiferina indica	GY77 (8-13)	0.68	0.09	9
Costiferina indica	GY74 (7-16)	0.60	0.11	16
Costiferina indica	GY76 (8-2)	0.49	0.09	10
Alatorthotetina sp.	EBHZ65-12	0.40	0.13	40
Alatorthotetina sp.	EBHZ65-9	0.45	0.06	17
Alatorthotetina sp.	EBHZ69-6	0.41	0.05	31
Alatorthotetina sp.	EBHZ70-8	0.47	0.09	45
Alatorthotetina sp.	EBHZ70-6	0.47	0.12	25
Alatorthotetina sp.	EBHZ71-2	0.53	0.15	68
Alatorthotetina sp.	EBHZ71-6	0.41	0.07	16
Alatorthotetina sp.	EBHZ80-16	0.45	0.09	8
Alatorthotetina sp.	EBHZ80-5	0.42	0.09	23
T. persica	IR314-11	0.41	0.08	25
T. yangtzeensis	IR314-16	0.30	0.05	20
T. persica	IR314-bis5	0.25	0.04	11
T. persica	IR329-5	0.33	0.05	15
T. yangtzeensis	IR867-4	0.38	0.08	14
T. yangtzeensis	IR871-7	0.39	0.10	23
Paryphella	CH136-2	0.36	0.04	29
Paryphella	CH4-3	0.37	0.04	36
Paryphella	CH5-9	0.36	0.04	15
Spinomariginifera	CH71-17	0.31	0.04	32
Spinomarginifera	CH71-3	0.31	0.04	34
Cathaysia	CH71-8	0.24	0.03	15
Cathaysia	CH72-13	0.31	0.03	16

Table 3. Mean, standard deviation (SD) and number of measures (N) for the width and area of fibers in some of the specimens under investigation with SEM.

		Width of fibers (µm)		Area of fibers (µm)		
Taxon	Specimen	Mean	SD	Mean	SD	N
Paracrurithyris pygmaea	CH128-11	12,00	1,67	29,16	6,75	6
Paracrurithyris pygmaea	CH128-21	14,08	2,27	43,62	14,03	115
Paracrurithyris pygmaea	CH134-7	20,05	3,40	110,26	42,25	21
Paracrurithyris pygmaea	CH85bis-4	10,81	1,47	22,41	3,11	14
Paracrurithyris pygmaea	CH85bis-6	12,73	2,94	31,01	11,63	110
Paracrurithyris pygmaea	CH86-4	12,55	2,10	27,33	6,90	12
Paracrurithyris pygmaea	CH87bis-16	14,72	4,10	30,37	9,50	94
Paracrurithyris pygmaea	CH87bis-17	8,73	1,15	23,03	5,09	274
Paracrurithyris pygmaea	CH87bis-3	11,79	2,33	31,26	8,74	26
Paracrurithyris pygmaea	CH87bis-5	17,01	3,54	38,39	11,30	83
Paracrurithyris pygmaea	CH87bis-8	10,56	2,17	31,13	10,99	143
Paracrurithyris pygmaea	CH87bis-9	14,60	3,38	45,57	20,60	123
Paracrurithyris pygmaea	CH87bis-11	11,48	2,09	27,46	7,00	201
Paracrurithyris pygmaea	CH87bis-12	10,30	2,17	25,76	9,21	172
Paracrurithyris pygmaea	CH87bis-14	13,51	2,14	33,41	10,20	155
Paracrurithyris pygmaea	CH87bis-15	16,76	3,36	51,64	19,13	42
Permopricodothyris sp.	GY10 (6-15)	10,88	1,30	20,72	3,73	6
Permopricodothyris sp.	GY19 (9-23)	5,95	0,59	8,17	1,01	10
Permopricodothyris sp.	GY44 (7-4)	7,77	0,54	NA	NA	6
Permopricodothyris sp.	GY46 (7-2)	10,15	1,62	48,44	10,01	5
Permopricodothyris sp.	GY5 (6-12)	9,34	0,83	NA	NA	6
Permopricodothyris sp.	GY57 (7-3)	7,40	1,65	NA	NA	13
Permopricodothyris sp.	GY83 (9-23)	6,09	0,82	NA	NA	10
Permopricodothyris sp.	GY9 (6-15)	8,0	1,6	NA	NA	26
Permopricodothyris iranica	IR164-3	16,1	1,7	34,8	1,9	5
Permopricodothyris iranica	IR367-2	10,3	1,4	18,3	3,9	11

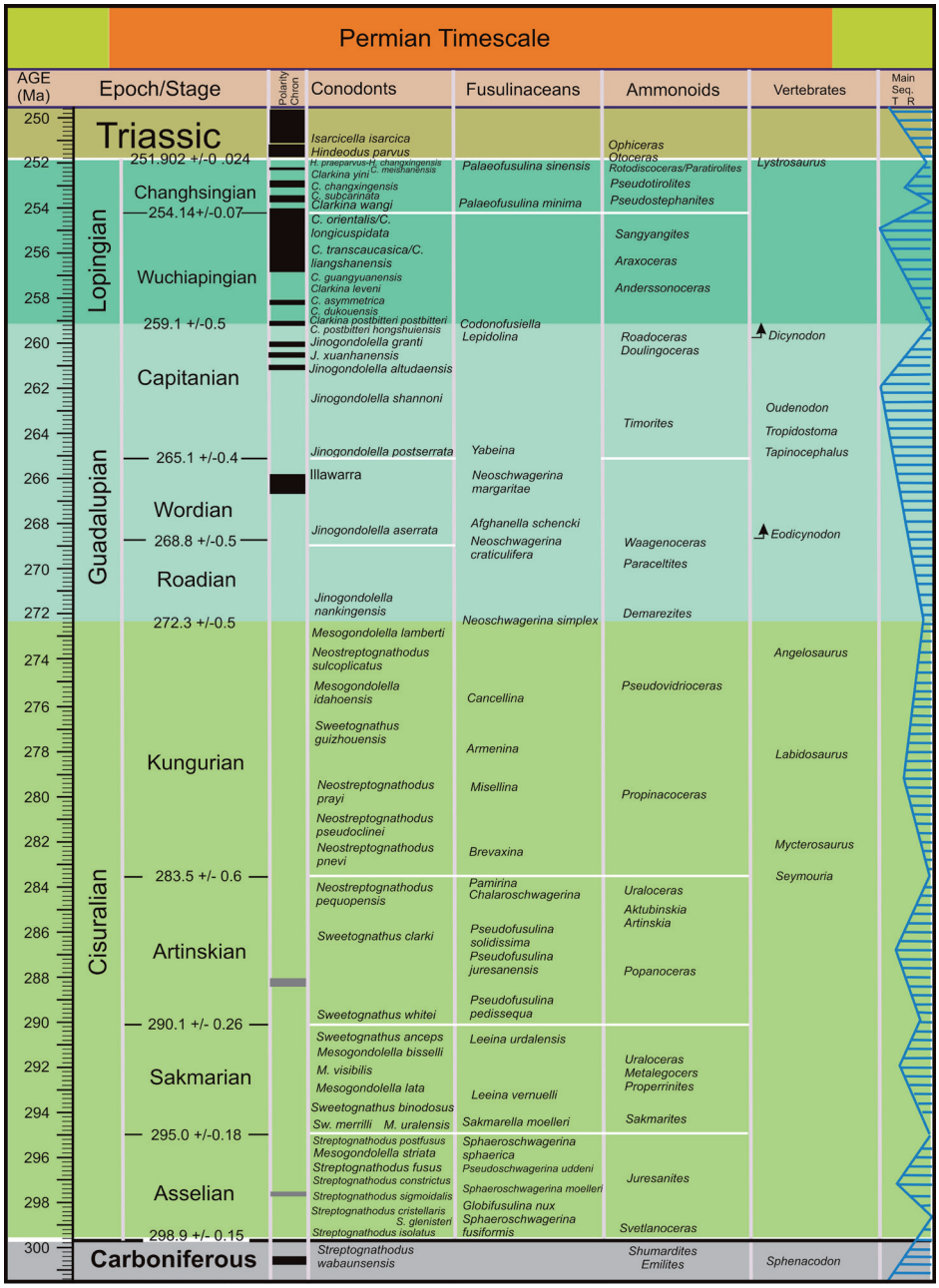

Note: This is the latest version of the Permian timescale which SPS recommends (Shen *et al.* 2013, New Mexico Museum of Natural History and Science, Bulletin 60, p. 411-416). We welcome any comments to improve it. All the information will be updated from time to time here. Geochronologic ages are combined from Burgess *et al.* (2014, PNAS 111, 9, p. 3316–3321); Shen *et al.* (2011, Science 334, p. 1367-1372) for the Lopingian; Zhong *et al.* (Lithos, in press) for the Guadalupian-Lopingian boundary; Schmitz and Davydov, (2012, GSA Bulletin 124, p. 549-577.) for the Cisuralian, Henderson *et al.* (2012, The Geologic Time Scale 2012 (vol. 2), p. 653-679) for the base of Kungurian and the Guadalupian. Tetrapod biochronology is after Lucas (2006, Geological Society London Special Publications 265, p. 65-93).